DIBENZOFURANS AND BENZO[b]NAPHTHOFURANS IN SOURCE ROCKS AND CRUDE OILS FROM TERTIARY NIGER DELTA BASIN, NIGERIA

ABIODUN BUSUYI **OGBESEJANA**
B.Sc. (Ado-Ekiti), M.Sc. (Ibadan)
MATRIC. No. : 153217

A Thesis in the Department of Chemistry,
Submitted to the Faculty of Science
in Partial Fulfillment of the requirements for the Degree of

DOCTOR OF PHILOSOPHY

of the

UNIVERSITY OF IBADAN

MARCH, 2019

ABSTRACT

Petroleum migration from source rock to the reservoir is one of the most critical geological processes responsible for the accumulation of hydrocarbon in sedimentary basins. The differential fractionation of dibenzofurans (DBFs) and benzo[b]naphthofurans during oil migration has made them useful as migration markers.The migration and filling history of hydrocarbon in the Niger Delta has not been fully understood. This study was designed to investigate the occurrence and distribution of dibenzofurans and benzo[b]naphthofurans in Niger Delta source rocks and crude oilsand their application in the determination of oil migration directions and distances in the basin.

Ninety-two source rocks and forty-one crude oil samples from five wells were collected from northern and offshore depobelts of the Niger Delta Basin. The rock samples were extracted with a mixture of dichloromethane/methanol (93/7, v/v) for 72 h in a Soxhlet extractor. The rock extracts and crude oils were fractionated using column chromatography. The total organic carbon (TOC), genetic potential (GP), maximum temperature of hydrocarbon generation (T_{max}) and production index (PI) were determined by Rock-Eval pyrolysis. The maceral composition and vitrinite reflectance were determined by petrographic analyses. The biomarkers and isotope composition of the rock extracts and crude oil fractions were analyzed by gas chromatography-mass spectrometry, elemental analyzer-isotope ratio mass spectrometry and gas chromatography-combustion-isotope ratio mass spectrometry. The oil migration directions and distances were determined based on the plot of total dibenzofurans concentrations. Data were analyzed using descriptive statistics and linear regression analysis.

The TOC and GP of the source rocks ranged from 0.46 to 27.52 wt% (2.86 ± 1.10) and 0.27 to 199.12 mg/g (9.24 ± 5.70), respectively. These mean values exceeded the minimum 0.5 wt% TOC and 2.0 mg/g GP required for potential source rocks. The T_{max} (295 to 446˚C), PI (0.05 to 0.61), vitrinite reflectance (0.23 to 0.50 %) and other maturity biomarker parameters indicated that the source rocks were at immature to early mature stage. The maceral analysis and source dependent parameters from biomarkers distributions indicated that the rocks were formed from type II/III kerogen. The relative concentrations of dibenzofuran, methyldibenzofurans (C_1-dibenzofurans) and dimethyldibenzofurans (C_2-dibenzofurans) in the source rock extracts ranged from 1.75 to 29.82 %, 27.60 to 40.67 % and 29.66 to 68.89 %, respectively. Benzo[b]naphthofurans were detected in high abundance in the rocks. The

distribution and abundance of dibenzofurans and benzo[b]naphthofurans in the rock samples were not influenced by source and maturity. The concentrations (µg/g) of dibenzofuran, methyldibenzofurans,dimethyldibenzofurans and benzo[b]naphthofurans in the oil samples ranged from 1.06 to 136.71, 9.64 to 570.64, 61.50 to 1346.81 and 2.75 to 352.60, respectively. The total DBFs concentrations decreased from 2380.59 to 76.39 µg/g in the longest migrated oil. This decrease in concentration was due to migration induced fractionation effect. The migration distances estimated for the crude oil samples ranged from 1.0 to 64.0 km.

The abundance and distributions of dibenzofurans and benzo[b]naphthofurans in the oils from similar source facies and thermal maturities were found to be effective in determining the oil migration directions and distances in the Niger Delta basin.

Keywords: Pyrolysis, Hydrocarbon migration, Oil biomarkers, Dibenzofurans,Benzo[b]naphthofurans.

Word count: 500

ACKNOWLEDGEMENTS

I give all the glory, honour and adoration to God for the successful completion of this PhD work. He is the author and the finisher of my faith. May His name be praised forever.

I sincerely appreciate the Head of the Department of Chemistry, Prof. T.I., Odiaka and the entire members of staff for the opportunity given to me to carry out my Ph.D research in the Department. I am particularly grateful to Prof. A.A. Adesomoju for providing enabling environment for learning and for his constructive criticism while he was the Head of the Department of Chemistry.

I am particularly indebted to my Supervisor and Mentor, Professor O.O. Sonibare, for his love, patience, tolerance, simplicity and thorough supervision of my research. You have taught me how to be an excellent researcher and imparted my life positively. I pray that God will uphold you and your family members to the end in Jesus' name. (Amen).

I want to appreciate the management of the Federal University Dutsin-Ma for releasing me to take up a Research Fellowship and granting me study leave towards this PhD programme. I appreciate the pioneer Head of Department of Applied Chemistry, Federal University Dutsin-Ma, Late Professor E.J. Ekanem, for recommending my employment at the University in absentia and approving my study leave towards this PhD programme. May your soul continue to rest in the bosom of our Lord Jesus Christ. Amen. I also appreciate the current Head of Department of Applied Chemistry, Federal University Dutsin-Ma for his understanding throughout the period of this programme.

I want to say a big thank you to the management of the China University of Petroleum Beijing for granting me International Visiting Research Fellowship which afforded me the opportunity to carry out my laboratory work at the State Key Laboratory of Petroleum Resources and Prospecting under the supervision of Professor Zhong Ningning. I owe Professor Zhong Ningning a lot for his care and love throughout my stay in China. This PhD research benefitted immensely from the constructive criticism of Professor Meijun Li of the State Key Laboratory of Petroleum Resources and Prospecting. You are appreciated sir. I thank Dr Luo Qinyong (Associate Professor), Dr Shi Shengbao, Mr Zhu Lei, Chen Quan, Zhao Jiang and some postgraduate students at the State Key Laboratory of Petroleum Resources and Prospecting, China University of Petroleum, Beijing for their assistance during my stay in China.

Special thanks to the Department of Petroleum Resources of Nigeria (DPR) for providing the source rock and crude oil samples used for this PhD research through the managements of Chevron Nigeria Limited and Total Nigeria Limited. I thank Mr. Tope Owolabi and Mr. Charles of DPR for their assistance in obtaining introduction letters from DPR to the oil companies. I also thank MR Seye Ekun, Mr Michael Nwume and Mr Chidi Ugbaja of Chevron Nigeria limited and TOTALFINAELF Nigeria limited for their assistance in getting the samples from their companies.

I salute my wife, Mrs Adebanke Ogbesejana who supported me throughoutthe period of this programme. You are the propelling force behind the success of this PhD research and to my children, Oluwakorede and Oluwaferanmi Ogbesejana.I pray that God would grant us sound health, long life and prosperity to reap the fruit of our labour in Jesus name. Amen

I appreciate my late parents, DSP Babatunde and Mrs. Anthonia Ogbesejana for giving birth to me. Though, I lost both of you when I was a kid, but this programme would not have been possible if you did not give birth to me. May you continue to rest in the bosom of our Lord Jesus Christ till we meet and part no more. I also say a big thank you to my elder brother and sister and my younger sisters who stood by my to ensure that I have sound education. May the Lord continue to bless you and your families in Jesus name. Amen.

My sincere appreciations go to CSP Victor Daramola, Major General Sunday Adebayo and ACP Abiodun Alabi for their financial supports during my postgraduate studies. May the almighty God reward you abundantly in Jesus' name (Amen). I also appreciate my spiritual father, Dr Gboyega Idowu for financial assistance and prayers during my postgraduate studies. More grace and anointing sir.

…….

Abiodun Busuyi OGBESEJANA

March, 2019.

DEDICATION

This thesis is dedicated to Almighty God, the Omnipotent and Omnipresent who guided me both physically and spiritually throughout the duration of this programme.

CERTIFICATION

This is to certify that Abiodun Busuyi OGBESEJANA in the Department of Chemistry, University of Ibadan, Ibadan carried out the work reported in this thesis under my supervision.

…….

Supervisor

Oluwadayo Olatunde Sonibare

B.Sc (Ago-Iwoye), M.Sc, Ph.D. (Ibadan)

Professor of Organic Chemistry

Department of Chemistry,

University of Ibadan, Ibadan.

TABLE OF CONTENTS

LIST OF TABLE

LIST OF FIGURES

CHAPTER ONE
INTRODUCTION

1.1 General Introduction

Organic Geochemistry is the study of the processes governing the origin and fate of organic materials in the geosphere. Petroleum geochemistry is a branch of organic geochemistry which deals with the application of chemical principles in the study of the origin, migration, accumulation and alteration of petroleum (Hunt, 1996). Petroleum is generated from organic matter during the process of sedimentation as it experiences increase pressure and temperature. Biomarkers present in the source rock extracts and crude oils are useful because they can provide reliable information on the source, depositional environment, thermal maturity and migration. Information about the processes governing petroleum migration from the source to the reservoir and hydrocarbon filling history are very useful in the discovery of new exploration plays, and this has been reported by many authors (Philp, 1985; Mackenzie, 1984; Tissot and Welte, 1984; Larter *et al*., 1996; Peters *et al*., 2005; Li *et al*., 2014).

Most of the early geochemical studies have been focused on the analyses of saturate and aromatic hydrocarbon fractions of source rocks and crude oil. However, the advancement in analytical and instrumental techniques has made the studies of other classes of compounds, especially the polar compounds (nitrogen, oxygen and sulphur compounds) very much possible. In more recent times, there have been growing interest in the application of aromatic sulphur, nitrogen and oxygen compounds in determining the extent and direction of oil migration (Li *et al.,* 1995; Larter *et al*., 1996; Li *et al*., 2011, 2014; Faboya *et al*., 2015; Li and Ellis, 2015; Fang *et al.,* 2016; Xiao *et al*., 2016; Yang *et al*., 2016; Chen *et al*., 2017; Li *et al*., 2018). These compounds have the capacity to interact with the surrounding environment via hydrogen and/ionic bonding. The resulting effect is the differential fractionation of these compounds and their derivatives during oil migration.

1.2 Origin of petroleum

Petroleum is a generic name for substances consisting of mainly hydrocarbons and smaller amount of non-hydrocarbons compounds. There aretwo competing concepts for the origin of petroleum, namely; the inorganic and organic origin.

1.2.1 Inorganic origin

The modern inorganic concept is rooted in the mid nineteenth century. Mendeleev (1877) proposed that surface water percolates deep into the earth and reacts with metallic carbides to form acetylene, which then condenses into larger hydrocarbons. Mendeleev's abiotic hypothesis, further refined in 1902, was attractive at the time because it offered an explanation for the growing awareness of widespread petroleum deposits that suggested some sort of deep, global process.

$$2CaC_{(s)} + 2H_2O_{(l)} \rightarrow C_2H_{2(g)} + 2CaO_{(s)} + H_{2(g)} \quad (1)$$

$$3C_2H_2 \rightarrow C_6H_6 \quad (2)$$

The modern version of Mendeleev hypothesis has emerged and this hypothesis relies on a thermodynamic argument, which states that hydrocarbons greater than methane cannot be formed spontaneously except at the high temperatures and pressures of the lower-most crust (Kenney *et al*., 2002). The hypothesis ignores the fact that all life is in thermodynamic disequilibrium.Geochemists recognize that some abiogenic hydrocarbons occur in the geosphere. Small amounts of abiotic hydrocarbon gases are generated by rock–water interactions involving serpentinization of ultramafic rocks (McCollom and Seewald, 2001), the thermal decomposition of siderite in the presence of water (McCollom and Sewald, 2003), and during magma cooling as a result of Fischer-Tropsch type reactions (Potter *et al*., 2001). Fischer–Tropsch synthesis (Fischer and Tropsch, 1926) is used to convert carbon monoxide or carbon dioxide generated from coal into synthetic hydrocarbons as follows:

$$nCO + (2n+1)H_2 = C_nH_{2n}+2+nH2O \quad (3)$$

$$nCO_2 + (3n+1)H_2 = CnH_{2n+2}+2nH_2O \quad (4)$$

Fischer–Tropsch synthesis generates complex mixtures that are always dominated by the lighter hydrocarbons. Commercial quantities of abiotic petroleum have never been found, and the contribution of abiogenic hydrocarbons to the global crustal carbon budget is inconsequential (Sherwood Lollar*et al*., 2002). However, support for the abiotic hypothesis dwindled with mounting evidence for a biogenic origin of petroleum (Peters *et al*, 2005)

1.2.2 Organic origin

Modern concepts of the origin of petroleum from ancient organic-rich sedimentary rocks emerged during the nineteenth century. Hunt (1996) reported that organic matter in some North American Paleozoic rocks came from marine animals or plants and that its transformation to bitumen must be similar to the process of coal formation. Lesquereux (1866), the American father of paleobotany, reached similar conclusions after studying Devonian shales from Pennsylvania, as did Newberry (1873) in his study of Devonian shales from Ohio. Early twentieth-century field and chemical studies by the US Geological Survey provided convincing evidence that crude oil in the Monterey Formation of California originated from diatoms in organic-rich shales (Clarke, 1916; Tissot and Welte, 1984). Studies of organic-rich shales in Europe also gave credence to organic origin of petroleum (Pompecki, 1901; Schuchert, 1915)

Support of the biogenic hypothesis became widespread in the mid twentieth century, with converging scientific advances in paleontology, geology, and chemistry. Alfred Treibs (1936) established a link between chlorophyll in living organisms and porphyrins in petroleum. Additional geochemical evidence followed with the discoveries that low- to moderate-maturity oils retain fractions that are optically active (Oakwood et al., 1952), that stable carbon isotope compositions of petroleum preserve evidence of biological isotope fractionation (Craig, 1953), and that oils contain many “chemical fossils” (biomarkers) in addition to porphyrins that can be traced to their biological precursors (Peters *et al*., 2005). Concurrent with these findings were field studies recognizing that organic-rich strata occur in all petroliferous sedimentary basins, that this organic matter (kerogen) originates from biota (Forsman and Hunt, 1958; Abelson,

1963), that has been chemically altered from its initial state, and that it generates oil and gas as the sediments are buried and heated (Tissot and Welte, 1984).

1.3 Petroleum Generation, Migration and Accumulation

1.3.1 Petroleum Generation

The generation of oil and gas in source rocks is a natural consequence of the increase of subsurface temperature during geologic time. The process of kerogen transformation with increasing temperatures is called maturation, which is subdivided into the diagenesis, metagenesis and catagenesis stages (Tissot and Welte, 1984).These three physico-chemical transformation processes are briefly discussed below:

1.3.1.1 Diagenesis

Diagenesis is a process through which the system tends to approach equilibrium under conditions of shallow burial, and through which the sediment normally becomes consolidated (Tissot and Welte, 1984). The depth interval concerned is in the order of a few hundred meters, occasionally to a few thousand meters. In the early diagenetic interval, the increase of temperature and pressure is small and transformations occur under mild conditions (Tissot and Welte, 1984). During early diagenesis, one of the main agents of transformation is microbial activity (Tissot and Welte, 1984). Aerobic micro-organisms that live in the uppermost layer of sediments consume free oxygen. Anaerobes reduce sulfates to obtain the required oxygen. The energy is provided by decomposition of organic matter, which in the process is converted into carbon dioxide, ammonia and water.

Previous biogenic polymers or "biopolymers" (proteins, carbohydrates are destroyed by microbial activity during sedimentation and early diagenesis (Tissot and Welte, 1984). Then their constituents become progressively engaged in new polycondensed structures ("geopolymers") precursing kerogen. The most important hydrocarbon formed during diagenesis is methane (Tissot and Welte, 1984).

At the end of diagenesis, the organic matter consists mainly of kerogen (Tissot and Welte, 1984). The end of diagenesis of sedimentary organic matter is most conveniently placed at the level where extractable humic acids have decreased to a

minor amount, and where most carboxyl groups have been removed (Tissot and Welte, 1984). This is equivalent to the boundary between brown coal and hard coal, according to the coal rank classification of Tissot and Welte (1984). It corresponds to a vitrinite reflectance of about 0.5 % .

1.3.1.2 Catagenesis

This results from consecutive deposition of sediments which will lead to further burial of previous beds to a depth reaching several kilometers of overburden in subsiding basins (Tissot and Welte, 1984). The sediment will experience increase in temperature and pressure as it passess through greater depth. Temperature may range from about 50 to 150'C and geostatic pressure due to overburden may vary from 300 to 1000 or 1500 bars (Tissot and Welte, 1984). Such increase places the system out of equilibrium andresults in new changes. Organic matter experiences major changes and through progressive evolution, the kerogen produces first liquid petroleum; then at a later stage "wet gas" and condensate; both liquid oil and condensate are accompanied by significant amounts of methane (Tissot and Welte, 1984). The end of catagenesis is reached in the range where the disappearance of aliphatic carbon chains in kerogen is completed, and where the development of an ordering of basic kerogen units begins (Tissot and Welte, 1984). This corresponds to vitrinite reflectance of about 2.0% which, according to various coal classifications, is approximately the beginning of the anthracite ranks (Tissot and Welte, 1984).

1.3.1.3 Metagenesis

This is the last stage of petroleum generation and dry gas is generated at this stage. Here temperature (above 200^{o}C) and pressure reach high values at greater depth; in addition, rocks are exposed to the influence of magma and hydrothermal effect (Tissot and Welte, 1984). At this stage, the organic matter is composed only of methane and a carbon residue, where some crystalline ordering begins to develop (Tissot and Welte, 1984). The constituents of the residual kerogen are converted to graphitic carbon (Tissot and Welte, 1984).

1.3.2 Petroleum Migration

Migration is the movement of petroleum from its place of origin in the source rock to the reservoir trap. The migration of petroleum from source rock to reservoir trap is controlled by physical and physico-chemical conditions of the sedimentary strata the oil is moving through.There are two types of migration; primary and secondary migration (Peters and Moldowan, 1993; Peters *et al*., 2005). These two types of migration are briefly discussed below:

1.3.2.1Primary Migration

Primary migration is the expulsion of petroleum from the fine-grained source rock into rocks with higher porosity and permeability. One of the main driving forces for primary migration is sediment compaction due to overburden load. Compaction is achieved by the reduction of pore spaces due to the expulsion of pore waters. Freshly deposited clay-rich sediments have 60-80% pore water contents. Most of this pore water is expelled due to compaction within the first 2,000 m of burial. However, at that stage petroleum generation by thermal degradation has not been initiated in most basins. With further burial, very little pore water remains for additional expulsion. This is why sediment compaction was long disputed as a major driving force for primary migration. Now it is known, however, that good quality source rocks experience further compaction with the expulsion of petroleum (Peters and Moldowan, 1993; Peters *et al*., 2005).

1.3.2.2 Secondary Migration

Secondary migration involves the movement of petroleum within permeable carrier beds to the reservoir (Wendebourg and Harbaugh, 1997, and references therein). It occurs over distances from a few kilometers to hundreds of kilometers, although typically it is on the order of tens of kilometers. Although rates of secondary migration are likely to be highly variable (England et al., 1991), laboratory experiments suggest that they are rapid on a geologic time scale (Tissot and Welte, 1984). The secondary migration process and the subsequent formation of pools are controlled by three parameters. These are the buoyancy rise of oil and gas in water-saturate porous rock, capillary pressures and hydrodynamic fluid flow (Tissot and Welte, 1984). If the aqueous pore fluids in the

subsurface are stationary, which is under hydrostatic conditions, the only driving force for secondary migration is buoyancy. But if there is water flow in the subsurface that is, under hydrodynamic conditions, the buoyant rise of oil and gas may be modified by this water flow.

1.3.3 Petroleum Accumulation

Petroleum is ultimately collected through secondary migration in permeable porous reservoir rocks in the position of a trap (Tissot and Welte, 1984). Traps are containers in the subsurface where petroleum accumulates. It is characterized by its upward convex shape in combination with a porous reservoir rock with a relatively impermeable sealing cap rock above (Tissot and Welte, 1984). Stratigraphic traps are mainly caused by depositional features, and structural traps by tectonic events. In some cases, there may be combination of these two traps. Typical examples of stratigraphic traps are barrier sand bars, deltaic distributory channel sandstones and carbonate reefs (Tissot and Welte, 1984). Typical examples of structural traps are anticlines, fault traps, and traps associated with salt domes (Tissot and Welte, 1984).

The majority of petroleum accumulations are found in clastic reservoir rocks, such as sandstones and siltstones. Another important reservoir rocks are carbonates. Fractured shales, igneous and metamorphic rocks play only a minor role. The maximum total holding capacity or closed volume of a trap is the volume between its highest point and the spilling plane or outflow level at the bottom (Tissot and Welte, 1984). Porosities in reservoir rocks usually range from 5 to 30%. Traps are never full in the sense that all available pore space is occupied by petroleum. There is always a certain residual amount of water, which cannot be displaced by migrating petroleum.

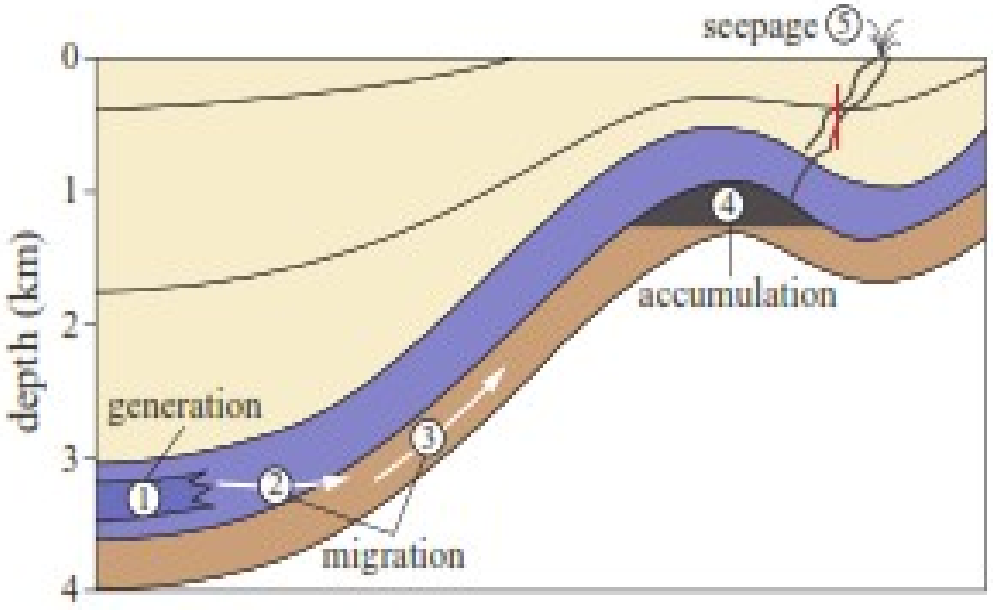

Fig. 1.1: Diagram to illustrate the main geological conditions and geochemical processesrequired for the formation of petroleum accumulations in sedimentary basins: (1) petroleum generation in source rocks; (2) primary migration ofpetroleum;(3) secondary migration of petroleum; (4) accumulation of petroleum in a reservoir trap; (5) seepage of petroleum at the Earth's surface as a consequence of a fractured cap rock (After Selley, 1998).

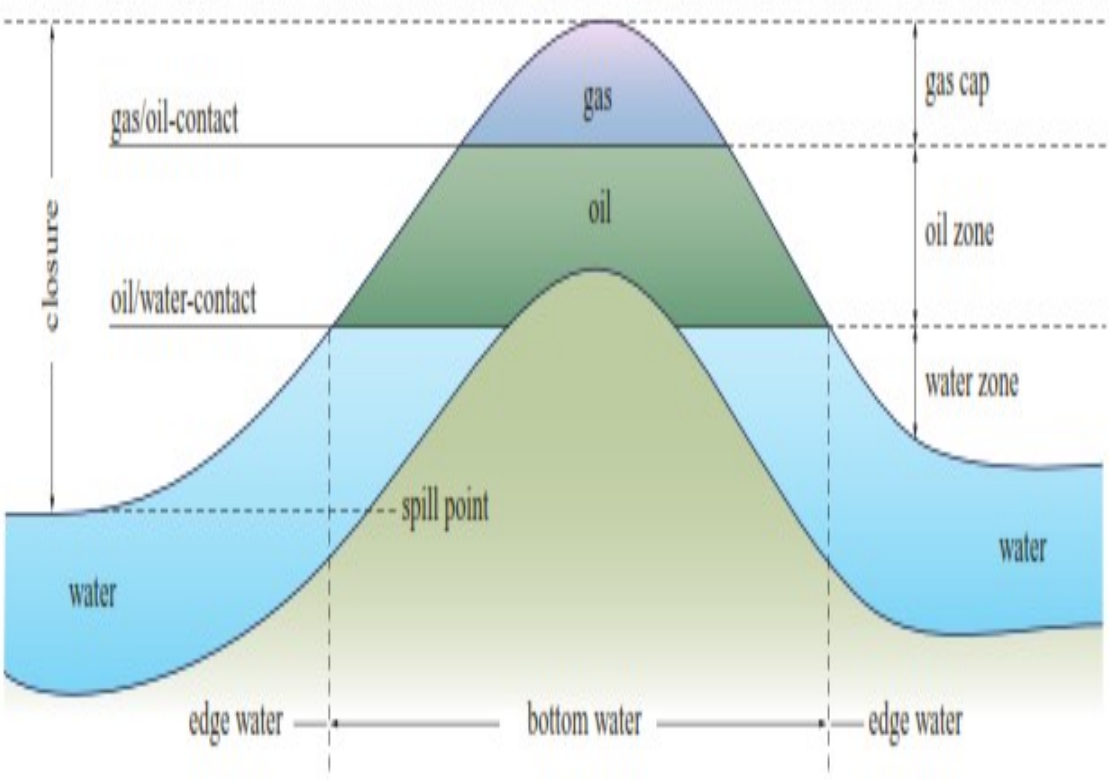

Fig.1.2: Diagram showing a folded sandstone layer representing a reservoir trap. At theapex of this anticline, natural gas and oil below has accumulated (After Selley, 1998)

1.4 Petroleum Source Rock Evaluation

Petroleum source beds are fine grained, clay-rich siliclastic rocks (mudstones, shales) or dark coloured carbonate rocks (limestones, marlstones), which have potential to generate hydrocarbons or have generated and effectively expelled hydrocarbons. A petroleum source rock is characterized by three essential conditions: it must have a sufficient content of finely dispersed organic matter of biological origin; this organic matter must be of a specific composition, i.e. hydrogen-rich; and the source rock must be buried at certain depths and subjected to proper subsurface temperatures in order to initiate the process of petroleum generation by the thermal degradation of kerogen (Killops and Killops, 1993, 2005). The parameters used for source rock evaluation are briefly discussed below:

1.4.1 Quantity of Organic Matter

The abundance of organic matter in sediments is usually expressed as the relative percentage of organic carbon on a dry weight basis. The total organic carbon (TOC) content is controlled by the input of organic matter into the sedimentary paleoenvironment, the preservation of the supplied organic matter, and the dilution of this organic matter by mineral matter. The minimum acceptable TOC values for various types of source rocks are 0.5 % for shales, 0.3 % for carbonates and 1.0 % for clastictype rocks (Killops and Killops, 1993). A minimum of 1.5-2.0 % TOC has generally been accepted for defining good source rocks (Hunt, 1996). The amount of hydrocarbon isolated from the bitumen extracted from finely ground rock samples can also provide a useful indication of whether any oil potential exists. Oil source rocks are generally considered to require a minimum hydrocarbon content of 200-300 ppm (Killops and Killops, 1993). The Genetic Potential (GP) expressed in milligram hydrocarbon per gramme of rock (mg/HC/g) can also be used to evaluate the maximum quantity of hydrocarbon that a particular rock had already generated (S1) and would be generated (S2) if exposed to a sufficient prolonged thermal stress i.e. (S1 + S2). Both the S1 and S2 values can be obtained from the Rock-Eval pyrolysis of rocks. The minimum GP value required for potential source rock is fixed at 2 mg/g (Tissot and Welte, 1984; Killops and Killops 1993; Peters et al., 2005).

1.4.2 Quality of Organic Matter

The type of sedimentary organic matter present is essential for evaluating source rocks, because different types of organic matter have different hydrocarbon potential. The three methods used in assessing the quality of source rocks are discussed below.

1.4.2.1 Optical Method

Optical microscopy can only be used to describe that part of the organic matter of a sediment occurring in particles large enough to be visible in an optical microscope (about 1μm or larger). However, also some finer "amorphous" organic matter can be identified, using transmitted light or fluorescence techniques. A significant number of publications for kerogen classification, using optical microscopy, are available in literature (e.g. Alpern, 1975; Alpern *et al*., 1972; Batten, 1973; Boulter, 1994; Boulter and Riddick, 1986; Bujak *et al*. 1977; Burgess, 1974; Bustin, 1988; Combaz, 1980; Correia, 1971; Gutjahr, 1983; Habib, 1979, 1983; Hart, 1986; Masran and Pocock, 1981; Ottenjann et al., 1975; Parry et al., 1981). Generally three different techniques are applied for microscopic studies of source rocks:

The principal macerals in coals and sedimentary rocks can be categorized into three groups (Stach *et al*., 1982; Taylor *et al*., 1998) as described below:

Liptinites: oil-prone macerals that have low reflectance, high transmittance, and intense fluorescence at low levels of maturity. Many liptinite phytoclasts have characteristic shapes and textures, e.g. algae (such as Tasmanites), resin (impregnating voids), and spores. Liptinites are divided broadly into alginites and exinites.

Vitrinites: gas-prone macerals that have angular shapes, usually gelified, but sometimes with cellular structure. The reflectance of vitrinite phytoclasts is used as an indicator of the thermal maturity for rock samples. Vitrinite macerals show intermediate reflectance (low-gray) (Bostick, 1973) and transmittance, usually with no fluorescence unless impregnated by liptinites.

Inertinites: an inert macerals that have angular shapes, typically with cellular structure. Inertinite phytoclasts show high reflectance, show no fluorescence, and are opaque in transmitted light

1.4.2.2 Physico-chemical Methods

This method offers a combination of techniques to describe the three basic types of kerogen found in sedimentary rocks. The Physicochemical classification of kerogens has been reported by many authors (Bordenave and Espitalié 1993, Cook and Sherwood 1991, Cooper and Barnard 1984, Espitalié *et al*. 1977, Horsfield 1984, Langford and Blanc-Valleron 1990, Larter 1985, Mukhopadhyay *et al*. 1985, Orr 1986, Tissot and Welte 1978, 1984, Waples, 1985). The most familiar method used to classify organic matter type in sedimentary rocks is the plot of atomic H/C versus O/C from elemental analysis or van Krevelen diagram. This diagram was originally developed to characterize coals (Van Krevelen, 1961; Stach *et al*., 1982; Taylor *et al*., 1998) during their thermal maturation or coalification, but Tissot *et al*. (1974) extended its use to include the kerogen dispersed in sedimentary rocks. Later, a combination of the S_2 and S_3 values from Rock-Eval pyrolysis was used to provide a graphic representation called a pseudo-van Krevelen diagram using the Hydrogen Index (S2/Corg) and Oxygen Index (S3/Corg). Both diagrams have been widely accepted to classify kerogens and the quality of organic-rich rocks.

The classification of the organic matter based on H/C and O/C atomic ratios (van Krevelen, 1961, 1993) typically distinguishes three main types of kerogens (Type I, Type II and Type III) in the order of decreasing H/C and O/C ratios. The various types of kerogens initially were associated to specific geological settings (Tissot and Welte, 1984). Thus, Type I kerogen occurred in lacustrine environments where selective accumulation of algal material or severe biodegradation of the organic matter took place; Type II was related to open marine sediments where autochthonous organic matter derived from a mixture of phyto- and zooplankton was deposited in a reducing environment, with a Type II-S that was a high sulfur variety of Type II; and finally, Type III kerogen was essentially derived from terrestrial plants and deposited in proximal environments (Durand, 1993). A secondary type of kerogen (Type IV) composed of aromatic carbonized organic matter (pre-deposition, during deposition, or during oil cracking) with no potential for hydrocarbon generation has also been described. Coals are classified as Type III kerogen (Durand *et al*., 1977).

Type I kerogen displays a very high potential for liquid hydrocarbon generation, which decreases in Type II kerogen, while the Type III kerogen has no potential to generate oil and will only generate abundant gas at greater depths.

1.4.2.3 Chemical methods

This method involves the use of biomarkers to determine the organic matter type in the source rocks. Extractable bitumen from source rocks contains geochemical fossils (biomarkers) which carry information about the origin of the organic matter (Tissot and Welte, 1984). The application of biomarker in the determination of organic matter type is fully discussed in chapter 2.

Table 1.1: Kerogen type and expelled products (After Peters and Cassa, 1994)

Kerogen (quality)	Hydrogen index(mg hydrocarbon/g TOC)	S2/S3	Atomic H/C	Main product at peak maturity
I	>600	>15	>1.5	oil
II	300-600	10-15	1.2-1.5	oil
II/III	200-300	5-10	1.0-1.2	Oil/gas
III	50-200	1-5	0.7-1.0	gas
IV	<50	<1	<0.7	none

1.4.3 Thermal Maturity of Organic Matter

Thermal evolution of the source rock, during diagenesis, catagenesis and metagenesis, changes many physical or chemical properties of the organic matter (Peters and Welte, 1984). These properties may be considered as indicators for maturation. Maturity of organic matter can be determined from Rock-Eval pyrolysis, geophysical and petrographic and biomarker analyses. These techniques are briefly discussed below:

1.4.3.1 Rock –Eval Pyrolysis

Rock-Eval Pyrolysis offers a rapid method for the characterization of kerogen types and for the determination of the maturity of organic matter (Espitalie *et al*., 1977). Rock-Eval pyrolysis parameters such as T_{max} and Production Index (PI) $(S_1/(S_1 + S_2)]$ can be used to estimate thermal maturity. T_{max} and PI less than ~435˚C and 0.1, respectively, indicate immature organic matter that generated little or no petroleum. Tmax values greater than 470˚C coincide with the wet-gas zone. PI reaches ~0.4 at the bottom of the oil window (beginning of the wet gas zone) and can increase to as high as 1.0 when the hydrocarbon-generative capacity of the kerogen has been exhausted. Usually, some S1 will remain as adsorbed dry gas, even in highly postmature rocks. T_{max} and PI are indices of thermal maturity but depend partly on other factors, such as the type of organic matter. The maturation range of T_{max} varies for different types of organic matter (Tissot and Welte, 1984; Peters, 1986; Bordenave, 1993). The range of variation of T_{max} is narrow for Type I kerogen, wider for Type II and much wider for Type III kerogen due to the increasing structural complexity of the organic matter (Tissot et al., 1987). The maturation window for oil/condensate generation from Types I and II organic matter ranges from 430 to 470˚C and greater than 470˚C for dry gas generation (Tissot et al., 1987; Peters, 1986). The oil window for Type III terrigenous organic matter ranges from 465 to 470˚C, while the condensate/wet gas window corresponds to T_{max} up to 540˚C(Bordenave, 1993). However, thermal maturity determination based on T_{max} or PI should be supported by other geochemical measurements such as vitrinite reflectance, TAI, or biomarker parameters.

1.4.3.2 Petrographic Method

The basis of organic petrography is optical microscopy that includes reflected and transmitted white light, fluorescence (UV and blue light excitation), and polarized light analysis of the organic matter in a broad sense.

1.4.3.2.1 Vitrinite reflectance

The optical properties of vitrinite from finely dispersed organic matter in sedimentary rocks could be used to assess thermal maturity or rank (Bostick, 1973). Vitrinite reflectance is now widely accepted by exploration geologists as a key measure of thermal maturity. Kerogen is organic matter that is insoluble in organic solvents, and vitrinite is one of the macerals common in kerogen. Although vitrinite reflectance is related more to thermal stress than to petroleum generation, approximate R_o values have been assigned to the beginning and end of oil generation (Table 1.2). Inter-laboratory comparison suggests that a differential of 0.1% vitrinite reflectance is significant for indicating different thermal maturities with a moderate confidence (68%), while a differential of 0.2% is required for a high confidence (95%) (Lin, 1995; Killops and Killops, 2005).

1.4.2.3.2 Thermal Alteration Index (TAI)

With increase in thermal maturation of organic matter a gradual change in color is observed in transmitted light, from yellow in immature samples through orange, brown and black, culminating in opaque organic debris. These palynomorphic coloration changes are produced as increasing burial depth and rise in temperature cause chemical changes in spores and pollens and can be used to evaluate the state of thermal alteration on a scale referred to as the Thermal Alteration Index (TAI) (Suárez-Ruiz *et al*., 2012). Thus, the TAI is based upon color changes of one variety of pollen or spore (Correia, 1967; Staplin, 1969) and can range from a value of 1 for strictly immature spores and pollen (pale-yellow in color) to a value of 5 for those having undergone a strong thermal evolution corresponding to the dry-gas zone or above (dark-brown color). For the Spore Coloration Index (SCI) the scale proposed by Fischer *et al*. (1981) ranges from 1 to 10. TAI generally is related to vitrinite reflectance and primarily has been used to assess the

hydrocarbon potential of rocks containing organic matter. Limitations of this method include the lack of standardization, subjectivity of the observation of color, and a limited ability to relate appropriate geochemical parameters to TAI (Senftle *et al*., 1993; Yule *et al*., 1998).

1.4.3.3 Biomarker Analysis

Biological markers which are present in extracts of sediments and crude oils can be used in maturity determination (Peters *et al*., 2005). Ratios of certain saturated and aromatic biomarkers are some of the most commonly applied thermal maturity indicators. These indicators result from two types of reactions i.e. (1) cracking reactions (including aromatizations) and (2) configurational isomerizations at certain asymmetric carbon atoms (Peters *et al*., 2005). The application of biomarker in the determination of organic matter maturity is discussed in detail in chapter 2.

1.5 Justification for this Study

The process of petroleum migration from source rock to the reservoir is one of the most important geological processes responsible for the accumulation of hydrocarbons in a sedimentary basin. The reconstruction of oil migration directions, distance and filling history is crucial to determine oil filling points and potential source kitchens/beds as well as to predict satellite reservoirs among petroleum reservoirs. The complex petroleum system in the Niger Delta basin has limited the understanding of hydrocarbons migration and accumulation processes. Oxygen-containing compounds such as dibenzofuran and its derivatives have proved to be potential oil migration dependent biomarkers. The dibenzofuran molecules can easily get adsorbed by the carrier bed during oil migration, thereby generating a geological chromatographic effect and this has attracted their use as oil migration marker. However, dibenzofuran compounds have not been studied or reported in the Niger Delta source rocks and crude oils.

1.6 Aims and Objectives of this study

The processes involved in the migration and filling history of hydrocarbon in the Niger Delta has not been fully understood. This study was designed to investigate the

application of dibenzofurans and its derivatives which are migration dependent, in understanding the petroleum migration and accumulation processes in the basin. The present study was conducted to:

a. re-examine the petroleum potential of source rock from the Niger Delta,
b. re-examine the source and maturity status of the crude oils and source rocks based on the distributions of saturate and aromatic biomarkers,
c. examine the occurrence and distributions of dibenzofurans and benzo[b]naphthofurans in the source rocks and crude oils,
d. evaluate the effect of source facie, maturity and migration on the occurrence and distributions of dibenzofurans and benzo[b]naphthofurans in the source rocks and crude oils,
e. describe the migration pattern of crude oils in the basin based on the results from (a) to (d) above.

CHAPTER TWO

LITERATURE REVIEW

2.1 Biomarker Geochemistry

Biomarkers are complex organic compounds that occur in sediments, rocks, and crude oils, and that show little or no change in structure from their parent organic molecules in living organisms (Peters and Moldowan, 1993). The distribution of these compounds is highly diagnostic of source organisms, and their subtle structural transformation could be indicative of depositional environment, thermal maturity and biodegradation (Asif, 2010). Biomarker molecules are believed to have definite chemical structures that can be linked either directly or indirectly through a set of diagenetic alterations to their biogenic precusors (Simoneit, 2002). Biomarkers are conventionally used as indicators of biogenic, paleoenvironmental, and geochemical processes (Brassel, 1992; Imbus and Mckirdy, 1993; Mitterer, 1993; Simoneit, 1998). Biomarkers have been extensively used in petroleum geochemical studies in source rock evaluation, oil-oil or oil-source rock correlations, basin evaluation and reservoir management (Peters *et al*., 2005). Some of the biomarkers that are used in geochemical studies are briefly described below.

2.1.1 Normal and branched Alkanes

Organisms normally show odd numbers of C-atoms, due to their biosynthesis from fatty acids via enzymatic decarboxylation (Killops and Killops, 1993). n-alkanes in the range of C_{27} to C_{31} members, especially, n-C_{27} and n-C_{29} relative to the total n-alkanes are characteristic of terrestrial higher plants, where they occur as main components of plant waxes. Short-chain n-alkanes with odd-to-even predominance (OEP) in the medium molecular weight region (C_{11}-C_{17}) maximizing at n-C_{16} are presumed to originate from algae (Tissot and Welte, 1984). The influence of different contributors to the distribution of n-alkanes can be expressed in ratios. The aquatic/terrigenous ratio (ATR) of hydrocarbons (Wilkes *et al*. 1999) is a parameter used to determine the amounts of aquatic to terrigenous derived n-alkanes, i.e. short-chain to long-chain n-alkanes:

$$ATR_{HC} = \frac{(C_{15} + C_{17} + C_{19})}{C_{15} + C_{17} + C_{19} + C_{27} + C_{29} + C_{31}}$$

Values below 0.5 indicate an enhanced input of long-chain n-alkanes, i.e. organic matter derived from terrestrial sources. The ratio also depends on the maturity of the samples and is only distinctive for immature organic matter. Samples of low maturity normally show the biogenic distribution of n-alkanes. This predominance of odd- over even-numbered n-alkanes becomes less pronounced with increasing maturity of the organic matter. Due to thermal cracking, an increase of short-chain n-alkanes can be observed, leading to equal proportions of odd and even- numbered n-alkanes (Killops and Killops, 1993). The ratio of odd/even carbon numbered n-alkanes has been used in estimating the thermal maturity of fossil fuels (Bray and Evans, 1961; Scalan and Smith, 1970; Tissot *et al*., 1977). These ratios are expressed as carbon preference index, CPI (Bray and Evans, 1961) or enhanced odd-to-even predominance, OEP (Scalan and Smith, 1970). The CPI and OEP values less or greater than 1.0 indicate low thermal maturity while values around 1.0 suggest, but do not prove, that an oil or rock extract is thermally mature. The CPI or OEP values below 1.0 are unusual and typify low maturity oils or bitumen from carbonate or hypersaline environments (Peters et al., 2005). These ratios are affected by organic matter type and therefore are mostly applied with caution.

$$\boldsymbol{CPI_{LHC}} = \frac{1}{2}\left(\frac{(C_{25} + C_{27} + C_{29} + C_{31})}{(C_{24} + C_{26} + C_{28} + C_{30})} + \frac{(C_{25} + C_{27} + C_{29} + C_{31})}{(C_{26} + C_{28} + C_{30} + C_{32})}\right)$$

2.1.2 Acyclic Isoprenoids

These compounds are known constituents of plants, animal tissues and bacterial cell walls and have been reported in all classes of geologic samples (González-Vila, 1995). The phytol side chain of chlorophyll-a accounts for the widespread occurrence of acyclic isoprenoids in the biosphere. They are chemically formed from various combinations of C_5, isoprene units through three main types of linkages: head-to-tail (the most common, and include compounds such as pristane (C_{19}), phytane (C_{20}) and homologues up to C_{45}); tail-to-tail (squalane, perhydro-β-carotane, lycopane, etc); and head-to-head (C_{32}-C_{40} typical of thermophilic and other archaebacteria) (González-Vila , 1995).

Pristane (2,6,10,14-tetramethylpentadecane) (**2.1**) and phytane (2,6,10,14-tetramethylhexadecane) (**2.2**) originate from the phytol side chain of chlorophyll-a (Fig. 2.1). Pristane and phytane are the most abundant isoprenoids in the aliphatic hydrocarbon fraction (Peters and Moldowan, 1993). Whereas pristane is derived by oxidation and decarboxylation of phytol, phytane is the product of its dehydration and reduction (Fig. 2.1). The ratio of pristane to phytane is used as an indicator of the redox potential in sediments. At maturity ranges of 0.65 to 1.3% R_r, values beyond 3 indicate an input of terrestrial derived organic matter deposited under oxic conditions. Values below 0.6 indicate anoxic, hypersaline environments. Values in the range of 0.8 to 2.5 are less significant and may indicate a lacustrine or marine origin of organic matter (Peters and Moldowan, 1993). The ratio is not sensitive to organic matter of low maturities (Volkman and Maxwell, 1986). The ratio of pristane / n-C_{17} is another useful tool to characterize the source of organic matter. Values beyond 0.6 are attributed to organic matter derived from terrestrial sources whilevalues below 0.5 indicate organic material derived from marine sources (Peters and Moldowan, 1993).

Botryococcane (**2.3**) is a branched hydrocarbon derived from the unsaturated hydrocarbon , botryococcene, which can be directly associated with an organism that will only grow in a specific type of environment (Philp and Lewis, 1987). The fresh or brackish water alga, *Botryococcus braunii*, was observed to contain concentrations of botryococcane as high as 70 to 90% in the senescent phase. The unique occurrence of this compound in *botryococcus braunii* has been used by Moldowan and Seifert (1980) as evidence that certain oil deposits in Sumatra, Indonesia, were generated principally from prehistoric source material in a fresh or brackish lagoonal-type environment. *B. braunii* exists as two physiologically distinct clonal races, and as such it can contribute both unsaturated hydrocarbons, which are potential precursors of botryococcanes, and long chain n-alkanes to fresh water (lacustrine) sediments (Philp and Lewis, 1987). A study of biomarkers present in coastal bitumens from the western Otway basin in Australia revealed the presence of significant concentrations of botryococcane, for the first time, in an Australian crude oil (Mckirdy et al., 1986). Deposition of *botryococcus* blooms under anoxic or micro-oxic conditions in deep lakes was proposed to account for the waxy

character of the three main bitumen types found in the Otway basin and their botryococcane content (Philp and Lewis, 1987).

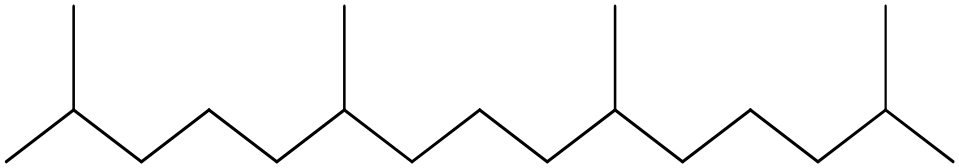

2.1

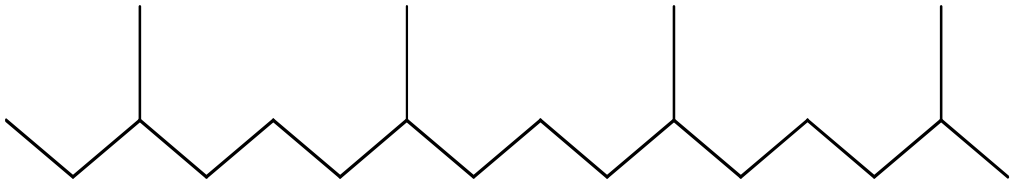

2.2

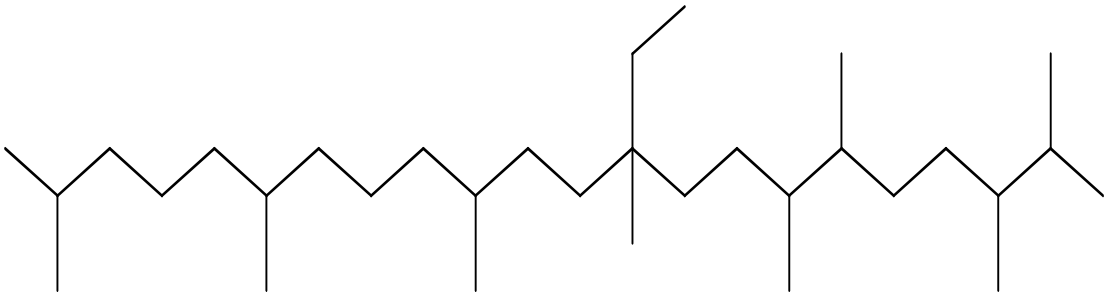

2.3

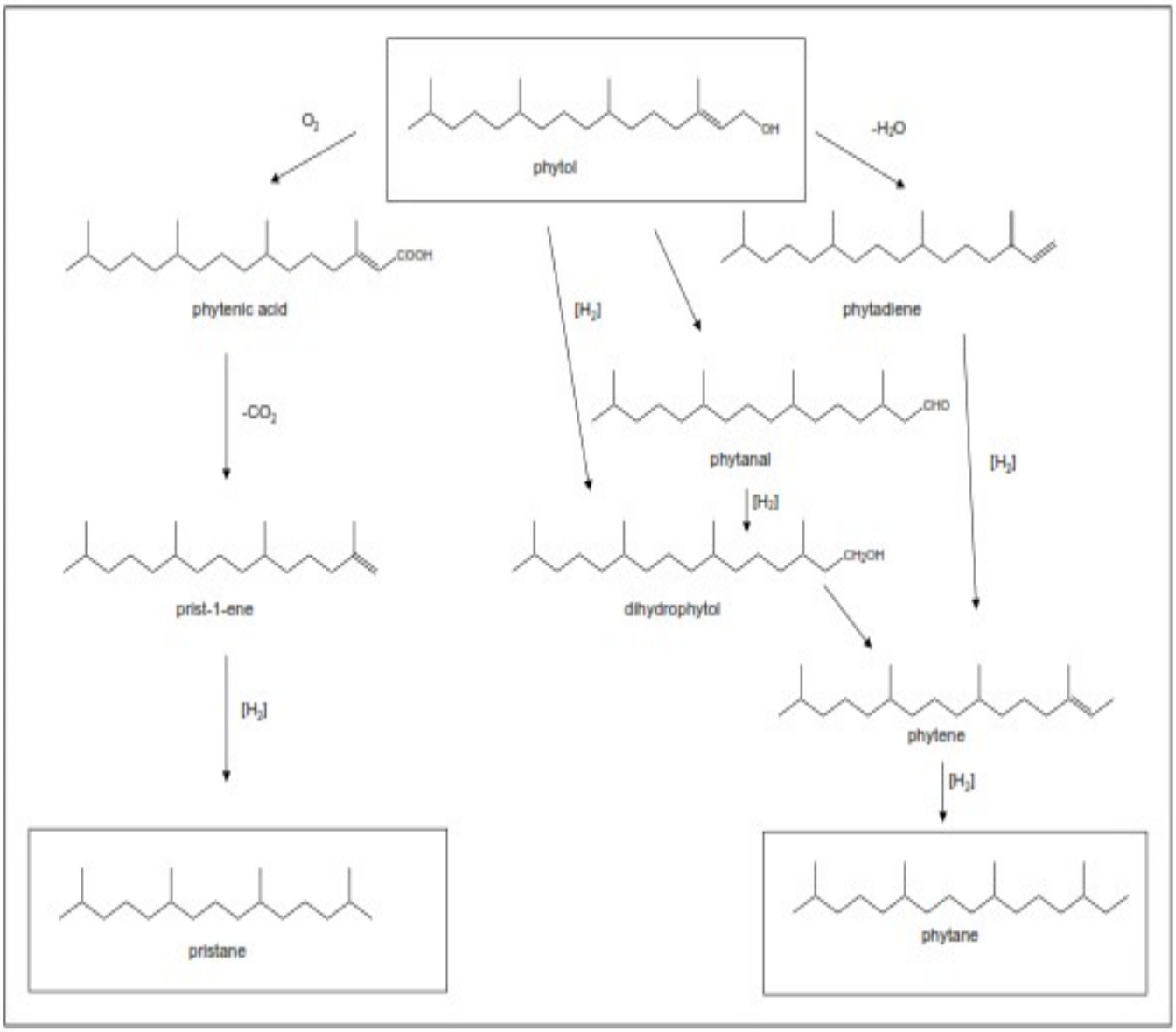

Fig.2.1: Formation of pristane and phytane from phytol

2.1.3 Triterpenoids

Triterpenoid are derived from the acyclic isoprenoid squalene, which is an ubiquitous component in organisms (Killops and Killops, 2005). Members of this group includes: tricyclic-, tetracyclic and pentacyclic. Several terpanes are also considered to be derived from prokaryotic bacteria membrane lipid (Ourisson *et al*., 1982). Few among the triterpenoids often used in biomarker studies are briefly discussed below:

2.1.3.1 Tricyclic and tetracyclic terpanes

The tricyclic terpanes (TT) (**2.4**), extensively found in source rock extracts and crude oils, occur as a pseudo-homologous series ranging from C_{19} to as high as C_{54}. They are commonly recognized up to the C_{29} compounds because the higher members of the series are often masked by hopanes in the m/z 191 mass chromatogram (Huang *et al*., 2015). The abundance of C_{22} TT and C_{27}TT is unusually low as a result of the requirement for the cleavage of twocarbon−carbon bonds to form these components (Peters *et al*., 2005). Ourisson *et al*. (1982) suggested that the tricyclic terpanes have been possibly sourced from prokaryotic cell membranes. Also, Aquino Neto *et al*. (1983) further proposed that highly abundanttricyclic terpane compositions in crude oils may be associated with a higher contribution of marine algae. The association between high concentrations of tricyclic terpanes and "tasmanite" oil shales infers a possible origin from Tasmanites algae (Simoneit *et al*., 1993; Marynowski *et al*., 2001; Revill *et al*., 1994). However, the ubiquitous occurrence in sediments and oils of varying ages demonstrates that additional sources must also exist (Peters *et al*., 2005).

The C_{23} TT is often dominant in marine sourced oils, while relatively high abundance of C_{19} TT and C_{24} tetracyclic terpane (TeT) normally indicates the input of terrigenous organic matter (Aquino Neto *et al*., 1981; Peters *et al*., 2005; Aquino Neto *et al*., 1986; Kruge *et al*., 1990; Philp and Gilbert, 1986). The relative amounts of C_{26}TT to C_{25}TT can be used to differentiate marine from lacustrine source rocks (Peters et al., 2005; Volk et al., 2005).

The relative distribution of tricyclic terpanes together with C_{24} tetracyclic terpanes (TeT) has been widely applied as molecular parameters to differentiate terrigenous versus marine organic matter input, correlate crude oils and source rock extracts, predict source

rock characteristics, and decipher source rock lithology (Peters *et al*., 2005; Philp and Gilbert, 1986; Volk *et al*., 2005; . Al-Ameri and Zumberge, 2012) However, Samuel *et al*. (2010) cautioned against such application because, globally, most oils have very similar distribution patterns of tricyclic terpanes and C_{24} TeT.

The effects of thermal maturation upon distributions of the tri- and tetracyclic terpanes have been investigated in numerous studies. C23 TT is usually the most abundant in crude oils and source rock extracts and was previously observed to become less abundant relative to the C_{21} and C_{24} compounds with increasing thermal maturity (Cassani *et al*., 1988; Ekweozor and Strausz, 1983). Data from laboratory heating experiments of a crude oil indicate an increase in C_{24} TeT relative to C_{23} TT with increasing maturation (Aquino Neto *et al*., 1981). However, Farrimond *et al*. (1999) observed an increase in the ratios of $C_{23}TT/C_{21}TT$, $C_{23}TT/C_{24}TeT$, and $C_{23}TT/C_{26}TT$ within the oil window, implying that $C_{23}TT$ is thermally more stable than other components. Huang et al. (2015) reported the continuous increase of $C_{19}TT/C_{20}TT$ ratio with maturity in palaeozoic oils from Tarim basin which suggests that $C_{19}TT$ is the most stable component during thermal evolution and additional $C_{19}TT$ may be formed from other components.

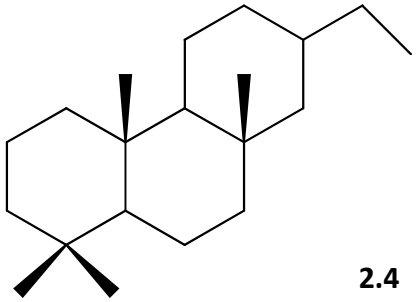

2.4

Tetracyclic terpanes (**2.5**) are usually present in a series from C_{24} to C_{27}. Differences in probable precursors of tetracyclic and tricyclic terpanes make the ratio of C_{24} tetracyclic terpane over C_{26} tricyclic terpane a source parameter (Johns, 1986). The abundant of C_{24} tetracyclic terpane in petroleum has also been reported in carbonate and evaporate source rock settings (Clark and Philp, 1989) and are widespread in most marine oils generated from mudstones to carbonate source rocks. C_{24}-C_{27} tetracyclic terpanes are often referred to as de-E-hopanes, or 17, 21-secohopanes and are suggested to be more

resistant against biodegradation and maturity effects than hopanes (Aquino Neto et al., 1983).

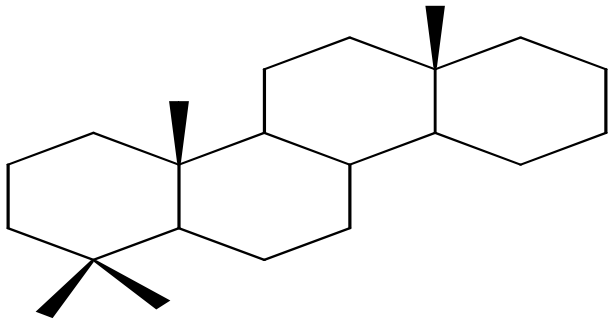

2.5

2.1.3.2 Pentacyclic triterpanes (hopane skeleton).

Hopanes (**2.6**) are group of aliphatic biomarkers consisting of a pentacyclic terpenic skeleton, incorporating a five membered E-ring . Hopanes in the range of $C_{27}$to C_{35} are present in sediments, petroleum and coals (Simoneit, 1986). They originate from natural precursors like C_{35} bacteriohopanetetrol and related C_{30} - or C_{35}-bacteriohopanoids, which are constituents of cell membranes in a great range of bacteria (Ourisson *et al*., 1979, 1987).

Hopanes and their biological precursors have been extensively studied for some decades but their transformation pathways during diagenesis and catagenesis have not been fully understood (Farrimond *et al*., 1996, 2000). They are often applied for both maturity and environmental assessment (Peters and Moldowan, 1993). High values of C_{35}-/$C_{31–35}$ hopanes (Table 2.1, HHI=homohopane index) for example indicate highly reducing marine environments (Peters and Moldowan, 1991). In non-reducing environments bacteriohopanetetrol is oxidised to C_{32}-hopanoic acid. Loss of the carboxylic group results in enhanced proportions of C_{30}- and C_{31}-hopanes. C_{31}/C_{30} (also expressed as C_{31} 22R/C_{30} hopane) hopane ratio is useful to distinguish between marine versus lacustrine source-rock depositional environments (Peters et al., 2005). Unlike crude oils from lacustrine source rocks, oils from marine shale, carbonate, and marl source rocks generally show high C_{31} 22R homohopane/C_{30} hopane ratio (C_{31}R/C_{30}>0.25). Marine and lacustrine crude oils are best distinguished using C_{30} hopane in combination with other parameters, such as the C_{30} n-propylcholestane and

C_{26}/C_{25} tricyclic terpanes, and the canonical variable from stable carbon isotope measurements (Peters *et al*., 2005).

Maturity parameters based on hopanes normally consider the relative proportions of different isomers (Table 2.1). Isomerisation of naturally occurring 22R homologues results in an equilibrium mixture of 22R- and 22S-isomers. Beyond maturities of 0.6% R_r an equilibrium value (0.6) of 22S/(22S + 22R) ratios is observed. The ratio of hopanes/(hopanes + moretanes) (Table 2.1) can also be used as maturity parameter. At elevated maturity ranges the relative proportions of moretanes show a decrease. Typically, C_{31}–or C_{32}-homohopane 22S/(22S + 22R) ratios are used to assess the maturity status of oils and source rock extracts.The 22S/(22S + 22R) ratio rises from 0 to ~0.6 (0.57–0.62 =equilibrium) (Seifert and Moldowan, 1980) during maturation. Samples showing 22S/(22S + 22R) ratios in the range 0.50–0.54 have barely entered oil generation, while ratios in the range 0.57–0.62 indicate that the main phase of oil generation has been reached or surpassed. Some oils exposed to very mild thermal stress apparently can have 22S/(22S +22R) ratios below 0.50.

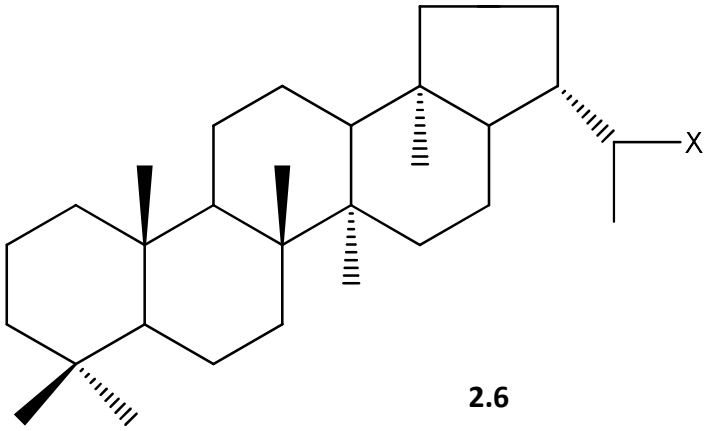

2.6

X= H; 30-norhopane (C29 Hopane
X= CH_3; C_{30} hopane
X=C_2H_5; C_{31} homohopane
X=C_3H_7; C_{32} homohopane
X=C_4H_9; C_{33} homohopane
X=C_5H_{11};C_{34} homohopane
X=C_6H_{13};C_{35} homohopane

2.1.3.3 Pentacyclic triterpapanes (non-hopanoid skeleton)

The biomarkers in this category include oleananes (**2.8**), Lupanes (**2.9**), fernane, gammacerane (**2.10**) and ursanes (**2.11**). Lupane, oleanane, fernane and ursane biomarkers which are characteristic of plant triterpenoids have been frequently found in coals and oils derived from terrigenous source materials (González-Vila , 1995). Their precursors are widely distributed in higher plants. C_{30} bicadinanes found in oils have been

shown to be characteristic cracking products of angiosperm fossil resins. The 18a(H)-oleanane has been observed in a number of deltaic sediments and crude oils related to them (Zumberge, 1987; Mello *et al*., 1988; Ekweozor *et al*., 1979; Ekweozor and Udo, 1988). The biogenic precursors of oleanane are presumed to be oleanene triterpenoids such as β-amyrin (**2.7**), which are associated with highly specialized terrigenous plants (Ekweozor *et al*., 1979; Ekweozor and Udo, 1988; Alberdi and Lopez, 2000).

Oleananes (**2.8**) are normally found in sediments younger than Late Cretaceous. It is age restricted and could therefore be used as indicator of geological age (Nytoft et al., 2002; Ozcelik and Altunsoy, 2005). Oleanane occurs in two isomeric forms; 18α(H)-oleanane and 18β(H)-oleanane. Their relative amount changes with the level of thermal maturation, and hence can be used as indicators of maturity (Ekweozor and Telnas, 1990). Oleanane index (oleanane/C_{30} hopane) has also been used to indicate the input of terrestrial and marine into source rock (Waples and Machiara, 1990).

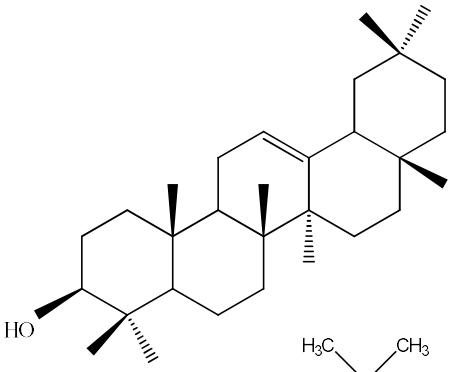

2.7

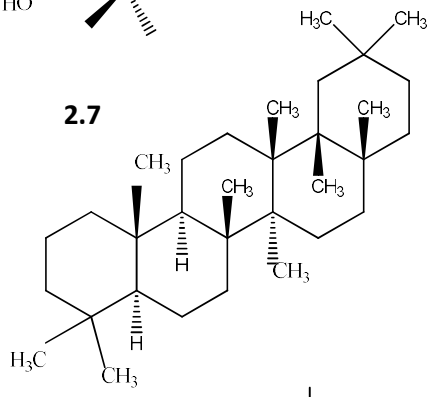

2.8

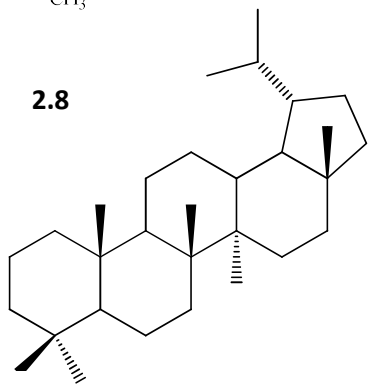

2.9

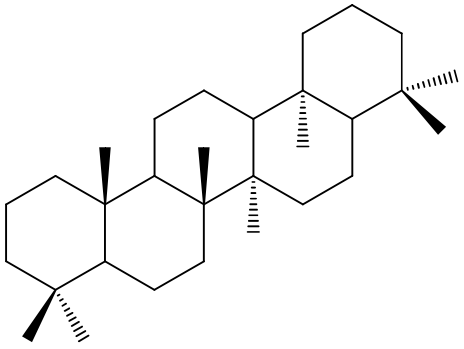

2.10

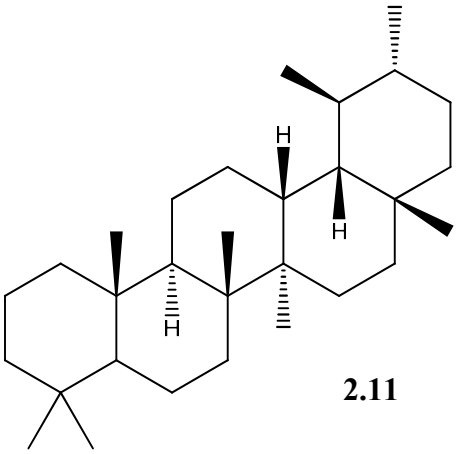

2.11

Gammacerane (**2.10**) was first reported to occur in extracts of Green River Shale (Henderson *et al*., 1969). The origin of gammaceraneoften used as indicator for salinity, is still unclear. TetrahymanoI, the only pentacyclic triterpenoid found in protozoa and fungus, is the only known potentiaI biological precursor of gammacerane (Venkatesan, 1988). Diagenetic conversion of tetrahymanol to gammacerane most likely proceeds by dehydration to formgammacer-2-ene, followed by hydrogenation. Gammacerane may also arise by sulfurization and subsequent cleavage of tetrahymanol (Sinninghe Damste et al., 1995). Gammacerane is present in many sampIes from various environments and its use as a biomarker for salinity is not based on its occurrence, but rather on its relative abundance (Mello *et al*., 1988). Gammacerane indicates a stratified water column in marine and non-marine source-rock depositional environments (Sinninghe Damste *et al*., 1995), commonly resulting from hypersalinity at depth. In addition to β-carotane and related carotenoids, gammacerane is a major biomarker in many lacustrine oils and bitumens, including the Green River marl and oils from China (Moldowan *et al*., 1985; Jiang Zhusheng and Fowler, 1986; FuJiamo *et al*., 1986; FuJiamo *et al*., 1988; Brassell *et al*., 1988; Grice *et al*., 1998). Gammacerane is also abundant in certain marine crude oils from carbonate-evaporite source rocks (Rohrback, 1983; Moldowan *et al*., 1985; Mello *et al*., 1988; Moldowan *et al*., 1991). Gammacerane is useful to distinguish petroleum families. For example, Poole and Claypool (1984) used gammacerane to distinguish oils and bitumens from different source rocks in the Great Basin.

2.1.4 Steranes

Steranes (**2.12**), commonly found in mature sediments and crude oils are derived via diagenesis from sterols which are widely dispersed in plants and micro-organisms (González-Vila , 1995). Sterols are the natural precursors of steranes and diasteranes (de Leeuw and Baas , 1986). During diagenesiss, sterols undergo transformations that result in the formation of steranes and diasteranes (Brassell, 1985). The most likely direct precursors of steranes and diasteranes are sterenes and diasterenes, respectively (de Leeuw and Baas, 1986). The saturated isomers are the result of hydrogenation. The relative proportions of C_{27}-, C_{28}- and C_{29}-steranes and diasteranes to some extend provide information on the origin of the organic matter (Peters and Moldowan, 1993). Whereas C_{29}-steranes are suggested to predominantly originate from higher plants, C_{27} and C_{28}-steranes are supposed to originate from phytoplankton (Huang and Menschein, 1979). However, significant concentrations of C_{29} steranes have been observed in oils and source rocks thought to be of predominantly marine origin (Palacas *et al*., 1984; Walters and Cassa, 1985). Similarly, an interesting paper by Grantham (1986) provided evidence that the C_{29} steranes of crude oils may not always be derived from terrestrial source materials.

During diagenesis and catagenesis isomerisation at the C-5, C-14, C-17 and C-20 atoms of the sterane skeleton results in an equilibrium mixture of ααα*R*, ααα*S*, αββ*R*, αββ*S*-steranes of about 1:1:3:3 (Peters and Moldowan, 1993). Isomerization at C-20 in the C_{29} 5α,14α,17α(H)steranes causes 20S/(20S + 20R) ratio to rise from 0 to ~0.5 (0.52–0.55 = equilibrium) with increasing thermal maturity (Seifert and Moldowan, 1986). Similarly, isomerization at C-14 and C-17 in the C_{29} 20S and 20R regular steranes causes an increase in ββ/(αα + ββ) from near-zero values to ~0.7 (0.67–0.71 = equilibrium) with increasing maturity (Seifert and Moldowan, 1986). This ratio appears to be independent of source organic matter input and somewhat slower to reach equilibrium than 20S/(20S + 20R), thus making it effective at higher levels of maturity (Peters *et al*., 2005). Plots of ββ/(αα + ββ) versus 20S/(20S + 20R) for the C_{29} steranes are particularly effective in determining the thermal maturity of source rocks and oils (Seifert and Moldowan, 1986).

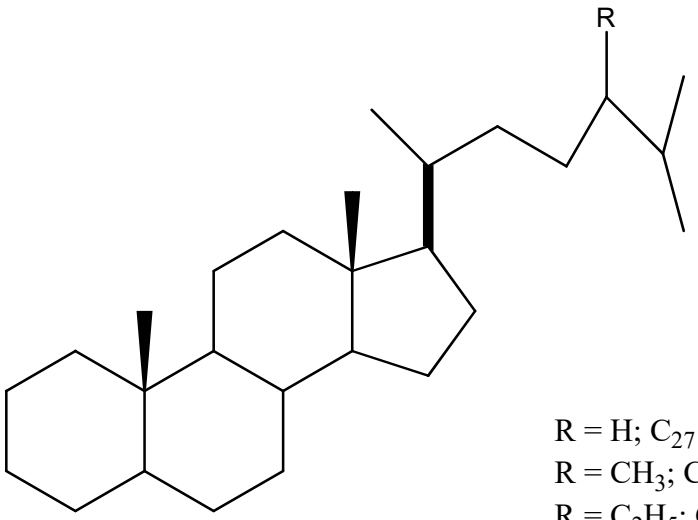

R = H; C_{27} sterane
R = CH_3; C_{28} sterane
R = C_2H_5; C_{29} sterane

2.12

2.1.5 Polycyclic Aromatic Hydrocarbons (PAHS)

Aromatic hydrocarbons are important constituents of petroleum and extracts of both recent and ancient sediments (Blumer and Youngblood, 1975; Radke, 1987; Radke *et al*., 2000; Radke *et al*., 2001). Polycyclic aromatic hydrocarbons (PAHs) are not synthesized in living organisms and almost absent in natural organic matter (Hase and Hites, 1976). The majority of PAHs in petroleum are the products of complex chemical transformations of naphthenic and/or olefinic biological ancestors during diagenesis and catagenesis (Radke, 1987). The biological origin of a given PAHs is obvious only in favorable conditions, where a characteristic part of the naphthenic structure has been preserved unchanged (Asif, 2010). Distributions of PAHs are potentially useful in many areas of applied petroleum geochemistry. Abundance of certain aromatic hydrocarbons in crude oils and sediments such as 1,2,5-trimethylnaphthalene (1,2,5-TMN), 1,2,5,6 tetramethylnaphthalene (1,2,5,6-TeMN), 9-methylphenanthrene (9-MP), 1,7-dimethylphenanthrene (1,7-DMP) originate from diterpenoid and triterpenoid natural products (Radke, 1987; Alexander et al, 1992). The most useful application of aromatic hydrocarbons is in evolution of thermal maturity of organic matter (Alexander et al., 1985; Radke et al., 1986).

Naphthalene (**2.13**) and its alkylated derivatives are common constituents of fossil fuels (Bastow et al., 1998, 2000; Van Aarssen et al., 1999). Terpenoids derived from terrestrial plants are the major precursors for methylated naphthalenes (Sivan *et al*., 2008). Their distributions in the geosphere are highly variable as they are controlled by the effects of source, thermal stress and biodegradation (Sivan *et al*., 2008). The ratios often computed from the methylated naphthalenes are considered to be a reflection of the increase in the abundance of the stable isomers relative to the less stable isomers and these are determined by 1,2-methyl shift and methyl transfer in the naphthalene carbon skeleton (Van Aarssen *et al*., 1999). Several molecular maturity parameters involving methylated naphthalenes have been developed over the years and used to assess maturities of crude oils (Alexander *et al*., 1985; Radke *et al*., 1990, 1994; Bastow *et al*., 1998).

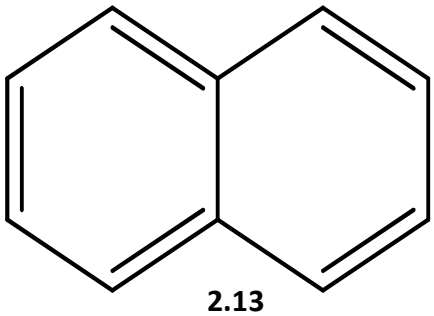

2.13

Phenanthrene (**2.14**) maturity parameters rely on the greater stability of 3-methylphenanthrene and 2-mehtylphenanthrene relative to 9-methylphenanthrene and 1-methylphenanthrene (Radke and Welte, 1983). The Methylphenanthrene Index (MPI) has been widely used as molecular maturity parameters (Radke and Welte, 1983; Radke, 1988). This parameter relies on a shift with maturity in the methylphenanthrene distribution towards a preponderance of more thermally stable β-type isomers. MPI-1 (1.5 (3-MP + 2-MP)/(P + 1-MP +9-MP)) has been used to assess maturity effect in oils from Sumatra basin, Indonesia (Hwang *et al*., 2002).

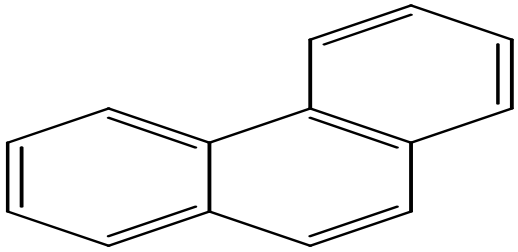

2.14

MPI-1 may be applied to evaluate the equivalent vitrinite reflectance value (%VRc) for crude oils as a result of its linear relationship with vitrinite relectance throughout conventional oil window (Radke and Welte, 1983). The addition of phenanthrene (parent compound) in the ratio is intended to compensate for facies-dependent variations in the degree of phenanthrene alkylation (Radke *et al*., 1982). The ratio 9-MP/1-MP has been successfully applied for biodegradation evaluation (Bennett *et al*., 2013).

The relative abundance of triaromatic steroids (**2.15**) (TAS) are influenced by multiple factors and thus can be used as indicators for differentsource inputs and depositional environments. C_{28}-TAS is usually found in high abundant in organic matter from fresh water environment while C_{26}-TAS is in high abundant inorganic matter from saline and brackish water environments (Ling and Zhihuan2009; Xiangchun *et al*., 2011). The ratio S/(S + R) C_{28}-TAS have been reported to be a potential maturity indicator (Xiangchun *et al*., 2011; Asif and Fazeelat, 2012).

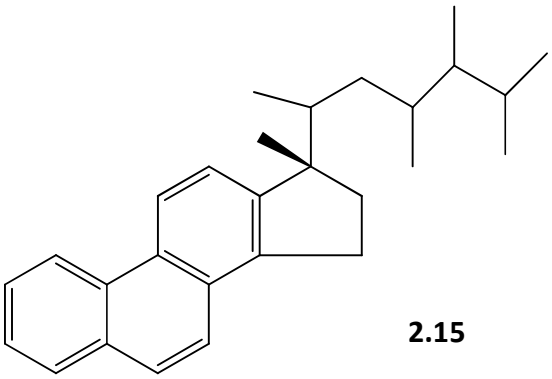

2.15

2.2 Nitrogen, Sulphur and Oxygen (NSO)- containing Compounds

2.2.1 Aromatic Sulphur Compounds

Sulfur (S) is the most abundant hetero-element in all types of sedimentary organic matter. The sulfate reducing bacteria is responsible for the production of sulphur at the water/sediment interface and results in its incorporation at early stage of diagenesis through abiotic reactions (Eglinton *et al*, 1994; Wakeham *et al*., 1995). The mechanism of sulphur incorporation into the organic matter depends on the nature of sulfurized functional groups and can be incorporated via intra- and intermolecular reactions (Sinninghe Damste *et al*., 1988). The former process results in the formation of cyclic alkyl sulfides (such asthiolanes, thianes and thiophenes (Brassell *et al*. 1986) while intermolecular sulfurization leads to the formation of (poly) sulfide linkages between alkyl chains (Richnow *et al*., 1992; Schaeffer *et al*, 1995). The occurrence of thiophenes in the S-rich kerogen pyrolysates does not necessarily reflect a ubiquitous contribution of thiophenic moieties to kerogen structure. However, such aromatic sulfur compounds may originate, at least partly, from secondary transformation of (poly) sulfide-containing moieties (Sinninghe Damste *et al*., 1990). In fact, heating (poly) sulfide-linked macromolecules results in the rapid formation of thiophenic compounds (Krein,and Aizenshtat, 1994; Schouten *et al*., 1994; Tomic *et al*., 1995). Secondary thermal reactions of (poly) sulfide-bound linear carbon skeletons were observed upon kerogen pyrolysis (Sinninghe Damste *et al*., 1998). These findings reflect the importance of incorporated sulphur in kerogen for the formation of sulfur compounds.

Dibenzothiophenes (DBTs) (**2.16**) and benzo[b]naphthothiophenes (BNTs) (**2.17 to 2.19**) are the main sulphur-containing heterocyclic aromatic compounds in crude oils and sedimentary rock extracts. A specific biological source of dibenzothiophene and alkyldibenzothiophenes is unknown. Indeed it is generally accepted that the major part of the organically-bound sulphur is generated in sediments randomly (Arpino *et al*., 1987; Sinninghe Damste and de Leeuw, 1990). It has been suggested that alkyldibenzothiophenes are formed via reactions of biomolecules with reduced sulphur (i.e. hydrogen sulphide and polysulphides under anoxic conditions and low concentrations of iron (Orr and Sinninghe Damste, 1990; Hughes *et al*., 1995). Therefore, the formation of alkyldibenzothiophenes is supposed to be controlled by environmental

factors, i.e. the availability of reduced sulphur in sediments. The availability of reduced sulphur in turn is related to the activity of sulphate-reducing bacteria and limited by the availability of sulphate as an electron acceptor for microbial oxidation of organic matter.

High proportions of dibenzothiophene and alkyldibenzothiophenes are characteristic for marine shales and carbonates, whereas their presence in continental facies is generally low (Radke *et al*., 1991). This relationship between alkyldibenzothiophene concentrations and organic facies is expressed in the ratio of dibenzothiophene to phenanthrene (Radke *et al*., 1991; Hughes *et al*., 1995). Ratios of dibenzothiophene to phenanthrene in the range of 0.06 to 0.2 are typical for coals, i.e. terrestrial organic matter (Requejo, 1994). The relative proportions of individual alkyldibenzothiophenes in contrast are suggested to depend on the maturity of organic matter. A relative increase of 4-methyldibenzothiophene during maturation is attributed to its higher thermal stability (Radke *et al*., 1986). The Methyldibenzothiophene Ratios (MDR and MDR^1) are based on a decrease of 1-methyldibenzothiophene with increasing maturity and accompanied by an increase of 4-methyldibenzothiophene. Dzou *et al*. (1995) found a constant amount of 1-methyldibenzothiophene within wide maturity ranges, and an increase of 4-methyldibenzothiophene with increasing maturityfor a set of Carboniferous coals and vitrinite concentrates. The authors therefore suggested that isomerisation reactions play a minor role in controlling the distribution of methyldibenzothiophenes. In contrast Chakhmakhchev *et al*. (1997) found no dependence of the MDR on the vitrinite reflectancesfor a set of oil and condensate samples from various geological periods. An influence of depositional environment and lithology on the distribution of alkyldibenzothiophenes below maturities of 1.35% R_r, especially for coals may account for these observations (Radke *et al*., 2000; Dzou *et al*., 1995). The ethyldibenzothiophene ratio (EDR,4,6-DMDBT/4-EDBT + 4,6-DMDBT) has also been applied to estimate the maturity of organic matter.

Recently, aromatic sulfur compounds such as dibenzothiophenes (DBTs) and benzo[b]naphthothiopnenes (BNTs) have been used to study oil migration based on the fact that they have similar structures and chemical properties like carbazoles and benzocarbazoles and that they are constrained by the same factors (Wang *et al*, 2004, Li *et al*., 2008, 2014, Fang *et al*., 2016). Li *et al*. (2014) proposed

[2,1]BNT/([2,1]BNT+[1,2]BNT) ratio as a potential molecular marker for tracing oil migration and observed that the ratio and the total concentrations of DBTs decreased with increasing migration distance in oil from Tahe field, Tarim basin China. It has been shown that the ratio of [2,1]BNT/([2,1]BNT+[1,2]BNT) (BNT ratio) exhibits a generally positive linear correlation with benzo[a]carbazole/(benzo[a]carbazole + benzo[c] carbazole which indicates that the relative concentration of the benzo[b]naphthothiophene (BNT) isomers may also be constrained by the same migration fractionation effects exerted on the benzocarbazole isomers (Li *et al*., 2014). Similarly, Fang *et al*. (2016) and Yang *et al*. (2016) have successfully applied [2,1]BNT/([2,1]BNT+[1,2]BNT) ratio and alkyldibenzothiophene parameters to trace the oil filling pathways in the carbonate reservoir of the Tarim Basin, China.

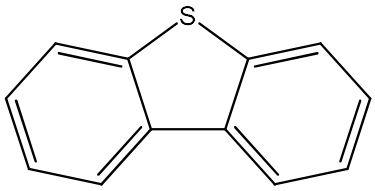

2.16

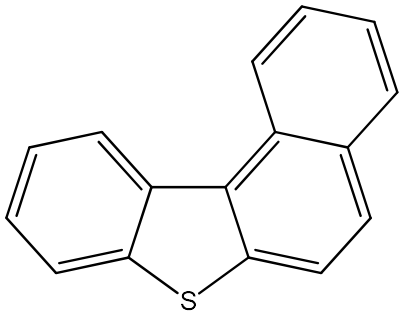

2.17

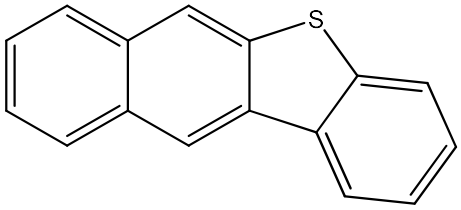

2.18

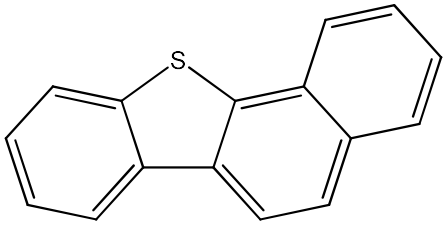

2.19

2.2.2 Oxygen-containing compounds

Oxygen containing compounds commonly found in geological samples include dibenzofurans, dibenzo[b]naphthofurans, fluoren-9-ones, xanthones, naphthaldehydes and acetylnaphthalenes**.** Dibenzofuran (DBF) (**2.20**), its alkylated homologues, and

benzo[b]naphthofurans (BNFs) (**2.21 to 2.23**) are important oxygen heterocyclic aromatic compounds in oils, coals, sediment extracts, and tar deposits. The origin of DBFs in oil and sedimentary organic matter remains a controversial issue. Previous studies suggest that DBFs may originate from dehydrated and condensed polysaccharides (Sephton *et al*., 1999; Pastorova et al., 1994) or from the oxidative coupling of phenols (Born *et al*., 1989). High abundances of DBF, DBT, and biphenyl in Permian rocks (East Greenland) probably derived from phenolic compounds of lignin of the woody plants (Fenton *et al.*, 2007). The majority of natural products related to dibenzofuran are metabolites of lichens or higher fungi. The lichen dibenzofurans appear to be formed by carbon−carbon oxidative coupling of orsellinic acid and its homologues (Sargent *et al*., 1984). Thus, Radke *et al*.(2000) proposed that DBFs in crude oil and sediment extracts are potential biomarkers for lichens. However, further work is needed to confirm the precursor-product relationship between lichens and DBFs (Li and Ellis, 2015).

Simulation experiments and geological observations have shown that biphenyl and oxygen can form dibenzofuran (Asif, 2010). Similarly, methyl-substituted biphenyls can react to yield the corresponding methylated DBFs. The derivatives of biphenyl are commonly used as reactants to synthesize dibenzofurans in the laboratory (Sargent et al., 1984). More geological evidence and laboratory experiments are still needed to fully understand the origin and evolution of DBFs in the geosphere. Dibenzofuran and its alkylated homologues (collectively abbreviated as DBFs) and benzo[b]naphthofurans have also been applied as important molecular markers in organic geochemistry. The occurrence and distribution of DBFs are mainly dependent on the source rock type and/or depositional environment (Fan *et al*., 1990; Fan *et al*., 1991; Radke *et al*., 2000). DBFs seem to prevail in freshwater source rocks, terrestrial oils, and coals (Fan *et al*., 1990, 1991; Li *et al*., 2013; Asif and Fazeelat, 2012), whereas their sulfur-heterocyclic counterparts dibenzothiophenes (DBTs) are more abundant in marine shales and carbonates (Li *et al*., 2013; Hughes, 1984; Hughes *et al*., 1995).The relative abundance of alkyldibenzothiophene (ADBT) with respect to alkyldibenzofuran (ADBF) has been proposed to distinguish depositional environments (Radke *et al*., 2000; Sephton *et al*., 1999; Kruge, 2000). Recently, researchers also observed that the absolute concentrations of DBFs in petroleum are also affected by secondary migration processes (Li *et al*., 2011,

2018). Thus, the DBFs in petroleum are potential molecular indices to indicate petroleum migration distances and filling pathways (Li *et al*, 2011). More recently, Li and Ellis (2015) identified benzo[b]naphthofurans (benzo[b]naphtho[2,1-d]furan (BN21F), benzo[b]naphtho[1,2-d]furan (BN12F) and benzo[b]naphtho[2,3-d]furan (BN23F)) in crude oils and rock extracts by co-injection of authentic standards and proposed that this ratio may be a potential molecular geochemical parameter to indicate oil migration pathways and distances.

Low molecular weight (C_0-C_3) alkylphenols are ubiquitous constituents of crude oils and formation waters of petroleum systems (Loppopo *et al*., 1992; Bennett *et al*., 1996) Alkylphenols are both oil- and water-soluble and their absolute and relative abundances in oils and associated formation waters are predictably determined by their partition coefficients, and the degree of oil/water interaction in the subsurface. As a result, alkylphenols have been proposed as potential parameters for delineating secondary migration pathways (Larter *et al*., 1996; Bennett and Larter, 1997; Taylor *et al*., 1997, 2001). Galimberti *et al*. (2000) have successfully defined a molecular migration index (MMI), based on relative abundance of phenol and alkylphenol.

A review of the occurrence of carboxylic acids in oils and sediments was reported by Seifert (1975). Jaffe and Gardinali (1990) described the generation and maturation of carboxylic acids in ancient sediments from the Maracaibo Basin, and these compounds have been proposed as indicators for crude oils biodegradation and migration (Jaffe and Gallardo, 1993).

Extended saturate and monoaromatic tricyclic terpenoid carboxylic acids have been found in Tasmanian tasmanite (Azevedo *et al*., 1994). Barakat and Rullkotter (1995) reported the occurrence of extractable and bound fatty acids in sediments from the Nordlinger Ries in Germany. Chromans have been identified in a number of sediment extracts and oils ranging in age from Pleistocene to Permian and it has been suggested that these compounds may be useful as palaeoenvironmental indicators (Sinninghe Damste *et al*., 1987, 1993).

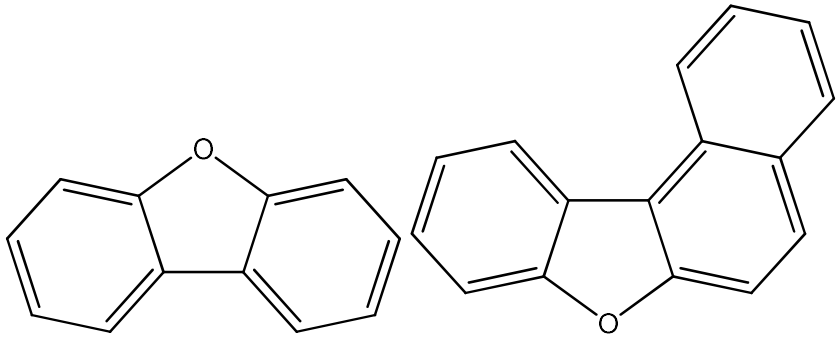

2.202.21

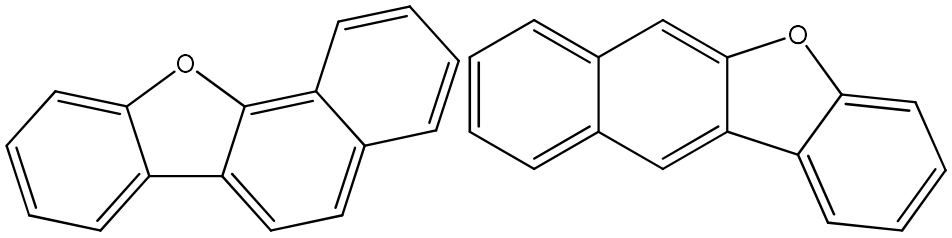

2.22 2.23

2.2.3Nitrogen-containing Compounds

Pyrrolic nitrogen compounds such as carbazoles (**2.24**) and alkylcarbazoles are constituents of crude oils and source rock extracts (Helm*et al*., 1960; Dorbon *et al*., 1984; Bakel and Philp, 1990; Li *et al*., 1997; Horsfield *et al*., 1998). The primary discussion on these compounds in recent years is based on their potential as indicators of maturity and primary/ secondary migration (Li *et al*., 1994, 1995; Horsfield *et al*., 1998; Clegg *et al*., 1998). Unlike most petroleum hydrocarbon compounds, polar species such as carbazoles and benzocarbazoles (**2.25 to 2.27**) do not rapidly get equilibrated over a few tens of meters in the reservoir petroleum columns (England, 1990). These compounds are capable of interacting with the surrounding environments via hydrogen and/or ionic bonding (Li *et al*., 1995). The consequential effect is the differential fractionation of these compounds within the geosphere. In general, the concentrations of the pyrrolic nitrogen compounds often show a decrease with increasing oil migration distance (Later *et al*., 1996; Hwang *et al*., 2002). This is usually accompany with enrichment of N-H shielded isomers to N-H exposed isomers, higher to lower molecular weight homologues,

alkylcarbazoles to alkylbenzocarbazoles, and benzo[c]carbazole to benzo[a]carbazole (Hwang *et al*., 2002). The ratio (benzo[a]carbazole/benzo[a]carbazole+benzo[c]carbazole has been proposed as migration distance indicator (Larter *et al*., 1996). It has been suggested that carbazoles might originate from alkaloids (Snyder, 1965) which are common constituents of blue-green algae (Cardellina *et al*., 1979) and terrestrial plants (Kapil, 1971; Hesse, 1974). This origin has been discussed in detail by Li *et al*. (1995), and concluded that alkaloids are not the major source of carbazoles. They pointed out that proteins and plant pigments might be a potential biological source. In contrast Dorbon *et al*. (1984) reported that alkaloids are not likely the precursors of alkylcarbazoles, but suggested a complex formation mechanism involving the condensation of ammonia or low molecular weight amines.

Carbazoles distributions have been used to differentiate two different facies of transgressive and regressive events in the carbonate source rocks of the Lower and Upper Keg River Formations (Clegg *et al*. (1997). The predominance of low molecular weight homologues (C_1- and C_2-carbazoles) relative to the high molecular weight compounds (C_3 to C_5-carbazoles) have been reported in the source rock from non-marine depositional environments in Qaidam and Turpan basin, Northwest China (Zhang *et al*., 2008). An increase of alkylcarbazoles with increasing thermal maturity has been observed for Posidonia Shale bitumen from Hils Syncline, northern Germany and crude oils from Thithonian source rocks in the Gulf of Mexico (Horsfield *et al*., 1998; Clegg *et al*., 1998). However, the concentrations of alkylcarbazoles do not generally increase with maturity. In the Thithonian source rocks a decrease up to maturities of 0.81% R_r, followed by an increase at higher maturity ranges up to 1.09% R_r has been observed (Horsfield *et al*., 1998; Clegg *et al*., 1998).

Although several maturity parameters based on the isomeric distribution of alkylcarbazoles have been established (Li *et al*., 1997; Clegg *et al*., 1997, 1998) but none of the parameters showed an unambiguous trend. Recently, Bakr and Wilkes (2002) suggested that the ratio of

$$\frac{(1{,}8-dimethylcarbazole)}{(1{,}8-dimethylcarbazole\ +1-ethylcarbazole)}$$

may depend on the environmental conditions. In crude oils from Egypt, the authors found a slight correlation between this ratio and the pristane/phytane-ratio.

Recently, Faboya *et al.* (2014, 2015) observed that the relative concentrations of carbazoles increased with increasing maturity in Niger Delta source rocks and crude oils and suggested that the increase of the carbazoles concentrations with increasing maturity indicate lateral hydrocarbon migration in the studied fields and that carbazoles may be a potential migration indicator in Niger Delta basin.

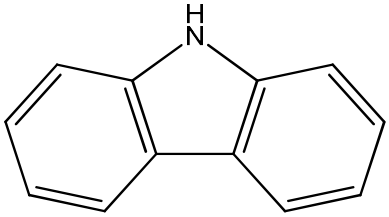

2.24

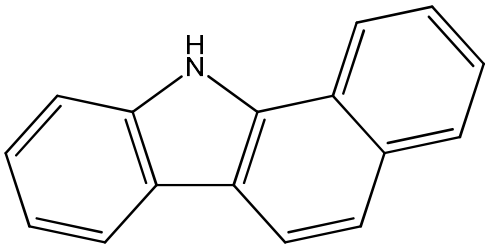

2.25

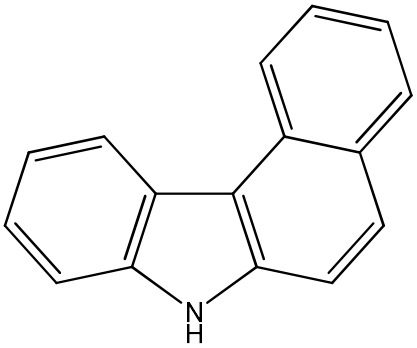

2.26

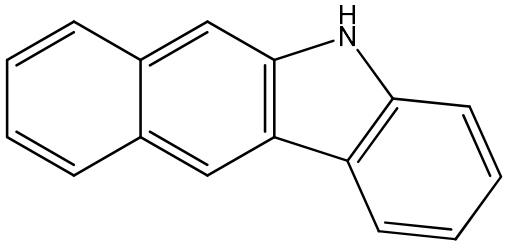

2.27

2.3 Isotope Geochemistry

Isotope measurements combined with the study of biomarkers, are common and very efficient approach in modern organic geochemistry. Isotope analyses of individual compounds have been applied for oil–oil and oil–source rock correlations and in the elucidation of petroleum generation mechanism (Hayes et al., 1990; Rooney et al., 1998). Several workers have shown that structures and isotope compositions of biomarkers provides valuable genetic information (Hayes *et al*.,1990; Grice *et al*., 2001; Lu *et al*.,

2003). The isotopic composition of the molecule can indicate parent organisms and in turn, reveal the carbon source utilized by the producer hence its position within the ancient ecosystem (Hayes, 1993). Isotopic fractionation occurs in nature during chemical, biochemicaland physical processes depending on the strength of bonds (Hoefs, 1987). Stable isotope composition is expressed as a ratio calculated by the δ (delta) notation and is expressed in per mil (‰):

$$\delta \text{ sample} = [(R_{sample} - R_{standard})/R_{standard}] \times 1000 \text{ ‰}$$

R connotes the isotopic abundance ratios, such as $^{13}C/^{12}C$, $^{18}O/^{16}O$, $^{34}S/^{32}S$, $^{15}N/^{14}N$, or D/H ($^{2}H/^{1}H$). The δ value for carbon for instance, is a convenient means to describe small variations in the relative abundance of the ^{13}C in organic matter. A negative δ value indicates that the sample is depleted in the heavy isotope relative to the standard while a positive value implies that the sample is isotopically enriched in the heavy isotope relative to the standard. For carbon, the terms ‘’light and heavy’’ are often avoided and the use of ‘’^{13}C-depleted’’ and ‘’^{13}C-enriched’’ are respectively preferred to describe relative isotope composition (Peters *et al*., 2005).

2.3.1 Stable Carbon Isotopes

Carbon isotope geochemistry has been extensively used to understand the processes that lead to the generation, maturation, migration and accumulation of oil and gas in a sedimentary basin. Of its several important applications, one has been the wide usage of stable carbon isotopic ratios in establishing the correlation between the source and the products related with gaseous hydrocarbons, as the natural mobility and alterations involved can mask the precise understanding of their origin and occurrence. Carbon isotopic and compositional ratios of light hydrocarbon gases, particularly methane, are utilized for the identification of varied locations or origins of diverse potential sources (Benner *et al.,* 1987; Hunt, 1996; Sofer, 1984; Tissot and Welte, 1978; Hayes *et al*.,1990; Grice *et al*., 2001; Lu *et al*., 2003). Also, it has been shown that n-alkane distribution in kerogen using conventional geochemical tools, without detailed stable carbon isotope data can sometimes lead to erroneous interpretations of the precursors contributing to the kerogen even with samples containing abundant biomarkers (Audino *et al*., 2002).

Bulk stable carbon isotope analysis involves measurement of the stable isotopic composition of the total carbon in a sample. Thus, it is used to determine the isotopic composition of all compounds in the whole mixture and consequently only gives an average value for the entire complex mixture (Sofer, 1984). Sofer (1984) used the bulk carbon isotopic ratios of aromatics againstsaturated fractions to separate oil families into waxy (terrigenous) and non-waxy (marine) oil types. This technique is the useful for correlation studies, but the source typing is less accurate. Chung *et al*. (1992) classified 621 post-Ordovician marine oils into four groupsin terms of their depositional environment and the age of their source rocks, on the basis of $\delta^{13}C$ distribution in conjunction with pristane/phytane ratios and sulfur contents. Andrusevich *et al*. (1998) reported bulk $\delta^{13}C$ values of the saturate and aromatic fractions of 514 oils and found that both fractions become enriched in ^{13}C values towards recenttimescales. In contrast to bulk stable carbon isotope analysis, carbon isotope specific analysis involves the measurement of $^{13}C/^{12}C$ of individual organic components in complex mixtures of petroleum and organic extracts from sedimentary materials (Matthews and Hayes, 1978). It has been reported that the distribution pattern of individual n-alkane carbon isotopes in different oil should reflect the variations in organic source character(Murray *et al*., 1994; Yangming *et al*., 2005), with terrestrial organic matter often displays depleted (light) values of n-alkane carbon isotopes (Murray *et al*., 1994; Yangming *et al*., 2005) while marine oils are characterized by enriched (heavy) values of carbon isotopes (Samuel *et al*., 2009).

In the subsurface, maturation has been reported to affect the stable isotopic composition of petroleum (Clayton, 1991). $\delta^{13}C$ values of kerogen, source rock extracts and crude oils, and their associated fractions, and individual compounds (e.g. n-alkanes) have been found to increase with thermal maturity. The enrichment of ^{13}C in kerogen is thought to be a result of the thermal release of isotopically lighter products (Clayton, 1991). Secondary processes such as biodegradation have been reported to alter$\delta^{13}C$ values. Biodegradation can lead to an enrichment of ^{13}C in residual compounds, with the level of enrichment gradually decreasing with increasing molecular weight (George *et al*., 2002; Sun *et al*., 2005; Samuel *et al*., 2009).

2.3.2 Oxygen Isotopes

Oxygen has three stable isotopes, ^{16}O, ^{17}O, and ^{18}O. Oxygen ratios are measured relative to Vienna Standard Mean Ocean Water (VSMOW) or Vienna Pee Dee Belemnite (VPDB). Variations in oxygen isotope ratios are used to track both water movement and paleoclimate, (James, 2002) and atmospheric gases such as ozone and carbon dioxide (Brenninkmeijer et al., 2003).Typically, the VPDB oxygen reference is used for paleoclimate, while VSMOW is used for most other applications (James, 2002). Oxygen isotopes appear in anomalous ratios in atmospheric ozone, resulting from mass-independent fractionation(James, 2002).Oxygen isotope ratios in fossilized foraminifera have been used to deduce the temperature of ancient seas (Emiliani and Edwards, 1953).

2.3.3 Sulphur Isotopes

Sulphur isotopes have been used for the correlation of source rocks and oils not altered by thermochemical sulfate reduction (TSR)in a rapidly buried basin (Thode, 1981; Orr, 1986; Cai *et al*., 2009a,b; Cai *et al*., 2015). In such a basin, hydrocarbons are generated rapidly and peak oil is likely to occur undersemi-closed to closed conditions. This feature, along with high H_2S solubility and rapid sulfur isotope homogenization, are believed to result in small differences (up to 2‰)in$\delta^{34}S$ values between mature kerogens and their generated oils in the case studies and experimental simulation (Cai et al., 2009aand references therein). Sulphur isotopes has been successfully applied to correlate the Cambrian derived oilswith Cambrian source rocks with the $\delta^{34}S$ values recorded in closed range in both the oils and source rocks (Cai *et al*., 2009a,b). Cai *et al*., 2015 applied bulk and individual n-alkane $\delta^{13}C$ and individual alkyl-dibenzothiophene $\delta\ ^{34}S$ values to determine the source of oils and oil-source rock correlations in oils and source rocks from the Tazhong area, Tarim Basin, China. These researchers found that most of the oils from the Tazhong area were probably derived from Cambrian source rocks and that $\delta^{13}C$ and $\delta^{34}S$ values can be used as effective tools to demonstrate oil–source rock correlation in the Tazhong uplift, Tarim Basin, China. Also, sulphur isotopes have been successfully applied for oil-oil correlations in oils from the Willston Basin of North

Dakota and Saskatchewan (Thode, 1981) and Iranian oils (Bordenave and Burwood, 1990).

2.3.4 Hydrogen Isotopes

Hydrogen isotope has been applied to oil-oil and oil-source rock correlations in petroleum geochemistry (Tuo *et al*., 2006; Asif *et al*., 2011). Hydrogen compound-specific isotope analysis (CSIA) has shown great potential in petroleum geochemistry hydrogen of all elements has the largest mass difference between its two stable isotopes (D and H) and hence the largest natural variations in stable isotope ratios. The capability of measuring δD values of individual compounds in a complex mixture (e.g. petroleum) was developed over ten years ago (Dawson *et al*., 2004; Schimmelmann *et al*., 2004; Pedentchouk *et al*., 2006). To date, there are has been relatively limited research into the D/H composition of petroleum particularly using compound-specific approach. The reports that exist have investigated the relationship between δD values of whole crude oils and bitumen sand and their sources (including organic matter type and depositional conditions), thermal maturity as well as secondary processes such biodegradation, mixing and migration (Li *et al*., 2001; Dawson *et al*., 2006; Asif *et al*., 2011). Sessions *et al* (1999) studied the fractionation of hydrogen isotopes in lipid biosynthesis by different organisms. Anderson *et al.* (2000) reported the δD values of individual n-alkanes and isoprenoids as evidence of large and rapid climate variability. Li *et al*., 2001 assessed the usefulness of hydrogen CSIA in petroleum correlation studies using a number of crude oil samples from Western Canada sedimentary basin. Dawson *et al*. (2005, 2006) have demonstrated the usefulness of δD values of sedimentary aliphatic hydrocarbons to evaluate the maturity of source rocks and crude oils from Perth Basin (WA) and Vulcan sub basin (Timor sea). Pristane (Pr) and Phytane (Ph) are significantly depleted in D values compare to n-alkanes, although this difference decreases with increasing maturity due to thermal hydrogen isotopic exchange. The work by Dawson *et al*. (2005 and 2006) suggests that the δD measurements of sedimentary hydrocarbons represents a useful maturity parameter which also accounts for source effects. Maslen *et al*. (2010) have shown the application of the D/H of biomarkers as maturity proxy for Devonian source rocks from the Western Canada sedimentary basin (WCSB).

2.4 Instrumental Techniques and Parameters used in Geochemical Studies

2.4.1 Rock-Eval Pyrolysis

The Rock-Eval pyrolysis method has been extensively used for the evaluation of the hydrocarbon potential of source rocks (Espitalie *et al*., 1977; Clementz *et al*., 1979; Larter and Douglas, 1982; Horsfield, 1985). This technique uses temperature programmed heating of a small amount of rock (70 mg) or coal (30-50 mg) in an inert atmosphere (helium or nitrogen) in order to determine the quantity of free hydrocarbons present in the sample (S_1 peak) and of those that can be potentially released after maturation (S_2 peak) (Behar *et al*., 2001). The Tmax value is a standardized parameter, calculated from the temperature at which the S_2 peak reaches its maximum and it is used as a maturity parameter for source rocks. The latest version of the Rock-Eval product line, i.e. the Rock-Eval 6, described by Lafargue *et al*. (1998), enables the determination of Rock-Eval parameters plus TOC. It is equipped with an oven for combustion of the rock residue after pyrolysis, and an infra-red cell ensuring the continuous monitoring of CO and CO_2 released during both pyrolysis and combustion. By studying the specific thermal decomposition of the carbonates during pyrolysis (Lafargue *et al*.,1998), it is now possible to subtract from the total carbon curves during the pyrolysis and combustion stages, the contribution of the mineral carbon and to get a precise organic carbon profile.

The parameters that can be generated from the Rock-Eval pyrolysis include Tmax (maximum temperarture), HI (hydrogen index), OI (oxygen index), PI (production index), S_1 (free hydrocarbons present in the samples), S_2 and S_3 (amounts of hydrocarbons produced during the thermal cracking of kerogen in the rock).

Behar *et al*. (2001) defined the thermal parameters based on which maximum temperature (Tmax) can be used to determine the dimensions of the oil window. According to that definition, the Tmax value for the beginning of the oil window is usually 435–445˚C, 445–450˚C peak and 450–470˚C for the end of oil generation (Peters and Cassa, 1994). Thermal maturity of samples can be determined by plotting Tmax values against HI. Furthermore, a cross plot of Tmax versus HI is used to estimate the organic matter type. A related index, the Production Index (PI), (PI=S1/[S1 +S2]) is used to indicate the amount of hydrocarbons already generated compared to the total amount capable of being

generated, or it is used as an additional maturity parameter (Peters, 1986, Behar *et al*., 2001). Other values are also obtained during the analysis and include the Hydrogen Index [HI] and the Oxygen Index [OI] (Behar et al., 2001; Peters et al., 2005). The hydrogen and oxygen indices *(HI=S2/TOCx* 100, *OI=S3/TOCx* 100) are related to the atomic *H/C* and *O/C* ratios and determine the quality of organic matter. Overall, the thermal maturity of the OM (organic matter) can then be estimated via two modes: the T max range, and via a plot of HI and OI on a graph (Peters and Cassa, 1994).

2.4.2 Gas Chromatography-Mass Spectrometry (GC-MS) and Gas Chromatography-Mass Spectrometry-Mass Spectrometry (GC-MS-MS).

The gas chromatography-mass spectrometry (GC-MS) analyses are quite sensitive, and extremely small amounts of material can be analyzed. The use of MS in connection with GC for detection provides a unique capacity to identify unknown substances, or to verify the presence of target molecules in complex mixtures. GC-MS is a core analytical technique with a broad range of applications, including the analysis of geological samples, pharmaceuticals, pesticides, environmental pollutants, xenobiotics and toxins. GC-MS instrumentation demands the use of elevated temperatures in the injector, column, detector and transfer line to the MS during the separation and detection of substances. The temperature in the injector must be higher than the boiling point of the main substance in the mixture to be analyzed (Brondz *et al*., 2012). The conventional capillary columns used in these analyses have a normal column length of 15 - 30 m. The mobile phase (gas) flow rate is low, at about 1 mL/min or less. Current GC-MS technology suffers from a major limitation in that a relatively small range of volatile, thermally stable compounds are amenable to analysis (Brondz *et al*., 2012). The electron impact (EI) ionization mass spectra suffer from the frequent absence of the molecular ion $[M]^+$, and this drawback reduces confidence in sample identification. Less volatile compounds tend to be more fragile and have a higher probability of being thermally labile. Furthermore, to prevent ion-source-induced peak tailing (and contamination) with less volatile compounds, the temperature of the ion source must be increased (Brondz *et al*., 2012); this causes a reduction in the relative abundance of the molecular ion for all sample compounds (due to increased sample vibrational energy content).

In view of the forgoing, a more powerful analytical technique is the Gas Chromatography coupled to Tandem Mass Spectrometry (GC/MS/MS).GC/MS/MS is most frequently applied to trace quantitative analysis in complex matrix including geological samples. The ability of the system to select against matrix (reduce chemical noise) is a critical performance factor to be taken into consideration. This can be demonstrated with a signal-to-noise ratio (S/N). In addition, a S/N ratio also provides a guarantee against instrument contamination on installation while low level precision and instrument detection limits (IDL) provide the complete picture.Samples being analyzed by GC-MS/MS are separated in a gaseous state based on the various physical and chemical properties of analytes of interest and their interaction with the analytical column's stationary phase. Upon exiting the analytical column the analytes enter the tandem mass spectrometer (MS/MS) which consists of two scanning mass analyzers separated by a collision cell. Fragments selected in the first analyzer are reacted with an inert gas in the collision cell, resulting in further fragmentation. These daughter product ions are then resolved in the third quadrupole for analysis.GC-MS/MS analysis can be performed on liquids, gases or solids.For liquids, the sample is directly injected into the GC. For gases, gastight syringes are used to transfer the gaseous components directly into the GC. For solids, the analysis is carried out either by solvent extraction, outgassing or pyrolysis analysis. The analytes of interest are then quantified through comparison to external or internal standards. In addition to the quantification, GC-MS/MS is well suited for the identification of unknown volatile components using the mass fragmentation patterns and mass transitions associated with the unknown analyte.

2.4.3 Gas Chromatography-Isotope Ratio Mass Spectrometer (GC-IRMS)

Compound-specific isotope analysis (CSIA) combines a separation technique (typically GC) with isotope measurement (often by IRMS) to determine isotope ratios of individual compounds within a mixed sample (Sessions, 2006). CSIA using multiple isotopes (i.e.,$\delta^{15}N$, $\delta^{34}S$,δD and $\delta^{13}C$) provides an additional dimension for sample fingerprinting (Schimmelmann *et al*.,2004).

The combustion interface eitherconsistsof a quartz tube containing CuO pellets

(850°C) or a ceramic tube containing twisted CuO/Pt wires (850°C) (Matthews and Haye s, 1978; Hayes, 1993).

2.5 Geological and stratigraphic setting of Niger Delta

Niger delta is a sedimentary basin situated in the re-entrant of the Gulf of Guinea, West Africa. The sub-aerial portion of the Niger Delta covers approximately 75,000 km^2 and stretches about 200 km from apex to mouth. The total sedimentary prism encompasses 140000 km^2, with a maximum stratigraphic thickness of about 12 km (Whiteman, 1982). The stratigraphy of the thick sedimentary sequence is divided into three lithostratigraphic units, namely the Akata, Agbada and Benin Formations (Short and Stauble, 1967).

The uppermost unit, the Benin Formation which ranges from Oligocene to recent in age, comprises continental/fluviatile sands, gravels, and backswamp deposits up to 2500 m thick. These are underlain by the Agbada Formation of paralic, brackish to marine, coastal and fluvio-marine deposits. These are mainly interbedded sandstones and shale with minor lignite organized into coarsening upward 'offlap' cycles. Underlying this unit is the Akata Formation, ranging in age from Paleocene to Miocene consists of mainly of overpressure shales deposited under fully marine conditions.

The depobelts are partitioned into 6-7east-west bound blocks corresponding to discrete periods of the deltas evolutionary history starting from the oldest in the north, northern delta to the youngest, offshore in the south (Doust and Omatsola, 1990). It is believed that each depobelt constitutes a more or less autonomous unit with respect to sedimentation, structural deformation and hydrocarbon generation and accumulation (Evamy et al., 1978). Available source rocks in the basin exist mainly in the lower parts of the paralic sequence (Agbada Formation) and uppermost strata of the continuous marine shale (Akata Formation; Evamy *et al*., 1978; Ekweozor and Daukoru, 1994). The hydrocarbon habitat of the Niger Delta is mostly the sandstone reservoir of the Agbada Formation where oil oil and gas are usually trapped in rollover anticlines associated with growth faults.

2.6 Faults, Traps and Overpressures in the Niger Delta

The Niger Delta basin evolved in a protracted style where subsidence and sedimentation within a depobelt may have been facilitated by large scale withdrawal and seaward movement of undercompacted and geopressured marine shales under the weight of advancing paralic clastic wedge (Doust and Omatsola, 1990). At a certain stage however, further subsidence and sedimentation could no longer be accommodated and the focus of deposition shifted basin ward to form a new depobelt. Similarly, syn-sedimentary and most post-sedimentary faulting ceased with the abandoned depobelt. Normal faults triggered by the movement of deep-seated, overpressured, ductile, marine shale have deformed much of the Niger Delta clastic wedge. Growth faults affecting the sequence within depobelts form the boundaries of macrostructures (or individual delta units), each with its own sand and shale distribution pattern and style. Depobelts or mega-structures comprise in fact families of genetically and temporally related growth fault trends, or macrostructures (Doust and Omatsola, 1990).

Most known traps in Niger Delta fields are structural although stratigraphic traps are not uncommon. The structural traps developed during syn-sedimentary deformation of the Agbada paralic sequence (Evamy *et al*., 1978; Stacher, 1995). Structural complexity increases from the north (earlier formed depobelts) to the south (later formed depobelts) in response to increasing instability of the under-compacted, overpressured shale. Doust and Omatsola (1990) describe a variety of structural trapping elements, including those associated with simple rollover structures, clay filled channels, structures with multiple growth faults, structures with antithetic faults, and collapsed crest structures. On the flanks of the delta, stratigraphic traps are likely as important as structural traps (Beka and Oti, 1995). In this region, pockets of sandstone occur between diapiric structures. Towards the delta toe (base of distal slope), this alternating sequence of sandstone and shale gradually grades to essentially sandstone. The primary seal rock in the Niger Delta is the interbedded shale within the Agbada Formation. The shale provides three types of seals; clay smears along faults, interbedded sealing units against which reservoir sands are juxtaposed due to faulting, and vertical seals (Doust and Omatsola, 1990). On the flanks of the delta, major erosional events of early to middle

Miocene age formed canyons that are now clay-filled. These clays form the top seals for some important offshore fields (Doust and Omatsola, 1990).

2.7 Niger Delta Source Rocks

There has been much discussion about the source rock for petroleum in the Niger Delta (e.g. Evamy *et al.*, 1978; Ekweozor *et al.*, 1979; Ekweozor and Okoye, 1980; Lambert-Aikhionbare and Ibe, 1984; Bustin, 1988; Doust and Omatsola, 1990). The Agbada Formation has intervals that contain organic carbon contents sufficient to be considered good source rocks (Ekweozor and Okoye, 1980; Nwachukwu and Chukwura, 1986). The intervals, however, rarely reach thickness sufficient to produce a world-class oil province and are immature in various parts of the delta (Evamy *et al.*, 1978; Stacher, 1995). However, the Akata shale is present in large volumes beneath the Agbada Formation and is at least volumetrically sufficient to generate enough oil for a world class oil province such as the Niger Delta**.** Based on organic-matter content and type, Evamy *et al.*(1978) proposed that both the marine shale (Akata Fm.) and the shale interbedded with paralic sandstone (lower Agbada Fm.) were the source rocks for the Niger Delta oils.

Ekweozor *et al*. (1979) used αβ-hopanes and oleananes to fingerprint crude with respect to their source and reported the shale of the paralic Agbada Formation on the eastern side of the delta and the Akata marine-paralic shale on the western side of the delta as the possible source. Ekweozor and Okoye (1980) further confirmed this hypothesis using geochemical maturity indicators, including vitrinite reflectance data that showed rocks younger than the deeply buried lower parts of the paralic sequence to be immature. Lambert-Aikhionbare and Ibe (1984) argued that the migration efficiency from the over-pressured Akata shale would be less than 12%, indicating that little fluid would have been released from the formation. They derived a different thermal maturity profile, showing that the shale within the Agbada Formation is mature enough to generate hydrocarbons. Ejedawe *et al.*(1984) use maturation models to conclude that in the central part of the delta, the Agbada shale sources the oil while the Akata shale sources the gas. In other parts of the delta, they believe that both shales source the oil. Doust and Omatsola (1990) reported that the source organic matter is in the deltaic offlap sequences and in the sediments of the lower coastal plain. Their hypothesis implies that both the

Agbada and Akata Formations likely have disseminated source rock levels, but the bulk will be in the Agbada Formation. In deep water, they favor delta slope and deep turbidite fans of the Akata Formation as source rocks. The organic matter in these environments still maintains a terrestrial signature, however, it may be enriched in amorphous, hydrogen-rich matter from bacterial degradation. Stacher (1995) proposes that the Akata Formation is the only source rock volumetrically significant and whose depth of burial is consistent with the depth of the oil window.

2.8 Hydrocarbons Generation and Migration in Niger Delta

Petroleum in the Niger Delta is produced from sandstone and unconsolidated sands predominantly in the Agbada Formation (Tuttle *et al*., 1999). However, several directional trends form an "oil-rich belt" having the largest field and lowest gas: oil ratio (Ejedawe, 1981; Evamy *et al*., 1978; Doust and Omatsola, 1990). The belt extends from the northwest offshore area to the southeast offshore and along a number of north-south trends. It roughly corresponds to the transition between continental and oceanic crust, and is within the axis of maximum sedimentary thickness. This hydrocarbon distribution was originally attributed to timing of trap formation relative to petroleum migration.

There are two main migration histories proposed for the Niger Delta. For those who favours Agbada formation the hydrocarbon must have migrated from a short distance up dip to the adjacent sandstone while for the other which favour Akata formation as the source rock, it is expected that the hydrocarbon migration will be vertical from Akata formation to Agbada Formation (reservoir rock). Fault migration through conductive fault zones have been recognized probably as the most effective way by which hydrocarbon and oil field waters may have migrated into the rollover anticlines. Other mechanism such as flank of a rollover may have contributed to the hydrocarbon accumulation (Waples and Mahadir, 2001).

It is observed that the dominant trapping mechanism for hydrocarbon pool in the Niger Delta is the crescent shaped growth fault and associated rollover anticlines, the best reservoirs are located in the upthrow side of the growth fault where shale smearing assists in the formation of effective seals by juxtaposition of reservoir against shale (Tuttle *et al*., 1999; Waples and Mahadir, 2001)

CHAPTER THREE

MATERIALS AND METHODS

3.1. SAMPLING AND SAMPLE PREPARATION

3.1.1 Sampling

A total of ninety-two (92) ditch cuttings were collected from five fields represented as ADL, OKN, MJO, MJI and WZB in the Niger Delta, Nigeria. Forty-one (41) crude oil samples were also collected at depth ranging from 2602 m to 3036 m from the five fields. The sample locations and geological information are presented in Fig. 3.1and Table 3.1, respectively.

3.1.2 Sample Preparation

3.1.2.1 Extraction of Soluble Organic Matter

The samples were crushed with agate mortar and powdered to less than 100 mesh size prior to extraction. About 50g powdered samples were Soxhlet extracted with azeotropic mixture of dichloromethane:methanol (93:7, v/v) for 72 h. Activated copper powder was added to remove elemental sulphur from the extracts. Excess solvent was distilled off using a rotary evaporator to an aliquot volume of about 3 mL. The aliquot was then transferred into a weighed clean vial with a micropipette and the remaining solvent removed under nitrogen gas flow at temperature below 50 ^{o}C.

3.1.2.2 Column Chromatography

To obtain dibenzofuran compounds, the rock extracts and crude oils were separately fractionated by column chromatography using silica gel/alumina as stationary phase into saturated and aromatic hydrocarbon fractions using n-hexane (50 mL) and dichloromethane/n-hexane (2:1 v/v, 50 mL), respectively, as eluents (Li and Ellis, 2015).

For carbazoles, the saturated, aromatics, and polar compounds were eluted using n-hexane (50 mL), toluene (50 mL), and dichloromethane/methanol (99:1, 70 mL), respectively. The polar fraction was further fractionated on 2g of silicic acid stationary phase by elution with n-hexane/toluene (1:1, 50ml) to obtain the pyrrolic nitrogen compounds (Li *et al*., 1995).

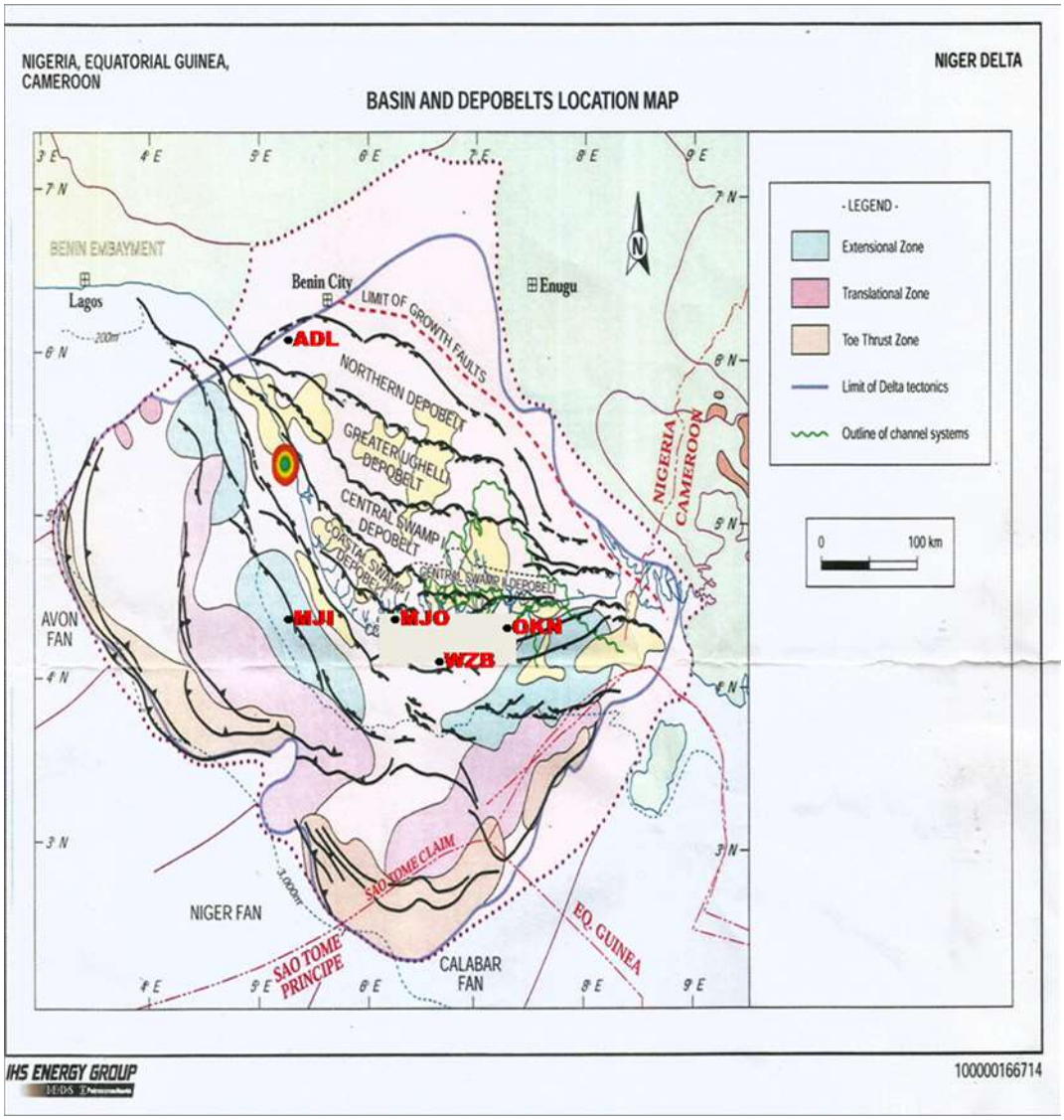

Fig. 3.1: Niger Delta depobelts and sample locations (after Tuttle *et al*., 1999).

Table 3.1: Geological information of crude oils from the Niger Delta, Nigeria

S/N	Sample	Well	Field	Depth (m)	Biodegradation ranking[a]	Formation	Depobelt
1	oil	ADL-1	ADL	2602	0	Agbada	Northern
2	oil	ADL-2	ADL	2607	0	Agbada	Northern
3	oil	ADL-3	ADL	2702	0	Agbada	Northern
4	oil	ADL-4	ADL	2718	0	Agbada	Northern
5	oil	ADL-5	ADL	2759	0	Agbada	Northern
6	oil	ADL-6	ADL	2766	0	Agbada	Northern
7	oil	ADL-7	ADL	2905	0	Agbada	Northern
8	oil	ADL-8	ADL	2964	0	Agbada	Northern
9	oil	ADL-9	ADL	3064	0	Agbada	Northern
10	oil	OKN-1	OKN	1749	3	Agbada	Offshore
11	oil	OKN-2	OKN	1892	0	Agbada	Offshore
12	oil	OKN-3	OKN	1905	2	Agbada	Offshore
13	oil	OKN-4	OKN	1952	3	Agbada	Offshore
14	oil	OKN-5	OKN	2050	1	Agbada	Offshore
15	oil	OKN-6	OKN	2369	1	Agbada	Offshore
16	oil	OKN-7	OKN	2377	1	Agbada	Offshore
17	oil	OKN-8	OKN	2469	1	Agbada	Offshore
18	oil	OKN-9	OKN	2485	1	Agbada	Offshore
19	oil	OKN-10	OKN	2489	1	Agbada	Offshore
20	oil	OKN-11	OKN	2521	1	Agbada	Offshore
21	oil	OKN-12	OKN	2530	1	Agbada	Offshore
22	oil	OKN-13	OKN	2566	3	Agbada	Offshore
23	oil	OKN-14	OKN	2677	1	Agbada	Offshore
24	oil	OKN-15	OKN	3148	3	Agbada	Offshore
25	oil	OKN-16	OKN	3593	1	Agbada	Offshore
26	oil	MJO-1	MJO	2070	4	Agbada	Offshore
27	oil	MJO-2	MJO	2091	4	Agbada	Offshore
28	oil	MJO-3	MJO	2096	4	Agbada	Offshore
29	oil	MJO-4	MJO	2207	1	Agbada	Offshore
30	oil	MJI-1	MJI	1607	1	Agbada	Offshore
31	oil	MJI-2	MJI	1777	4	Agbada	Offshore
32	oil	MJI-3	MJI	1795	4	Agbada	Offshore
33	oil	MJI-4	MJI	1920	1	Agbada	Offshore
34	oil	MJI-5	MJI	1936	1	Agbada	Offshore
35	oil	MJI-6	MJI	1944	2	Agbada	Offshore

Table 3.1: contd.

S/N	Sample	Well	Field	Depth (m)	Biodegradation ranking[a]	Formation	Depobelt
35	Oil	MJI-6	MJI	1944	4	Agbada	Offshore
36	Oil	MJI-7	MJI	1948	1	Agbada	Offshore
37	Oil	MJI-8	MJI	1979	1	Agbada	Offshore
38	Oil	MJI-9	MJI	2442	1	Agbada	Offshore
39	Oil	MJI-10	MJI	3030	1	Agbada	Offshore
40	Oil	WZB-1	WZB	NA	2	Agbada	Offshore
41	Oil	WZB-2	WZB	NA	2	Agbada	Offshore

[a]Biodegradation Ranking scale 1 – 10 (Peters and Moldowan, 1993)
NA: not available

3.2 ANALYTICAL METHODS

3.2.1 Total Organic Carbon and Sulphur Determination

Total organic carbon (TOC) and total sulphur (TS) were measured by LECO analyzer. Carbon and sulphur concentrations in whole rock samples were measured in duplicate by combustion in an induction furnace in a flow of oxygen, using a LECO carbon-analyzer IR 112. Total organic carbon (TOC) was measured using samples that had been pretreated with hydrochloric acid to remove carbonate.

3.2.2 Rock Eval Pyrolysis

Rock-Eval pyrolysis was performed on the rock samples using Rock-Eval 6 analyzer. 100 mgof powdered rock sample was progressively heated to 850^{o}C using a special temperature program. Four characteristic peaks were obtained during the heating. S_1 which is the first peak represents hydrocarbons already present in the sample which are mainly stripped at temperatureat about 300^{o}C. The second peak, S_2 represents hydrocarbons generated through thermal cracking of kerogen at temperatures between 300 and 650 ^{o}C, while S_3 peak represents the CO_2 which is generated from the kerogen at the same time the S_2 hydrocarbons are being generated. The fourth peak, S_4 indicates the amount of CO_2 produced through oxidation during combustion at a temperature of about 850^{o}C. OPTKIN software was used for acquisition of pyrolysis kinetic parameters. The parameters include S_1, S_2, S_3, hydrogen index (HI), oxygen index (OI), S_2/S_3, S_1, S_2, S_3, production index (PI) and T_{max} for the assessment of rocks qualities and maturation. Standards were run in between the analyses to ensure reproducibility and accuracy of the data generated.

3.2.3 Gas chromatography-mass spectrometry (GC-MS)

The GC-MS analyses of the saturate and aromatic fractions were performed on an Agilent 5975i gas chromatograph (GC) equipped with an HP-5MS (5% phenylmethylpolysiloxane) fused silica capillary column (60m x 0.25mm i.d., x 0.25µm film thickness) coupled to an Agilent 5975i mass spectrometer (MS). The GC operating conditions are as follows: the oven temperature was held isothermally at 80˚C for 1 min, ramped to 310˚C at 3˚C/min and held isothermal for 16 min (Li *et al*., 2012). Helium was

used as the carrier gas with constant flow rate of 1.2 mL/min. The MS was operated in the electron impact (EI) mode at 70eV, an ion source temperature of 250 ^{o}C and injector temperature of 285^{o}C

GC-MS analysis of the dibenzofurans and pyrrolic nitrogen fractions was performed on an Agilent 5975i gas chromatograph equipped with a 60 m long fused-silica capillary column (HP-5MS, 0.25 mm i.d., 0.25 m film thickness) coupled with an Agilent 5975i mass spectrometer. The GC ovens was held isothermally at 80 ˚C for 1 min, and was ramped to 150˚C at 15˚C/min and then to 290˚C at 5˚C/min with a final temperature hold time of 20 min. The mass spectrometer was operated in selective-ion monitoring (SIM) mode (m/z 85, 191, 217, 178, 192, 168, 194, 234, 198, 231, 170, 228, 242, 202, 216, 182, 196 and 218) with electron impact ionization of 70 eV. The identification of dibenzofurans and carbazoles was based on elution orders from the literature and comparison of their mass spectra with those reported in literature and library data (Chakhmakhchev *et al*, 1997; Lee *et al*., 1979; Mossner *et al*., 1999; Schade and Andersson, 2006; Li *et al*., 2012; Alexander *et al*., 1991; Bowler *et al*., 1997; Clegg *et al*., 1997;). Quantification of aromatic oxygen compounds was done using dibenzothiophene-d8 (DBT-d8; molecular formular: $C_{12}D8S$; molecular mass: 192.31; purity = 99.5%, Laboratory of Dr. Ehrenstorfer, Augsburg, Germany). The absolute and relative concentrations of carbazoles and benzocarbazoles were obtained following the same procedure described by Li *et al*. (1995) and using 9-phenylcarbazoles as an internal standard.

3.2.4 Gas chromatography-isotope ratio mass spectrometry (GC-IRMS).

The carbon isotope analysis of individual compounds was performed on a Delta Plus XP gas chromatograph-combustion-isotope ratio mass spectrometer. The gas chromatography was performed using a Thermo Finnigan GC COMBUSTION III system equipped with a DB-5 fused silica capillary column (30 m x 0.25 mm) and helium was used as carrier gas at a flow rate of 1 mL/min. The GC oven temperature was isothermal for 5 min at 70 ^{o}C and then programmed from 70-290 ^{o}C at 3 ^{o}C/min and isothermal for 30 min at 290 ^{o}C.

Isotopic values were calculated by integrating the m/z 44, 45 and 46 ion currents of the peaks produced by combustion (880 ^{o}C) of chromatographically separated compounds and those of CO_2 standard spikes admitted at regular intervals. The reproducibility and accuracy were evaluated routinely using laboratory standards of known $\delta^{13}C$ values (C_{13}-C_{32} n-alkanes). Laboratory standard was injected for every six-sample analysis. The isotope values are given with respect to the PDB standard. The analysis was repeated three times and the results presented as an average value.

3.2.5 Elemental Analysis-Isotope Ratio Mass Spectrometry (EA-IRMS)

Bulk isotope analysis was performed on a micromass IsoPrime isotope ratio mass spectrometer interfaced to a EuroVector EuroEA3000 elemental analyzer. For bulk $\delta^{13}C$ analysis, the sample was accurately weighed (0.05-0.15 mg) into a small tin capsule which was then folded and compressed carefully to remove any tracers of atmospheric gases. The tin capsule containing sample was dropped into a combustion reactor at 1025 °C with help of autosampler. The sample and capsule melted in an atmosphere temporarily enriched with oxygen, where the tin promoted flash combustion. The combustion products, in a constant flow of helium, passed through an oxidation catalyst (chromium oxide). The oxidation products then passed through a reduction reactor containing copper granules at 650 °C, where any oxides of nitrogen (NO, N_2O and N_2O_2) were reduced to N_2 and SO_2 and separated on a 3 m chromatographic column (PoropakQ) at ambient temperature. After the removal of oxides of nitrogen, oxidation products were then passed through a thermal conductivity detector (TCD) followed by elemental analysis. Isotopic compositions are reported in the delta notation relative to Vienna Peedee belemnite (VPDB).

3.2.6 Vitrinite reflectance measurement

This analysis was carried out on the polished rock samples using a Zeiss standard universal reflected microscope equipped with 100x oil immersion objective and a 40x air objective. Measurements were done at 546 nm (wavelength) on clear spots of vitrinite particles (with distinct shape) of size approximately equal to or greater than 10 μm. The microscope set up was calibrated with standard (glass) of known vitrinite reflectance

within the range to be measured before each series of measurements. Reflectance values were read off directly from the digital read out.

3.2.7 Organic petrology

The organic petrological study was carried out on Reichert Jung Polyvar photomicroscope equipped with halogen and HBO lambs, photomultiplier and a computer unit. The shale samples were crushed to a maximum particle size of 2mm, mounted in epoxy resin, and then ground and polished in the same way as coal samples are prepared for incident light microscopy (Bustin *et al*., 1983). The composition of organic matter was determined by maceral analysis using a semi-automated Swift Point Counter, with each maceral analysis based on at least forty counts in view of the sparse phytoclast distribution in the shales. Standard classification scheme was used for the interpretation of organic materials present in the samples (Kalkreuth and Macauley, 1984, 1987, 1989).

CHAPTER FOUR
RESULTS AND DISCUSSION

4.1 Source rock evaluation

The hydrocarbon potential of the source rocks was assessed based on the Rock-Eval pyrolysis data. The Rock-Eval pyrolysis data are presented in Table 4.1

4.1.1 Quantity/ Amount of Organic Matter

The quantity of organic matter contained in the rock samples was evaluated based on the total organic carbon (TOC) contents, genetic potential (GP) values and plot of S_2 versus TOC (Fig. 4.1)

4.1.1.1 ADL Field

The total organic carbon (TOC) values for the source rock range from 0.61 to 5.13 wt% (Table 4.1). The coaly shales in some section of the well have TOC values varying from 37.53 to 39.23 wt% with a mean value of 38.38 wt%. The TOC values in all the samples exceeded the minimum 0.5 wt% required for a potential source rock (Tissot and Welte, 1984; Killops and Killops 1993, 2005; Hunt, 1996; Peters *et al*. 2005). The GP values for the source rock range between 0.40 and 6.45 mg/g with a mean value of 3.57 mg/g. The coaly shales have GP values ranging between 74.37 and 114.60 mg/g with a mean value of 94.49 mg/g. Most of the samples have GP values greater than 2 mg/g required for a potential source rock (Tissot and Welte, 1984; Killops and Killops 1993, 2005; Hunt, 1996; Peters *et al*. 2005). The plot of S_2 against TOC values classifies the source rocks as very good to excellent source rocks (Peters and Cassa, 1994) (Fig. 4.1). However, the majority of the source rock samples fall in the region of very good source rock (Fig. 4.1).

4.1.1.2 OKN Field

The total organic carbon (TOC) values range from 2.27 to 3.89 wt%. (Table 4.1). The TOC values in all the samples exceeded the minimum 0.5 wt% required for a potential source rock (Tissot and Welte, 1984; Killops and Killops 1993, 2005; Hunt,

Table 4.1: Rock-Eval pyrolysis and Petrological data for rock samples from Niger Delta, Nigeria

Field	Depth (m)	TOC	Tmax	S1	S2	S3	(S1 + S2)	PI	HI	OI	Maceral compositions (%)				(%)Ro
		(%)	(℃)	(mg/g)	(mg/g)	(mg/g)	GP		(mg/g.TOC)	(mg/g.TOC)	vit.	ex.	iner.	sap.	
ADL	1442-1451	0.61	423	0.24	0.16	1.76	0.40	0.59	26	289					nd
ADL	1835-1860	39.23	415	4.72	69.65	37.48	74.37	0.06	178	96					0.30
ADL	1902-1933	37.53	418	5.59	109.01	37.73	114.60	0.05	290	101					nd
ADL	2030-2061	5.13	425	0.32	6.13	4.53	6.45	0.05	119	88					nd
ADL	2213-2238	3.09	435	0.27	4.15	3.22	4.42	0.06	134	104					0.35
ADL	2305-2329	2.19	427	0.17	1.62	2.42	1.79	0.09	74	111					nd
ADL	2390-2409	2.51	426	0.37	2.18	2.28	2.55	0.14	87	91	77.00	13.00	4.00	6.00	nd
ADL	2457-2482	2.01	432	0.24	2.10	2.54	2.34	0.10	104	126	81.00	15.00	2.00	2.00	0.42
ADL	2579-2598	1.76	430	0.20	1.38	1.38	1.58	0.13	78	78					nd
ADL	2622-2646	2.45	432	0.34	2.66	1.56	3.00	0.11	109	64	72.00	15.00	2.00	12.00	nd
ADL	2713-2738	2.99	431	0.30	3.55	3.44	3.85	0.08	119	115					0.33
ADL	2793-2817	3.62	436	0.53	5.38	1.86	5.91	0.09	149	51					nd
ADL	2878-2902	3.32	436	0.66	4.73	2.05	5.39	0.12	142	62					nd
ADL	2970-2994	2.80	438	0.54	4.47	1.50	5.01	0.11	160	54	69.00	17.00	4.00	10.00	0.42
ADL	3030-3055	2.31	438	0.58	3.16	2.04	3.74	0.15	137	88					nd
OKN	1454-1463	3.54	396	2.46	15.56	3.22	18.02	0.14	440	91					0.23
OKN	1500-1518	3.26	393	2.06	13.58	4.60	15.64	0.13	417	141					nd
OKN	1537-1555	3.21	394	1.39	13.49	3.21	14.88	0.09	420	100	61.00	30.00	3.00	6.00	0.23
OKN	1582-1601	2.52	401	0.71	10.25	3.15	10.96	0.06	407	125					nd
OKN	1619-1628	2.27	413	0.66	9.81	2.63	10.47	0.06	432	116	60.00	26.00	4.00	10.00	nd
OKN	1646-1665	2.36	409	0.67	9.66	3.45	10.33	0.06	409	146					0.29
OKN	1729-1747	2.74	409	0.80	10.65	3.10	11.45	0.07	389	113					nd
OKN	2332-2341	2.79	418	1.18	15.58	2.29	16.76	0.07	558	82					nd
OKN	2369-2378	3.89	414	2.25	22.82	2.92	25.07	0.09	587	75	48.00	39.00	5.00	9.00	nd

Table 4.1 contd.

Field	Depth (m)	TOC	Tmax	S1	S2	S3	(S1 + S2)	PI	HI	OI	Maceral compositions (%)				(%) Ro
		(%)	(°C)	(mg/g)	(mg/g)	(mg/g)	GP		(mg/g.TOC)	(mg/g.TOC)	vit.	ex.	iner.	sap.	
OKN	2625-2643	3.77	400	2.36	20.23	4.05	22.59	0.10	537	107					0.29
OKN	2671-2689	2.55	414	3.37	25.32	3.18	28.69	0.12	993	125					nd
OKN	2707-2726	3.76	410	3.05	22.23	3.59	25.28	0.12	591	95					0.31
OKN	`2780-2799	3.62	403	5.36	20.29	3.08	25.65	0.21	560	85					nd
OKN	2817-2835	3.47	388	3.61	19.32	2.72	22.93	0.16	557	78					nd
OKN	2863-2881	3.60	383	4.94	17.26	2.93	22.20	0.22	479	81					0.27
OKN	2863-2881	3.54	387	5.64	17.78	2.64	23.42	0.24	502	75					nd
OKN	2890-2899	3.39	381	5.90	16.80	2.49	22.70	0.26	496	73					0.27
OKN	2909-2927	3.09	401	3.31	16.53	2.98	19.84	0.17	535	96					0.30
MJI	1860-1878	0.78	426	0.03	0.37	2.00	0.40	0.08	47	256					0.21
MJI	1970-1988	1.33	425	0.06	0.62	2.54	0.68	0.09	47	191					nd
MJI	2079-2098	0.73	426	0.02	0.28	1.39	0.30	0.06	38	190	73.00	11.00	6.00	10.00	0.29
MJI	2189-2207	0.88	425	0.02	0.35	1.73	0.37	0.05	40	197					nd
MJI	2299-2308	0.63	430	0.01	0.28	1.44	0.29	0.05	44	229					nd
MJI	2390-2409	1.01	428	0.03	0.47	1.52	0.50	0.06	47	150					0.46
MJI	2527-2546	0.83	429	0.02	0.41	1.27	0.43	0.05	49	153					nd
MJI	2637-2655	1.26	427	0.03	0.49	1.49	0.52	0.05	39	118					nd
MJI	2701-2720	0.96	429	0.03	0.37	1.25	0.40	0.06	39	130					nd
MJI	2793-2811	1.05	428	0.05	0.46	1.86	0.51	0.09	44	177					nd
MJI	2857-2875	0.94	430	0.04	0.43	1.23	0.47	0.08	46	131					nd
MJI	2893-2912	1.10	429	0.04	0.47	1.42	0.51	0.09	43	129					0.37
MJI	2927-2936	1.07	439	0.15	1.35	2.26	1.50	0.10	126	211					0.36
MJI	2994-3012	0.78	433	0.04	0.42	1.31	0.46	0.09	54	168					nd

Table4.1 Contd.

Field	Depth (m)	TOC	Tmax	S1	S2	S3	(S1 + S2)	PI	HI	OI	Maceral compositions (%)				(%) Ro
		(%)	(℃)	(mg/g)	(mg/g)	(mg/g)	GP		(mg/g.TOC)	(mg/g.TOC)	vit.	ex.	iner.	sap.	
MJI	3040-3058	1.03	432	0.04	0.48	1.22	0.52	0.07	47	118					nd
MJI	3085-3104	1.06	432	0.04	0.61	1.16	0.65	0.07	58	109					0.41
MJI	3131-3149	0.81	436	0.05	0.48	1.02	0.53	0.09	59	126	75.00	13.00	3.00	8.00	nd
MJI	3232-3250	1.21	436	0.06	0.59	0.82	0.65	0.09	49	68					nd
MJI	3259-3277	1.12	438	0.07	0.53	0.79	0.60	0.12	47	71					0.43
MJI	3323-3332	1.40	434	0.12	0.75	0.85	0.87	0.14	54	61					0.37
MJI	3360-3378	1.05	435	0.11	0.51	0.93	0.62	0.18	49	89	75.00	11.00	5.00	9.00	nd
MJI	3405-3424	0.84	443	0.12	0.64	1.49	0.76	0.16	76	177					0.5
MJO	820-838	2.13	406	0.17	0.67	3.48	0.84	0.20	31	163					nd
MJO	1003-1012	0.76	425	0.84	0.55	1.23	1.39	0.61	72	162					nd
MJO	1616-1625	1.07	419	0.43	0.73	2.59	1.16	0.37	68	242					nd
MJO	1698-1707	0.63	425	0.10	0.50	1.59	0.60	0.17	79	252					nd
MJO	1771-1790	0.86	419	0.09	0.45	1.62	0.54	0.17	52	188					0.26
MJO	1854-1872	1.23	421	0.07	0.63	1.92	0.70	0.10	51	156					nd
MJO	1918-1936	1.88	413	0.43	0.83	2.34	1.26	0.34	44	124					nd
MJO	2091-2101	1.79	419	0.18	1.36	2.00	1.54	0.12	76	112	80.00	11.00	3.00	6.00	0.30
MJO	2220-2238	1.55	424	0.27	1.69	2.96	1.96	0.14	109	191					nd
MJO	2293-2311	1.36	424	0.12	1.32	2.25	1.44	0.08	97	165					nd
MJO	2348-2366	1.22	423	0.08	1.00	1.70	1.08	0.07	82	139					nd
MJO	2412-2430	1.38	432	0.19	1.71	2.21	1.90	0.10	124	160					0.38
MJO	2466-2485	1.32	427	0.19	1.32	1.62	1.51	0.12	100	123					nd
MJO	2524-2543	1.33	425	0.09	1.14	1.41	1.23	0.08	86	106					nd
MJO	2570-2588	1.01	422	0.06	0.68	1.30	0.74	0.09	67	129	58.00	26.00	6.00	9.00	0.40
MJO	2616-2671	1.83	429	0.31	3.98	2.57	4.29	0.07	217	140					nd
MJO	2689-2726	1.56	432	0.23	2.38	2.34	2.61	0.09	153	150					nd

Table4.1 Contd

Field	Depth (m)	TOC	Tmax	S1	S2	S3	(S1 + S2)	PI	HI	OI	Maceral compositions (%)				(%) Ro
		(%)	(℃)	(mg/g)	(mg/g)	(mg/g)	GP		(mg/g.TOC)	(mg/g.TOC)	vit.	ex.	iner.	sap.	
MJO	2744-2771	1.42	434	0.29	2.47	2.82	2.76	0.10	174	199					0.38
MJO	2808-2817	1.18	438	0.15	1.65	1.44	1.80	0.08	140	122					0.43
MJO	2881-2899	1.05	435	0.17	1.32	2.16	1.49	0.12	126	206	75.00	12.00	3.00	10.00	0.35
WZB	880-900	1.4	295	0.71	1.28	2.67	1.99	0.36	91	91					0.28
WZB	1020-1040	0.79	349	0.45	0.47	3.37	0.92	0.49	60	141					nd
WZB	1040-1060	0.46	342	0.09	0.29	1.44	0.38	0.24	63	100					nd
WZB	1060-1080	0.59	411	0.08	0.23	1.84	0.31	0.26	39	125					nd
WZB	1100-1120	0.56	304	0.27	0.6	2.24	0.87	0.31	107	116					nd
WZB	1120-1140	0.65	370	0.12	0.28	2.04	0.4	0.3	43	146					0.31
WZB	1260-1280	27.52	431	26.75	172.37	2.83	199.12	0.13	626	113					nd
WZB	1340-1360	0.96	335	1.75	1.67	1.99	3.42	0.51	174	82					nd
WZB	1460-1480	0.76	397	0.16	0.36	1.69	0.52	0.31	47	75					nd
WZB	1500-1520	0.97	361	0.64	1.15	1.71	1.79	0.36	119	107					0.35
WZB	1520-1540	1.06	323	0.29	1.03	2.19	1.32	0.22	97	125					0.35
WZB	1540-1560	1.17	368	0.35	0.73	2.52	1.08	0.32	62	95					0.36
WZB	1560-1580	0.72	446	0.1	0.17	1.96	0.27	0.37	24	85					0.33
WZB	1600-1620	1.76	352	0.62	1.22	2.67	1.84	0.34	69	78					nd
WZB	1640-1660	1.2	363	0.3	0.79	2.64	1.09	0.28	66	81					nd
WZB	1660-1680	3.89	419	0.69	7.05	2.7	7.74	0.09	181	75					nd
WZB	1680-1700	1.4	368	0.36	1.3	1.93	1.66	0.22	93	73					0.41
Mean		2.86	411.7	1.13	8.11	2.97	9.24	0.16	176.80	148.32					
		±1.1	±1.52	±0.47	±3.42	±0.97	±5.7	±0.05	±19.6	±17.3					

Vit.: vitrinite; Ex.: exinite; Iner.: inertinite; Sap.: sapropelinite; Ro: vitrinite reflectance; TOC: total organic carbon; S_1: free hydrocarbons; S_2: pyrolyzable hydrocarbons; S_3: carbon dioxide yield; GP: S_1+S_2, PI: S_1/S_1+S_2; HI: S_2/TOC*100(mg HC/g TOC); OI: S_3/TOC*100(mg CO_2/g TOC)

1996; Peters *et al*. 2005). The GP values for the source rocks range between 10.33 and 28.69 mg/g with a mean value of 19.27mg/g. The GP values are greater than 2 mg/g required for a potential source rock (Tissot and Welte, 1984; Killops and Killops 1993, 2005; Hunt, 1996; Peters *et al*. 2005). The plot of S_2 versus TOC values classifies the source rocks as very good source rocks (Peters and Cassa, 1994) (Fig. 4.1).

4.1.1.3 MJI Field

The total organic carbon (TOC) values for the source rocks range from 0.6 to 1.4 wt% (Table 4.1). The TOC values in all the samples exceeded the minimum 0.5 wt% required for a potential source rock (Tissot and Welte, 1984; Killops and Killops 1993, 2005; Hunt, 1996; Peters *et al*. 2005). The GP values for the source rocks range from 0.29 to 1.50 mg/g with a mean value of 0.57 mg/g. The GP values are less than 2 mg/g required for a potential source rock (Tissot and Welte, 1984; Killops and Killops 1993, 2005; Hunt, 1996; Peters *et al*. 2005). Plot of S_2 against TOC values classifies the source rocks as fair to good source rocks (Peter and Cassa, 1994) (Fig. 4.1)

4.1.1.4 MJO Field

The total organic carbon (TOC) values range from 0.63 to 1.88 wt% (Table 4.1). The TOC values in all the samples exceeded the minimum 0.5 wt% required for a potential source rock (Tissot and Welte, 1984; Killops and Killops 1993, 2005; Hunt, 1996; Peters *et al*. 2005). The GP values for the source rocks range between 0.54 to 4.29 mg/g with a mean value of 1.54 mg/g. The GP values are less than 2 mg/g required for potential source rock in most of the samples (Tissot and Welte, 1984; Killops and Killops 1993, 2005; Hunt, 1996; Peters *et al*. 2005). The plot of S_2 versus TOC classifies the source rocks as fair to good source rocks (Peters and Cassa, 1994) (Fig.4.1).

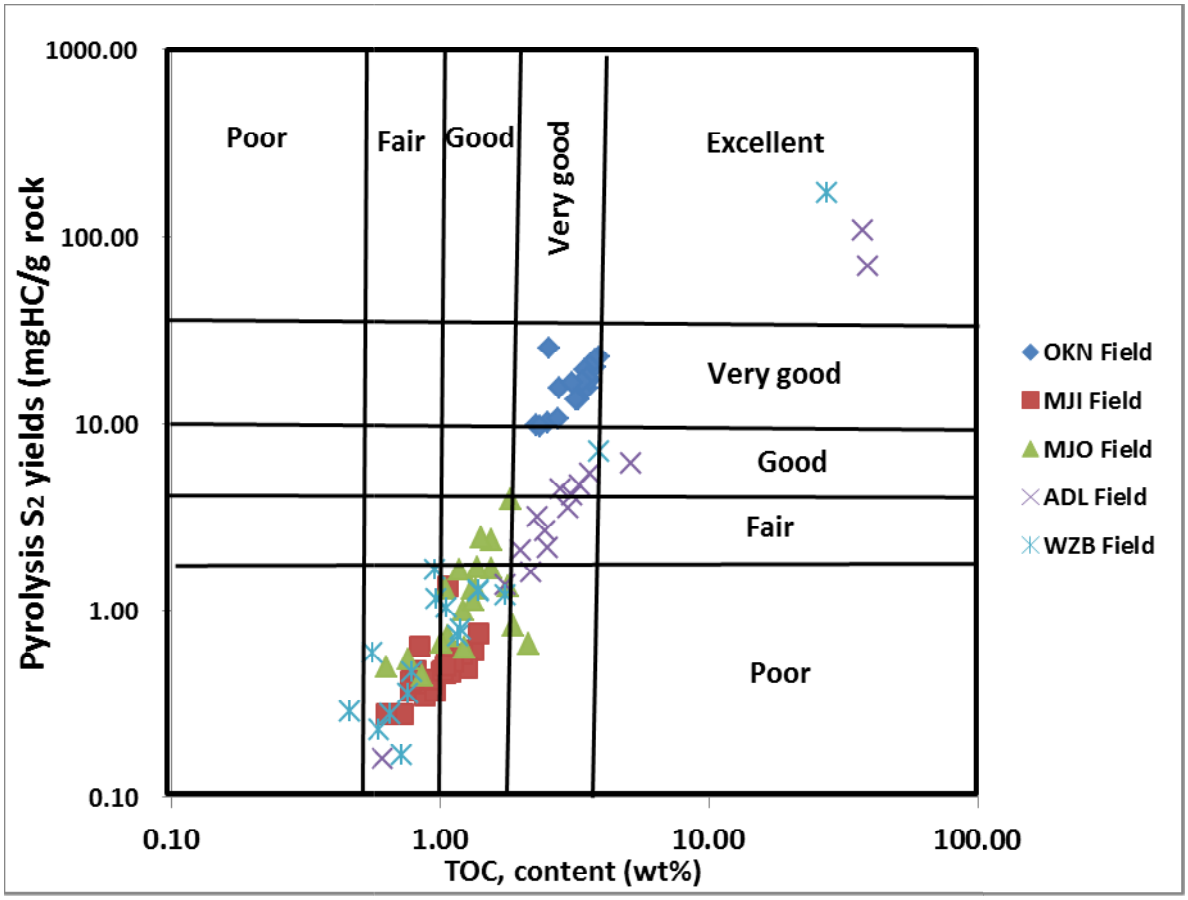

Fig. 4.1: Plot of S_2 versus total organic carbon (TOC) for the source rocks from Niger Delta Basin (modified after Peters and Cassa, 1994)

4.1.1.5 WZB Field

The total organic carbon (TOC) values for the source rocks range between 0.46 and 3.89 wt% while the coaly shales within the well has the TOC value of 27.52 wt% (Table 4.1). The TOC values in most of the samples exceeded the minimum 0.5 wt% required for a potential source rock (Tissot and Welte, 1984; Killops and Killops 1993, 2005; Hunt, 1996; Peters *et al*. 2005) except one sample with the TOC value of 0.46wt%. The GP values for the source rock range from 0.27 to 7.74 mg/g with a mean value of 1.60 mg/g while the coaly shale has GP value of 199.12 mg/g. Most of the samples have GP values less than 2mg/g required for a potential source rock (Tissot and Welte, 1984; Killops and Killops 1993, 2005; Hunt, 1996; Peters *et al*. 2005). The plot of S_2 against TOC values classifies the source rocks as fair to excellent source rocks (Peters and Cassa, 1994) (Fig. 4.1). However, most of the source rock samples fall in the regions of fair to good source rock (Fig. 4.1).

4.1.2 Organic Matter Quality

The quality of the organic matter contained in the rock samples was evaluated from their Hydrogen Index (HI), plots of HI vs. OI (equivalent to van Krevelen diagram), plot of Tmax vs HI, plots of S_2 vs. TOC and petrological data (Table 4.1).

4.1.2.1 ADL Field

The source rocks have HI values that vary between 26 and 290 mgHC/g TOC. These low HI values indicate type II/III kerogen, capable of generating gas only (Peters 1986; Sachsenhofer *et al*. 1995; Peters *et al*., 2005). Most of the samples fall within type III kerogen fields on the plots of HI against OI and S_2 against TOC (Figs. 4.2 and 4.3) The T_{max} vs HI plot (Fig. 4.4), further reveal that the samples have potential to generate mainly gas (Killops and Killops 1993, 2005).

A predominantly terrestrial origin (Type III kerogen) of organic matter in the source rocks is supported by the petrological data (Table 4.1) and ternary plots of the major macerals group in Fig. 4.5. The dominant component of all the samples is vitrinite (69 to 81%) which indicates type III kerogen (Bustin *et al*., 1983, 1988). The samples are characterized by very low abundances of liptinite (13 to 17%) and inertinite (2 to 4%).

Fig. 4.5 reveals a duroclaritic nature of the maceral distribution showing a strong similarity, indicating similar rank (Akande *et al*., 2005).

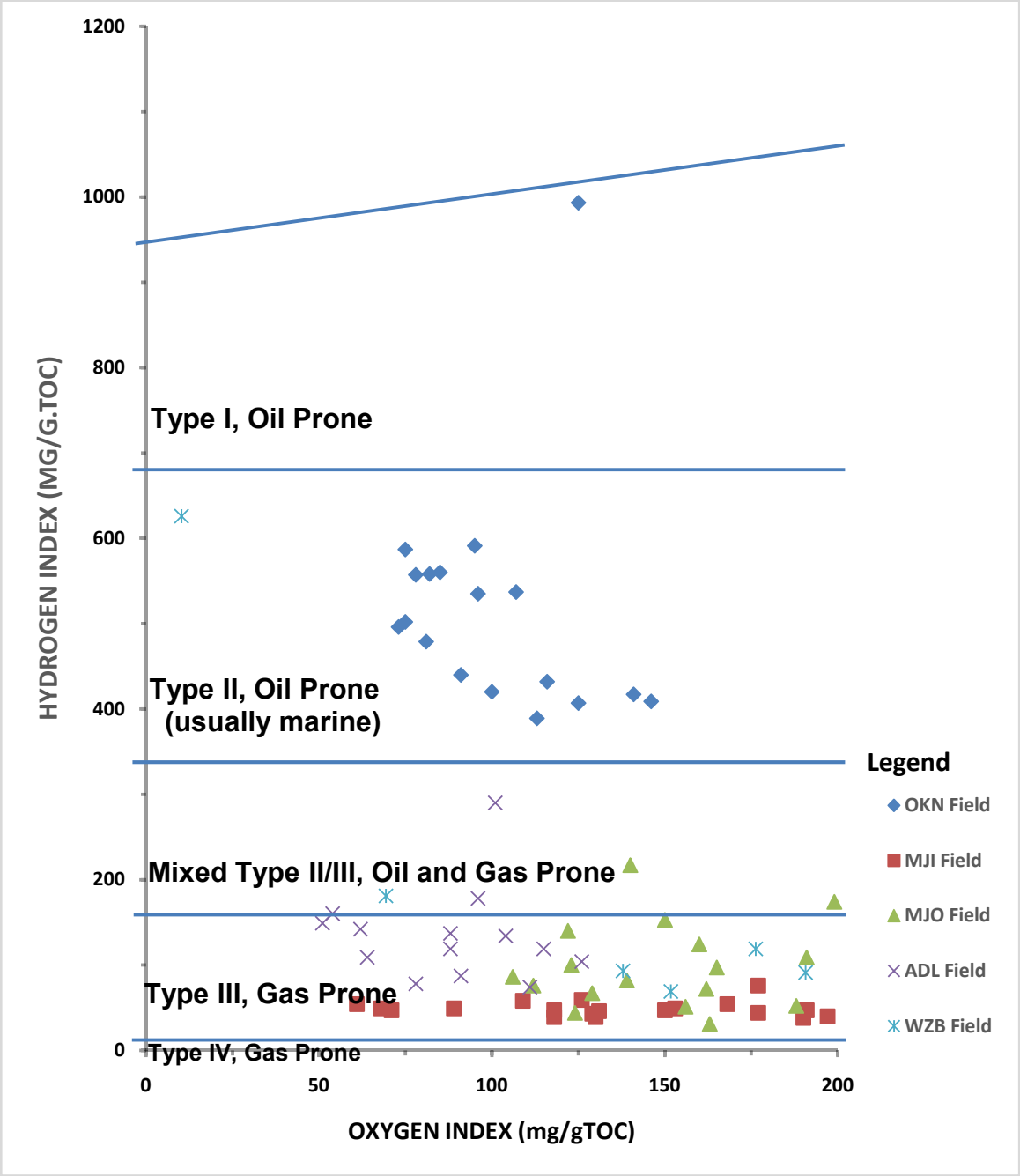

Fig. 4.2: Plots of HI vs OI of rock samples from Niger Delta, Nigeria (After Van Krevelen *et. al*., 1961)

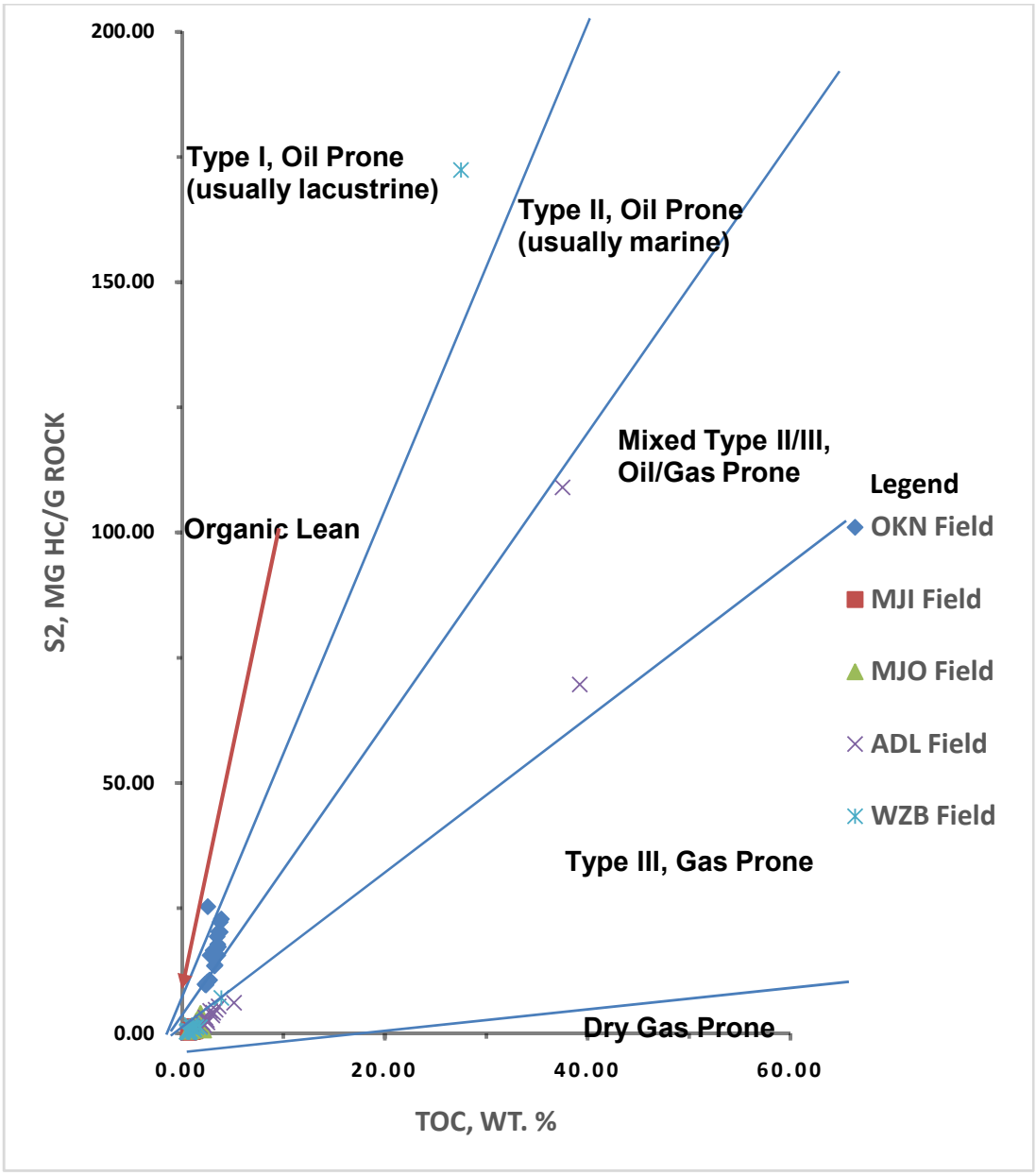

Fig. 4.3: Plots of S_2 vs TOC of rock samples from Niger Delta, Nigeria (After Langford and Blanc-Valleron, 1990)

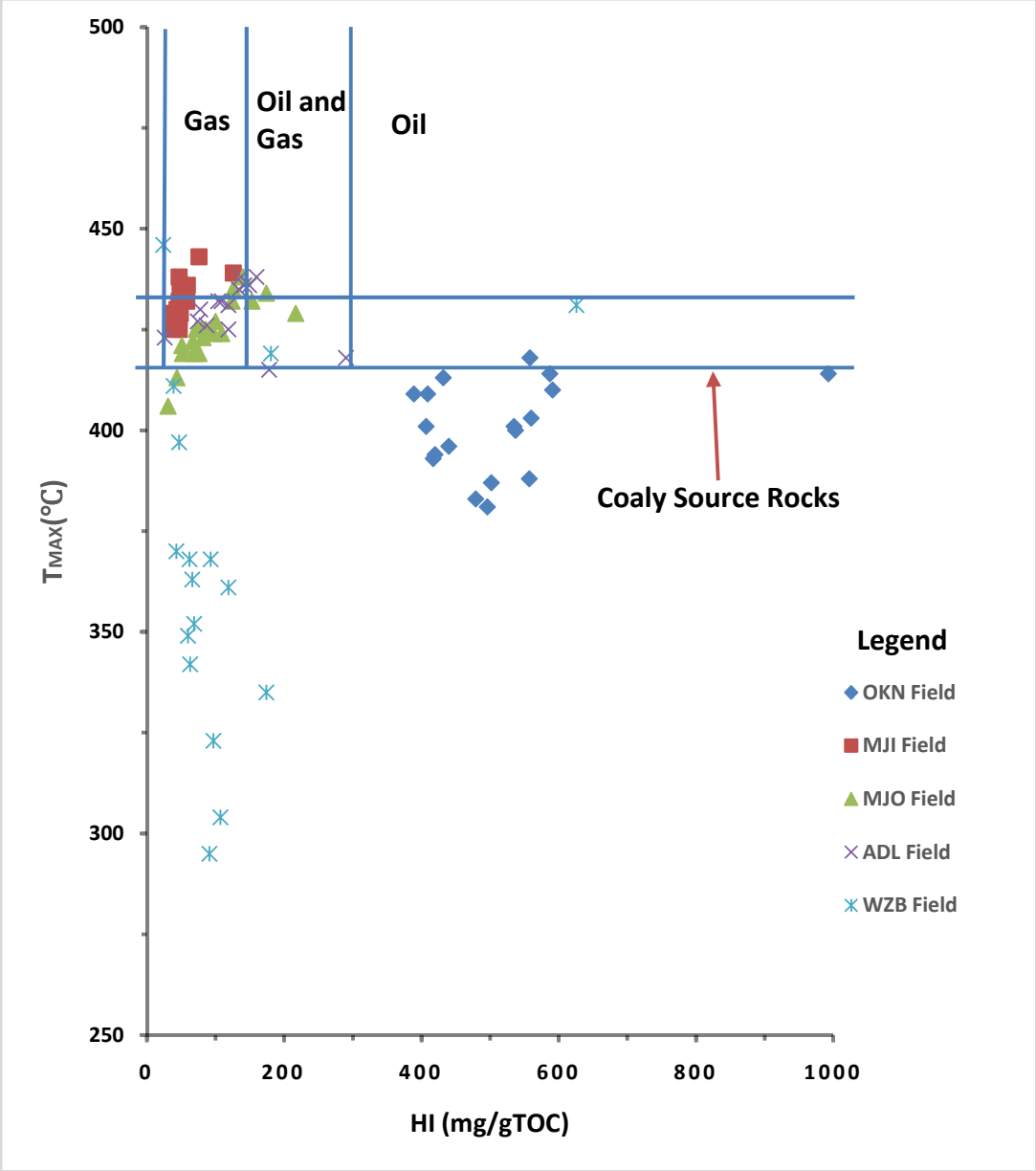

Fig. 4.4: Plots of Tmax vs HI. of rock samples from Niger Delta, Nigeria (modified after Van Krevelen *et. al*., 1961).

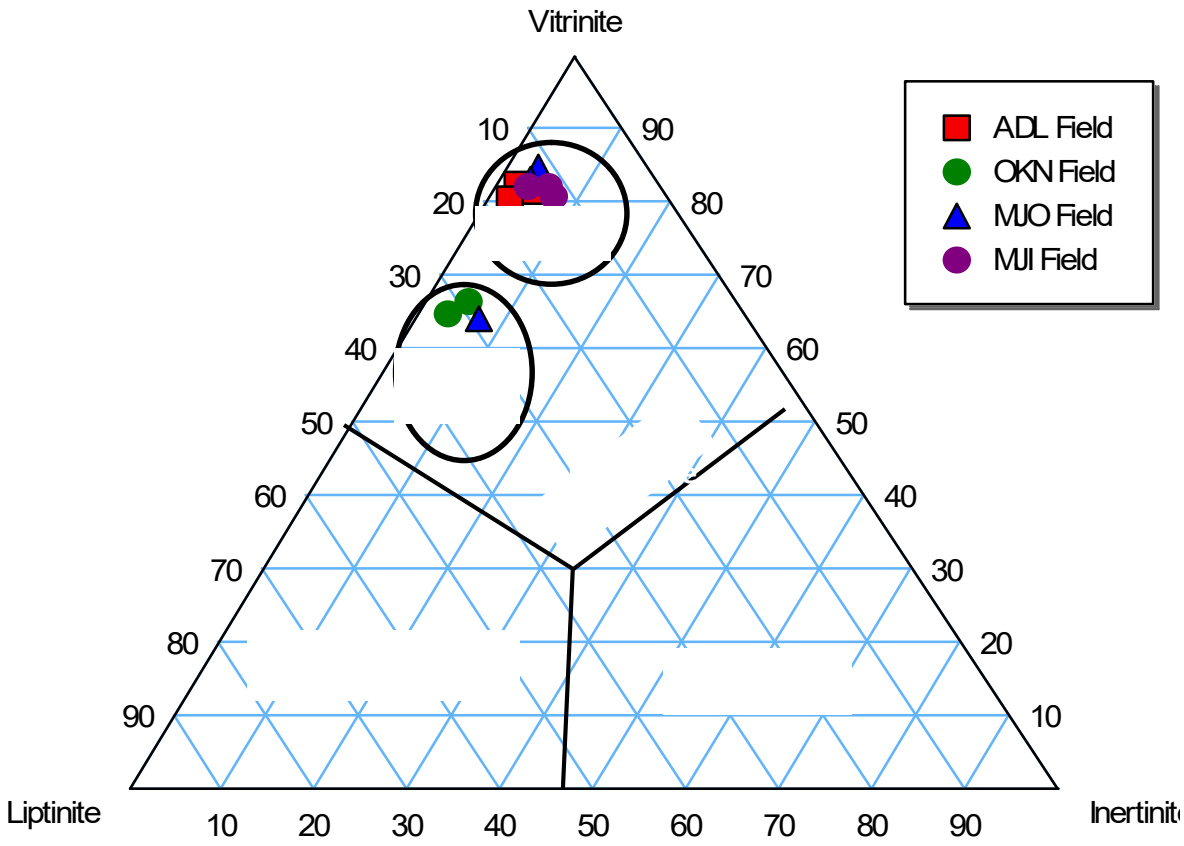

Fig. 4.5: Ternary plot of the maceral groups found in the Niger Delta source rocks (modified after Bustin *et al*. 1983).

4.1.2.2 OKN Field

The HI values for OKN samples range between 389 and 993 mgHC/g TOC with an average value of 517.17 mgHC/g TOC. These values indicate type II kerogen, capable of generating oil (Peters 1986; Sachsenhofer *et al.* 1995; Peters *et al*. 2005). The samples fall within type II evolution path on the plots of HI against OI and S_2 against TOC (Fig.s 4.2 and 4.3), indicating oil prone source rock. The T_{max} vs HI plot (Fig. 4.4) further reveal the oil generative potential of the samples The data obtained from the petrological study did not support type II kerogen for OKN samples (Table 4.1). The maceral composition of the organic matter is consistent with the source rocks of Type III kerogen. Fig. 4.5 shows that the dominant component of the samples in OKN field is vitrinite (48 to 61%). However, the rock samples have significant values of liptinite (26-39%) and low amounts of inertinite (3-5%). The liptinite values indicate significant marine contribution to the organic matter (Bustin *et al*., 1983, 1988). A ternary plot of the three major maceral groups in the source rocks (Fig. 4.5) reveals a duroclaritic nature of the maceral distribution indicating similar rank (Akande *et al*., 2005).

4.1.2.3 MJI Field

The HI values in the rock samples range from 38 to 126 mgHC/g TOC. Most of the samples are of type IV kerogen with HI values < 50 mg/g while few samples are of type III. (Peters 1986; Sachsenhofer *et al*. 1995).However, the samples fall within type III evolution path on the plots of HI against OI and S_2 against TOC (Fig.s 4.2 and 4.3), indicating gas prone (Killops and Killops 1993, 2005). The potential of the samples to generate mainly gas was further confirmed on the plot of T_{max} vs HI where all the samples plotted within the gas prone zone (Fig.4.3).

A predominantly terrestrial origin (Type III kerogen) of organic matter in the MJI source rocks is supported by the petrological data (Table 4.1). The maceral composition of the organic matter is consistent with a higher plant source. Fig. 4.5 shows that the dominant component of all the rock samples is vitrinite (73 to75%) (Bustin *et al*., 1983, 1988). The rock samples are characterized by very low abundances of liptinite (11 to 13%) and inertinite (3 to 6%). The low liptinite values indicate low marine contribution to the organic matter that formed the source rocks (Bustin et al., 1983, 1988). A ternary

plot of the three major maceral groups in the source rocks from MJI field (Fig. 4.5) reveals a duroclaritic nature of the maceral distribution showing a strong similarity, indicating similar rank (Akande *et al*., 2005).

4.1.2.4 MJO Field

The HI values vary from 31 - 217mg/g TOC (Table 4.1). These low HI values indicate Type III kerogen, capable of generating mainly gas (Peters 1986; Sachsenhofer *et al*. 1995). The samples fall within Type III kerogen zone on the plots of HI against OI and S_2 against TOC (Fig.s 4.2 and 4.3). The T_{max} vs HI plot (Fig. 4.4), further reveal that the samples are gas prone. These features confirm their gas generative potential. However, two samples fall within oil and gas zone.

A predominantly terrestrial origin (Type III kerogen) of organic matter in the source rocks is supported by the petrological data (Table 4.1). The maceral composition of the organic matter is consistent with a higher plant source. The dominant component of all the study samples is vitrinite (58-80%) (Fig. 4.5) indicating Type III kerogen (Bustin *et al*., 1983, 1988). Most of the samples are characterized by very low abundances of liptinite (11-26%) and inertinite (3-6%). The low liptinite values indicate low marine contribution to the organic matter that formed the source rocks (Bustin *et al*., 1983, 1988). A ternary plot of the three major maceral groups in the source rocks (Fig. 4.5) reveals a duroclaritic nature of the maceral distribution showing a strong similarity among the majority of the samples (Akande *et al*., 2005).

4.1.2.5 WZB Field

The HI values in the rock samples range from 24 - 174 mgHC/g TOC while the coaly shale has HI value of 626 mg/HCg TOC. These low HI values indicate Type III kerogen, capable of generating mainly gas (Peters 1986; Sachsenhofer *et al*. 1995; Peters et al., 2005). The samples fall within type III evolution path on the plots of HI vs OI (Fig. 4.2) and S2 vs. TOC (Fig. 4.3), indicating gas prone (Killops and Killops 1993, 2005). The potential of the samples to generate mainly gas was further confirmed on the plot of Tmax vs HI where all the samples plotted within the gas prone zone (Fig. 4.4). However, the coaly shale plotted within the oil zone.

4.1.3 Thermal Maturity of Organic Matter

The thermal maturity status of the rock samples was determined using Rock –Eval pyrolysis parameters (T_{max}, Production index (PI), plots of PI vs. T_{max} and plots of HI vs. T_{max}) and Vitrinite reflectance measurements from petrographic analyses.

4.1.3.1 ADL Field

The T_{max} and PI values of the rock samples range from 415 to 438 ˚C and 0.05 to 0.59, respectively (Table 4.1). These values suggest immature to early mature source rocks (Peters *et al*., 2005). The vitrinite reflectance (Ro) values range from 0.30 to 0.42 %Ro. These values show that the samples are immature (Killops and Killops, 2005; Peters et al., 2005).

The Vitrinite reflectance values estimated from the plot of HI vs. T_{max} (Fig. 4.6) range from 0.25 to 0.65 %Ro reflecting immature to early oil window. The samples plotted within immature and oil zones on the plot of PI vs. T_{max} (Fig.4.7) indicating immature to early mature source rocks (Peters *et al*., 2005).However, measured vitrinite reflectance is more reliable than the estimated vitrinite reflectance.

4.1.3.2 OKN Field

The T_{max} and PI values in the rock samples range from 381 to 418˚C and 0.06 to 0.26 respectively (Table 4.1). The low T_{max} values indicate immature source rock while the PI values indicate immature to peak of oil window (Peters *et al*., 2005). The vitrinite reflectance (Ro) values of the samples range from 0.23 to 0.31 %Ro. These values indicate that the source rocks are thermally immature (Killops and Killops, 2005; Peters *et al*., 2005). The vitrinite reflectance values estimated from the plot of HI vs. T_{max} (Fig.4.6) show VR values that are less than 0.5 %Ro reflecting diagenetic stage. These values agree with the vitrinite reflectance data obtained from the petrographic analysis. The plot of PI vs. T_{max} (Fig.4.7) further reveals that the samples are thermally immature

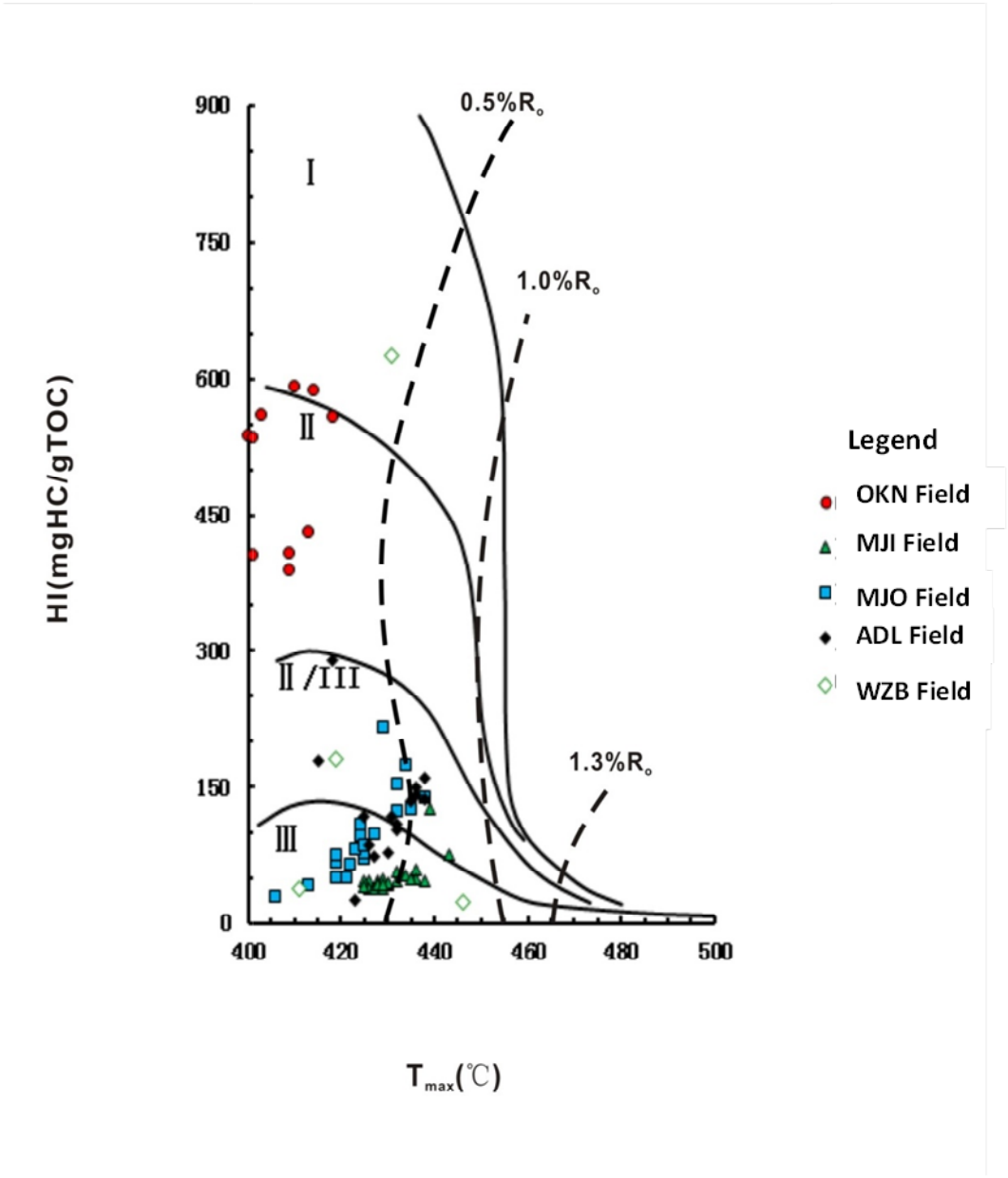

Fig. 4.6 : Plots of HI vs T_{max} of rock samples from Niger Delta, Nigeria (after Mukhopadhyay *et al*., 1995)

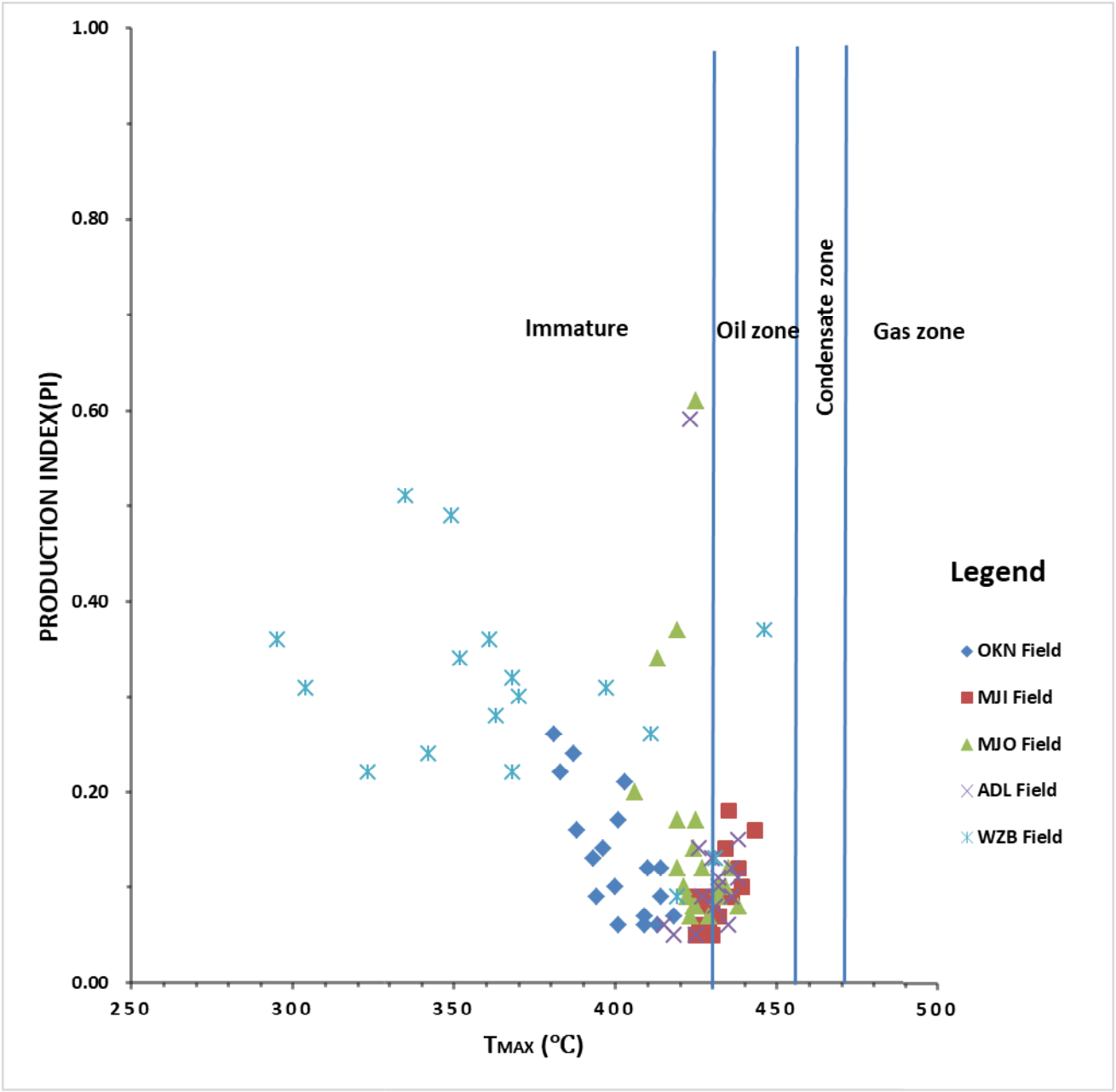

Fig. 4.7: Plots of PI vs Tmax of rock samples from Niger Delta, Nigeria

4.1.3.3 MJI Field

The T_{max} and PI values in the samples range from 425 to 443˚C and 0.05 to 0.18 respectively (Table 4.1). These values suggest immature to early mature source rocks (Peters *et al*., 2005).However, most of the samples are thermally immature. The vitrinite reflectance (Ro) values of the samples range from 0.21 to 0.50 %Ro. These values indicate diagenesis to early oil window (Killops and Killops, 2005; Peters *et al*., 2005). Vitrinite reflectance values estimated from the plots of HI vs. T_{max} for the samples range from 0.42 to 0.75 %Ro with most of the samples having VR of less than 0.5 %Ro (Fig. 4.6). These values further confirmed diagenesis to early oil window maturity stage. However, there is subtle difference between the vitrinite reflectance data obtained from the petrographic analysis and estimated vitrinite reflectance. The samples plotted within immature and oil zones on the plot of PI vs. T_{max} (Fig.4.7), indicating immature to early mature source rocks (Peters *et al*., 2005).

4.1.3.4 MJO Field

The T_{max} and PI values of the rock samples range from 406 to 438 ˚C and 0.07 to 0.61 respectively (Table 4.1). These values indicate immature to early mature source rocks (Peters *et al*., 2005). The vitrinite reflectance (Ro) values of the samples range from 0.2 to 0.43 %Ro (av. 0.36 %Ro). These low values indicate diagenetic stage (Killops and Killops, 2005; Peters *et al*., 2005). The vitrinite reflectance values estimated from the plot of HI vs. T_{max} (Fig. 4.6) range from 0.12 to 0.65 %Ro indicating immature to early oil window. However, there is subtle difference between the vitrinite reflectance data obtained from the petrographic analysis and estimated vitrinite reflectance. The plot of PI vs. T_{max} (Fig. 4.7) further reveals that the samples are at immature to early maturity stage.

4.1.3.5WZB Field

The T_{max} and PI values of the samples range from 295 to 446 ˚C and 0.09 to 0.51 respectively (Table 4.1). The T_{max} values suggest that the source rocks are at the stage of immature to peak of oil window while the PI values imply immature to late oil window (Peters et al., 2005). Most of the samples plotted in the immature zones on the plot of PI

versus T_{max} (Fig. 4.7). The vitrinite reflectance (Ro) values of the samples range from 0.28 to 0.41 %Ro (av. 0.34 %Ro). These values show that the samples are immature (Killops and Killops, 2005; Peters *et al*., 2005). The Vitrinite reflectance values estimated from the plot of HI vs. T_{max}. (Fig.4.6) gave VR values ranging from 0.16 to 0.83 %Ro indicating early diagenesis to peak of oil window.

4.2 Biomarker Geochemistry of Niger Delta Source Rocks

The source, depositional environment and thermal maturity status of the organic matter contained in the rock samples were determined based on the distributions and abundance of aliphatic biomarkers in the source rock extracts.

4.2.1 Source and Depositional Environment of Organic Matter

The m/z 85, 191 and 217 mass chromatograms showing the distribution of n-alkane/ acyclic hydrocarbons, terpanes and steranes in the saturate fraction of the rock extracts are presented in Fig.s4.8, 4.9, 4.10, 4.11 and 4.12. Peak identities are listed in Table 4.2. Geochemical parameters calculated from the abundances of the biomarkers are given in Table 4.3.

4.2.1.1 OKN Field

The n-alkanes in the samples show a unimodal distribution from C_{13}-C_{18} maximizing at n-C_{15}(Fig.4.8). This pattern of distribution indicates organic matter with significant marine contribution (Peters *et al*., 2005). The pristane/phytane (Pr/Ph) ratios for the samples range from 1.51-2.61 (Table 4.3). The Pr/Ph values are consistent with the source rock deposited in suboxic paleoenvironment (Mello and Maxwell, 1990; Roushdy *et al*., 2010). The ratios of Pr/nC_{17} and Ph/nC_{18} range from 0.51 to 2.82 and 0.72 to 6.79, respectively. The rock samples fall within algal organic matter zone on the plot of Pr/nC_{17} against Ph/nC_{18} (Fig.4.13).

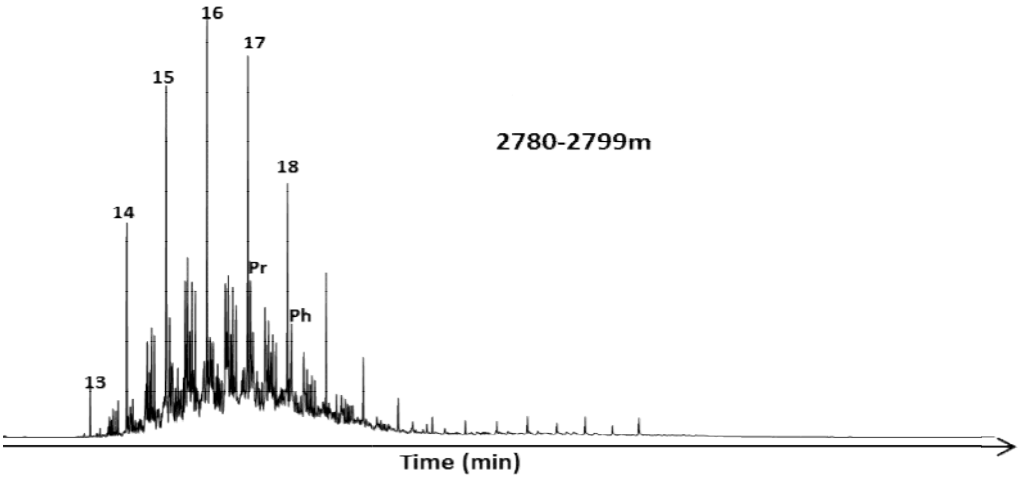
16
17
15
18
14
Pr
Ph
13
2780-2799m
Time (min)

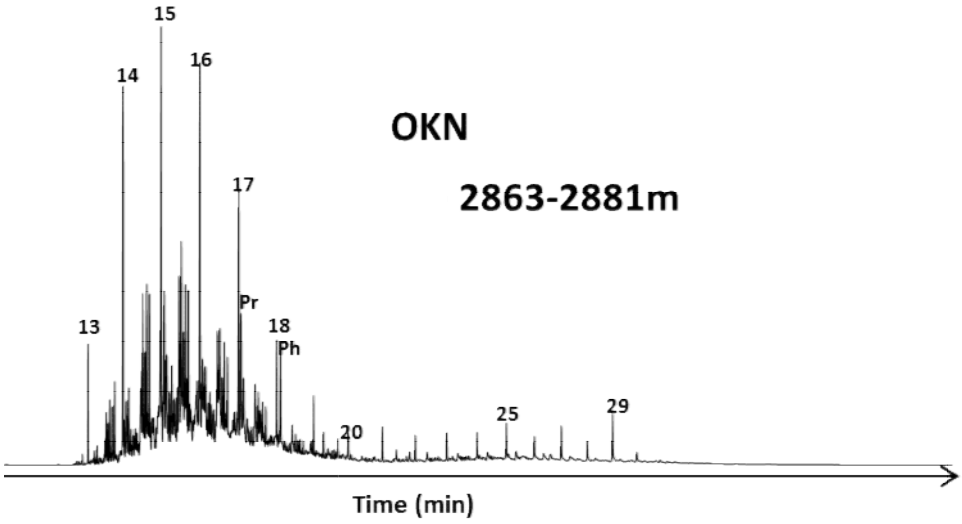
15
16
14
OKN
17
2863-2881m
Pr
13
18
Ph
25
29
20
Time (min)

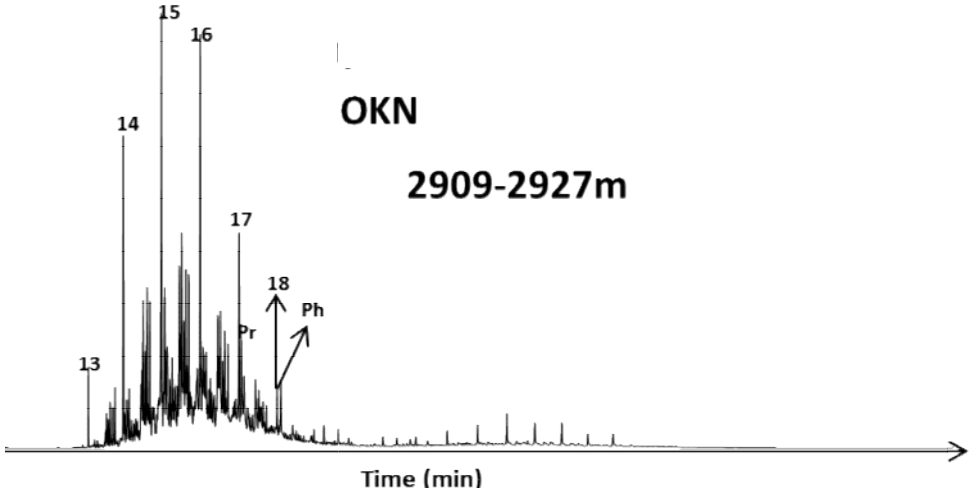
15
16
14
OKN
2909-2927m
17
18
Ph
Pr
13
Time (min)

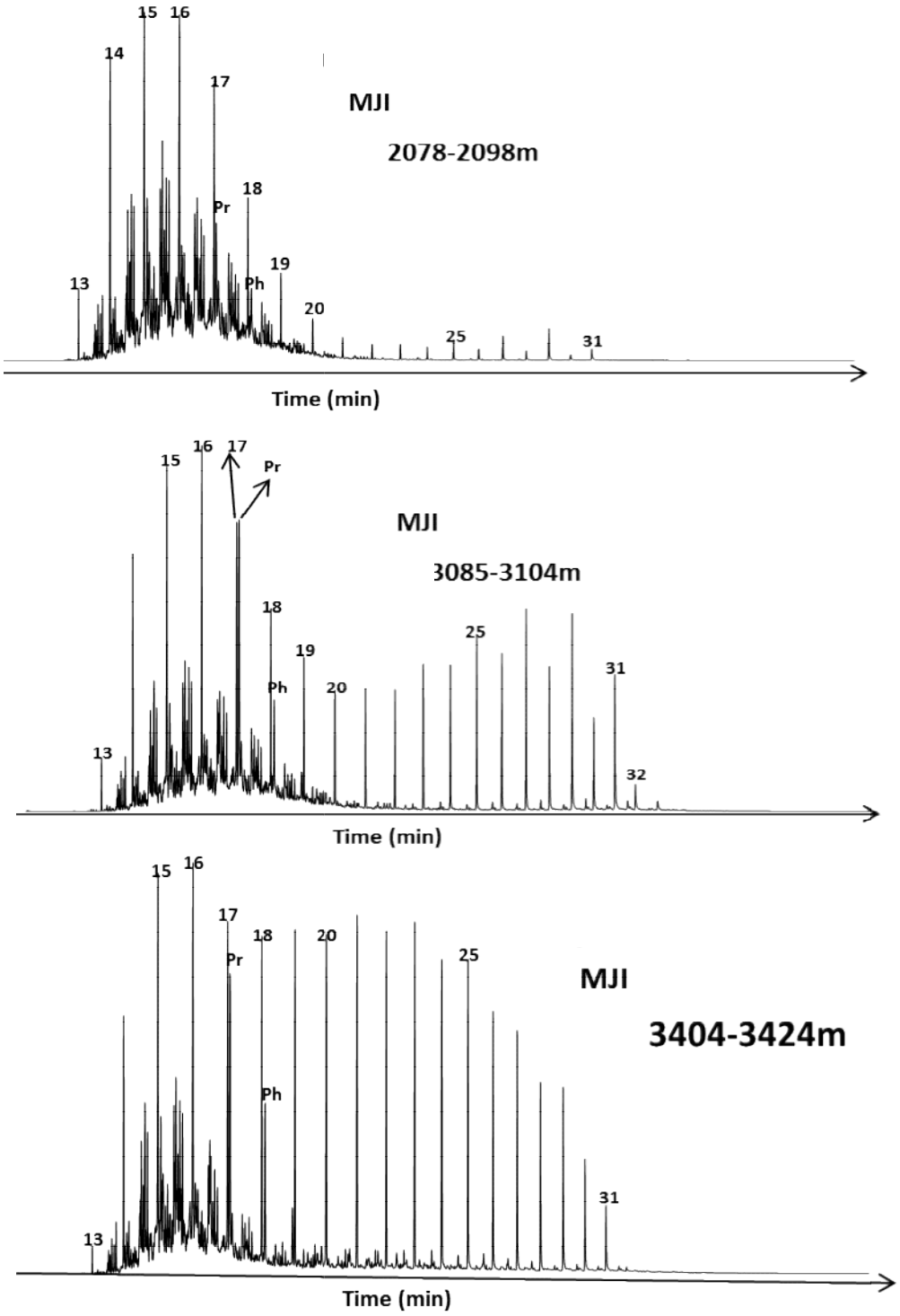

Fig. 4.9: m/z 85 Mass chromatograms of aliphatic fractions of representative rock samples from MJI field showing the distributions of n-alkanes

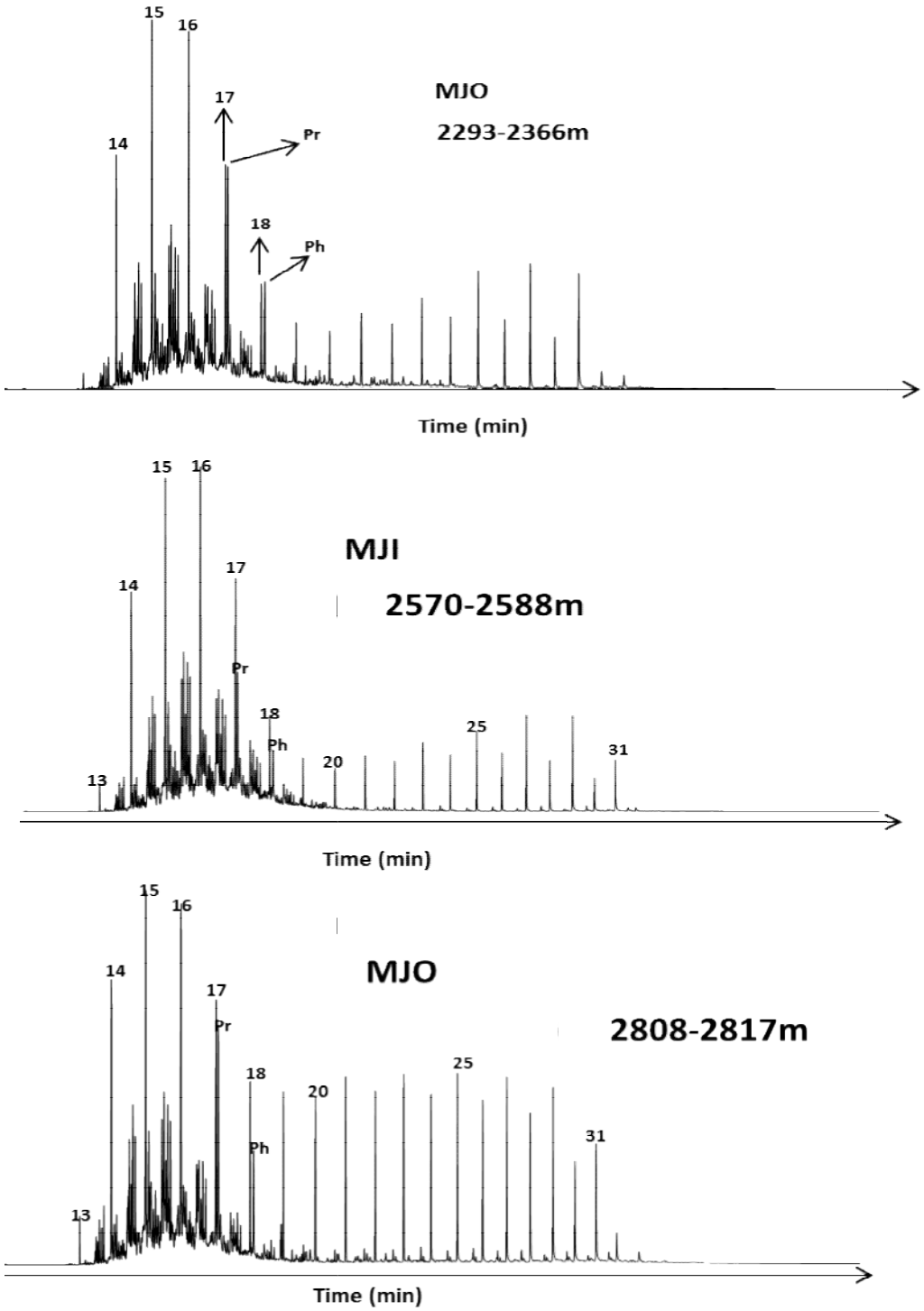

Fig. 4.10: m/z 85 Mass chromatograms of aliphatic fractions of representative rock samples from MJO field showing the distributions of n-alkanes.

Table 4.2: Peak identification on m/z 191 and 217 Mass chromatogram of the Niger Delta source rocks and crude oils

Peak	Compound
Ts	18α(H), 22,29,30-trisnorneohopane
Tm	17α(H),22,29,30-trisnorhopane
C_{29}	17α,21β(H)-norhopane
α-Ole	α-oleanane
$C_{30}H$	17α,21β(H)-hopane
Mor	17β,21α(H)-mortane
Ga	Gammacerane
C_{31}(22S)	17α,21β(H)-30-homohopane (22S)
C_{31} (22R)	17α,21β(H)-30-homohopane (22R)
C_{32}(22S)	17α,21β(H)-30,31-dihomohopane (22S)
C_{32} (22R)	17α,21β(H)-30,31-dihomohopane (22R)
C_{33} (22S)	17α,21β(H)-30,31,32-trihomohopane (22S)
C_{33} (22R)	17α,21β(H)-30,31,32-trihomohopane (22R)
C_{34} (22S)	17α, 21β(H)-30,31,32,33-tetrakishomohopane (22S)
C_{34} (22R)	17α, 21β(H)-30,31,32,33-tetrakishomohopane (22R)
C_{35} (22S)	17α, 21β(H)-30,31,32,33,34-pentakishomohopane (22S)
C_{35} (22R)	17α, 21β(H)-30,31,32,33,34-pentakishomohopane (22R)
S21	C_{21} sterane
S22	C_{22} sterane
27ααaS	C_{27} 5α,14α(H), 17α(H)-sterane (20S)
27ααaR	C_{27} 5α,14α(H), 17α(H)-sterane (20R)
28ααaR	C_{28} 5α, 14α(H), 17α(H)-sterane (20R)
29ααaS	C_{29} 5α, 14α(H), 17α(H)-sterane (20S)
29ααaR	C29 5α, 14α(H), 17α(H)-sterane (20R)

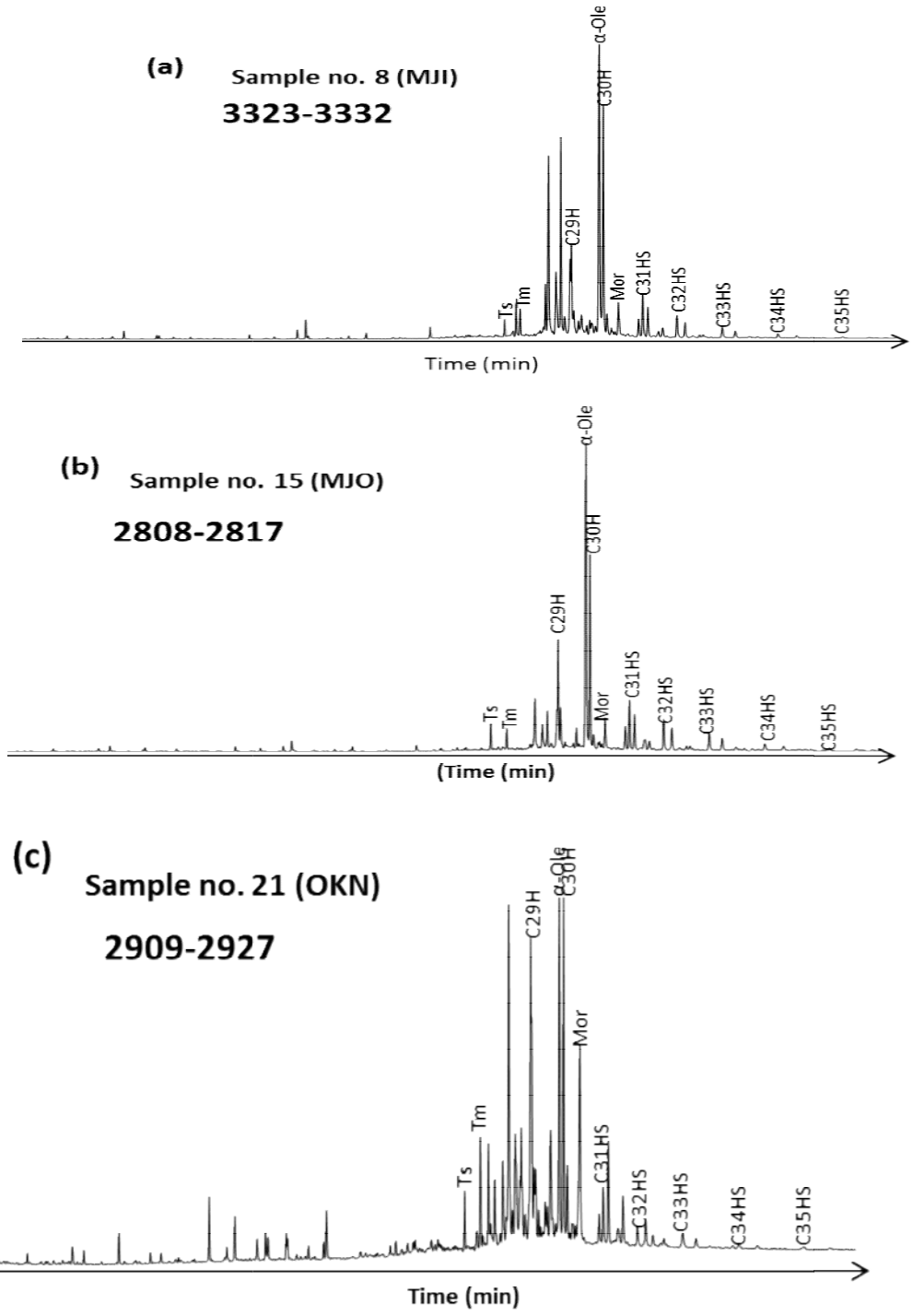
(a)
Sample no. 8 (MJI)
3323-3332
α-Ole
C30H
C29H
Ts
Tm
Mor
C31HS
C32HS
C33HS
C34HS
C35HS
Time (min)
(b)
Sample no. 15 (MJO)
2808-2817
α-Ole
C30H
C29H
Ts
Tm
Mor
C31HS
C32HS
C33HS
C34HS
C35HS
(Time (min)
(c)
Sample no. 21 (OKN)
2909-2927
C29H
α-Ole
C30H
Mor
Tm
Ts
C31HS
C32HS
C33HS
C34HS
C35HS
Time (min)

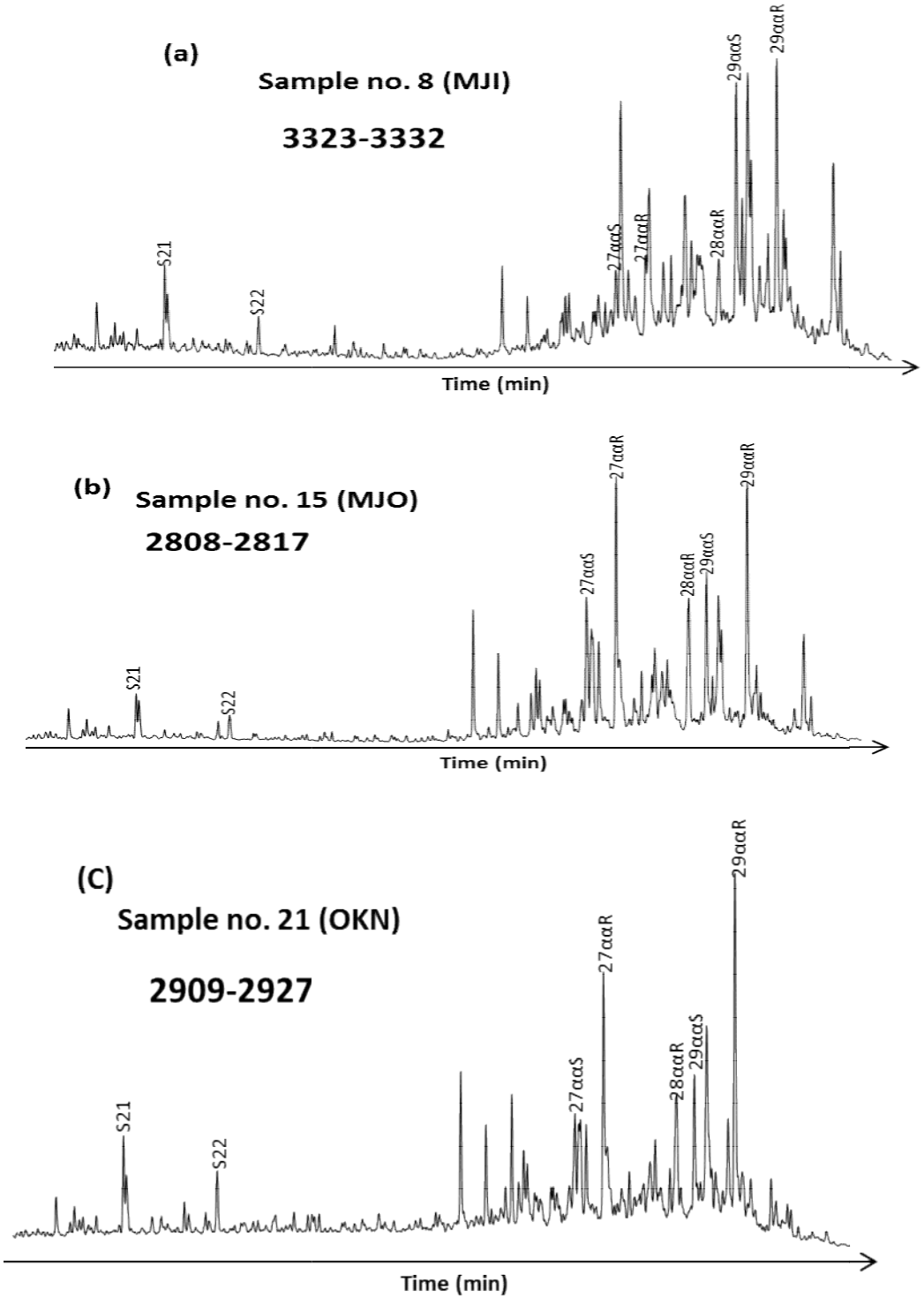
(a)
Sample no. 8 (MJI)
3323-3332
S21
S22
27ααS
27ααR
28ααR
29ααS
29ααR
Time (min)
(b)
Sample no. 15 (MJO)
2808-2817
S21
S22
27ααS
27ααR
28ααR
29ααS
29ααR
Time (min)
(C)
Sample no. 21 (OKN)
2909-2927
S21
S22
27ααS
27ααR
28ααR
29ααS
29ααR
Time (min)

Table 4.3: Source and maturity parameters computed from the saturate hydrocarbon compounds in the rock samples

Sample no.	Field	Depth m	Pr/ Ph	Pr/ C17	Ph/ C18	Olean. index	Ts/ (Ts+Tm)	22S/(22S+22R) C31 hopane	20S/(20S+20R) C29 sterane	Sterane, %		
										C27	C28	C29
1	OKN	1537-1555	1.85	2.82	6.79	0.54	0.59	0.29	0.18	38.15	17.85	44.00
2	OKN	1729-1747	2.61	0.58	0.72	0.52	0.55	0.35	0.14	33.28	18.36	48.36
3	OKN	2625-2643	1.51	1.71	3.63	0.57	0.48	0.35	0.30	39.49	21.25	39.26
4	OKN	2780-2799	1.73	0.64	0.76	1.37	0.25	0.35	0.24	20.66	27.45	51.89
5	OKN	2863-2881	2.06	0.88	1.31	1.33	0.31	0.37	0.34	24.92	27.42	47.66
6	OKN	2909-2927	2.27	0.51	1.42	1.14	0.34	0.35	0.28	31.52	25.18	43.31
7	MJI	2078-2098	3.2	0.54	0.4	1.23	0.24	0.24	0.15	16.51	25.49	58.00
8	MJI	2299-2308	2.31	0.59	0.56	1.26	0.19	0.36	0.15	18.53	21.98	59.49
9	MJI	2637-2655	3.91	0.96	0.64	2.17	0.19	0.46	0.21	17.39	22.24	60.37
10	MJI	2857-2875	3.98	1.13	0.71	2.16	0.27	0.52	0.29	20.15	21.75	58.10
11	MJI	2994-3012	4.26	1.33	0.65	1.43	0.34	0.53	0.30	20.65	23.30	56.05
12	MJI	3085-3104	4.53	1.91	0.79	2.00	0.35	0.58	0.40	16.80	20.31	62.89
13	MJI	3232-3250	2.87	2.8	0.9	1.30	0.34	0.59	0.46	19.85	18.59	61.56
14	MJI	3323-3332	4.46	2.58	0.92	1.46	0.37	0.59	0.52	19.64	20.04	60.32
15	MJI	3405-3424	2.92	1.46	0.63	1.58	0.57	0.58	0.48	29.79	27.84	42.37
16	MJO	1616-1707	4.31	1.03	1.21	0.81	0.24	0.25	0.16	19.02	28.60	52.38
17	MJO	1771-1872	2.16	1.02	1.15	0.59	0.29	0.35	0.41	17.85	27.78	54.37
18	MJO	2091-2101	2.08	2.23	5.94	3.37	0.17	0.30	0.21	17.28	28.78	53.94
19	MJO	2293-2366	2.96	1.73	1.66	1.11	0.18	0.42	0.13	24.44	26.46	49.11
20	MJO	2570-2588	3.5	0.99	1.07	1.70	0.32	0.54	0.19	27.78	28.58	43.64
21	MJO	2808-2817	3.6	1.51	0.84	2.09	0.57	0.57	0.38	34.65	27.05	38.30

*OI:Oleanane index = 18α(H)-oleanane/17α(H), 21β(H)-hopane

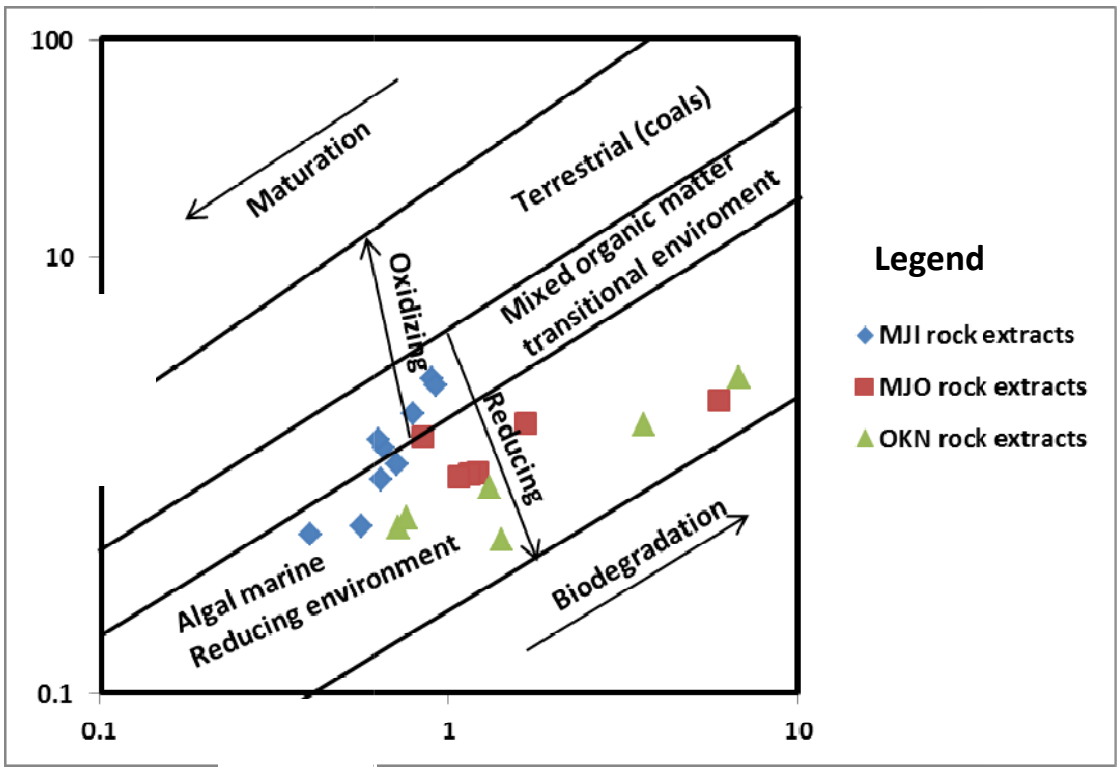

Fig. 4.13: Cross plot of Pr/nC_{17} against Ph/nC_{18} of rock samples from Niger Delta (Modified after Shanmugan, 1985)

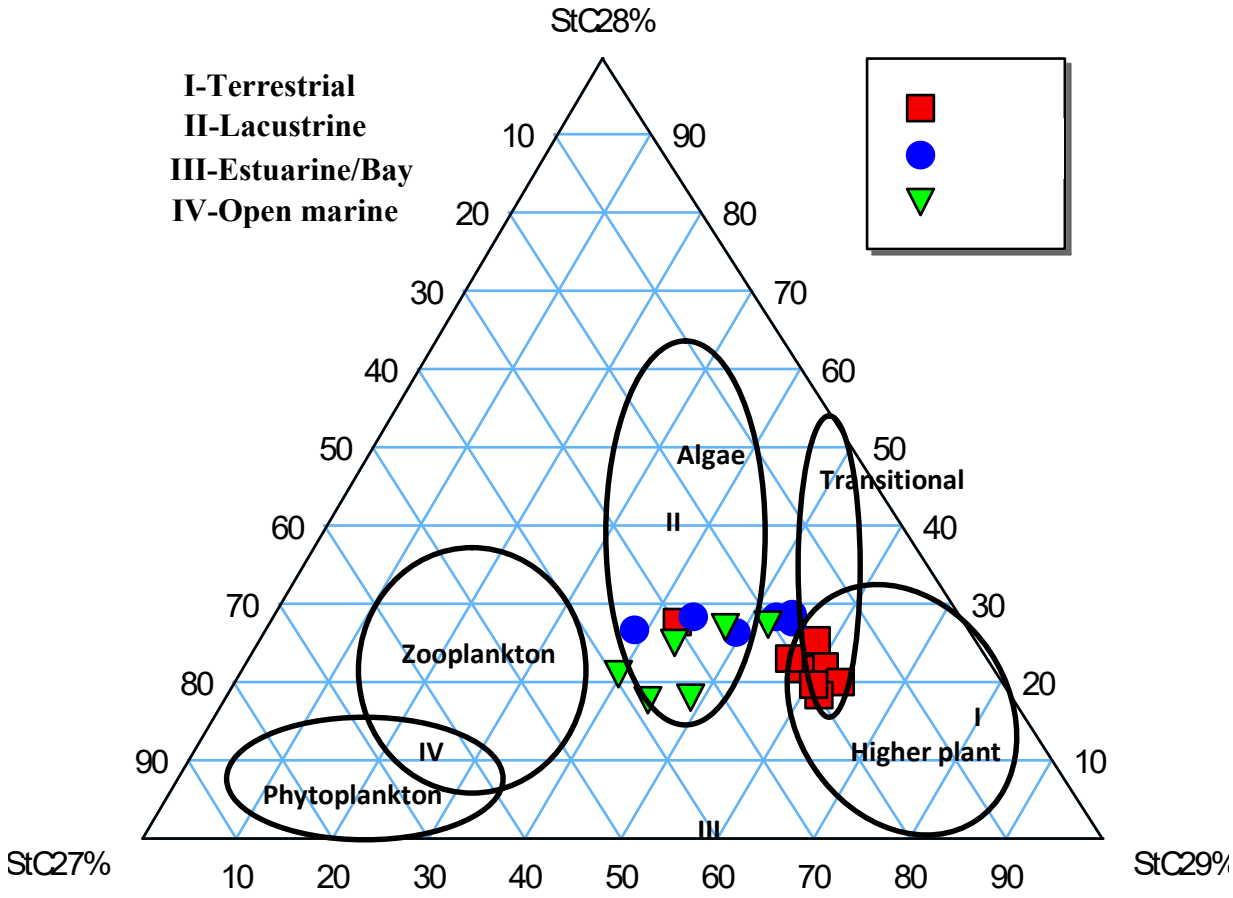

Fig. 4.14: Ternary plot of C_{27}, C_{28} and C_{29} sterane distributions in source rocks from Niger Delta (after Huang and Meinschein, 1979).

The presence of appreciable amounts of oleanane (Fig. 4.11c) in the rock samples indicate an input of terrestrial higher plants into the source rocks and deltaic depositional environment (Whitehead, 1974; Ekweozor *et al*., 1979; Philp and Gilbert, 1986). The abundance of C_{27}-C_{29} steranes (Fig.s 4.12c and 4.14) in the source rocks (Table 4.2) indicates mixedorigin for the source rocks but with higher contribution from marine organic matter(Huang and Meinscchein, 1979).

4.2.1.2 MJI Field

The n-alkanes in the samples show a bimodial distributions maximizing at n-$C_{16}$and n-C_{27}(Fig.s 4.9). This pattern of distribution indicates organic matter derived from mixed (marine and terrestrial) organic matter (Peters *et al*., 2005). The pristane/phytane (Pr/Ph) ratios for the samples range from 2.31 to 4.46 (Table 4.3). The high Pr/Ph ratios suggest source rock with a significant terrestrial contribution, deposited in an oxic paleoenvironment (Didyk *et al*., 1978; Mello and Maxwell, 1990). The Pr/nC_{17} and Ph/nC_{18} ratios range from 0.54 to 2.58 and 0.40 to 0.92 respectively. A plot of Pr/nC_{17} against Ph/nC_{18} ratios in Fig.4.13 indicate that the samples are of mixed origin (Connan and Cassou, 1980). This is consistent with the previous studies on source rocks from Niger Delta (Okoh and Nwachukwu, 1997; Akinlua and Torto, 2011; Faboya *et al*., 2014.

The presence of oleanane (Fig. 4.9a) in the samples indicates source rocks with input of terrestrial higher plants and deposited in a deltaic environment (Whitehead, 1974; Philp and Gilbert, 1986). The abundance of C_{27}-C_{29} steranes (Fig.s. 4.12a and 4.14) in the source rocks (Table 4.2) further support the mixed origin (terrestrial and marine) of the source rocks but with major contribution from terrestrial plants(Huang and Meinschein, 1979).

4.2.1.3 MJO Field

The n-alkanes in samples show a bimodial distributions maximizing at n-C_{15} and n-C_{27}(Fig. 4.10). This pattern of distribution indicates organic matter derived from mixed (marine and terrestrial) organic matter (Peters *et al*., 2005). The pristane/phytane (Pr/Ph) ratios for the samples range from 2.08 to 3.60 (Table 4.3). The Pr/Ph ratios suggest source rock of strong terrestrial origin, deposited in an oxic to suboxic

Paleoenvironment (Didyk *et al*., 1978; Mello and Maxwell, 1990). The Pr/nC_{17} and Ph/nC_{18}ratios range from 1.02 to 2.23 and 0.84 to 5.94 respectively. The rock samples fall within the marine organic matter zone on the plot of Pr/nC_{17} and Ph/nC_{18} ratios (Fig. 4.13).

The rock samples also show abundance of oleanane (Fig. 4.9b), an indication of input of terrestrial higher plants into the source rocks and deltaic depositional environment (Whitehead, 1974; Ekweozor *et al*., 1979; Philp and Gilbert, 1986). The abundance of C_{27}-C_{29} steranes (Figs. 4.12b and 4.14) in the source rocks (Table 4.2) also gives credence to the mixed origin of the source rocks (terrestrial and marine) (Huang and Meinschein, 1979).

4.2.2 Thermal Maturity of Organic matter

4.2.2.1 OKN Field

The values of Ts/(Ts+Tm) ratios in the rock samples range from 0.25 to 0.59 (Table 4.3). These values indicate immature to mature source rocks (Peters *et al*., 2005). The 22S/(22S+22R) C_{31} hopane and 20S/(20S+20R) C_{29} sterane values range from 0.29 to 0.37 and 0.14 - 0.34, respectively (Table 4.3). Cross plots of these two parameters revealed that most of the samples are thermally immature (Fig. 4.15). These maturity parameters show no trend with increasing depths (Fig. 4.16).

4.2.2.2MJI Field

The Ts/(Ts + Tm) ratios for the rock samples range from 0.19 to 0.57 (Table 4.3). These values indicate immature to early mature source rocks (Peters *et al*., 2005). The 22S/(22S+22R) C_{31}hopane and 20S/(20S+20R) C_{29} sterane values range from 0.24 to 0.59 and 0.15 to 0.52, respectively. Cross plot of this parameter supports the immature to early oil window maturity status of the samples (Fig. 4.15). The maturity of the rock samples generally increases with increasing depths (Fig. 4.16).

4.2.2.3 MJO Field

The Ts/(Ts + Tm) ratios range from 0.17 to 0.57 (Table 4.3), indicating immature to early oil window (Peters *et al*., 2005). The 22S/(22S+22R) C_{31} hopane and

20S/(20S+20R) C_{29} sterane values range from 0.25 to 0.57 and 0.13 to 0.38, respectively (Table 4.3). Cross plots of these two parameters indicate that the samples have immature to early mature maturity status (Fig. 4.15). The maturity of the samples increases with increasing depths (Fig. 4.16).

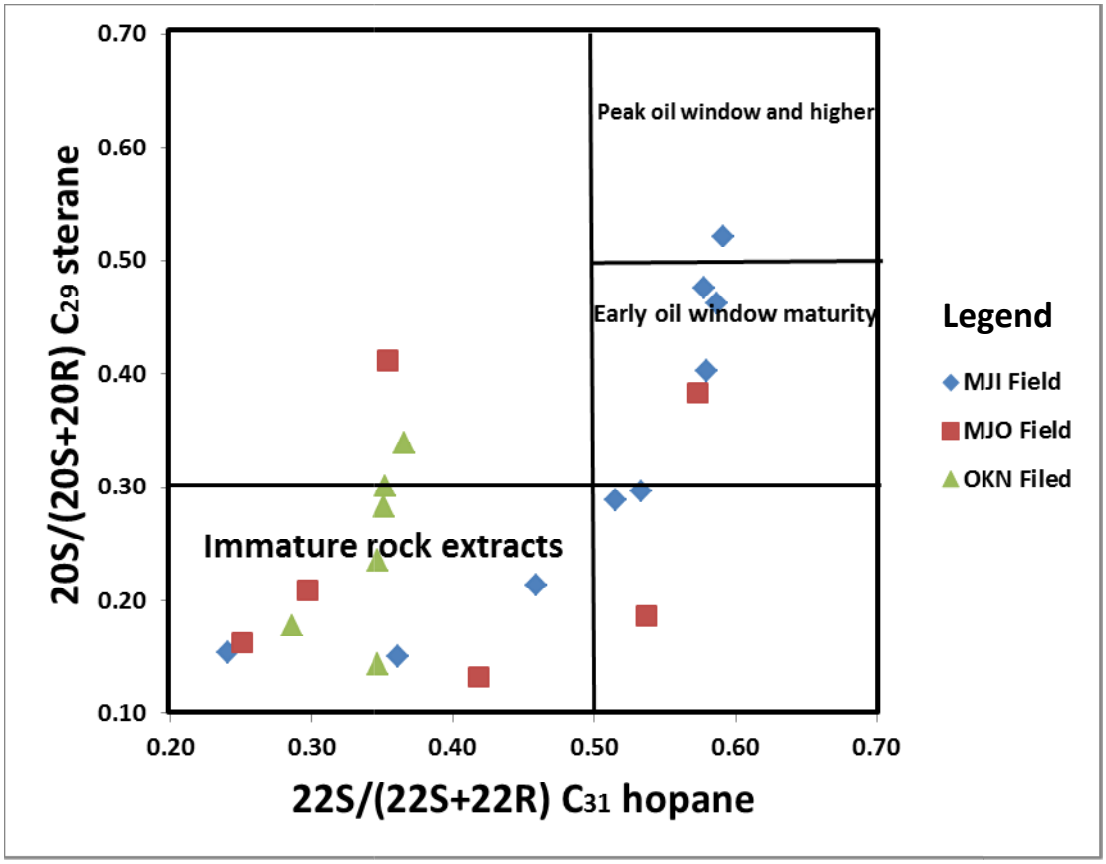

Fig. 4.15: Cross plots of 22S/(22S+22R) C_{31} hopane versus 20S/(20S+20R) C_{29} steraneof source rocks from Niger Delta (modified after Peters and Moldowan, 1993)

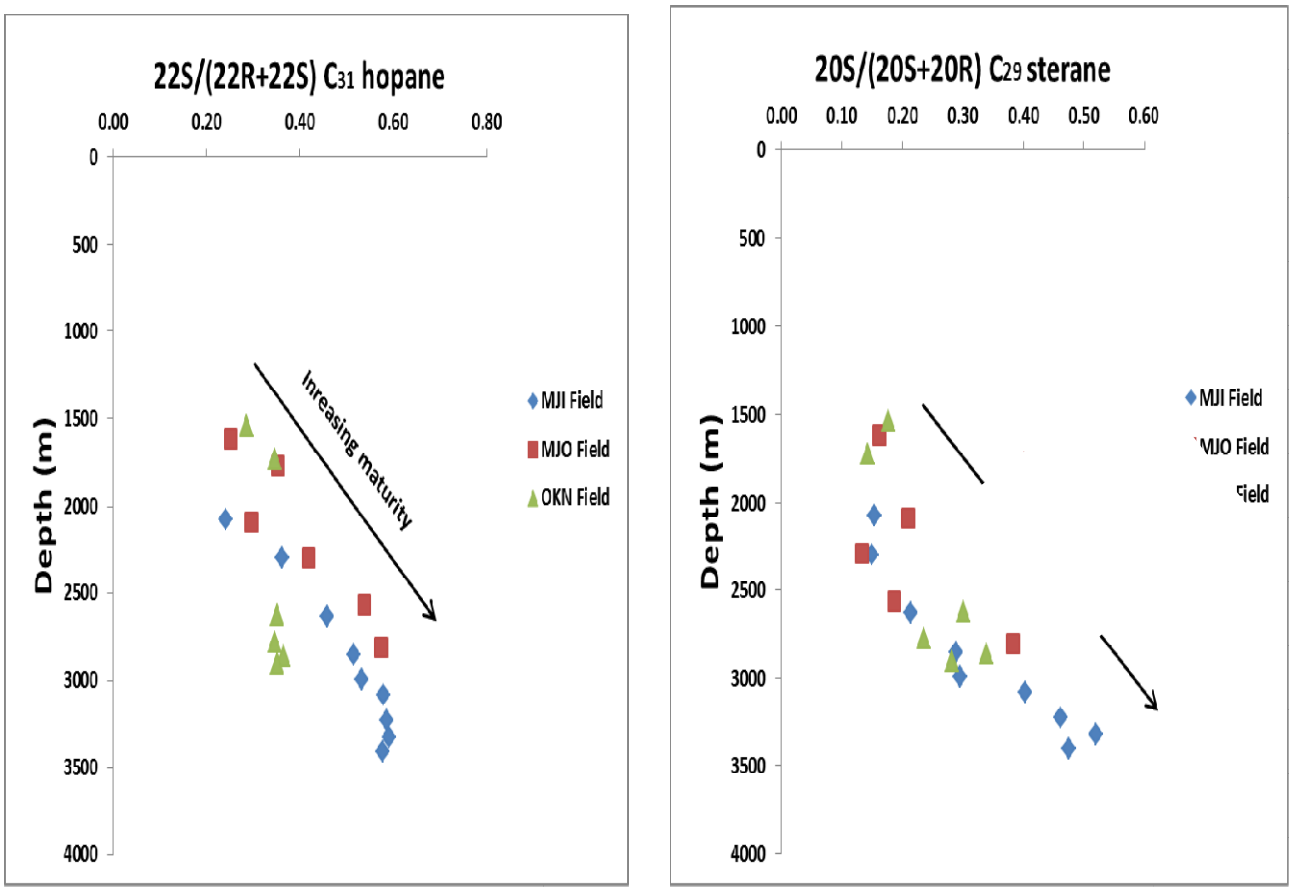

Fig. 4.16: Plots of source rocks maturity parameters with increasing depths (modified after Peters *et al*., 2005)

4.3 Aromatic Hydrocarbon distributions

The m/z 170, 184, 192, 231, 228+242, 202 and 216 mass chromatograms showing the distributions of methylnaphthalene, methylphenanthrenes, methylbenzothiphenes, triaromatic steroids, Chrysene, methylchrysenes, pyrene and methylpyrenes in the aromatic fractions of the representative source rocks are shown in Fig.s 4.17, 4.18, 4.19, 4.20, 4.21, 4.22 and 4.23, respectively. Peak identities are given in Table 4.4 while parameters calculated from the aromatic hydrocarbon distributions are shown in Table 4.5. These compounds were used to assess the origin, depositional environment and thermal maturity of the source rocks.

4.2.3.1 OKN Field

The occurrence of 9- and 1-methylphenanthrene in the rock samples indicates source rocks of mixed origin (marine and terrestrial) (Budzinski et al., 1995). Also, the presence of 1,7-DMP (pimanthrene) in the samples indicate terrestrial organic matter (Simoneit et al., 1986). The plots of 9-MP/1-MP+9-MP ratio against Paq (nC_{23} + nC_{25}/ nC_{23} + nC_{25} + nC_{29} + nC_{31} – alkanes) for the samples indicate that the samples are from different sources (Fig.4.24a). The dibenzothiophene/phenanthrene (DBT/P) ratio of the rock samples range from 0.05 to 0.09, indicating source rock with significant contribution from higher plant organic matter and deposited in deltaic environment (Requejo, 1994; Sivan *et al*., 2008). A plot of dibenzothiophene/phenanthrene (DBT/P) versus Pr/Ph ratios further confirmed the marine or lacustrine shale origin of the rock samples (Fig. 4.24b). The ratios C_{26}/C_{28} 20S and C_{27}/C_{28} 20R of triaromatic steroids in the studied source rocks range from 0.08 to 0.34 and 0.79 to 1.43, respectively. This indicates that the rock samples were formed strongly from marine organic matter.

The presence of 1,6-, 1,7-, and 2,6-DMNs in all the samples indicate terrestrial organic matter input (Day and Edman, 1963; Achari *et al.*, 1973).The presence of 1,2,5- and 1,2,7-TMN in the rock samples indicate both angiosperm and gymnosperms material contribution to the source rocks (Killops and Killops, 2005). The occurrence of 1,2,6-TMN in the rock samples indicate microbial input into the organic material from which the source rocks were formed (Killops and Killops, 2005; Alexander *et al*., 1992).

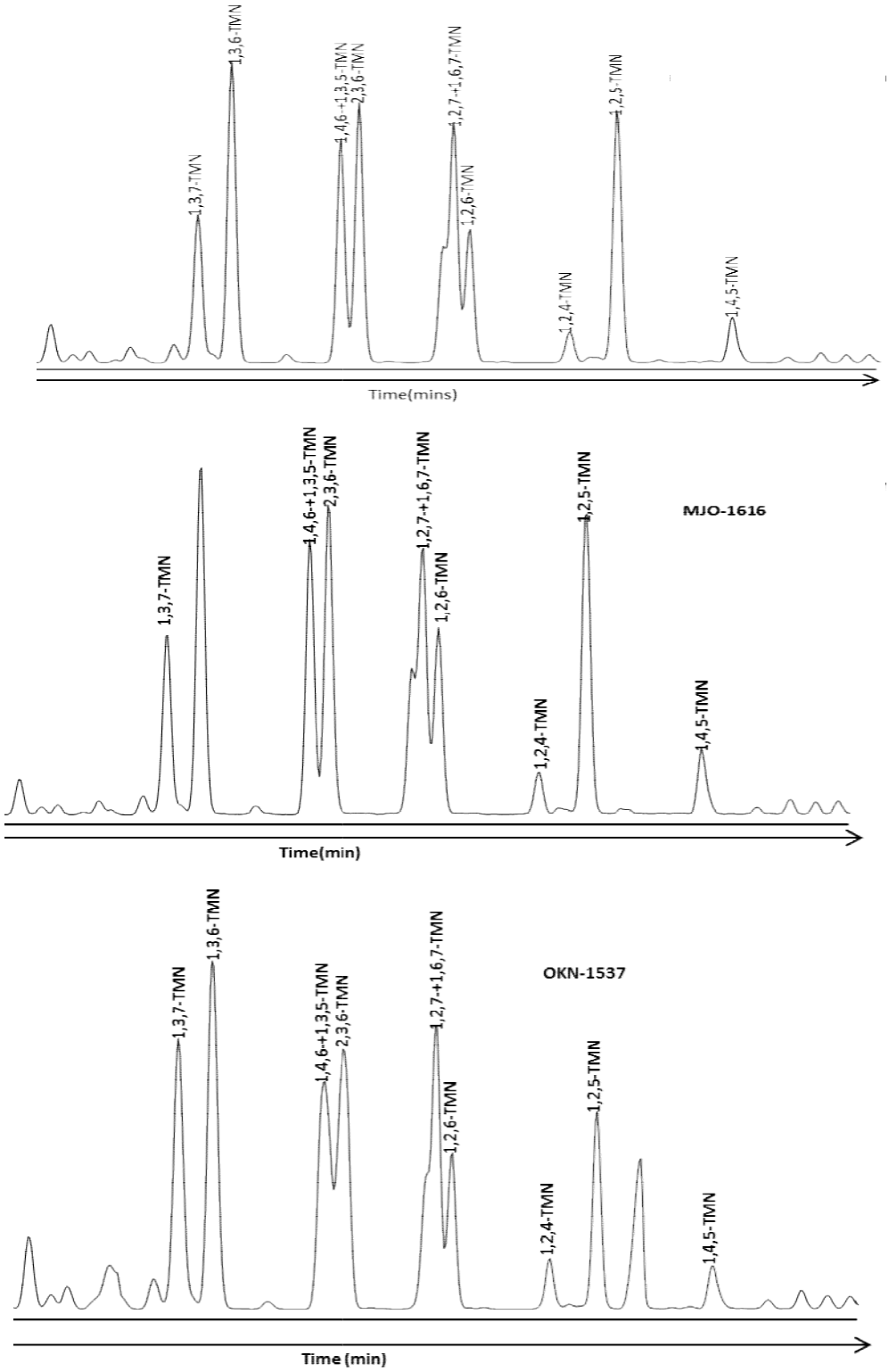

Fig.4.17 :m/z 170 Mass chromatogram showing the distribution of trimethylnaphthalenes in representative rock sample from Niger Delta

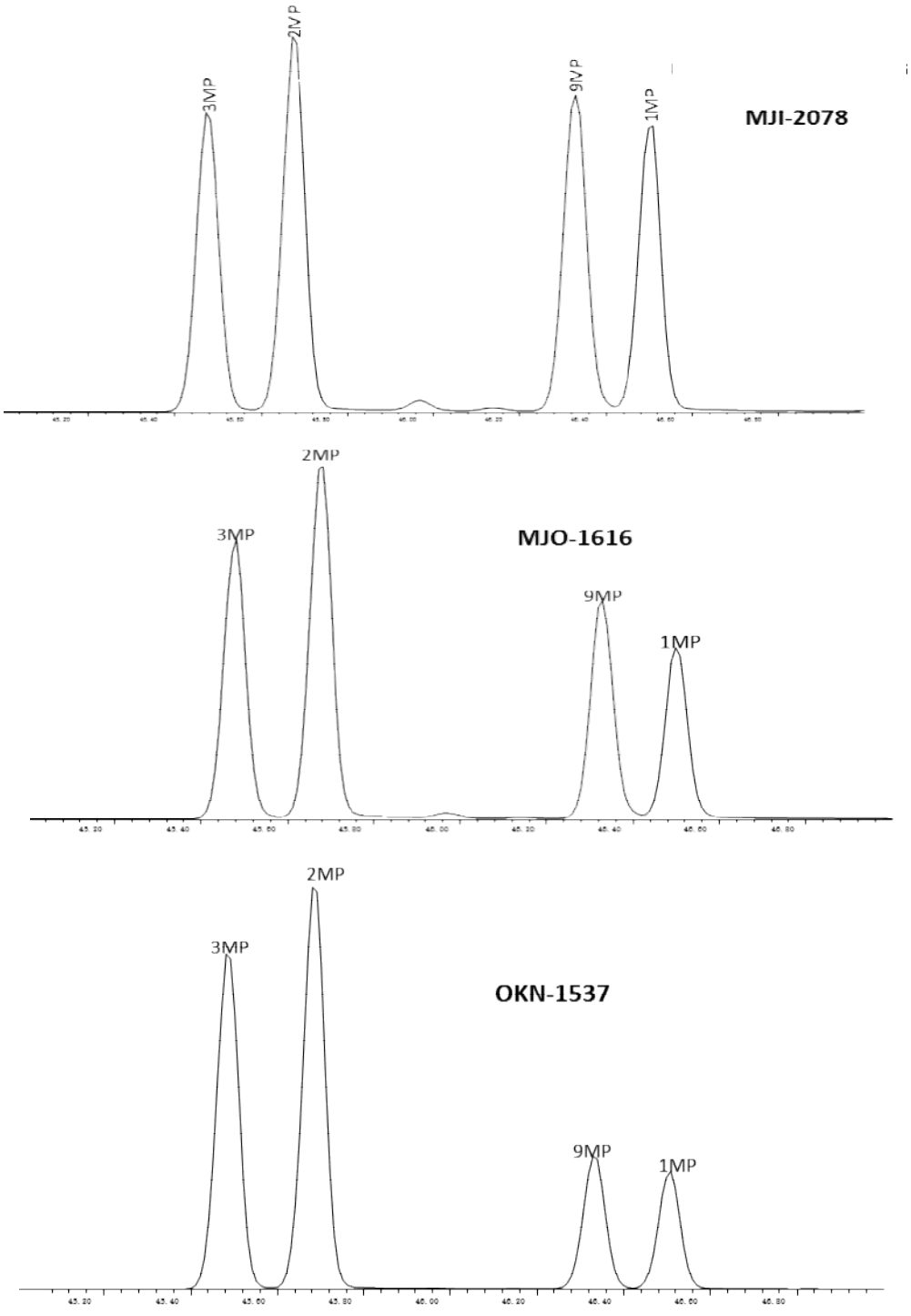

Fig. 4.18: m/z 192 Mass chromatograms showing the distribution of Methylphenanthrenes in representative rock samples from Niger Delta

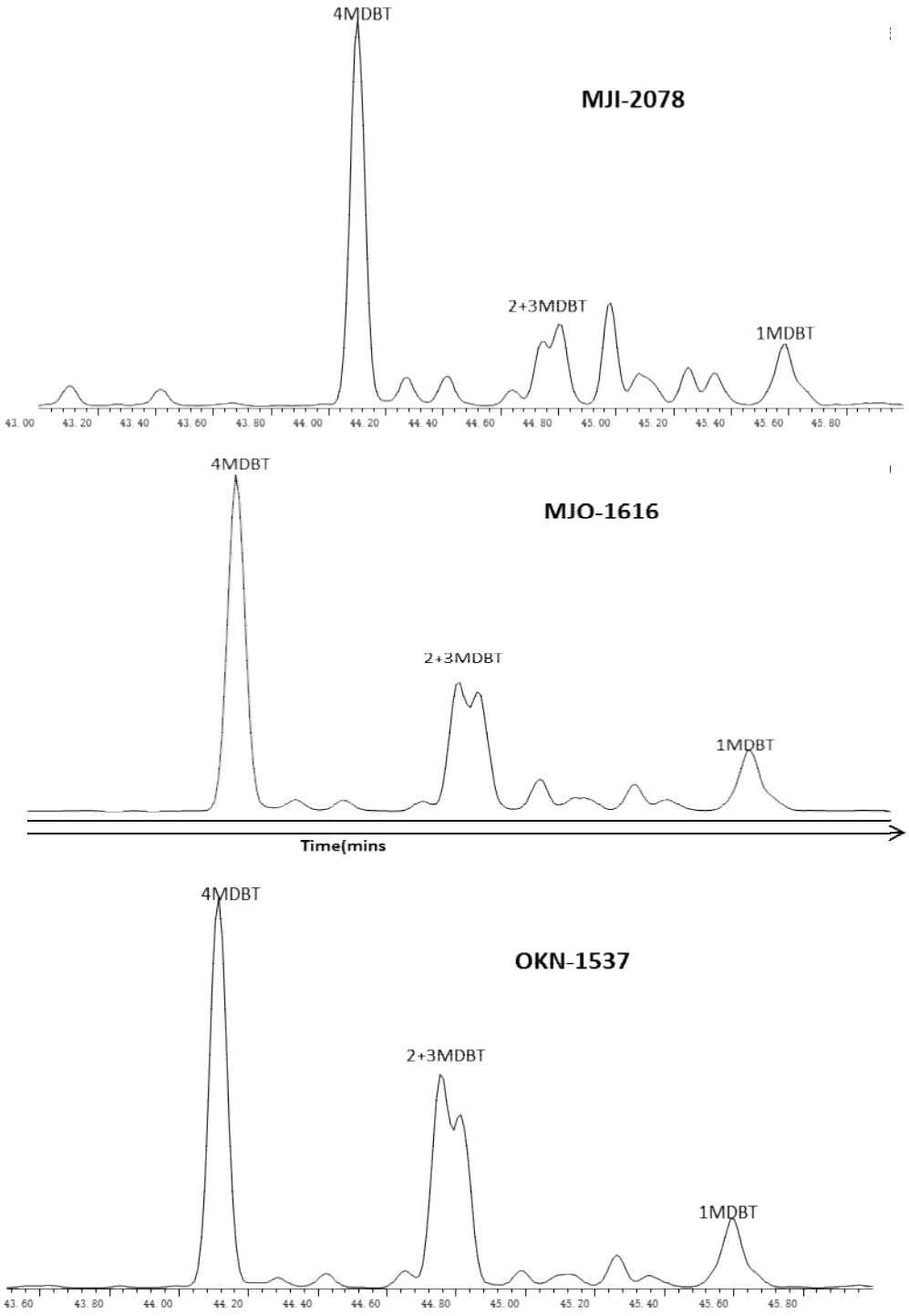

Fig.4.19 :m/z 198 Mass chromatograms showing the distribution of methyldibenzothiophenes in representative rock samples from Niger Delta

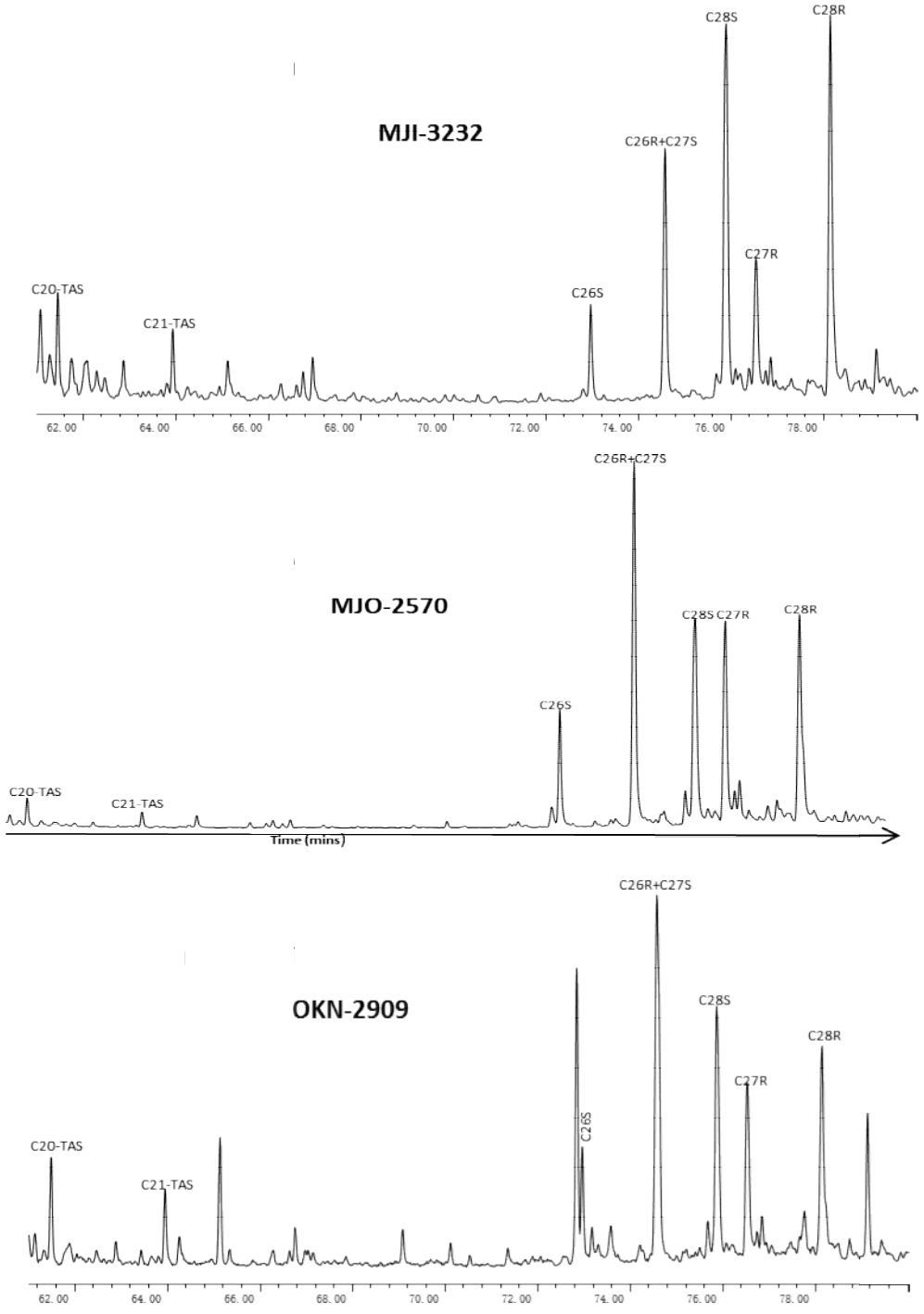

Fig.4.20 :m/z 231 Mass chromatograms showing the distribution of triaromatic steroids in representative rock samples from Niger Delta

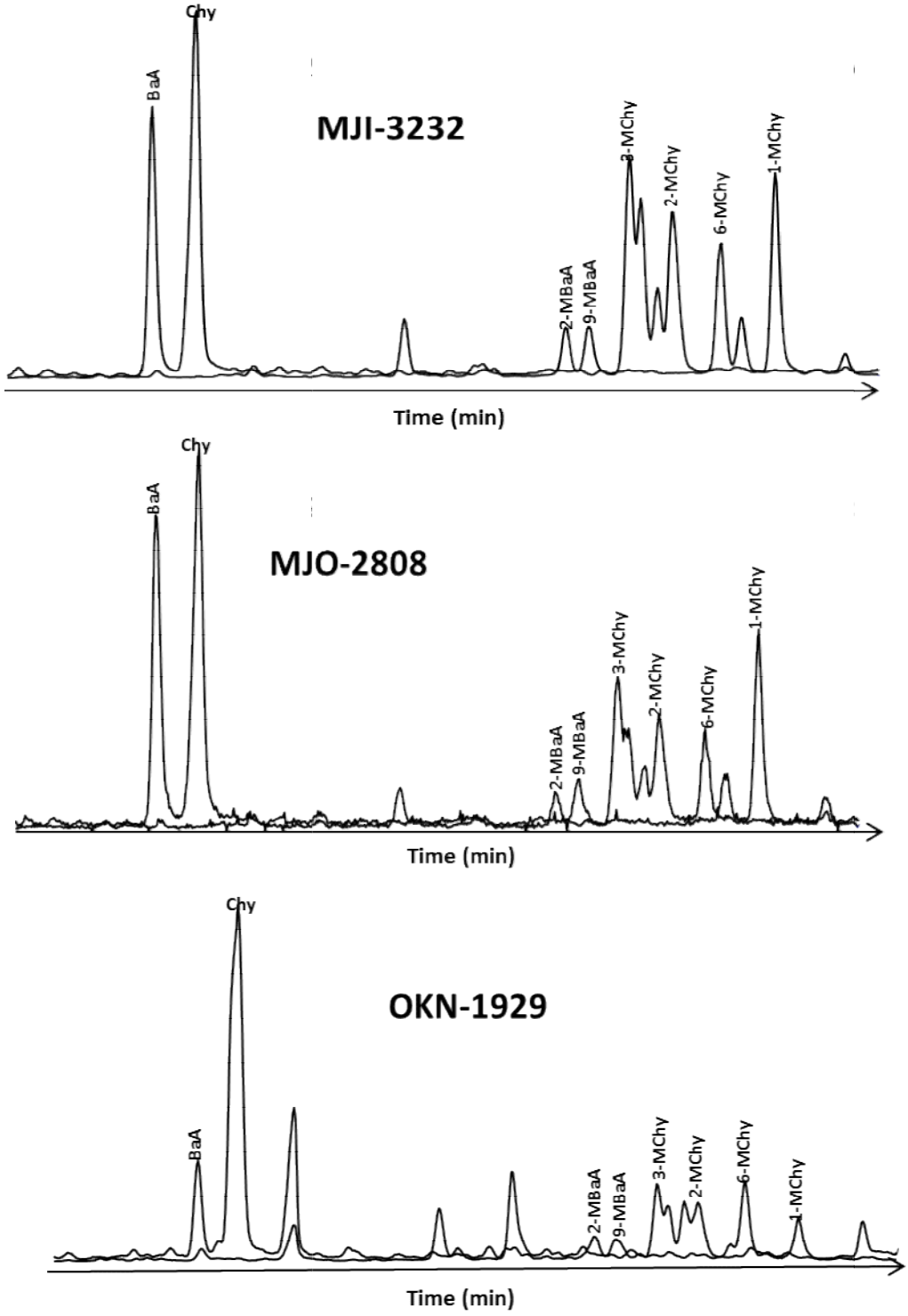

Fig. 4.21: m/z 228+242 mass chromatograms showing the distributions of chrysene, methylchrysenes and their isomers in source rock from Niger Delta.

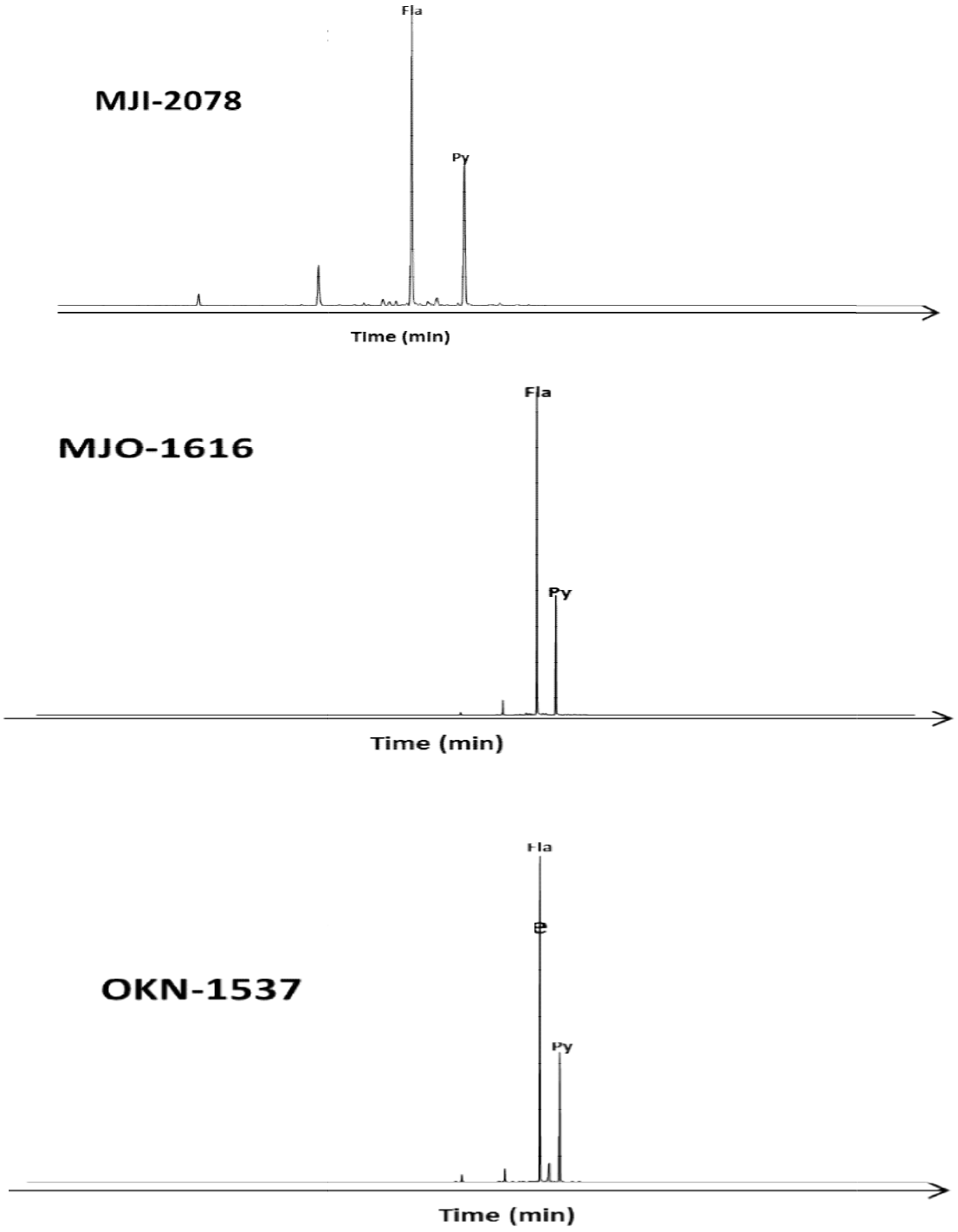

Fig. 4.22: m/z 202 mass chromatograms showing the distributions of pyrene and fluoranthene in source rocks from Niger Delta, Nigeria

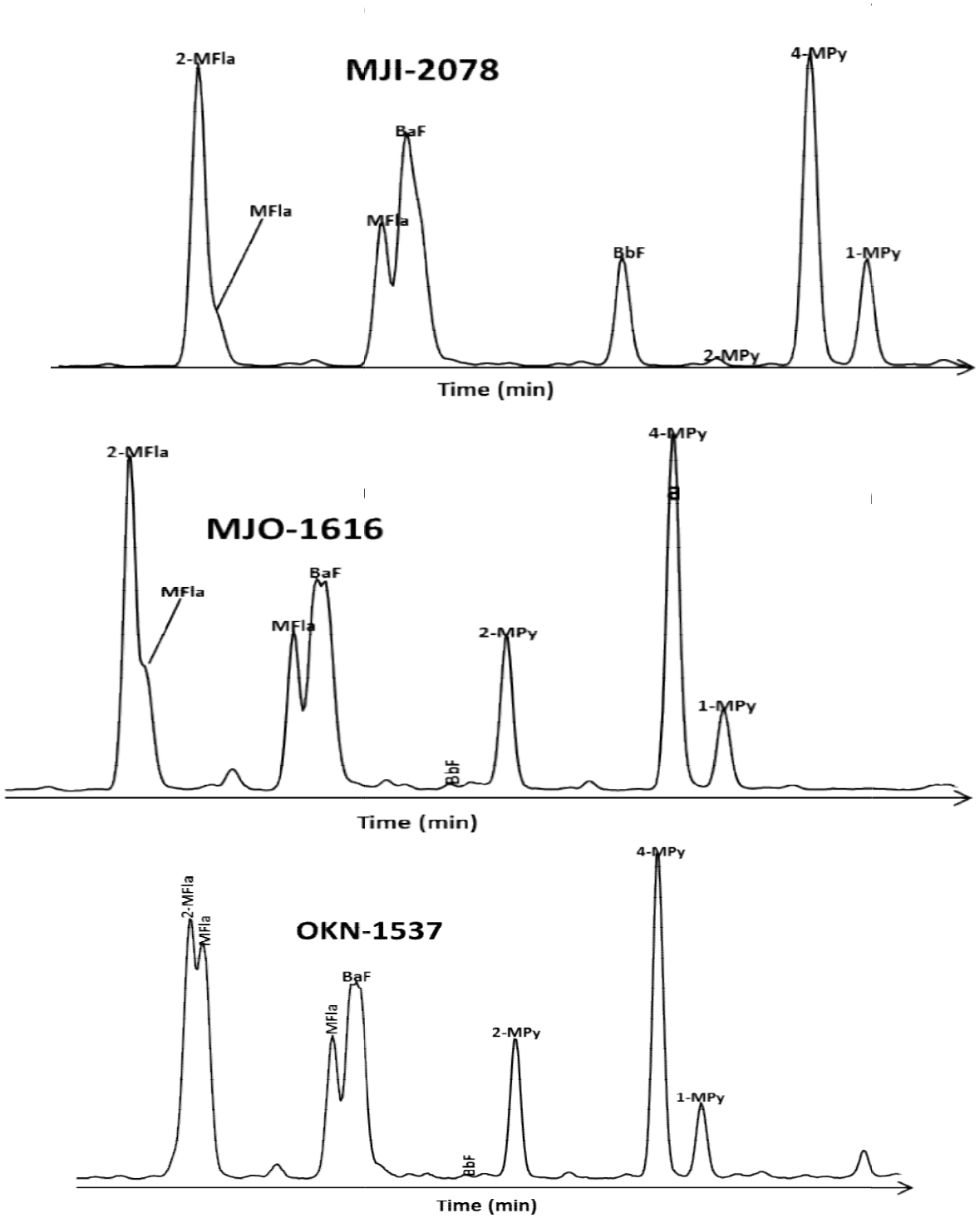

Fig. 23: m/z 202 and 216 mass chromatograms showing the distributions of (a) pyrene and fluoranthene and (b) methylfluoranthenes and methylpyrenes in source rock from Niger Delta, Nigeria.

Table 4.4: Peak identification of aromatic biomarkers in Niger Delta source rocks and crude oils

Peak	Compound
1,3,7-TMN	1,3,7-Trimethylnaphthalene
1,3,6-TMN	1,3,6-Trimethylnaphthalene
1,4,6- + 1,3,5-TMN	1,4,6- + 1,3,5-Trimethylnaphthalene
2,3,6-TMN	2,3,6-Trimethylnaphthalene
1,2,7- + 1,6,7-TMN	1,2,7- + 1,6,7-Trimethylnaphthalene
1,2,6-TMN	1,2,6-Trimethylnaphthalene
1,2,4-TMN	1,2,4-Trimethylnaphthalene
1,2,5-TMN	1,2,5-Trimethylnaphthalene
1,4,5-TMN	1,4,5-Trimethylnaphthalene
P	Phenanthrene
3-MP	3-Methylphenanthrene
2-MP	2-Methylphenanthrene
9-MP	9-Methylphenanthrene
1-MP	1-Methylphenanthrene
4-MDBT	4-Methyldibenzothiophene
2+3-MDBT	2+3-Methyldibenzothiophene
1-MDBT	1-Methyldibenzothiophene
C_{20}-TAS	C_{20}-Triaromatic steroid
C_{21}-TAS	C_{21}-Triaromatic steroid
C_{26}S-TAS	C_{26}S-Triaromatic steroids
C_{26}R + C_{27}S-TAS	C_{26}R + C_{27}S-Triaromatic steroids
C_{28}S-TAS	C_{28}S-Triaromatic steroids
C_{27}R-TAS	C_{27}R-Triaromatic steroids
BaA	Benzo[a]anthracene
Chy	Chrysene
2-MBaA	2-methylbenzo[a]anthracene
9-MBaA	9-methylbenzo[a]anthracene

3-MChy	3-methylchrysene
2-MChy	2-methylchrysene
6-MChy	6-methylchrysene
Fla	Fluoranthene
APA	Acephenanthrylene
Py	Pyrene
2-MFla	2-methylpyrene
MFla	methylpyrene
MFla	methylpyrene
BaF	Benzo[a]fluorene
BbF	Benzo[b]fluorene
2-MPy	2-methylpyrene
4-MPy	4-methylpyrene
1-MPy	1-methylpyrene

Table 4.5: Source and maturity parameters computed from the aromatic hydrocarbon distribution in the rock extracts

Field	Depth(m)	MPI-1	MPI-2	VRc	TMNR-1	TMNR-2	MDR	Rcb	DBT/P	S/(S+R) C28 TAS	1,2,5-/ 1,2,7-T	1,2,5,6-/ 1,2,5,7-Te	9-MP/ (9-MP+1-MP)	Paq
OKN	1537-1555	0.16	0.18	0.50	1.09	0.92	4.06	0.95	0.09	0.86	0.48	1.28	0.54	0.49
OKN	1729-1747	0.14	0.15	0.48	1.17	0.96	3.04	0.97	0.08	0.87	0.47	1.29	0.55	0.38
OKN	2625-2643	0.12	0.13	0.47	0.96	0.87	3.08	0.92	0.07	0.82	0.58	1.42	0.57	0.65
OKN	2780-2799	0.16	0.18	0.50	0.96	0.86	3.56	0.91	0.06	0.70	0.55	1.64	0.54	0.30
OKN	2863-2881	0.18	0.20	0.51	0.88	0.80	3.40	0.88	0.06	0.59	0.60	1.66	0.56	0.43
OKN	2909-2927	0.22	0.24	0.53	1.01	0.85	3.04	0.91	0.05	0.54	0.67	1.74	0.53	0.60
MJI	2079-2098	0.25	0.28	0.55	1.13	0.79	4.33	0.87	0.04	0.60	0.78	2.34	0.53	0.31
MJI	2299-2308	0.25	0.28	0.55	1.40	0.87	3.75	0.92	0.03	0.51	1.18	3.26	0.53	0.43
MJI	2637-2655	0.22	0.24	0.53	1.43	0.84	3.74	0.90	0.04	0.55	1.04	3.20	0.52	0.52
MJI	2857-2875	0.37	0.41	0.62	1.36	0.84	3.71	0.90	0.06	0.51	1.03	3.09	0.53	0.43
MJI	2994-3012	0.54	0.60	0.72	1.56	0.88	4.80	0.93	0.04	0.52	0.95	2.30	0.55	0.54
MJI	3085-3104	0.36	0.40	0.62	1.42	0.87	3.73	0.92	0.05	0.51	1.08	0.59	0.52	0.35
MJI	3232-3250	0.45	0.50	0.67	1.54	0.89	3.36	0.94	0.05	0.51	1.06	2.06	0.50	0.49
MJI	3323-3332	0.46	0.50	0.68	1.38	0.86	3.62	0.92	0.13	0.51	0.86	1.80	0.52	0.52
MJI	3405-3424	0.62	0.68	0.77	1.47	0.89	4.44	0.93	0.05	0.51	0.68	1.23	0.53	0.68
MJO	1616-1707	0.23	0.26	0.54	1.16	0.81	3.80	0.88	0.06	0.63	0.78	1.94	0.56	0.21
MJO	1771-1872	0.31	0.35	0.59	1.28	0.84	3.93	0.91	0.04	0.59	0.90	2.09	0.56	0.60
MJO	2091-2101	0.21	0.24	0.53	1.24	0.82	3.57	0.91	0.04	0.63	0.90	2.74	0.58	0.24
MJO	2293-2366	0.47	0.50	0.68	1.42	0.92	4.98	0.95	0.07	0.50	0.77	1.78	0.55	0.50
MJO	2570-2588	0.38	0.42	0.63	1.37	0.85	5.34	0.91	0.07	0.51	0.92	2.22	0.55	0.44
MJO	2808-2817	0.35	0.38	0.61	1.32	0.85	5.92	0.91	0.07	0.49	0.84	1.97	0.54	0.46

*MPI-1= 1.5(2- + 3-methylphenanthrene)/(Phenanthrene +1 - + 9-methylphenanthrene); MPI-2= 3(2-methylphenanthrene)/(phenanthrene +1- + 9-methylphenanthrene); VRc= 0.6(MPI-1) + 0.4; MDR= 4-MDBT/1-MDBT; DBT/P: Dbenzothiophene/phenanthrene; Paq=(nC_{23}+nC_{25})/(nC_{23}+nC_{25}+nC_{29}+nC_{31})–alkanes;Rcb=0.6(TMNr-2)+0.4;TAS:triaromaticsteroids;

Table 4.6: Source and maturity parameters computed from the chrysenes, pyrenes and triaromatic steroids distribution in the rock extracts

Field	Depth (m)	2-/1-Mpy	MPYR	Fla/ (Fla+Py)	2-/1-Mchy	BaA/ (BaA+Chy)	C26/C28 20S TAS	C27/C28 20R TAS
OKN	1537	1.88	0.65	0.74	1.88	0.20	0.21	1.07
OKN	1729	1.10	0.52	0.74	1.60	0.15	0.08	1.14
OKN	2625	0.99	0.50	0.72	1.55	0.24	0.13	1.43
OKN	2780	1.08	0.52	0.75	0.86	0.29	0.17	0.93
OKN	2863	1.28	0.56	0.74	1.25	0.27	0.34	0.98
OKN	2909	1.71	0.63	0.73	1.15	0.30	0.31	0.79
MJI	2078	1.03	0.51	0.68	0.75	0.31	0.19	1.09
MJI	2299	1.44	0.59	0.68	0.83	0.33	0.26	0.62
MJI	2637	1.34	0.57	0.63	0.88	0.42	0.19	0.63
MJI	2857	1.46	0.59	0.57	0.93	0.38	0.27	0.62
MJI	2994	1.64	0.62	0.57	1.44	0.20	0.25	0.5
MJI	3085	1.58	0.61	0.61	0.91	0.40	0.19	0.37
MJI	3232	1.51	0.60	0.57	1.02	0.37	0.18	0.34
MJI	3323	1.30	0.57	0.59	1.15	0.31	0.15	0.34
MJI	3405	2.10	0.68	0.60	1.07	0.15	0.2	0.37
MJO	1616	1.87	0.65	0.73	1.04	0.19	0.32	1.01
MJO	1771	1.17	0.54	0.72	1.17	0.13	0.29	0.14
MJO	2091	1.46	0.59	0.69	1.15	0.28	0.39	1.2
MJO	2293	2.19	0.69	0.68	0.92	0.26	0.54	0.66
MJO	2570	2.11	0.68	0.72	0.85	0.31	0.31	0.78
MJO	2808	2.38	0.70	0.73	0.70	0.41	0.38	0.84

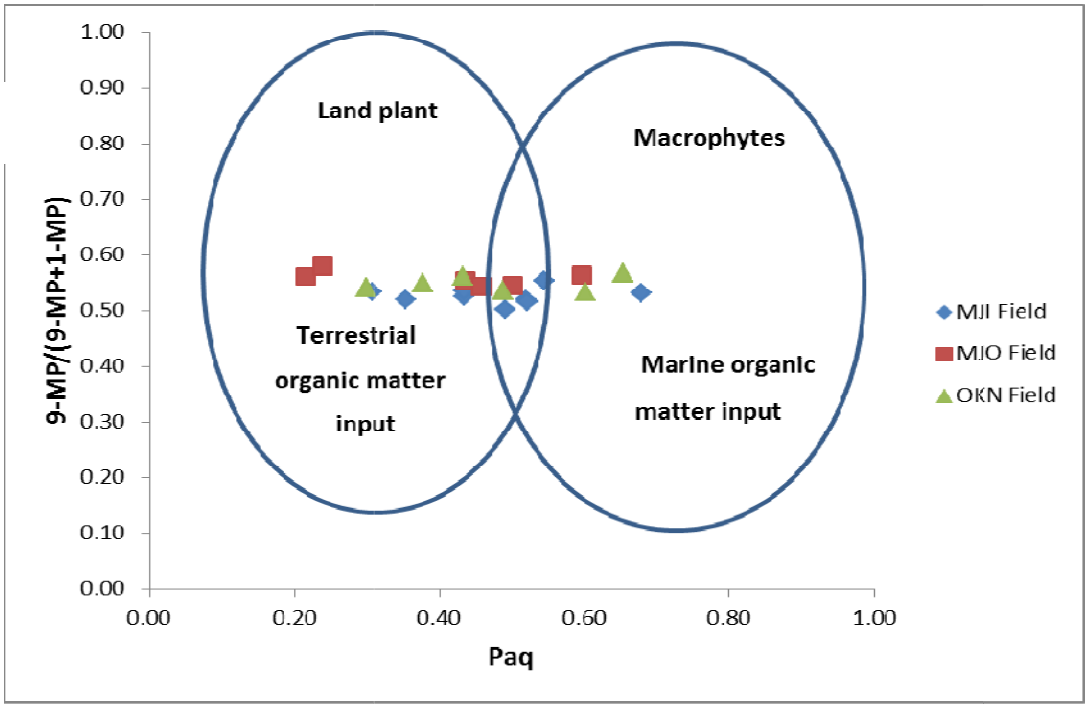

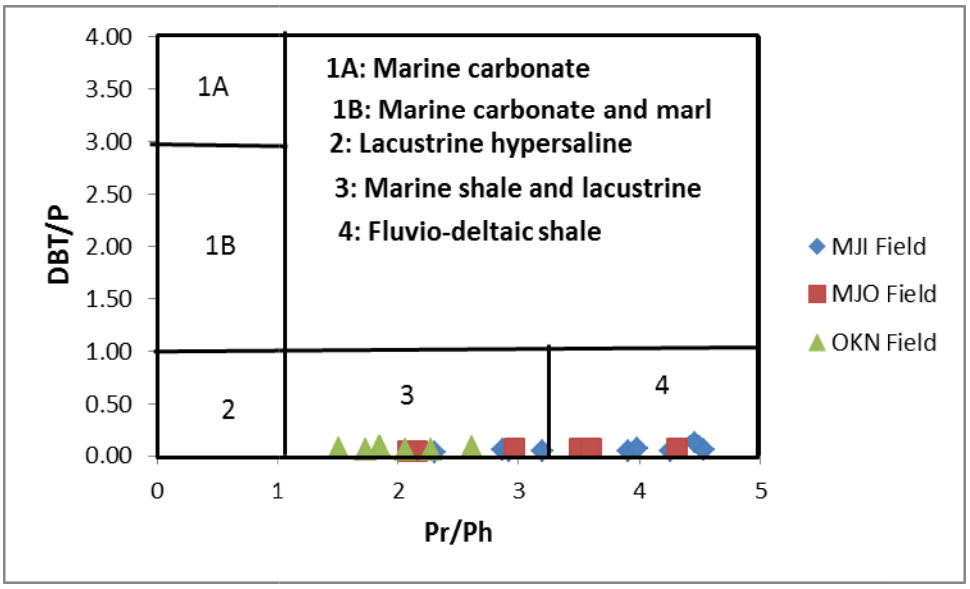

Fig.4.24 : Cross plots of (a) 9-MP/(9-MP+1-MP) versus Paq (modified after Ficken et al., 2000) and (b) dibenzothiophene/phenanthrene (DBT/P) versus pristane/phytane (Pr/Ph) ratios (after Hughes *et al*., 1995) for Niger Delta rock samples.

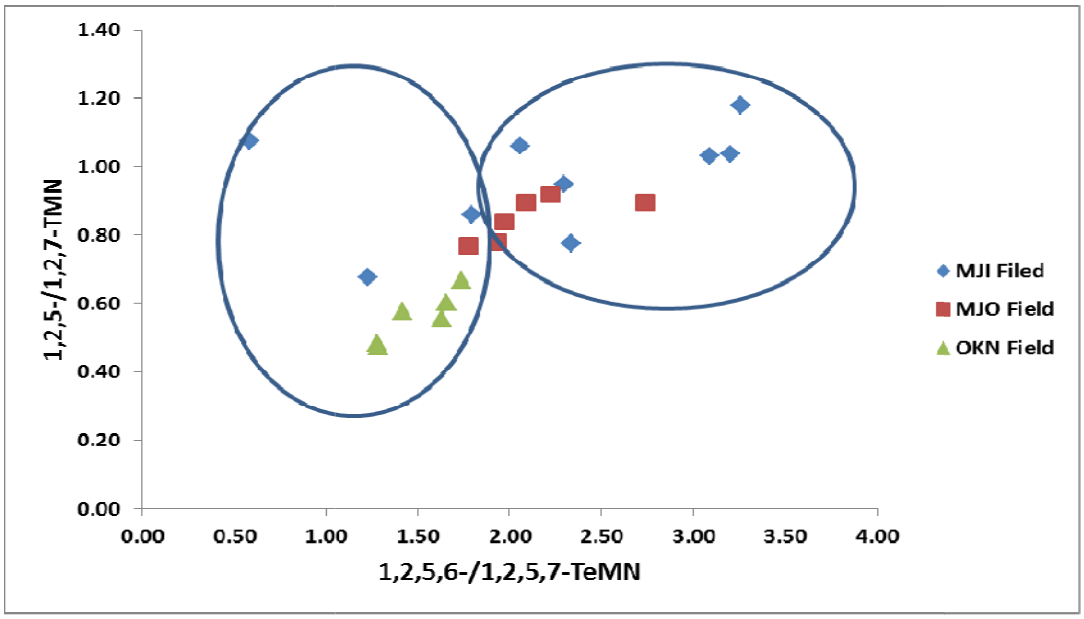

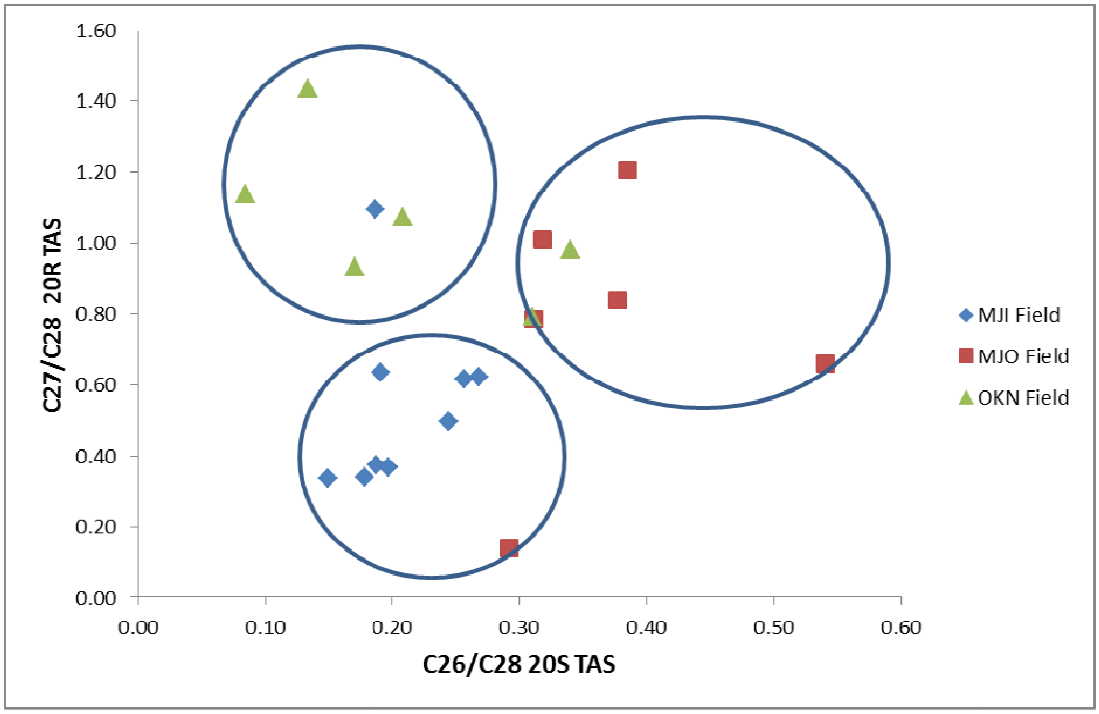

Fig. 4.25: Cross plots of (a) 1,2,5-/1,2,7-TMN versus 1,2,5,6-/1,2,5,7-TeMN and (b) C_{27}/C_{28} 20R TAS versus C_{26}/C_{28} 20S TAS for Niger Delta rock samples. (modified after Peters *et al*., 2005).

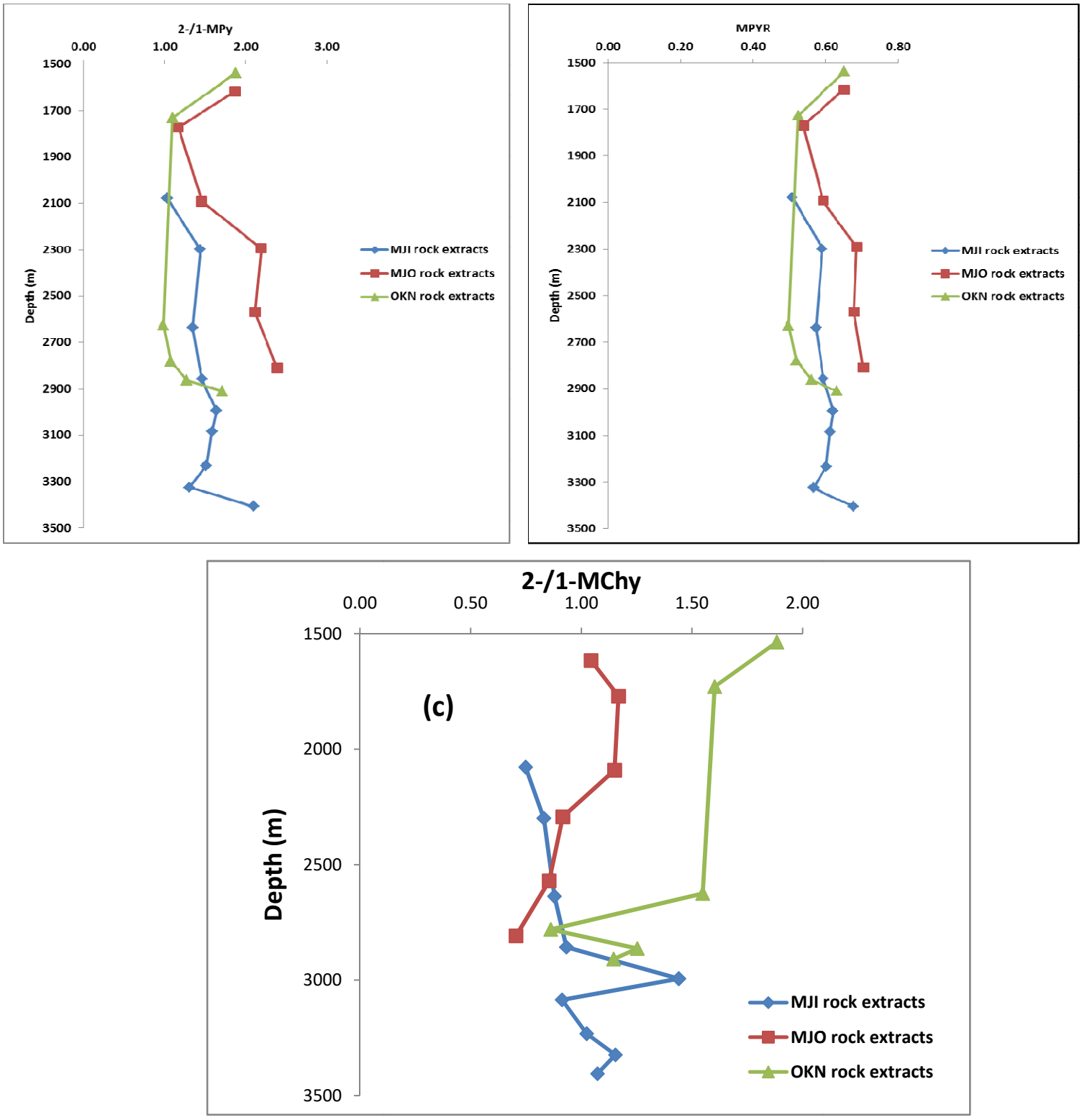

Fig. 4.26: Variations of (a) 2-/1-MPy, (b) MPYR and (c) 2-/1-MChy with depths for source rocks from Niger Delta, Nigeria.

Cross plot of 1,2,5-/1,2,7-TMN versus 1,2,5,6-/1,2,5,7-TeMN showed that the rock samples are derived predominantly from the marine source (Fig.4.25a). The C_{26}/C_{28} 20S ratios indicate a lake environment of brackish saline water (Xiangchun *et al*., 2011). Cross plots between these two parameters indicate that the source rocks are not from the same source (Fig.4.25b). The Fla/(Fla+Py) and BaA/(BaA + Chy) ratios range from 0.72 to 0.75 and 0.15 to 0.29 respectively, indicating source rocks were derived from mixed organic matter (Grice *et al.*, 2007, 2009; Li *et al*., 2012; Fang *et al*., 2015).

The MPI-1, MPI-2 and MDR values range from 0.12 to 0.22, 0.13 to 0.24 and 3.04 to 0 .56, respectively (Table 4.5). These values indicate that the rock samples are within narrow range of maturity. The calculated vitrinite reflectance (VRc%) values range from 0.47 to 0.53%, suggesting that the rock samples were formed at early oil generation window (Radke, 1987). The alkylnaphthalene maturity patrameters TMNr-1, TMNr-2 and calculated vitrinite reflectance values Rcb % (TMNr-2) of the rock samples range from 0.88 to 1.17, 0.80 to 0.96 and 0.88 to 0.97, respectively (Table 4.5) .These values show narrow range, indicating similar maturity status. The TMNr-1 values for some samples are < 1 while the Rcb values are < 0.95 (Table 4.5). These values indicate that the rock samples are at the peak of oil generation window (Radke, 1986). The triaromatic steroids maturity parameter, C_{28}S-TAS/(C_{28}R + C_{28}S-TAS) range from 0.54 to 0.84, indicating that the source rocks are thermally mature (Lewan, 1989). The 2-/1-MPy, MPYR and 2-/1-MChy ratios range from 0.99 to 1.88, 0.50 to 0.65 and 0.86 to 1.88, respectively, indicating that the source rocks are within oil window (Garrigues *et al*., 1988; Kruge, 2000; Li *et al*., 2012; Fang *et al*., 2015). However, the maturity parameters show no significant pattern with increasing burial depths (Fig.4.26).

4.2.3.2 MJI Field

The samples show equal distribution of 9-MP and 1-MP, indicating organic matter of mixed (terrestrial and marine) origin. The relative abundances of various alkylphenanthrenes have been suggested to be source dependent with a higher abundance of 9-MP attributed to marine organic matter while the predominance of 1-MP has been attributed to terrigenous organic matter (Budzinski *et al*., 1995). Plots of 9-MP/1-MP+9-MP ratio against Paq ($nC_{23} + nC_{25}$/ $nC_{23} + nC_{25} + nC_{29} + nC_{31}$ – alkanes) for the samples

is shown in Fig.4.24a. This plot has been proposed to discriminate between terrestrial and marine organic matter (Fickens *et al*., 2000). The samples fall under different zones on the plot of 9-MP/(9-MP + 1-MP) against Paq(Fig.4.24a), an indication that the source rocks were derived from organic matter formed from the mixture of terrestrial and marine materials. The dibenzothiophene/phenanthrene (DBT/P) ratios of the rock samples range from 0.03 to 0.13 (Table 4.5), indicating source rocks with predominant higher plant organic matter input and deposited in deltaic environment (Requejo, 1994; Sivan *et al*., 2008). Most of the rock samples fall within the zone of fluvial/deltaic zone on the plot of DBT/P versus Pr/Ph ratios as shown in Fig.4.24b.

Also the occurrence of 1,7-DMP (pimanthrene) in the samples also suggested terrestrial organic matter (Simoneit *et al*., 1986). The presence of appreciable amounts of 1,6-, 1,7-, and 2,6-DMNs in all the samples indicate terrestrial organic matter input (Day and Edman, 1963; Achari *et al*., 1973). The presence of 1,2,5- and 1,2,7-TMN in all the samples indicate both angiosperm and gymnosperms material contribution to the organic matter that formed the source rocks (Killops and Killops, 2005). The presence of 1,2,6 TMN in the samples also indicates microbial input to the biomass (Alexander et al., 1992). The presence of appreciable amount of 1,2,5,6-TeMN and 1,3,6,7-TeMN indicate terrigenous and marine input respectively (Puttmann and Villar, 1987). Fig. 4.25a shows the cross plot of 1,2,5-/1,2,7-TMN versus 1,2,5,6-/1,2,5,7-TeMN. This plot has been used to indicate the predominance of particular source input (marine versus terrigenous) in sedimentary organic matter (Alexander *et al*., 1992; Asif and Fazeelat, 2012).

The samples are characterized by higher abundance of C_{28} 20S and C_{28} 20R isomers relative to their respective homologues (Fig.4.21), indicating organic matter formed in fresh water environment (Linqiang and Renzi, 2005). The C_{26}/C_{28} 20S and C_{27}/C_{28} 20R ratios for triaromatic steroids have been shown to be source and depositional environments dependent and have been used in oil-oil and oil-source rock correlations (Picha and Peters, 1998; Xiangchun *et al*., 2011; Li *et al*., 2012). The ratios C_{26}/C_{28} 20S and C_{27}/C_{28} 20R in the studied source rocks are within the range of 0.19 to 0.26 and 0.34 to 1.09, respectively. The low C_{26}/C_{28} 20S ratios indicate organic matter formed in the fresh water environment (Xiangchun et al., 2011). However, the cross plots between

these two parameters indicate that the source rocks did not receive similar organic material (Fig. 4.25b).

The majority of the samples plotted together, indicating source rocks of similar source. The occurrence of fluoranthene and pyrene in the source rocks may suggest microbial metabolism of fungi, higher plants or insects (Grice *et al*., 2009; Fang et al., 2015) while the occurrence of chrysene and its isomers may be due to the degradation products of hopanes by cleavage of ring E and successive aromatization from ring D to ring A (Borrego *et al*., 1997) or terrestrial contribution to the source rocks organic matter (Jinggui *et al*., 2005). The Fla/(Fla+Py) in the rock samples range from 0.57 to 0.68 (Table 4.6), indicating terrigenous contribution into the source rocks organic matter (Grice *et al*., 2009; Yunker *et al*., 2002, 2011, Fang *et al*., 2015). The ratios also show a narrow range of values which indicate that the rock samples were formed from similar organic material. The BaA/(BaA + Chy) ratios in MJI samples range from 0.22 to 0.33 (Table 4.5), reflecting a mixed origin (marine and terrestrial).

The MPI-1 and MPI-2 values range from 0.22 to 0.62 and 0.24 to 0.68, respectively. These values show that the source rocks have some variation in maturity status. The methyldibenzothiophene ratios (MDR) values range from 3.36 to 4.44 (Table 4.5). These values fall within a narrow range reflecting similar maturity. The vitrinite reflectance (%VRc) of the source rocks was calculated from methylphenanthrene index (MPI1). The %VRc values range from 0.53 to 0.77 (Table 4.5). These values indicate a narrow maturity range of the source rocks and also show that the source rocks are within early oil window to the peak of oil generation. The maturity status (%VRc) predicted from the methylphenanthrene ratios is higher than those of sterane and hopane maturity indices. The saturate biomarker maturity parameters have been reported to reach equilibrium at the onset of oil generation window and therefore may not be providing the true reflection of the maturity status of the source rocks. The TMNr-1, TMNr-2 and calculated vitrinite reflectance (Rcb%) for the rock samples range from 1.13 to 1.56, 0.79 to 0.89 and 0.87 to 0.94, respectively. These values show narrow range indicating similar maturity status. TMNr-1 values for MJI samples are > 1, indicating that the source rocks are at the peak of oil generation window (Alexander et al., 1985). The Rcb values (< 0.95) also indicate that the rock samples are at the peak of oil generation window (Radke

et al., 1986). The triaromatic steroids maturity parameter, C_{28}S-TAS/(C_{28}R + C_{28}S-TAS) range from 0.51 to 0.60, indicating that the source rocks are thermally mature (Lewan, 1989). The 2-/1-methylpyrene (2-/1-MPy), methylpyrene ratio (MPYR) and 2-/1-methylchrysene (2-1-MChy) ratios in the rock samples range from 1.03 to 2.10, 0.51 to 0.68 and 0.75 to 1.44 (Table 4.5), indicating that the source rocks are within oil window (Garrigues *et al*., 1988; Kruge, 2000, Li *et al*., 2012; Fang *et al*., 2015). These maturity parameters lack particular trend with increasing burial depth (Fig. 4.26).

4.2.3.3 MJO Field

The presence of appreciable amounts of 9- and 1-methylphenanthrene in the rock samples indicates source rocks of mixed origin (marine and terrestrial) (Budzinski et al., 1995). The occurrence of 1,7-DMP (pimanthrene) in the samples is attributed to terrestrial organic matter (Simoneit et al., 1986). The Plots of 9MP/1MP+9MP ratio against Paq (nC_{23} + nC_{25}/ nC_{23} + nC_{25} + nC_{29} + nC_{31} – alkanes) for the samples revealed that most of the samples are of terrestrial organic matter, one from marine origin while a few are ofmixed origin (Fig. 4.24a). The dibenzothiophene/phenanthrene (DBT/P) ratio of the rock samples range from 0.04 to 0.07, indicating source rock with predominant higher plant organic matter input, deposited in deltaic environment (Requejo, 1994; Sivan *et al*., 2008). The samples plotted within marine, lacustrine and fluvial/deltaic zones on the plot of dibenzothiophene/phenanthrene (DBT/P) versus Pr/Ph ratios (Fig. 4.24b) and this further confirmed that the samples have varied organic matter background.

The presence of appreciable amounts of 1,6-, 1,7-, and 2,6-DMNs in all the samples indicate terrestrial organic matter input (Day and Edman, 1963; Achari *et al*., 1973). The presence of 1,2,5- and 1,2,7-TMN in all the samples indicate both angiosperm and gymnosperms material contribution to the organic matter that formed the source rocks (Killops and Killops, 2005). Also, the occurrence of 1,2,6-TMN in the rock samples indicate microbial input into the organic material from which the source rocks were formed (Killops and Killops, 2005; Alexander et al., 1992). Cross plot of 1,2,5-/1,2,7-TMN versus 1,2,5,6-/1,2,5,7-TeMN showed that the rock samples are derived from the same source (Fig.4. 25a). The presence of pyrene and its isomers in the source rocks may be derived from microbial metabolism of fungi, higher plants or insects (Grice

et al., 2009) while the presence of chrysene may reflect degradation products of hopanes by cleavage of ring E and successive aromatization from ring D to ring A (Borrego *et al*., 1997) or terrigenous organic matter input (Jinggui *et al*., 2005). For MJO samples, the Fla/(Fla+Py) and BaA/(BaA + Chy) ratios range from 0.68 to 0.73 and 0.13 to 0.41 respectively, indicating that the source rocks were formed from mixed sources with significant contribution from terrigenous organic matter (Grice *et al*., 2007, 2009; Li *et al*., 2012; Fang *et al*., 2015). The ratios C_{26}/C_{28} 20S and C_{27}/C_{28} 20R of triaromatic steroids in the studied source rocks are within the range of 0.29 to 0.54 and 0.66 to 1.20 respectively. The C_{26}/C_{28} 20S ratios indicate a lake environment of brackish saline water (Xiangchun et al., 2011). However, the cross plots of C_{26}/C_{28} 20S versus C_{27}/C_{28} 20R somehow show that the source rocks were not formed from the same source (Fig. 4.25b).

The MPI-1, MPI-2 and MDR values range from 0.21 to 0.47, 0.24 to 0.50 and 3.57 to 5.92, respectively (Table 4.5).These values indicate that the rock samples are within a narrow range of maturity. The calculated vitrinite reflectance (VRc%) values range from 0.54 to 0.68%, suggesting that the rock samples were formed at the early oil generation window (Radke, 1987). The alkylnaphthalene maturity patrameters TMNr-1, TMNr-2 and Rcb % (TMNr-2) of the rock samples range from 1.16 to 1.42, 0.81 to 0.92 and 0.88 to 0.95 respectively (Table 4.5) .These values indicate similar maturity status. The TMNr-1 (> 1) and Rcb values (≤ 0.95) indicate that the rock samples are at the peak of oil generation window (Radke, 1986). The triaromatic steroids maturity parameter, C_{28}S-TAS/(C_{28}R + C_{28}S-TAS) range from 0.49 to 0.63, indicating that the source rocks are thermally mature (Lewan, 1989). The 2-/1-MPy, MPYR and 2-/1-MChy ratios range from 1.17 to 2.38, 0.54 to 0.70 and 0.70 to 1.17, respectively, indicating that the source rocks are within oil window (Garrigues *et al*., 1988; Kruge, 2000; Li *et al*., 2012; Fang *et al.,* 2015). However, these maturity parameters did not show a particular trend with increasing burial depths (Fig. 4.26).

4.3 Stable Carbon Isotopic Composition of Niger Delta Source Rocks

The bulk stable carbon isotopic compositions and compound specific-isotope of individual n-alkanes were used to examine the origin and depositional environments of the Niger Delta source rocks. The bulk stable carbon isotope data of the rock extracts are

presented in Table 4.7. The $\delta^{13}C$ isotopic values for whole saturate fraction and individual n-alkanes of the rock extracts are presented in Tables 4.8

4.3.1 OKN Field

The carbon isotopic values of the rock samples in OKN field range from -28.5 to -28.0‰ (Table 4.7). The isotopic differences between the rock extracts are not than greater than 0.5‰, reflecting source rocks of similar organic matter source (Peters and Moldowan, 1993). The $\delta^{13}C$ isotopic values for the n-alkanes range from –29.1 to –28.1 δ^{13} ‰. The isotopic values are characteristics of higher plant derived n-alkanes (Canuel *et al.*, 1997; Tuo *et al*., 2007; Samuel *et al*., 2009; Cai *et al*., 2015)). The average carbon isotopic compositions of individual alkanes (nC_{12}-nC_{33}) in the samples range from –32.3 to –29.7 ‰. The most depleted values were observed for the long chain alkanes, which are characteristics of plant wax derived n-alkanes of C_3-plants (Schouten *et al*., 2000; Hu *et al*., 2002; Samuel *et al*., 2009; Cai *et al*., 2015).

Significant contribution from marine organic matter is reflected in light $\delta^{13}C$ isotope values observed in the short chain (nC_{12}-nC_{18}) alkanes in all the samples (Fig. 4.27). The $\delta^{13}C$ isotope ratios of Pr and Ph range from –29.2 to –28.4 ‰ (av.–28.8‰) and –30.2 to –28.7 ‰ (av. –29.5‰), respectively. There is no significant difference between the ^{13}C-values of Pr and Ph, which suggest that the rocks were formed from similar organic source materials (Schwab and Spangenberg, 2007; Cai *et al*., 2015).

However, there is notably flat portion pattern of the n-alkane profile between nC_{14} nC_{24} and nC_{27}-nC_{31} (Fig. 4.27), which is an indication of marine incursion (Murray et al., 1994). These features show that OKN samples consist of both terrestrial and marine organic matter deposited in lacustrine-fluvial/deltaic settings.

Table 4.7: The bulk stable carbon isotope data of the rock extracts from Niger Delta

		$\delta^{13}C$, ‰			
Field	Depth(m)	Extr.	Sat	Aro	Polar
OKN	1537-1555	-28.2	-28.4	-26.7	-26.2
OKN	1729-1747	-28.0	-29.1	-28.1	-25.6
OKN	2625-2643	-28.5	-28.4	-27.8	-25.0
OKN	2780-2799	-28.2	-28.6	-27.3	-29.2
OKN	2863-2881	-28.2	-28.3	-26.8	-28.3
OKN	2909-2927	-28.5	-28.1	-27.6	-28.7
MJI	2079-2098	-28.7	-29.0	-28.5	-28.2
MJI	2299-2308	-28.4	-29.2	-28.4	-28.2
MJI	2637-2655	-28.0	-27.6	-27.6	-28.2
MJI	2857-2875	-27.9	-28.6	-28.0	-27.6
MJI	2994-3012	-28.2	-28.8	-27.8	-28.0
MJI	3085-3104	-28.2	-28.8	-27.8	-27.7
MJI	3232-3250	-27.6	-27.8	-27.2	-28.0
MJI	3323-3332	-27.9	-28.4	-27.8	-27.9
MJI	3405-3424	-27.5	-27.6	-27.2	-27.2
MJO	1616-1707	nd	-28.8	-27.7	-28.3
MJO	1771-1872	-27.7	-27.2	-26.9	-28.0
MJO	2091-2101	-28.1	-28.3	-27.7	-28.2
MJO	2293-2366	-27.8	-28.8	-27.1	-27.2
MJO	2570-2588	-27.6	-28.8	-27.9	-27.7
MJO	2808-2817	-26.8	-28.1	-26.8	-26.6

Table 4.8: Carbon Isotopic Composition of n-Alkanes in Niger Delta Source Rocks (o/oo)

Field	Depth (m)	C_{12}	C_{13}	C14	C15	C17	C18	C19	C20	C21	C22	C23	C24
OKN	1729	-30.8	-30.7	-30.6	-30.0	nd	nd	Nd	nd	-30.6	-30.0	-29.3	-28.7
OKN	2625	-29.4	-30.0	nd	nd	nd	nd	-30.0	-31.3	-28.9	-30.2	-31.4	-30.0
OKN	2780	-30.5	-29.9	-30.1	nd	nd	nd	-30.5	-30.4	-30.4	-29.7	-29.7	-30.5
OKN	2863	nd	Nd	nd	nd	nd	-30.4	-29.5	-29.5	-30.4	-29.5	-29.7	-29.5
Ave.		-30.2	30.2	-30.3	-30.0		-30.4	-30.0	-30.4	-30.1	-29.9	-30.0	-29.7
MJI	2078						nd	-29.5	-30.3	-30.4	-30.6	-30.4	-30.7
MJI	2857						nd	-29.7	-29.5	-30.2	-30.2	-30.3	-30.3
MJI	3085						nd	-29.6	-29.9	-30.5	-30.7	-30.9	-30.7
MJI	3405						28.2	-28.1	-28.0	-27.9	-28.2	-28.2	-28.4
Ave.							28.2	-29.2	-29.4	-29.7	-29.9	-29.9	-30.0
MJO	1616					nd	-29.6	-28.9	-28.7	-30.9	-30.1	-31.1	-32.2
MJO	2293					nd	nd	Nd	nd	nd	nd	-31.7	-32.6
MJO	2570					nd	-31.0	-31.5	-31.8	-33.1	33.2	-33.2	-32.4
MJO	2808					-29.2	-28.4	-28.0	-28.0	-28.3	-28.2	-28.3	-28.2
Ave.						-29.2	29.7	-29.5	-29.5	-30.8	-30.8	-31.1	-31.4

Table 4.8 contd: Carbon Isotopic Composition of n-Alkanes in Niger Delta Source Rocks (o/oo)

Field	Depth (m)	C25	C26	C27	C28	C29	C30	C31	C32	C33	A.	Pr	Ph
OKN	1729	-31.8	-29.7	-30.3	-29.8	-32.5	nd	Nd	nd	nd	-30.4		
OKN	2625	-30.3	-30.6	-32.3	-30.4	-30.4	nd	Nd	nd	nd	-30.4	-28.0	-30.2
OKN	2780	-30.9	-32.0	-30.6	-32.8	-30.7	-32.0	Nd	nd	nd	-30.7		
OKN	2863	-32.6	-29.2	-30.0	-29.7	-31.3	-30.0	-32.0	-31.0	-32.3	-30.4	-29.2	-28.7
Ave		-31.4	30.4	-30.8	-30.7	-31.2	-31.0	-32.0	-31.0	-32.3		-28.8	-29.5
MJI	2078	-29.9	-30.4	-31.0	-31.7	-32.1	-32.1	-33.5	nd	nd	-31.0		
MJI	2857	-30.2	-30.8	-31.2	-31.8	-31.6	-32.2	-33.2	-33.2	32.6	-31.1	-29.0	-28.1
MJI	3085	-31.0	-31.3	-31.5	-32.0	-31.8	-32.4	-33.2	-33.1	-33.5	-31.5	-29.1	-29.0
MJI	3405	-28.4	-28.9	-29.2	-30.1	-30.8	-31.2	-31.4	-32.3	-32.7	-29.5	-28.3	-27.4
Ave.		-29.9	-30.3	-30.7	-31.4	-31.6	-32.0	-32.8	-32.9	-32.9		-28.6	-28.2
MJO	1616	-30.6	-30.9	-31.4	-31.6	-32.4	-32.8	-33.7	-33.8	nd	-31.3		
MJO	2293	-31.0	-31.8	-31.7	-31.7	-32.1	-31.8	-31.3	-32.7	nd	-31.8	-29.0	-29.1
MJO	2570	-31.8	-32.0	-32.0	-31.7	-31.8	-32.2	-33.6	-34.5	nd	-32.4	-29.1	-28.9
MJO	2808	-28.4	-28.6	-28.8	-29.2	-30.2	-30.9	-32.4	-33.1	-34.9	-29.6	-28.0	-27.9
Ave.		-30.4	-30.8	-31.0	-31.1	-31.6	-31.9	-32.7	-33.5	-34.9		-29.0	-28.6

*Ave.: average of individual n-alkanes; A: weighted average; nd: not determined. The data presented represent the average of three readings.

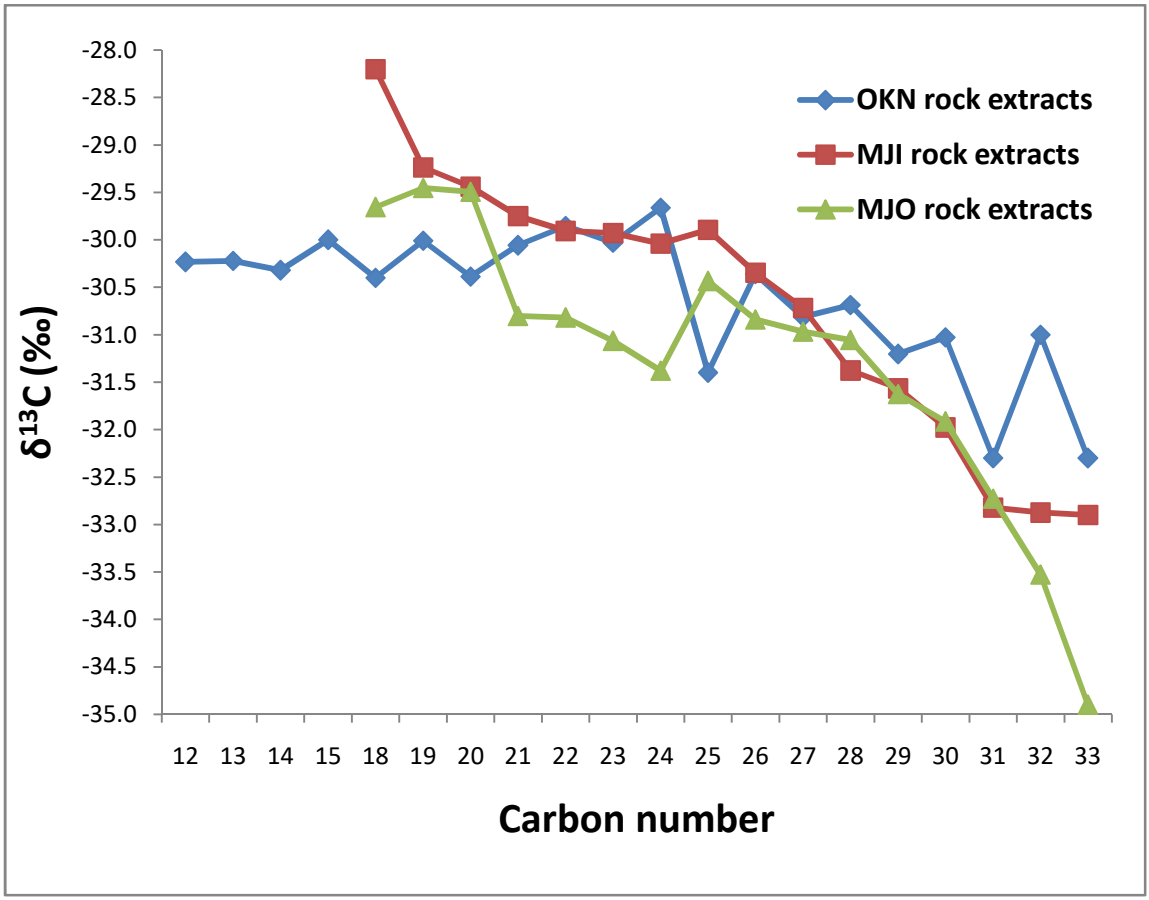

Fig. 4.27: Carbon isotopic compositions of individual n-alkanes in Niger Delta rock samples (after Murray *et al*., 1994).

4.3.2 MJI Field

The $\delta^{13}C$ isotopic value of the rock extracts range from -28.7 to -27.5‰ (Table 4.7). The isotopic differences between the rock extracts are not greater than 1.2‰, indicating similar organic matter source for all the source rocks (Peters and Moldowan, 1993). MJI samples have the average carbon isotopic compositions of individual n-alkanes (nC_{18}-nC_{33}) ranging from -32.9 to -28.2 ‰ (Tables 4.8). The most depleted values were noted for the long chain alkanes (nC_{24}-nC_{33}). These features are characteristics of higher plants organic matter input (Schouten *et al*., 2000; Hu *et al*., 2002; Cai *et al*., 2015). Low contribution from marine organic matter (i.e.C_3 algae or cyanobacteria) is shown in enriched $\delta^{13}C$ isotope values of medium molecular weight (nC_{18}-nC_{23}) n-alkanes. A negatively sloping n-alkane profile is obtained for the rock samples (Fig. 4.27). This profile shows lighter (more negative) carbon isotope ratio with increasing n-alkane chain length (Murray et al., 1994; Wilhelms et al., 1994; Samuel et al., 2009; Cai *et al*, 2015). This negative slope fingerprint has been described as characteristic of source rocks derived from deltaic and terrigenous organic matter (Murray *et al*., 1994; Wilhelms *et al*., 1994; Samuel *et al*., 2009; Cai *et al*., 2015). The carbon isotopic composition of n-alkanes for the samples that range between –31.5 and –29.5 ‰ are also characteristics of plant wax derived n-alkanes of C_3-plants (Canuel *et al*., 1997; Tuo *et al*., 2007; Samuel *et al*., 2009; Cai *et al*., 2015).

The $\delta^{13}C$ isotope ratios of Pr and Ph range from –29.1 to –28.3 ‰ (av.–28.6‰) and –29.0 to –27.4 δ^{13}‰ (av. –28.2‰), respectively. There is no substantial variation between the ^{13}C-values of the Pr and Ph suggesting that the source rocks were formed from similar organic matter (Schwas and Spangenberg, 2007; Cai *et al*., 2015).

4.3.3 MJO Field

In MJO samples, the $\delta^{13}C$ isotopic composition of the rock extracts range from -28.1 to -26.8‰, (Table 4.7). The differences in the isotopic values did not exceed 1.3‰, suggesting that the rocks were derived from the same organic source material (Peters and Moldowan, 1993). The average carbon isotopic compositions of individual n-alkanes (nC_{17}-nC_{33}) values (Tables 4.8) ranged from -34.9 to -29.2 ‰. The long chain alkanes (nC_{21}-nC_{33}) were noted to have the most depleted values. These are characteristics of

higher plant-derived organic matter (Schouten *et al*., 2000; Hu *et al*., 2002; Cai *et al*., 2015). A negatively sloping n-alkane profile is obtained for the rock samples in MJO field (Fig. 4.27) which reflects lighter (more negative) carbon isotope ratio with increasing n-alkane chain length (Murray *et al*., 1994; Wilhelms *et al*., 1994; Samuel et al., 2009). A negative slope n-alkane profile have been described as feature of source rocks derived from deltaic and terrigenous organic matter (Murray *et al*., 1994; Wilhelms *et al*., 1994; Samuel *et al*., 2009; Cai *et al*., 2015). The carbon isotopic compositions of n-alkanes for the samples range from –32.4 to –29.6 ‰. This also reflect higher plant contribution to the organic matter that formed the source rocks (Canuel *et al*., 1997; Tuo *et al*., 2007; Samuel *et al*., 2009; Cai *et al*., 2015).

The $\delta^{13}C$ isotope ratios of Pr and Ph range between –29.2 and –28.2 ‰ (av.–28.8‰) and –29.1 to –27.9‰ (av. –28.6‰) respectively. There is no substantial variation between the ^{13}C-values of Pr and Ph, which indicates that the source rocks were formed from similar organic material (Schwas and Spangenberg, 2007; Cai *et al*., 2015).

4.4 Biomarker Geochemistry of the Niger Delta Oils

The geochemical evaluation of the crude oils in terms of organic matter source, depositional environment and thermal maturity was carried out based on the distribution and abundance of saturate and aromatic biomarkers and stable carbon isotopic compositions in the oils.

4.4.1 Source, Depositional Environment and Maturity of the Oils

The m/z 85, 191 and 217 mass chromatograms of the representative samples showing the distribution of n-alkane/isoprenoids, terpanes and steranes of the oil samples are shown in Fig.s 4.28, 4.29 and 4.30, respectively. Peak identities are listed in Table 4.2. The source, depositional environment and maturity parameters computed from the distribution of biomarker in the oil samples are presented in Table 4.9.

4.4.1.1 ADL Field

The mass chromatograms of the saturate fractions of the oils showed a unimodal distribution of n-alkanes in the range of n-C_{11} to n-C_{34} with the predominance of short

chain n-alkanes (n-C_{11} to n-C_{23}) over the long chain n-alkanes (Fig. 4.28a). The distribution of n-alkanes indicates that the oils are not biodegraded (Volkman *et al*., 1984). The pristane/phytane ratios ranged from 3.61 to 5.48 (Table 4.9), indicating oils that originated from terrigenous organic matter deposited under an oxic paleo-environment (Mello and Maxwell, 1990). The Pr/nC_{17} and Ph/nC_{18} ratios range from 0.51 to 056 and 0.14 to 0.16 (Table 4.9). All the samples have Ph/nC_{18} less than one (< 1.0), suggesting that these samples are non-biodegraded (Hunt; 1996). The cross plot of the Pr/nC_{17} and Ph/nC_{18} ratios indicate that the crude oils are from mixed origin (Fig.4.31).

The oleanane/C_{30} hopane ratios (Oleanane Index) for the oils range between 0.30 and 0.32. The presence of the oleanane is a good indicator of a terrestrial input into the oil-prone source rocks deposited in a deltaic environment (Ekweozor *et al*., 1979; Philp and Gilbert, 1986; Peters *et al*., 2005). The distribution of C_{27}-C_{29} steranes in the oils (Table 4.9) reflect oil derived from source rock of mixed origin (terrestrial and marine) (Fig. 4.32). However, the higher abundance of C_{29} (49.5 – 53.7%) regular steranes compared with the C_{27} (19.7 – 25.8%) and C_{28} (23.5 – 30.4%) steranes indicates higher contribution of terrestrial relative to marine organic matter (Huang and Meischein, 1979; Volkman 1988; Peters *et al*., 2005). All the samples fall within algal/oxic zone on the plot of Pr/Ph against C_{29}/C_{27} (Hakimi *et al*., 2011) in Fig. 4.33, suggesting oxic depositional conditions.

The Ts/(Ts + Tm) and 22S/(22S+22R) C_{31} hopane ratios for the oils range from 0.46 to 0.61 and 0.56 to 0.57 (Table 4.9), respectively, which suggest oils derived at the onset of oil generative window (Seifert and Moldowan, 1986; Peters and Moldowan, 1993; Peters *et al*., 2005). The 20S/(20S+20R) and ββ/(ββ+αα) C_{29} sterane values range from 0.41 to 0.47 and 0.37 to 0.39, respectively (Table 4.9). These values also indicate that the oils were formed at the early oil generative window (Seifert and Moldowan, 1986; Peters *et al*., 2005). The cross plot of 22S/(22S+22R) C_{31} hopane versus 20S/(20S+20R) C_{29} sterane (Fig. 4.34) further support early oil generative window for the oils.

4.4.1.2 OKN Field

The chromatogram showed a bimodal distribution of n-alkanes from C_{11} – C_{35}, indicating oils derived from source rocks of mixed origins (marine and terrestrial) (Peters *et al*., 2005). The Pr/Ph ratios in the oils range from 2.10 to 2.83 (Table 4.9), suggesting source rocks deposited in sub-oxic conditions. The Pr/nC17 and Ph/nC18 ratios for the oils range from 0.36 to 9.49 and 0.19 to 2.97, respectively. These values show that some samples in OKN oils are biodegraded (Volkman *et al*., 1984). The cross plot of the Pr/nC_{17} and Ph/nC_{18} ratios indicate that the crude oils are from mixed origin, deposited in sub-oxic environments (Fig. 4.31).

The oleanane/C_{30} hopane ratio (Oleanane Index) for the oils range from 0.54 to 1.44 (Table 4.9).The presence of the oleanane is a good indicator of a terrestrial input into the oil-prone source rocks deposited in a deltaic environment (Ekweozor et al., 1979; Philp and Gilbert, 1986; Moldowan *et al*., 1994; Peters *et al*., 2005). The relative abundance of C_{27}, C_{28} and C_{29} steranes range from 30.0 to 33.6, 29.3 to 32.6 and 34.6 to 39.0%, respectively (Table 4.9). These distributions indicate oil derived from source rock of mixed origin (terrestrial and marine) but with nearly equal contributions from marine and terrigenous organic matter (Fig. 4.32). All the oil samples fall within algae/oxic region on the cross plot of Pr/Ph versus C_{29}/C_{27} ratios (Fig. 4.33).

The Ts/(Ts + Tm) ratios range from 0.40 to 0.62 (Table 4.9), indicating oils generated at the early mature stage (Peters and Moldowan, 1993; Peters *et al*., 2005). The 22S/(22S+22R) C_{31} hopane values in the samples range from 0.52 to 0.54 (Table 4.9). 20S/(20S+20R) and ββ/(ββ+αα) C_{29} sterane ratios range from 0.33 to 0.43 and 0.36 to 0.42, respectively (Table 4.9). These values indicate oil generated at the onset of oil generative window (Seifert and Moldowan, 1986; Peters and Moldowan, 1993). Plots of 22S/(22S+22R) C_{31} hopane versus 20S/(20S+20R) C_{29} sterane (Fig. 4.34) further support oils generated at the early stage of oil generative window.

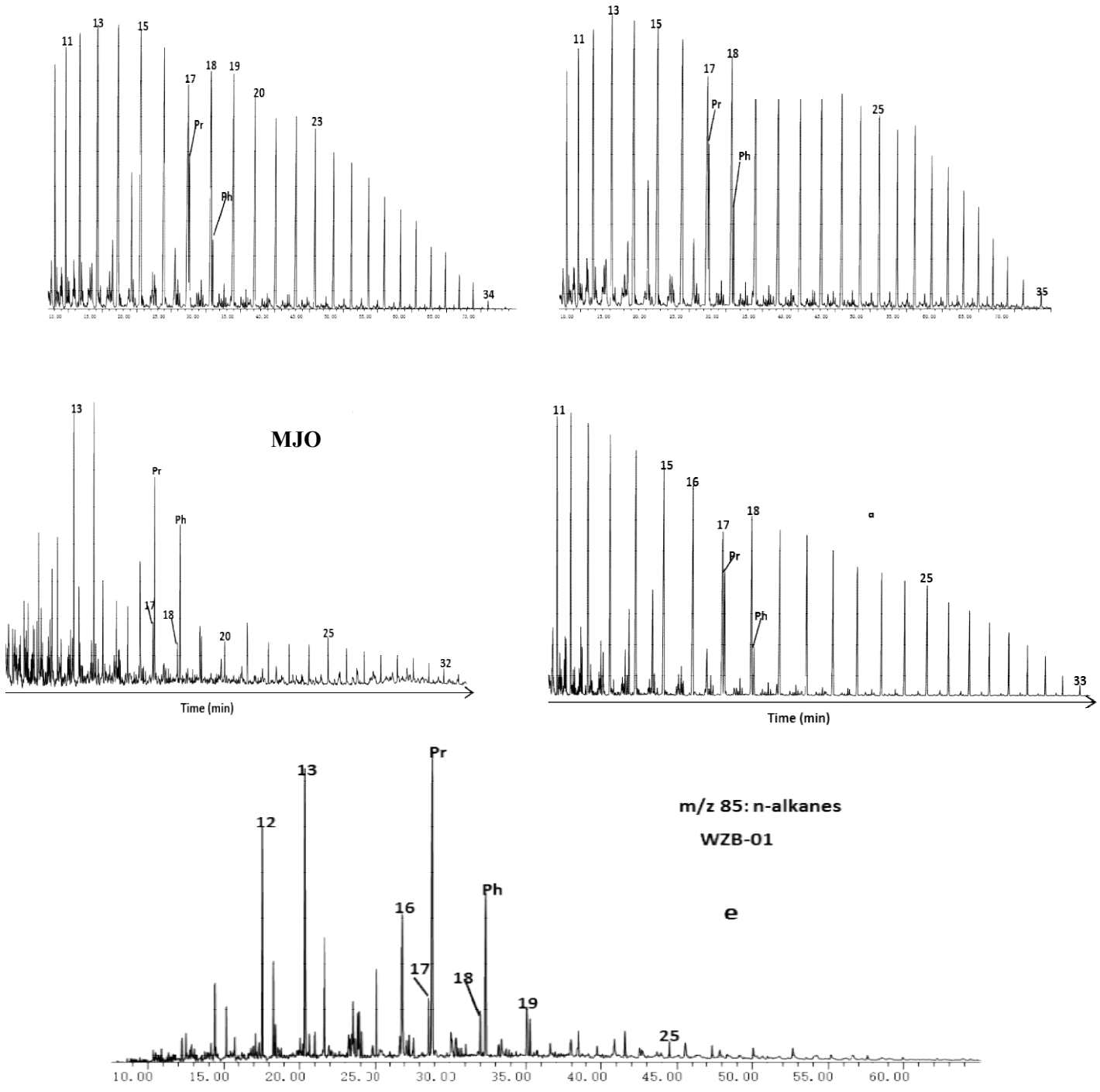

Fig. 4.28: m/z 85 mass chromatograms showing the distribution of n-alkanes in representative crude oils from Niger Delta

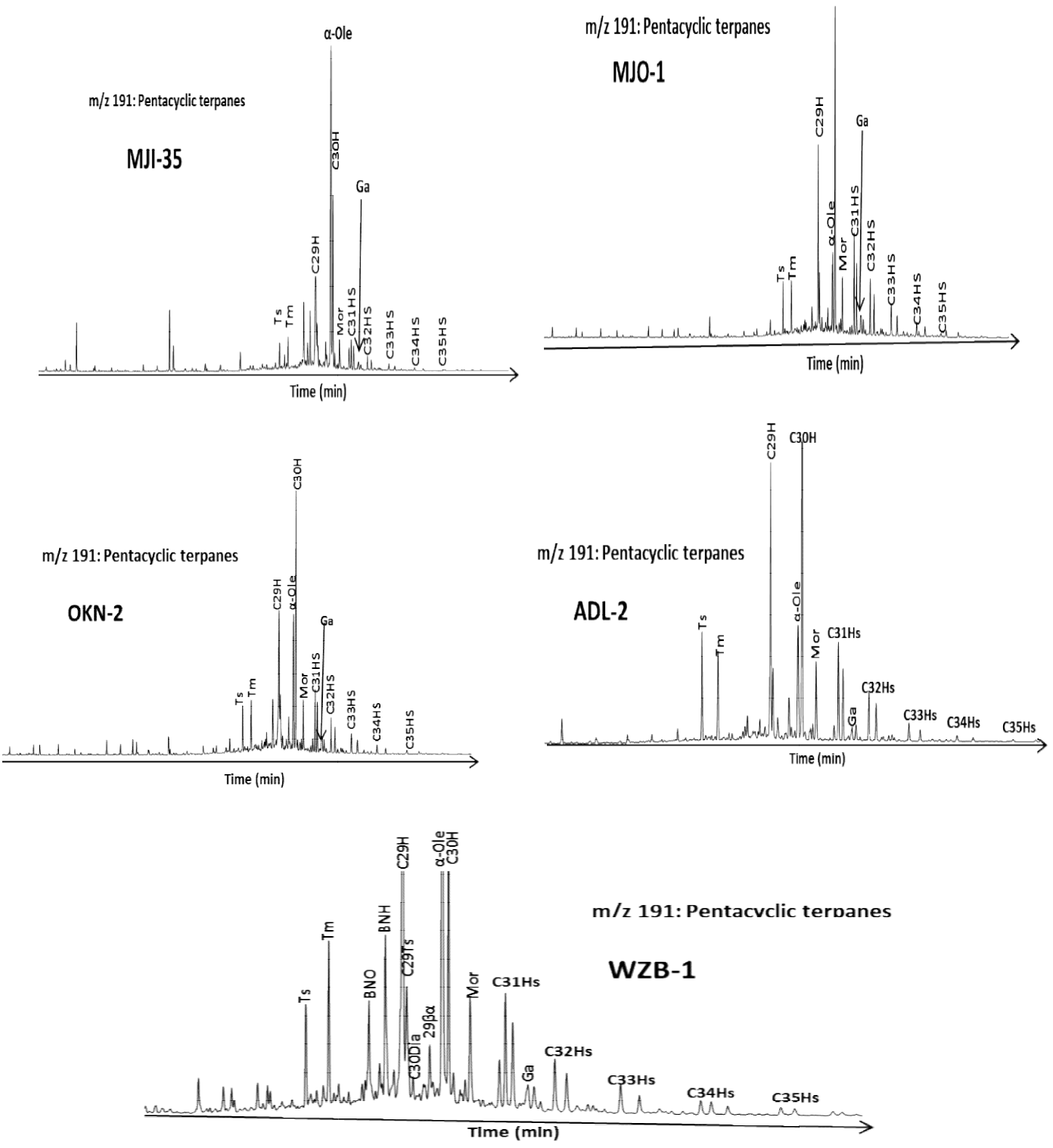

Fig. 4.29: m/z 191 Mass chromatograms showing the distributions of pentacyclic terpanes in representative crude oils from Niger Delta.

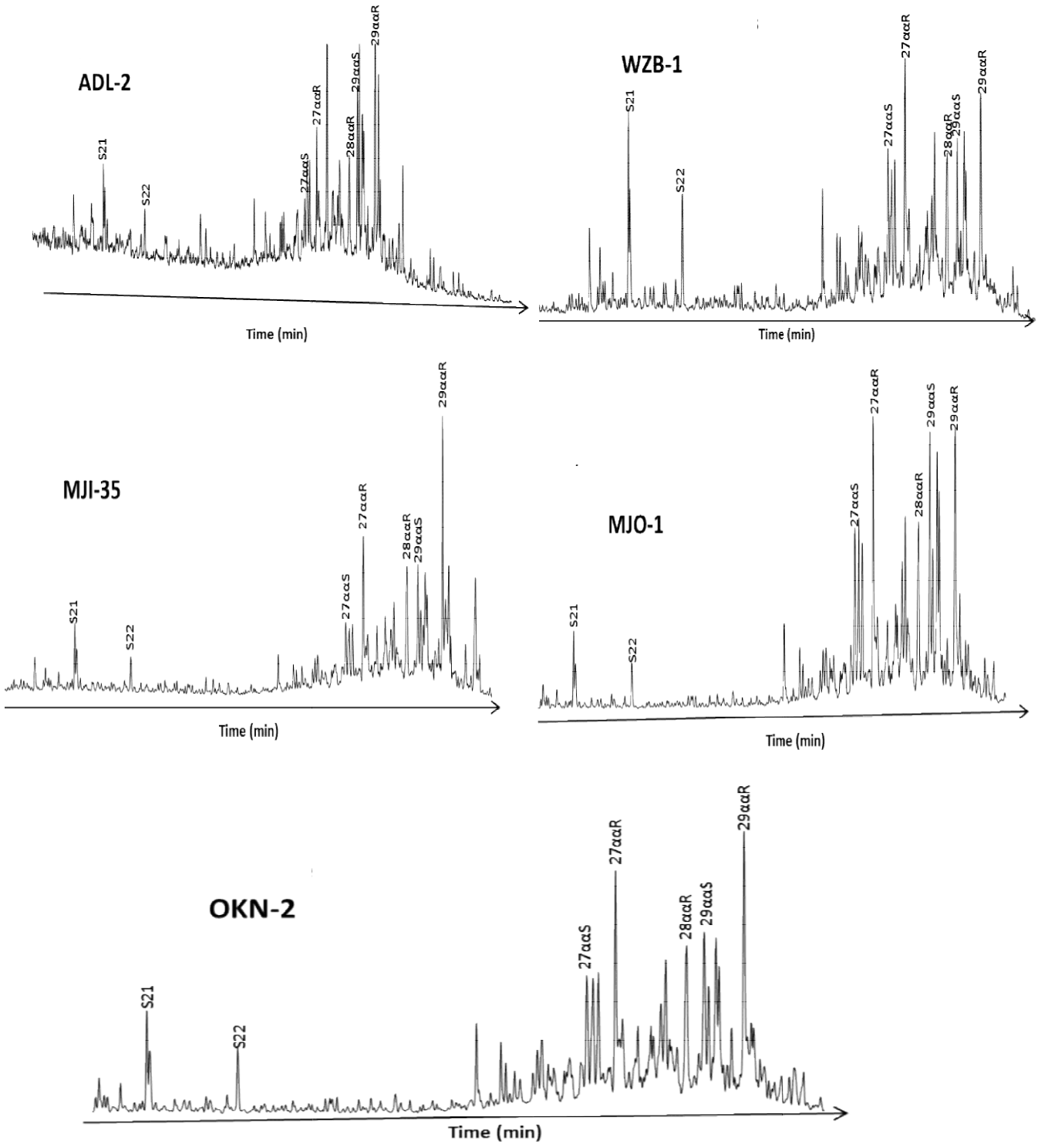
ADL-2
S21
S22
27ααS
27ααR
28ααR
29ααS
29ααR
Time (min)
WZB-1
S21
S22
27ααS
27ααR
28ααR
29ααS
29ααR
Time (min)
MJI-35
S21
S22
27ααS
27ααR
28ααR
29ααS
29ααR
Time (min)
MJO-1
S21
S22
27ααS
27ααR
28ααR
29ααS
29ααR
Time (min)
OKN-2
S21
S22
27ααS
27ααR
28ααR
29ααS
29ααR
Time (min)

Table: 4.9: Source and maturity parameters computed from the saturate hydrocarbon compounds in the Niger Delta crude oils

Well	Pr/Ph	Pr/C_{17}	Ph/C_{18}	OI	Ts/ (Tm+Ts)	22S/22S+22R C_{31}	20S/20S+20R C_{29}	ββ/ββ+αα C_{29}	Sterane, % C_{27}	C_{28}	C_{29}
ADL-1	3.61	0.51	0.16	0.30	0.48	0.56	0.41	0.37	20.8	27.8	51.5
ADL-2	3.95	0.54	0.16	0.31	0.52	0.56	0.40	0.37	19.7	26.6	53.7
ADL-3	5.48	0.56	0.15	0.32	0.46	0.56	0.40	0.37	25.8	23.5	50.7
ADL-4	5.40	0.55	0.14	0.31	0.48	0.56	0.44	0.38	23.9	24.4	51.7
ADL-5	4.13	0.56	0.15	0.30	0.50	0.56	0.43	0.38	20.2	28.0	51.8
ADL-6	4.30	0.53	0.15	0.03	0.51	0.56	0.45	0.38	21.9	27.2	50.9
ADL-7	4.08	0.52	0.15	0.31	0.49	0.56	0.45	0.39	20.1	30.4	49.5
ADL-8	3.61	0.51	0.16	0.32	0.51	0.56	0.44	0.39	21.1	28.1	50.8
ADL-9	3.61	0.51	0.15	0.32	0.61	0.57	0.47	0.38	24.9	25.5	49.5
OKN-1	2.39	5.84	2.33	1.44	0.40	0.52	0.36	0.36	31.3	30.3	38.4
OKN-2	2.19	2.67	1.57	0.72	0.43	0.53	0.40	0.39	31.1	31.9	37.1
OKN-3	2.11	2.80	1.63	0.71	0.43	0.53	0.40	0.40	32.8	31.3	35.9
OKN-4	2.39	4.78	2.97	1.30	0.41	0.53	0.33	0.41	30.0	32.3	37.7
OKN-5	2.18	2.77	1.60	0.72	0.46	0.53	0.41	0.39	33.6	31.8	34.6
OKN-6	2.29	2.43	1.34	0.72	0.43	0.53	0.39	0.38	31.7	30.3	38.0
OKN-7	2.10	2.87	1.65	0.70	0.43	0.53	0.43	0.39	32.5	32.6	34.9
OKN-8	2.25	0.39	0.20	0.58	0.61	0.53	0.39	0.42	31.7	29.3	39.0
OKN-9	2.18	2.61	1.50	0.71	0.43	0.53	0.41	0.37	32.6	32.1	35.3
OKN-10	2.72	0.49	0.22	1.02	0.47	0.54	0.36	0.39	31.0	31.8	37.2
OKN-11	2.62	0.51	0.23	1.02	0.46	0.54	0.33	0.38	30.8	32.0	37.2
OKN-12	2.83	0.52	0.22	1.24	0.48	0.53	0.37	0.37	31.2	30.3	38.5

Table 4.9 contd

Well	Pr/Ph	Pr/C_{17}	Ph/C_{18}	OI	Ts/ (Tm+Ts)	22S/22S+22R C_{31}	20S/20S+20R C_{29}	ββ/ββ+αα C_{29}	Sterane, % C_{27}	C_{28}	C_{29}
OKN-13	2.49	9.49	2.45	1.43	0.39	0.53	0.35	0.36	30.4	31.0	38.6
OKN-14	2.10	1.99	1.15	0.76	0.43	0.53	0.41	0.37	31.0	32.0	37.0
OKN-15	2.28	0.40	0.20	0.54	0.51	0.54	0.38	0.39	33.1	31.1	35.8
OKN-16	2.17	0.36	0.19	0.55	0.62	0.53	0.41	0.42	33.3	30.5	36.2
MJI-1	2.93	2.50	1.17	2.86	0.45	0.54	0.28	0.33	26.0	27.9	46.1
MJI-2	3.33	15.29	6.25	2.66	0.45	0.54	0.40	0.40	26.7	27.9	45.4
MJI-3	3.33	7.86	2.77	2.95	0.47	0.54	0.36	0.43	26.5	26.2	47.4
MJI-4	4.37	0.73	0.19	2.44	0.55	0.54	0.37	0.39	26.0	26.5	47.5
MJI-5	2.74	2.27	0.95	2.8	0.43	0.55	0.35	0.36	25.2	31.0	43.9
MJI-6	3.24	15.16	3.53	2.71	0.58	0.54	0.34	0.36	25.9	29.7	44.4
MJI-7	4.71	7.36	2.17	2.71	0.45	0.54	0.39	0.40	23.7	27.8	48.5
MJI-8	3.08	4.03	1.52	2.91	0.42	0.54	0.36	0.37	25.2	28.2	46.5
MJI-9	3.26	6.99	2.65	2.27	0.48	0.54	0.38	0.39	24.6	32.5	42.9
MJI-10	4.43	0.75	0.20	2.27	0.48	0.54	0.38	0.39	24.6	32.5	42.9
MJO-1	1.76	4.12	4.83	0.32	0.47	0.55	0.45	0.43	34.6	30.4	36.0
MJO-2	1.76	4.98	6.77	0.30	0.78	0.61	0.46	0.42	36.9	27.6	35.5
MJO-3	1.68	nd	nd	0.30	0.46	0.56	0.45	0.41	34.4	30.4	35.2
MJO-4	1.70	4.13	3.70	0.33	0.47	0.85	0.45	0.42	34.1	30.4	35.5
WZB-1	2.35	9.90	3.37	1.39	0.39	0.55	0.42	0.44	43.3	26.6	30.1
WZB-2	1.48	6.25	5.01	1.75	0.4	0.55	0.37	0.43	37.7	26.4	35.9

Oleanane index (OI) = 18α(H)-Oleanane/17α(H),21β(H)-hopane
nd: not determined

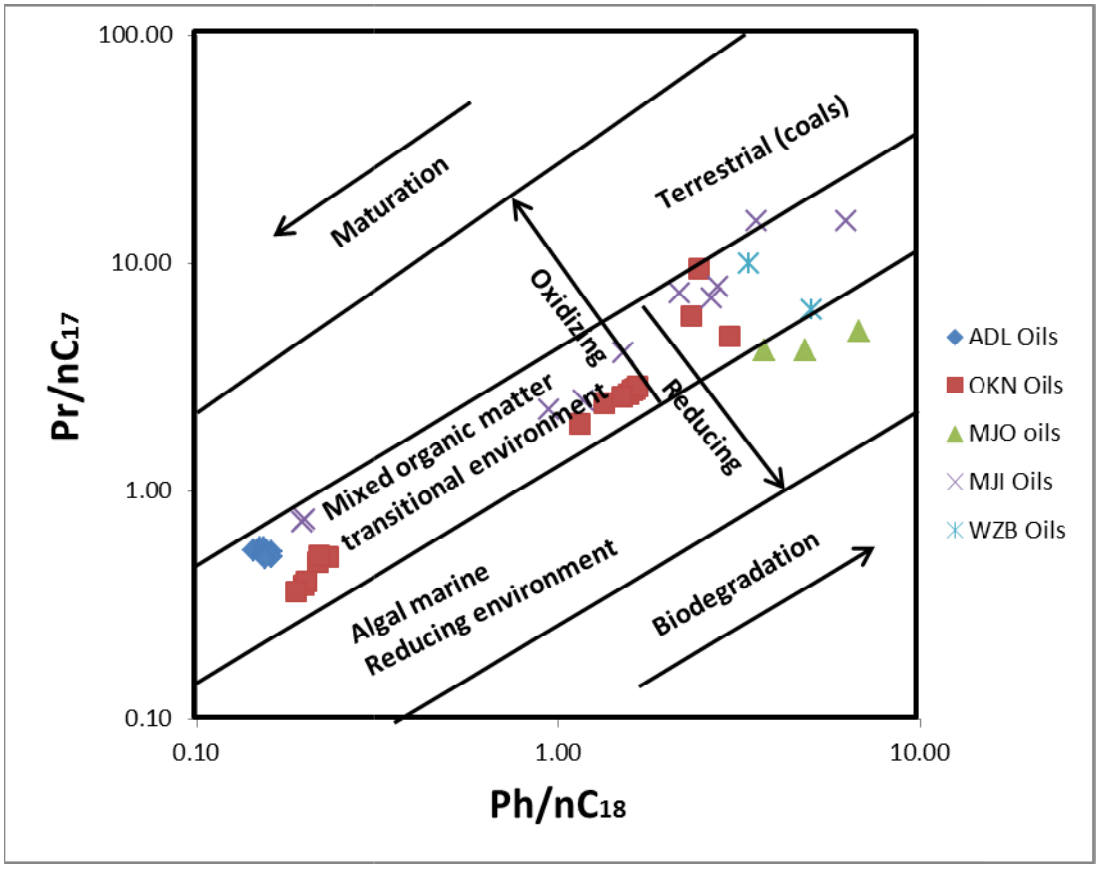

Fig. 4.31: Plot of Pr/nC17 against Ph/nC18 ratios of oils from Niger Delta (modified after Shanmugan, 1985)

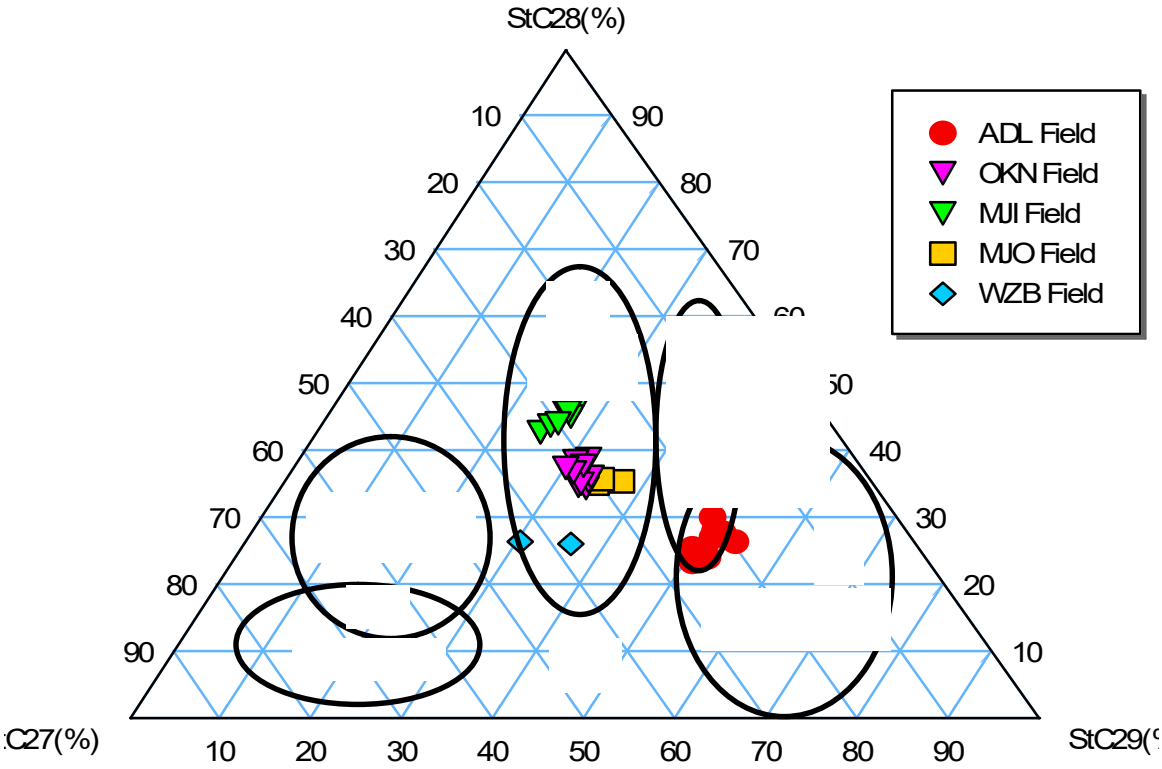

Fig. 4.32: Ternary plot of C_{27}, C_{28} and C_{29} sterane distributions in oils from Niger Delta (after Huang and Meinschein, 1979)

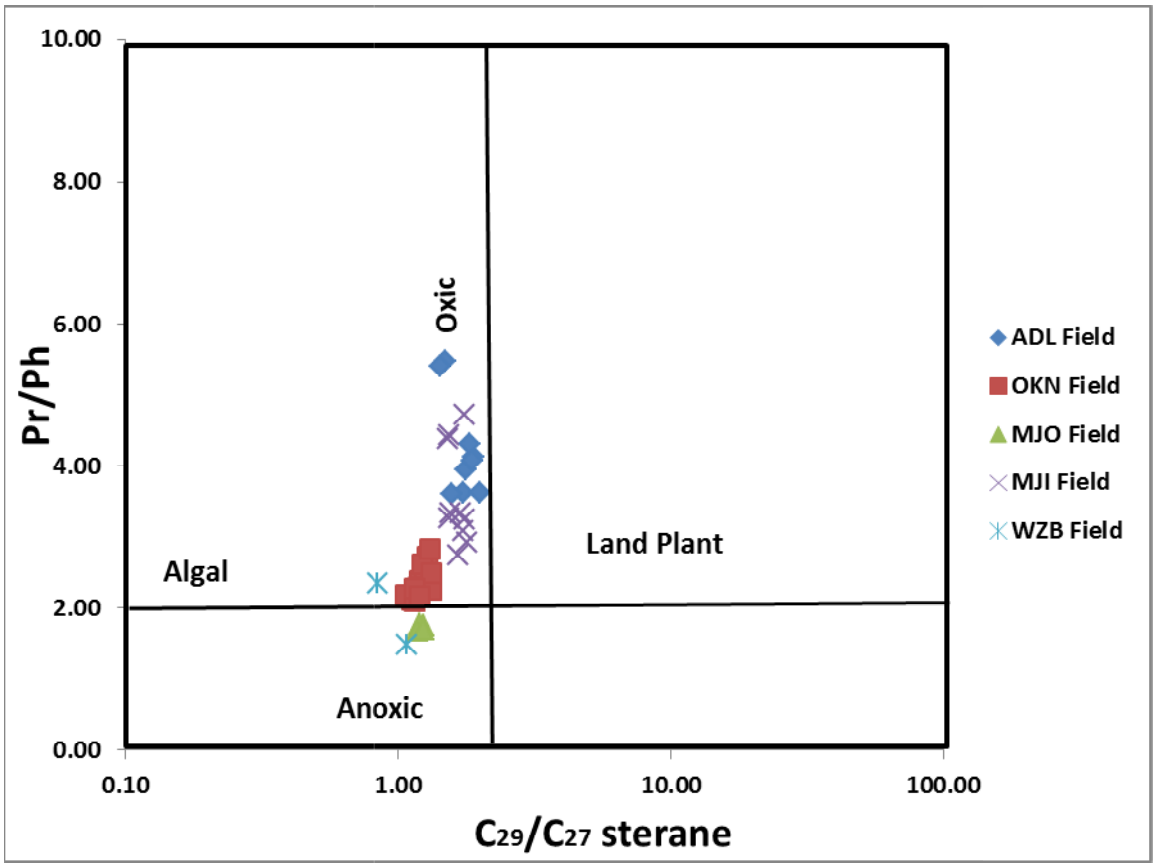

Fig. 4.33: Plot of Pr/Ph versus C_{29}/C_{27} steranes in Niger Delta crude oils (after Hakimi *et al*., 2011)

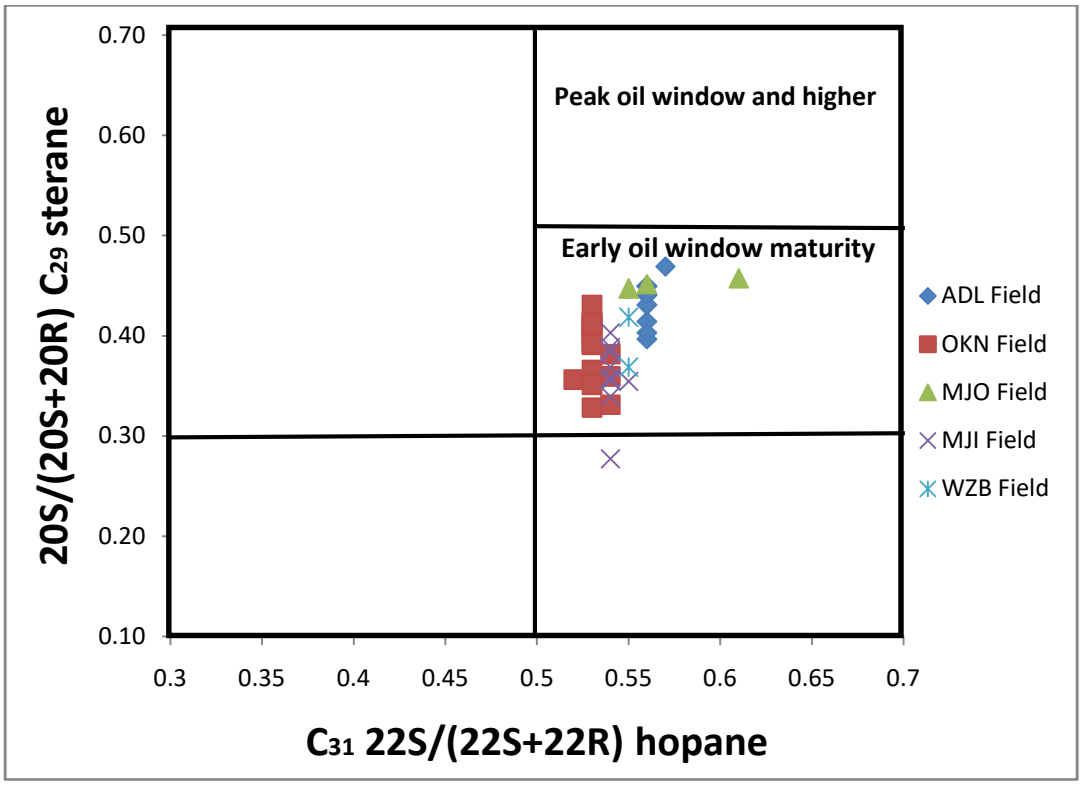

Fig. 4.34: Cross plots of 22S/(22S+22R) C_{31} hopane versus 20S/(20S+20R) C_{29} steranein Niger Delta oils (modified after Peters and Moldowan, 1993)

4.4.1.3MJI Field

The saturate fractions of the oils are dominated by n-alkanes in the range of n-C_{11} to n-C_{32} This mode of distribution reflects mixed (marine and terrestrial) origin (Hunt, 1996; Peters *et al*., 2005). The samples are characterized by Pr/Ph ratios in the range of 2.74 to 4.71 (Table 4.9). The high Pr/Ph values suggests oils derived from source rocks of significant terrestrial contribution, deposited in an oxic to sub-oxic paleoenvironment (Mello and Maxwell, 1990). Pr/n-C_{17} and Ph/n-C_{18} ratios range from 0.75 to 15.29 and 0.19 to 6.29, respectively. A plot of Pr/n-C_{18} versus Ph/n-C_{17} (Fig. 4.31) further supports mixed origin (terrestrial and marine) of the oils.

The oleanane/C_{30} hopane ratio (Oleanane Index) for the oils range from 2.27 to 2.95, indicating the input of terrestrial material into the organic matter of the oil source rocks (Ekweozor *et al*., 1979; Philp and Gilbert, 1986). The relative abundance of C_{27}, C_{28} and C_{29} steranes range from 23.7 to 26.7, 26.2 to 32.5 and 42.9 to 48.5%, respectively (Table 4.9). These distributions indicate oil derived from mixed origin (Fig. 4.32). However, the higher abundance of C_{29} sterane over C_{27} sterane (Table 4.9) suggests greater contributions from terrestrial source (Peters and Moldowan, 1993). Cross plot of Pr/Ph versus C_{29}/C_{27} ratios further confirmed terrestrial origin of the oils (Fig. 4.33).

The Ts/(Ts + Tm) ratios range from 0.42 to 0.58 (Table 4.9), indicating oils generated at the early maturity stage (Peters and Moldowan, 1993; Peters *et al*., 2005). The 22S/(22S+22R) C_{31} hopane values in the samples range from 0.54 to 0.55 (Table 4.9). The 20S/(20S+20R) and ββ/(ββ+αα) C_{29} sterane ratios range from 0.28 to 0.40 and 0.33 to 0.43, respectively (Table 4.9). These values indicate oils generated at the onset of oil generative window (Seifert and Moldowan, 1986; Peters and Moldowan, 1993). Plots of 22S/(22S+22R) C31 hopane versus 20S/(20S+20R) C29 sterane (Fig. 4.34) also indicate oils generated at the onset of oil generative window.

4.4.1.4 MJO Field

The m/z 85 mass chromatograms of the crude oil show a unimodal pattern with predominance of C_{11}-C_{20} over C_{22}-C_{33} which reflects significant contributions from marine. (Fig. 4.28c). The Pr/Ph ratio of oil samples range from 1.68 to 1.76 (Table 4.9), reflecting oils derived from mixed organic matter but with significant marine contribution

deposited under suboxic conditions (Mello and Maxwell, 1990, Hunt, 1996; Ten Haven, 1996). The Pr/n-C_{17} and Pr/n-C_{18} ratios range from 4.12 to 4.98 and 3.70 to 6.77, respectively. A plot of Pr/n-C_{17} versus Ph/n-C_{18} (Fig. 4.31) showed that the oils were derived from marine source.

The oleanane/C_{30} hopane ratios (Oleanane Index) for the oils range from 0.30 to 0.33. The presence of oleanane is good indicator of terrestrial input into the oil- source rocks (Ekweozor *et al*., 1979; Philp and Gilbert, 1986) and source age not older than Cretaceous (Hakimi *et al*., 2011). The relative abundance of C_{27}, C_{28} and C_{29} steranes range from 34.1 to 36.9, 27.6 to 30.4 and 35.2 to 36.0%, respectively (Table 4.9). The distributions of C_{27}-C_{29} steranes in the oils (Table 4.9) indicate oils derived from source rock of mixed origin (terrestrial and marine) (Fig. 4.32). The plot of Pr/Ph versus C_{29}/C_{27} further showed that the oil source rock received significant input from algal materials (Hakimi *et al*., 2011) (Fig. 4.33).

The Ts/(Ts + Tm) ratios range from 0.46 to 0.78 (Table 4.9), indicating oil generated at the early stage of oil generative window to peak of oil generation (Peters et al., 2005). The 22S/(22S+22R) C_{31} hopane ratios for the oils range from 0.55 to 0.85 (Table 4.9). These values are consistent with oils generated from source rocks at early stage of thermal maturity to late oil generation window (Seifert and Moldowan, 1986; Peters ans Moldowan, 1993). The 20S/(20S+20R) and ββ/(ββ+αα) C_{29} sterane values range from 0.45 to 0.46 and 0.41 to 0.43, respectively (Table 4.9). These values indicate oils generated at the onset of oil generative window (Seifert and Moldowan, 1986). The samples also fall within the zone of oil generated at early oil window maturity on the cross plot of 22S/(22S+22R) C_{31} hopane against 20S/(20S+20R) C_{29} sterane (Fig. 4.34).

4.4.1.5 WZB Field

The gas chromatograms of the crude oil samples are characterized by the n-alkanes in the range of n-C_{12} to n-C_{29} and a predominance of medium molecular weight compounds (n-C_{12} to n-C_{19}) (Fig. 4.28e). The distributions of n-alkanes showed that the samples are lightly biodegraded (Volkman *et al*., 1984). The Pr/Ph ratios of the oil samples range from 1.48 to 2.35 (Table 4.9), reflecting oils derived from mixed organic matter but with significant marine contribution deposited under sub-oxic conditions (Mello and Maxwell,

1990, Hunt, 1996; Ten Haven, 1996). Pr/n-C_{17} and Ph/n-C_{18} ratios of the oils range from 6.25 to 9.90 and 3.37 to 5.01, respectively (Table 4.9). A plot of Pr/n-C_{17} versus Ph/n-C_{18} (Fig. 4.31) showed that the crude oils were derived from source rocks of mixed origin (terrestrial and marine).

The oleanane/C_{30} hopane values (Oleanane Index) range from 1.39 to 1.75 (Table 4.9). The presence of oleanane suggests the input of terrestrial material into the organic matter of the oil source rocks. The relative abundance of C_{27}, C_{28} and C_{29} steranes range from 37.7 to 43.3, 26.4 to 26.6 and 30.1 to 35.9%, respectively (Table 4.9). The relative distribution of these compounds indicate oil derived from source rock of mixed origin (terrestrial and marine) (Huang and Meinschein, 1979). Ternary plots of C_{27}, C_{28} and C_{29} steranes further confirm the mixed origin of the source rocks (Fig. 4.32). The relative higher abundance of C_{27} over C_{29} steranes indicates more input of algal materials into the source rocks (Huang and Meinschein, 1979; Peters and Moldowan, 1993). A plot of Pr/Ph versus C_{29}/C_{27} also confirms greater input of algal material (Fig. 4.33).

The Ts/(Ts + Tm), 22S/(22S+22R) C_{31} hopane, 20S/(20S+20R) C_{29} sterane and ββ/(ββ+αα) C_{29} sterane ratios in the crude oils range from 0.39 to 0.40, 0.55, 0.37 to 0.42 and 0.43 to 0.44, respectively (Table 4.9). These values are within the range expected for oil generated at the onset of oil generative window (Seifert and Moldowan, 1986; Peters and Moldowan, 1993; Peters *et al*., 2005) (Fig. 4.34).

4.5 Aromatic Hydrocarbons Distributions in the oils

The representative m/z 170, 178, 192, 198, 231, 228+242 and 202+216 mass chromatograms showing the distribution of methylnaphthalenes, phenanthrene, methylphenanthrenes, methyldibenzothiophenes, triaromatic steroids, chrysene and methylchrysenes, pyrene and methylpyrenes in the aromatic fractions of crude oils are presented in Fig.s 4.35, 4.36a, 4.36b, 4.37a, 4.37b, 4.38 and 4.39, respectively. Peak identities are presented in Table 4.4. These compounds were used to assess the origin, depositional environment and thermal maturity of the oil samples. Geochemical parameters computed from the aromatic compounds are presented in Tables 4.10 and 4.11.

4.5.1 ADL Field

The presence of significant amounts of 1,6-, 1,7-, and 2,6-DMNs in the samples indicate terrigenous organic matter contribution (Day and Edman, 1963; Achari *et al*., 1973). The presence of 1,2,5- and 1,2,7-TMN in the samples indicate oils derived from organic matter with angiosperm and gymnosperms material contribution (Killops and Killops, 2005). The occurrence of 1,2,6 TMN in sediments has been linked to microbial source (Alexander *et al*., 1992). Therefore its presence in the samples also indicates microbial contribution to the organic matter. The occurrence of 9- and 1-MP in the oils indicates oils derived from source rock of mixed origin (terrestrial and marine). The occurrence of fluoranthene and pyrene in the oils may suggest microbial metabolism of fungi, higher plants or insects (Grice *et al*., 2009; Fang et al., 2015) while the occurrence of chrysene and its isomers may be due to the degradation products of hopanes by cleavage of ring E and successive aromatization from ring D to ring A (Borrego *et al*., 1997) or terrestrial contribution to the source rocks organic matter (Jinggui *et al*., 2004, 2005). The Fla/(Fla+Py) and BaA/(BaA+Chy) values for ADL oils range from 0.38 to 0.50 and 0.20 to 0.39 respectively, indicating mixed organic sources.

The dibenzothiophene/phenanthrene (DBT/P) ratios of the oils range from 0.13 to 0.38 (Table 4.10), indicating oils derived from source rock with predominant higher plant organic matter input and deposited in deltaic environment (Requejo, 1994; Sivan *et al*., 2008). All the oil samples fall within the zone of fluvial/deltaic zone on the plot of DBT/P against Pr/Ph ratios as shown in Fig. 4.40. The C_{26}/C_{28}-TAS 20S and C_{27}/C_{28}-TAS 20R ratios in the oils range from 0.21 to 0.32 and 0.43 to 0.52, respectively. The low C_{26}/C_{28} values indicate oils derived from source rocks deposited in freshwater environment (Xiangchun *et al*., 2011). The cross plot of C_{26}/C_{28}-TAS 20S versus C_{27}/C_{28}-TAS 20R showed that the oils were derived from similar organic materials (Fig. 4.41).

The TMNr-1, TMNr-2 and calculated vitrinite reflectance (Rcb%) for the oils range from 0.59 to 0.70, 0.66 to 0.69 and 0.76 to 0.81, respectively (Table 4.10). These values show narrow range indicating similar maturity status. TMNr-1 values for the oils are < 1, indicating that the source rocks that generated these oils are just at the peak of oil generation window (Alexander *et al*., 1985). The Rcb values (< 0.95, Table 4.10) also indicate that the oil samples were formed at the peak of oil generation window. The

methylphenanthrenes ratios, MPI-1 and MPI-2 values range from 0.61 to 0.91 and 0.70 to 0.82, respectively (Table 4.10). These values show little or no variation in the maturity status of the oils. The vitrinite reflectance (%VRc) of the oils was calculated from themethylphenanthrene index (MPI-1). The %VRc values range from 0.81 to 0.90 (Table 4.10). These values support the narrow maturity range of the oils and also indicate that the oils were generated at the peak of oil generative window (Radke, 1988). The %VRc ratios are higher than sterane and hopane maturity indices. The saturate biomarker maturity parameters have been reported to reach equilibrium at the onset of oil generation window and therefore may not be providing the true reflection of the maturity status of the oils. The methyldibenzothiophene ratios (MDR) range from 1.52 to 7.04 (Table 4.10). The MDR values show that the oils are thermally mature. The triaromatic steroids maturity ratio C_{28}S-TAS/(C_{28}R+C_{28}S-TAS) range from 0.54 to 0.59, indicating that the oils are thermally mature (Lewan *et al*., 1986). The pyrene and chrysene maturity ratios 2-/1-methylpyrene (2-/1-MPy), methylpyrene ratio (MPYR) and 2-/1-methylchrysene (2-/1-MChy) range from 0.69 to 0.98, 0.41 to 0.49 and 0.70 to 0.89, respectively. These values show that the oils are thermally mature (Garrigues *et al*., 1988; Kruge, 2000; Li *et al*., 2012; Fang *et al*., 2015).

4.5.2 OKN Field

The Fla/(Fla+Py) and BaA/(BaA+Chy) values for the oils range from 0.43 to 0.64 and 0.18 to 0.33 respectively, reflecting oil derived from mixed organic matter (Borrego *et al*., 1997; Jinggui *et al*., 2005; Grice *et al*., 2009; Li *et al*., 2012; Fang *et al*., 2015).

The dibenzothiophene/phenanthrene (DBT/P) ratio of the crude oils range from 0.10 to 0.14, indicating oils derived from marine or lacustrine shales (Sivan *et al*., 2008). A plot of dibenzothiophene/phenanthrene (DBT/P) against Pr/Ph ratios further confirmed the marine or lacustrine origin of the oils (Fig. 4.40). The C_{26}/C_{28}-TAS 20S and C_{27}/C_{28}-TAS 20R ratios in the oils range from 0.43 to 0.49 and 0.66 to 0.78, respectively. The C_{26}/C_{28} values indicate oils derived from source rocks deposited in brackish/lacustrine environment (Xiangchun *et al*., 2011). The cross plots of the C_{26}/C_{28}-TAS 20S and C_{27}/C_{28}-TAS 20R ratios showed oils derived from source rocks of similar organic matter (Fig. 4.41).

The TMNr-1, TMNr-2 and calculated vitrinite reflectance values Rcb% (TMNr-2) computed for the oils range from 0.73 to 1.55, 0.72 to 1.05 and 0.83 to 1.03, respectively (Table 4.10). The MPI-1 and MPI-2 values in the oils range from 0.62 to 0.95 and 0.66 to 0.99, respectively (Table 4.10). These values indicate that the oils are within a narrow range of maturity. The calculated vitrinite reflectances (VRc%) values range from 0.77 to 0.97%, suggesting that the oils were generated at the peak of oil window (Radke, 1987, 1988). The MDR values in the oils range from 3.52 to 4.51 (Table 4.10). These values fall within a narrow range indicating similar maturity. The triaromatic steroids maturity ratio, C_{28}S-TAS/(C_{28}R+C_{28}S-TAS) range from 0.52 to 0.55, indicating that the oils are thermally mature (Lewan *et al*., 1986). The Fla/(Fla+Py) and BaA/(BaA+Chy) values for the oils range from 0.43 to 0.64 and 0.18 to 0.33, respectively, reflecting oil derived from mixed organic matter (Borrego *et al*., 1997; Jinggui *et al*., 2005; Grice *et al*., 2009; Li *et al*., 2012; Fang *et al*., 2015). The pyrene and chrysene based maturity parameters, 2-/1-methylpyrene (2-/1-MPy), methylpyrene ratio (MPYR) and 2-/1-methylchrysene (2-/1-MChy) range from 0.88 to 1.39, 0.47 to 0.58 and 1.06 to 1.67, respectively. These values further show that the oils are thermally mature (Garrigues *et al*., 1988; Kruge, 2000; Li *et al.*, 2012; Fang *et al*., 2015).

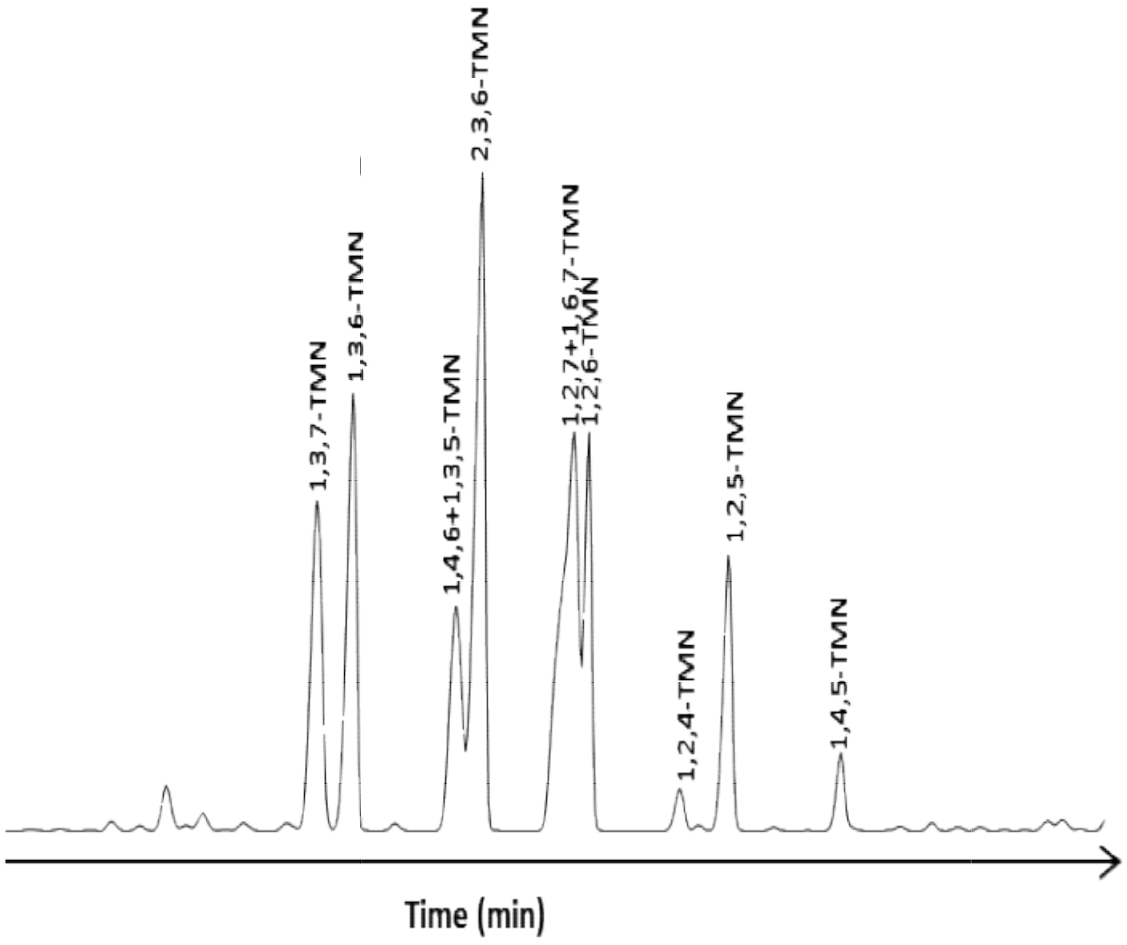

Fig. 4.35: m/z 170 Mass chromatogram showing the distribution of trimethylnaphthalenes in representative oil samples from Niger Delta

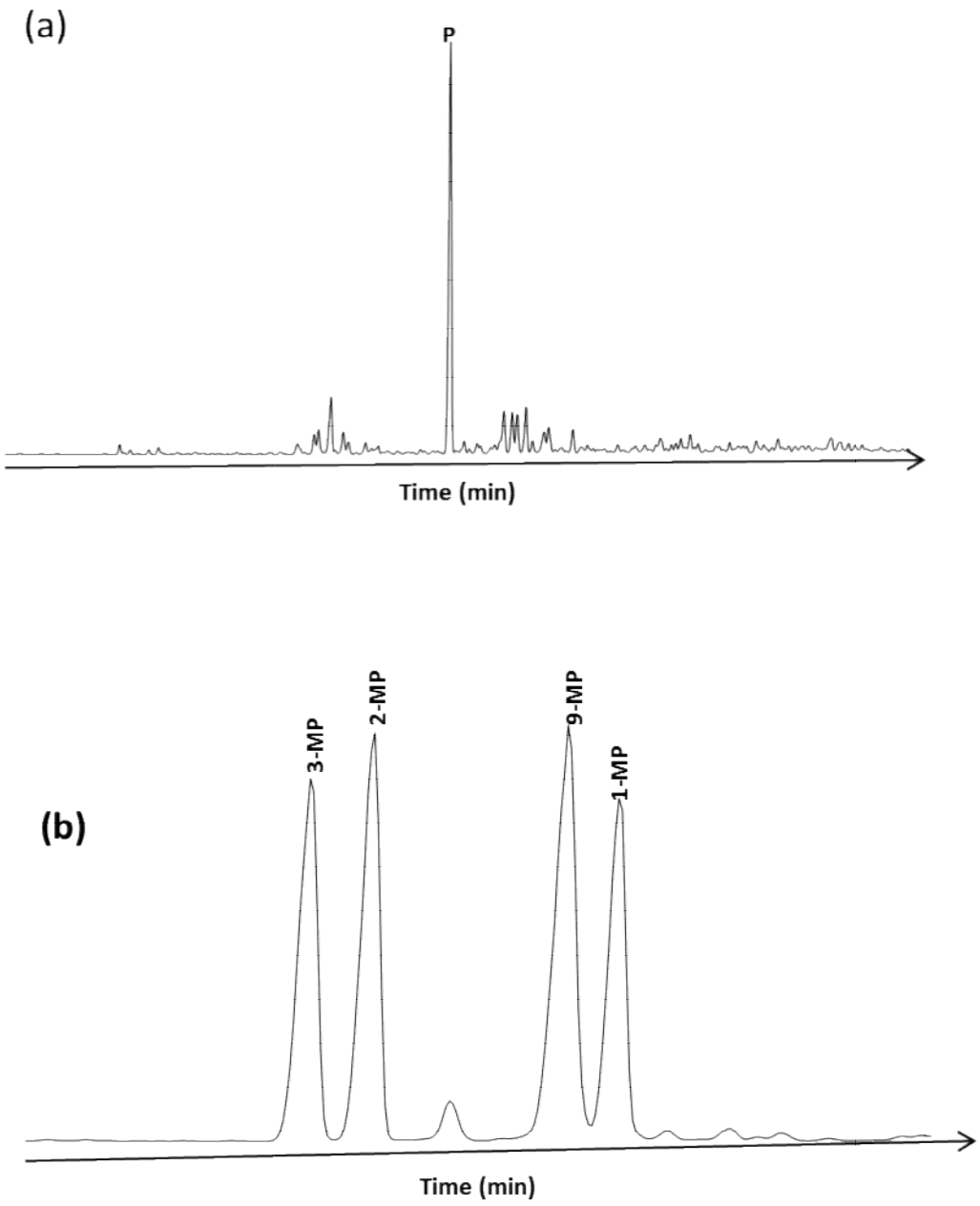

Fig. 4.36: m/z 178 and 192 Mass chromatograms showing the distribution of (a) phenanthrene and (b) methylphenanthrenes in representative oil samples from Niger Delta

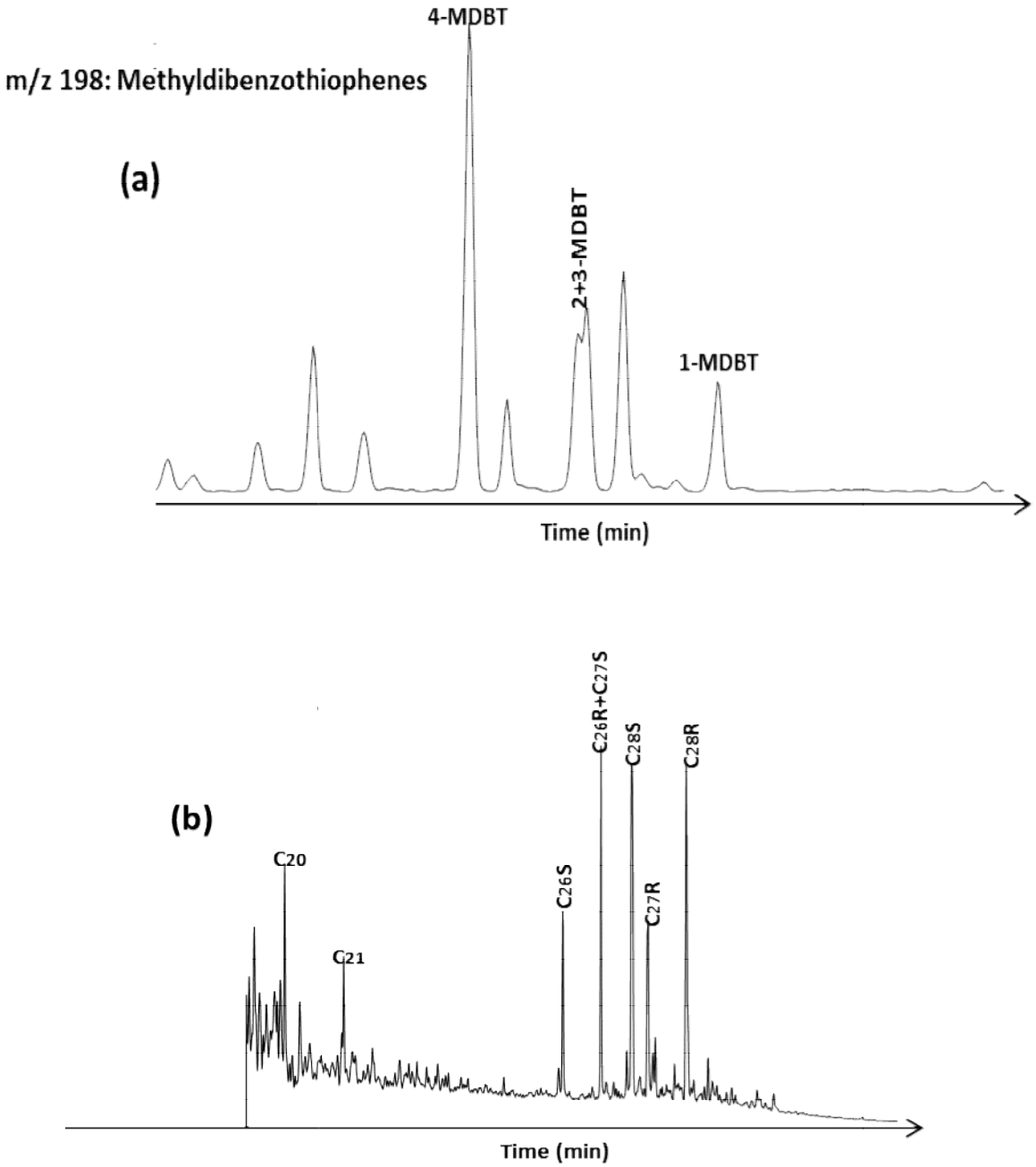

Fig. 4.37: m/z 198 and 231 Mass chromatograms showing the distribution of (a) methyldibenzothiophene and (b) triaromatic steroids in representative oil samples from Niger Delta.

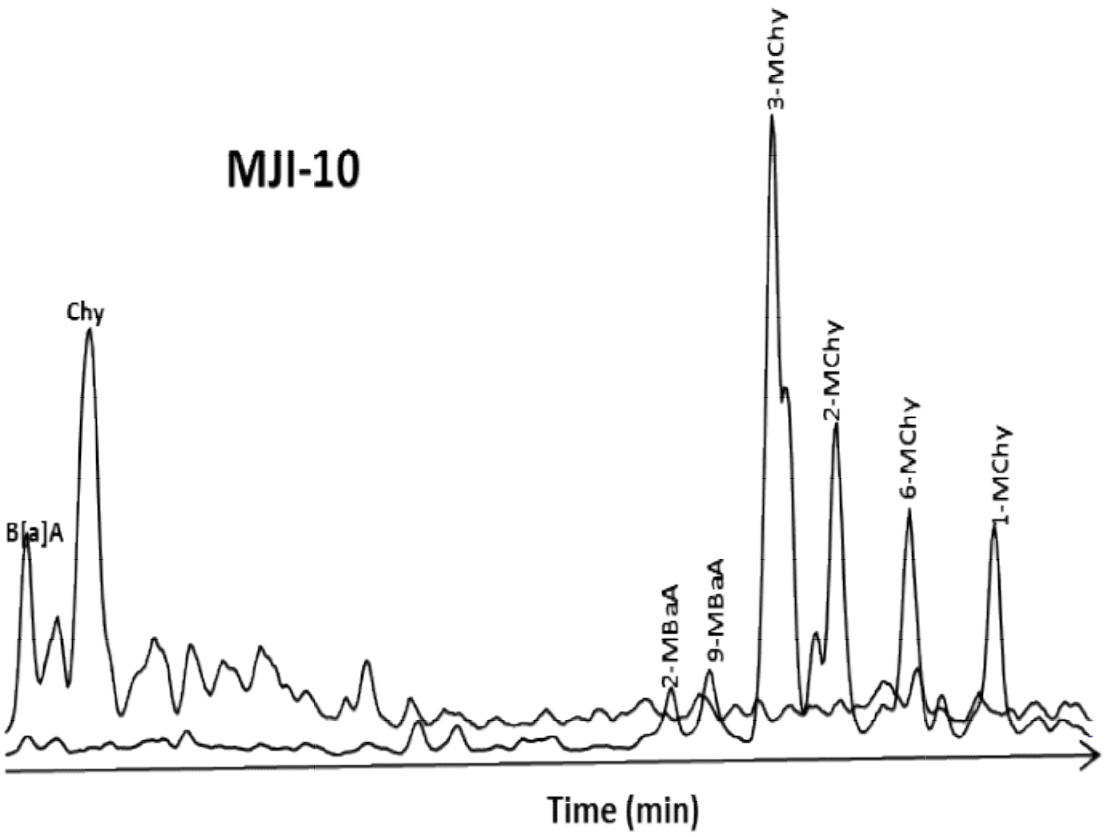

Fig. 4.38: m/z 228+242 mass chromatograms showing the distributions of chrysene, methylchrysenes and their isomers in crude oils from Niger Delta.

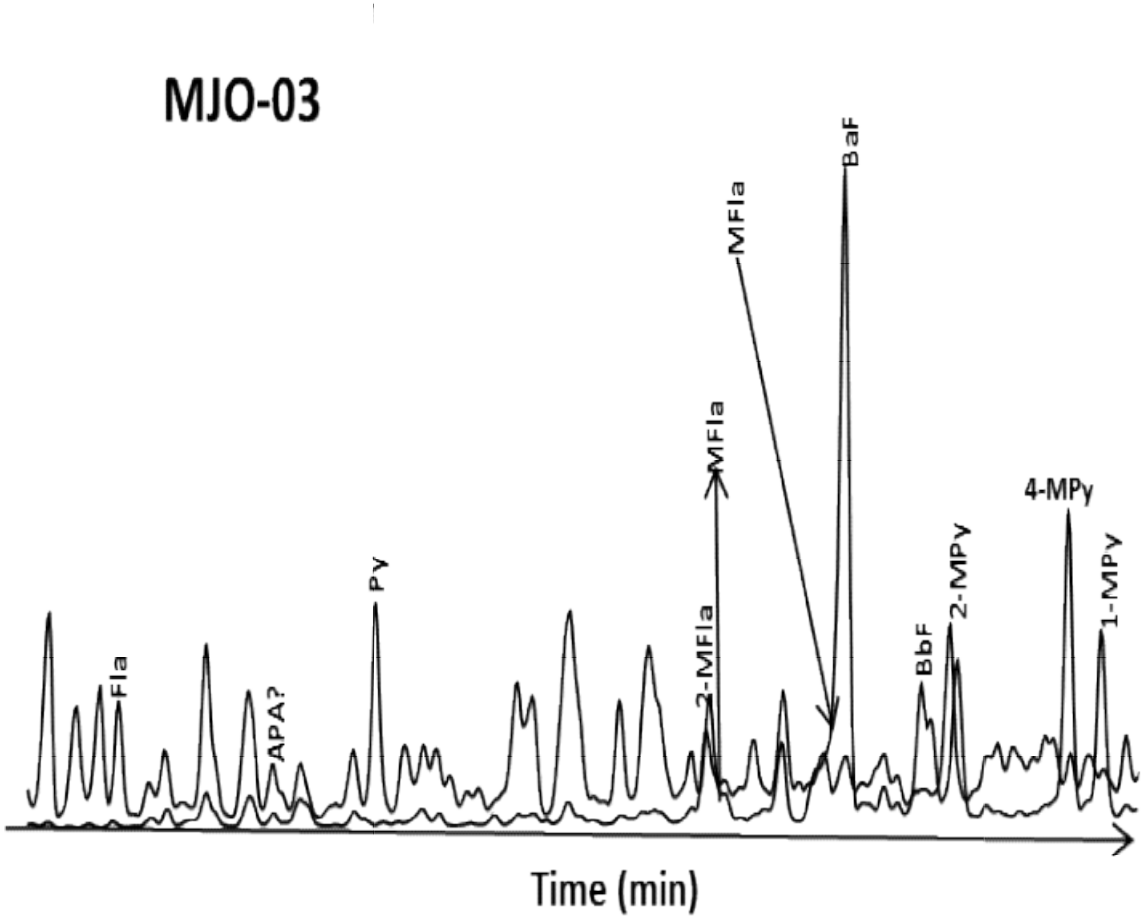

Fig. 4.39: m/z 202 + 216 mass chromatograms showing the distributions of pyrene , fluoranthene , methylfluoranthenes and methylpyrenes in crude oils from Niger Delta, Nigeria.

Table 4.10: Source and maturity parameters computed from the aromatic hydrocarbon distributions in crude oils

Sample	MPI-1	MPI-2	VRc	TMNR-1	TMNR-2	MDR	Rcb	DBT/P	C27/C28 20R TAS	C26/C28 20S TAS	20S/(20S+20R) C28 TAS
ADL-1	0.73	0.73	0.84	0.66	0.66	3.25	0.80	0.22	0.48	0.21	0.55
ADL-2	0.71	0.71	0.83	0.66	0.67	3.17	0.80	0.21	0.48	0.21	0.56
ADL-3	0.61	0.71	0.81	0.59	0.60	7.04	0.76	0.38	0.50	0.32	0.52
ADL-4	0.73	0.72	0.84	0.62	0.64	6.88	0.78	0.13	0.51	0.23	0.59
ADL-5	0.70	0.70	0.82	0.66	0.66	2.43	0.80	0.20	0.52	0.24	0.55
ADL-6	0.78	0.77	0.87	0.68	0.68	3.17	0.81	0.19	0.45	0.23	0.55
ADL-7	0.79	0.77	0.87	0.69	0.69	1.52	0.81	0.15	0.52	0.22	0.54
ADL-8	0.82	0.81	0.89	0.69	0.69	2.59	0.81	0.18	0.45	0.23	0.56
ADL-9	0.91	0.82	0.90	0.70	0.69	3.05	0.81	0.15	0.43	0.22	0.54
OKN-1	0.95	0.98	0.97	1.55	1.05	3.61	1.03	0.13	0.71	0.45	0.55
OKN-2	0.91	0.95	0.95	0.92	0.78	3.80	0.87	0.12	0.77	0.49	0.53
OKN-3	0.91	0.95	0.95	0.87	0.77	3.66	0.86	0.13	0.77	0.48	0.54
OKN-4	0.93	0.97	0.96	1.03	0.84	3.52	0.91	0.14	0.69	0.45	0.54
OKN-5	0.90	0.93	0.94	0.92	0.79	3.92	0.87	0.11	0.76	0.49	0.53
OKN-6	0.95	0.99	0.97	1.00	0.79	3.64	0.87	0.10	0.75	0.49	0.52
OKN-7	0.90	0.93	0.94	0.84	0.77	4.03	0.86	0.10	0.75	0.49	0.53
OKN-8	0.89	0.92	0.93	1.15	0.91	4.29	0.94	0.10	0.75	0.48	0.53
OKN-9	0.91	0.94	0.94	0.92	0.77	3.87	0.86	0.12	0.78	0.48	0.54
OKN-10	0.76	0.77	0.85	0.91	0.77	4.07	0.86	0.14	0.70	0.46	0.54
OKN-11	0.70	0.70	0.82	0.82	0.74	3.30	0.85	0.14	0.72	0.46	0.55
OKN-12	0.76	0.76	0.85	0.87	0.76	3.88	0.86	0.13	0.70	0.45	0.54

Table 4.10: contd

Sample	MPI-1	MPI-2	VRc	TMNR-1	TMNR-2	MDR	Rcb	DBT/P	C27/C28 20R TAS	C26/C28 20S TAS	20S/(20S+20R) C28 TAS
OKN-13	0.94	0.96	0.96	1.07	0.86	3.82	0.92	0.12	0.69	0.45	0.55
OKN-14	0.62	0.63	0.77	0.73	0.72	3.76	0.83	0.13	0.68	0.45	0.54
OKN-15	0.65	0.66	0.79	0.81	0.73	3.85	0.84	0.13	0.69	0.48	0.54
OKN-16	0.70	0.72	0.82	0.83	0.75	4.51	0.85	0.11	0.66	0.43	0.53
MJI-1	0.76	0.78	0.86	0.43	0.59	4.16	0.75	0.11	0.59	0.35	0.55
MJI-2	0.84	0.86	0.90	1.80	1.14	5.29	1.08	0.11	0.56	0.32	0.56
MJI-3	0.83	0.86	0.90	1.13	0.85	5.40	0.91	0.11	0.56	0.32	0.55
MJI-4	0.96	0.99	0.97	1.09	0.83	5.82	0.90	0.11	0.55	0.32	0.55
MJI-5	0.78	0.80	0.87	0.47	0.60	3.71	0.76	0.12	0.59	0.36	0.55
MJI-6	0.82	0.85	0.89	0.89	0.78	4.51	0.87	0.12	0.54	0.33	0.54
MJI-7	0.86	0.89	0.92	1.47	0.99	5.17	0.99	0.11	0.54	0.31	0.56
MJI-8	0.82	0.85	0.89	0.87	0.76	4.30	0.86	0.12	0.59	0.34	0.55
MJI-9	0.83	0.86	0.90	1.34	0.96	4.84	0.97	0.12	0.53	0.34	0.55
MJI-10	0.83	0.86	0.90	1.05	0.82	4.72	0.89	0.13	0.59	0.37	0.53
MJO-1	0.71	0.80	0.81	3.29	1.83	4.13	1.50	0.10	0.70	0.44	0.52
MJO-2	0.77	0.81	0.86	2.09	1.32	3.99	1.19	0.11	0.70	0.44	0.53
MJO-3	0.78	0.81	0.84	2.46	1.49	4.14	1.29	0.11	0.70	0.45	0.53
MJO-4	0.89	0.81	0.87	1.38	1.00	4.30	1.00	0.11	0.71	0.44	0.53
WZB-1	0.86	0.89	0.91	3.99	2.18	2.31	1.71	0.18	0.84	0.50	0.52
WZB-2	0.86	0.88	0.92	4.17	2.26	2.74	1.76	0.16	0.75	0.46	0.52

TMNr-1=2,3,6-trimethylnaphthalene/[(1,4,6- + 1,3,5-trimethylnaphthalene)]; TMNr-2= 2,3,6-trimethylnaphthalene/[(1,4,6- + 1,3,5-trimethylnaphthalene) + (1,3,6- + 1,3,7-trimethylnaphthalene)]; Rcb = 0.6(TMNr-2) + 0.4; TAS: triaromatic steroids.
MPI-1(methylphenanthrene index-1) =1.5(2- + 3-methylphenanthrene)/(phenanthrene + 1- + 9-methylphenanthrene).
MPI-2 (methylphenanthrene index-2) =3(2-methylphenanthrene)/(phenanthrene + 1- + 9-methylphenanthrene).
VRc =0.6(MPI-1) + 0.4; MDR : 4-MDBT/1-MDBT; DBT/P: dibenzothiophene/phenanthrene

Table 4.11: Source and maturity parameters computed from the chrysenes and pyrenes distributions in crude oils

Sample	Depth(m)	2-/1-Mpy	MPYR	Fla/(Fla+Py)	BaA/(BaA+Chy)	2-/1-Mchy
ADL-1	2602-2607	0.69	0.41	0.43	0.39	0.79
ADL-2	2602-2607	0.70	0.41	0.41	0.39	0.81
ADL-3	2702-2704	0.71	0.42	0.50	0.20	0.77
ADL-4	2718-2720	0.75	0.43	0.48	0.28	0.88
ADL-5	2759-2763	0.70	0.41	0.43	0.35	0.81
ADL-6	2766-2770	0.73	0.42	0.43	0.37	0.82
ADL-7	2905-2908	0.80	0.44	0.39	0.34	0.70
ADL-8	2964-2967	0.97	0.49	0.38	0.36	0.89
ADL-9	3064-3052	0.98	0.49	0.38	0.34	0.80
OKN-1	1749-1750	1.33	0.57	0.61	0.20	1.61
OKN-2	1892-1895	0.94	0.49	0.46	0.21	1.67
OKN-3	1905-1907	1.04	0.51	0.46	0.19	1.55
OKN-4	1952-1955	1.39	0.58	0.61	0.20	1.56
OKN-5	2050-2059	1.10	0.52	0.46	0.20	1.56
OKN-6	2369-2555	0.88	0.47	0.45	0.19	1.64
OKN-7	2377-2672	1.05	0.51	0.43	0.21	1.61
OKN-8	2469-2782	1.15	0.54	0.43	0.18	1.55
OKN-9	2485-2793	1.04	0.51	0.44	0.20	1.50
OKN-10	2489-2491	1.39	0.58	0.58	0.33	1.32
OKN-11	2521-2523	1.10	0.52	0.57	0.32	1.06
OKN-12	2530-2537	1.07	0.52	0.56	0.31	1.23
OKN-13	2566-2568	1.24	0.55	0.62	0.21	1.27
OKN-14	2677-2683	1.27	0.56	0.64	0.30	1.13
OKN-15	3148-3154	0.89	0.47	0.63	0.29	1.26
OKN16	3593-3605	1.22	0.55	0.61	0.27	1.02
MJI-1	1607-1611	1.29	0.56	0.71	0.33	1.08
MJI-2	1777-1779	1.15	0.53	0.61	0.27	1.40
MJI-3	1795-1797	1.06	0.51	0.62	0.27	1.61
MJI-4	1920-1921	1.08	0.52	0.55	0.27	1.84
MJI-5	1936-2342	0.90	0.47	0.70	0.28	1.19
MJI-6	1944-1947	1.18	0.54	0.65	0.29	1.46

Table 4.11: contd

Sample	Depth(m)	2-/1-Mpy	MPYR	Fla/(Fla+Py)	BaA/(BaA+Chy)	2-/1-Mchy
MJI-7	1948-1950	1.38	0.58	0.60	0.24	1.60
MJI-8	1979-2398	1.11	0.53	0.66	0.26	1.40
MJI-9	2442-2444	1.16	0.54	0.62	0.24	1.50
MJI-10	3030-3036	1.06	0.51	0.44	0.22	1.33
MJO-1	2207-2216	0.91	0.48	0.31	0.20	1.34
MJO-2	2070-2081	0.86	0.46	0.34	0.19	1.40
MJO-3	2091-2104	0.92	0.48	0.34	0.21	1.37
MJO-4	2096-2101	0.95	0.49	0.33	0.20	1.26
WZB-1		0.96	0.49	0.43	0.46	1.06
WZB-2		0.97	0.49	0.47	0.43	1.21

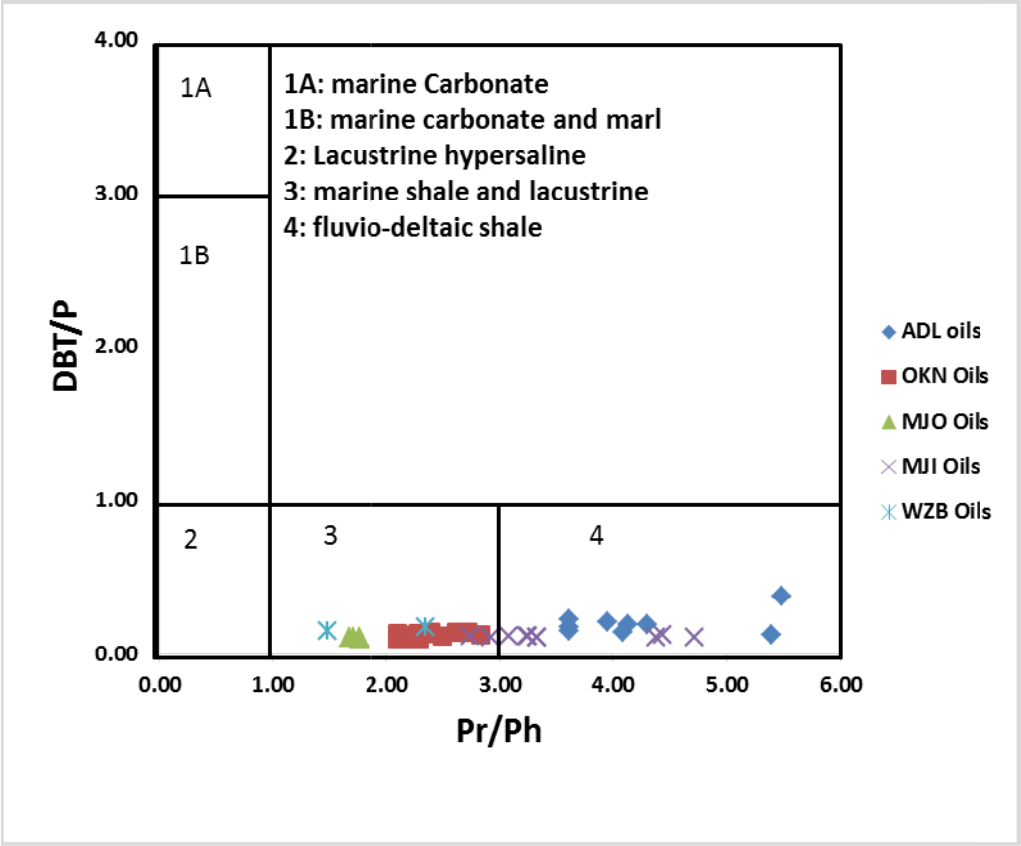

Fig.4.40: A cross plot of dibenzothiophene/phenanthrene (DBT/P) and pristane/phytane(Pr/Ph) ratios for the Niger Delta oils (after Hughes *et al*., 1995)

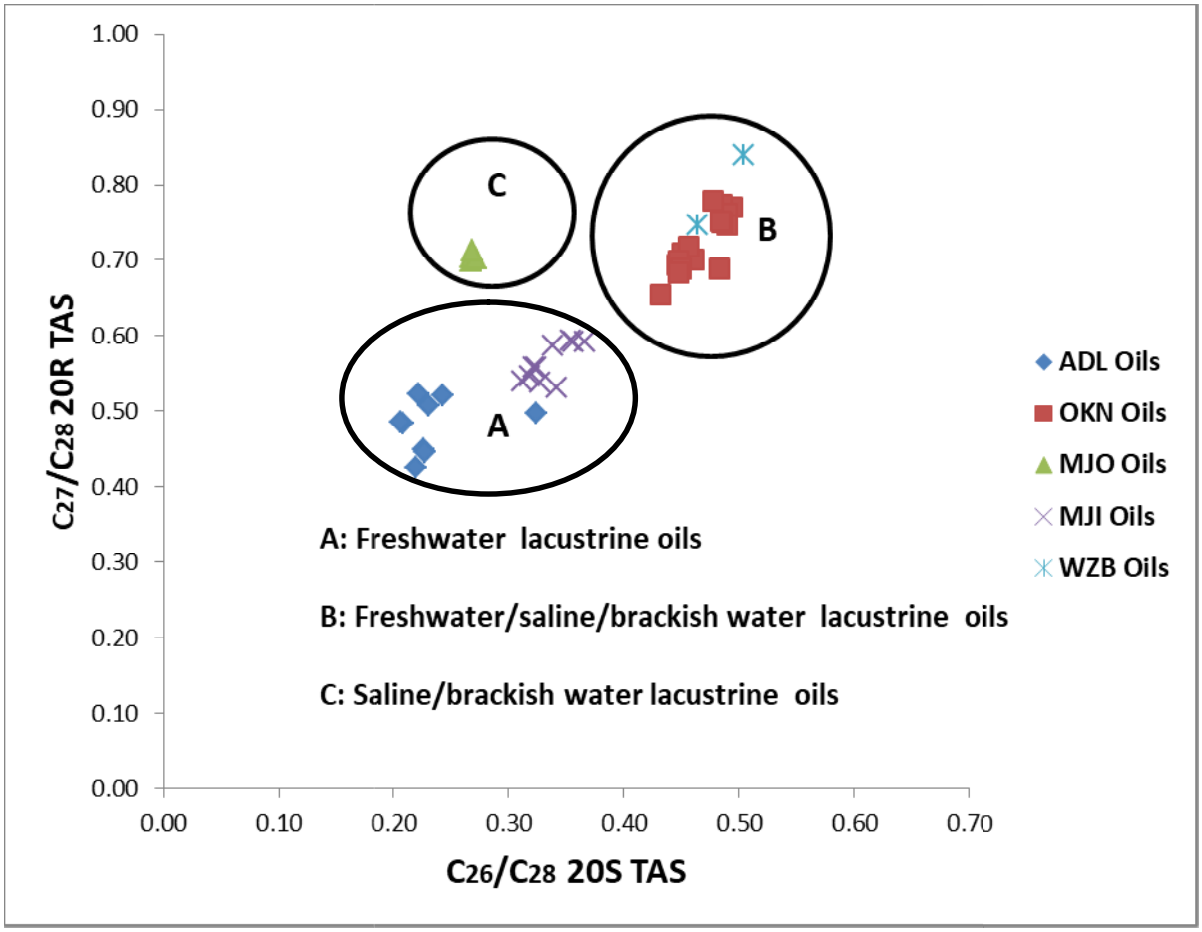

Fig. 4.41: Cross plot of C_{27}/C_{28} 20R TAS versus C_{26}/C_{28} 20S TAS for Niger Delta crudeoils (after Peters *et al*., 2005).

4.5.3 MJI Field

The Fla/(Fla+Py) and BaA/(BaA+Chy) values for the oils range from 0.44 to 0.71 and 0.22 to 0.33 respectively, reflecting oil derived from mixed organic matter with higher terrigenous organic matter input (Borrego *et al*., 1997; Jinggui *et al*., 2005; Grice *et al*., 2009; Li *et al*., 2012; Fang *et al*., 2015). The dibenzothiophene/phenanthrene (DBT/P) ratio of the crude oils range from 0.11 to 0.13, indicating that the oils were derived from source rock with predominant higher plant organic matter input, deposited in deltaic environment (Requejo, 1994; Sivan *et al*., 2008). A plot of dibenzothiophene/phenanthrene (DBT/P) against Pr/Ph ratios further confirmed fluvial/deltaic origin of the oils (Fig. 4.40). The C_{26}/C_{28}-TAS 20S and C_{27}/C_{28}-TAS 20R ratios in the oils range from 0.31 to 0.37 and 0.53 to 0.59, respectively. The C_{26}/C_{28} values indicate oils derived from source rocks deposited in freshwater environment (Xiangchun *et al*., 2011). The cross plots between the C_{26}/C_{28}-TAS 20S and C_{27}/C_{28}-TAS 20R ratios showed oils derived from source rocks of similar organic matter (Fig. 4.41).

The alkylnaphthalene maturity parameters TMNr-1, TMNr-2 and calculated vitrinite reflectance values Rcb% of the oils range from 0.43 to 1.34, 0.59 to 0.99 and 0.75 to 1.08, respectively (Table 4.10). The MPI-1 and MPI-2 values range from 0.76 to 0.96 and 0.78 to 0.99, respectively (Table 4.10). These values indicate that the oils are within a narrow maturity range. The calculated vitinite reflectance (VRc%) values range from 0.86 to 0.97% , suggesting that the oils were generated at the peak of oil window (Radke, 1987, 1988). The MDR values of the oilsamples range from 3.71 to 5.82 (Table 4.10). These values fall within a narrow range indicating similar maturity. The triaromatic steroids maturity ratio C_{28}S-TAS/(C_{28}R+C_{28}S-TAS) range from 0.53 to 0.56, indicating that the oils are thermally mature (Lewan et al., 1989). The pyrene and chrysene based maturity parameters, 2-/1-methylpyrene (2-/1-MPy), methylpyrene ratio (MPYR) and 2-/1-methylchrysene (2-/1-MChy) range from 0.90 to 1.38, 0.47 to 0.58 and 1.08 to 1.84 respectively. These values show that the oils are thermally matured (Garrigues *et al*., 1988; Kruge, 2000; Li *et al*., 2012; Fang *et al*., 2015).

4.5.4 MJO Field

The Fla/(Fla+Py) and BaA/(BaA+Chy) values for the oils range from 0.31 to 0.34 and 0.19 to 0.31 respectively, which show oil derived from mixed organic matter (Borrego *et al.*, 1997; Jinggui *et al*., 2005; Grice *et al*., 2009; Li *et al*., 2012; Fang *et al*., 2015). The dibenzothiophene/phenanthrene ratio of the oils range between 0.10 and 0.11 (Table 4.10), indicating oils formed from marine or lacustrine shales (Sivan *et al*., 2008). Cross plot of dibenzothiophene/phenanthrene (DBT/P) versus Pr/Ph ratios further confirmed the marine or lacustrine shale origin of the oils (Fig. 4.40). The C_{26}/C_{28}-TAS 20S and C_{27}/C_{28}-TAS 20R ratios in the oils range from 0.44 to 0.45 and 0.70 to 0.71, respectively. The C_{26}/C_{28} values indicate oils derived from source rocks deposited in brackish/lacustrine environments (Xiangchun *et al*., 2011). The cross plots of these parameters showed oils derived from source rocks of similar organic matter (Fig. 4.41).

The TMNr-1, TMNr-2 and calculated vitrinite reflectance values for the oils range from 1.38 to 3.29, 1.00 to 1.83 and 1.00 to 1.50, respectively (Table 4.10). The MPI-1 and MPI-2 values of the oilsamples range from 0.71 to 0.89 and 0.78 to 0.81, respectively (Table 4.10). These values fall within a narrow range reflecting similar maturity status of the oils. The calculated vitrinite reflectance (VRc%) values range between 0.81 and 0.87%, suggesting that the oils were generated at the peak of oil window (Radke, 1987, 1988). The MDR values in the oils range from 3.99 to 4.30 (Table 4.10). The triaromatic steroids maturity ratio C_{28}S-TAS/(C_{28}R+C_{28}S-TAS) range from 0.52 to 0.53, indicating that the oils are thermally mature (Lewan *et al*., 1986). The pyrene and chrysene based maturity parameters, 2-/1-methylpyrene (2-/1-MPy), methylpyrene ratio (MPYR) and 2-/1-methylchrysene (2-/1-MChy) range from 0.86 to 1.95, 0.46 to 0.49 and 1.26 to 1.40, respectively. These values further confirmed that the oils are thermally matured (Garrigues *et al*., 1988; Kruge, 2000; Li *et al*., 2012; Fang *et al*., 2015).

4.5.5 WZB Field

The Fla/(Fla+Py) and BaA/(BaA+Chy) values for the oils range from 0.43 to 0.47 and 0.43 to 0.46 respectively. These values are within a narrow range which reflects oil derived from similar organic matter.

The dibenzothiophene/phenanthrene ratio of the oils range from 0.16 to 0.18 (Table 4.10), suggesting oils derived from marine or lacustrine shales (Sivan *et al*., 2008). Cross plot of dibenzothiophene/phenanthrene (DBT/P) against Pr/Ph ratios further confirmed the marine or lacustrine shale origin of the oils (Fig. 4.40). The C_{26}/C_{28}-TAS 20S and C_{27}/C_{28}-TAS 20R ratios in the oils range from 0.46 to 0.50 and 0.75 to 0.84, respectively. The C_{26}/C_{28} values suggest oils derived from source rocks deposited in brackish/lacustrine environments (Xiangchun *et al*., 2011). The plots of C_{26}/C_{28}-TAS 20S versus C_{27}/C_{28}-TAS 20R ratios showed oils derived from source rocks of similar organic matter (Fig. 4.41).

The TMNr-1, TMNr-2 and calculated vitrinite reflectance values in the oils range from 3.99 to 4.17, 2.18 to 2.26 and 1.71 to 1.76, respectively (Table 4.10). The MPI-1 value is 0.86 for both samples while MPI-2 values in the oils range from 0.88 to 0.89 (Table 4.10). These values indicate that the oils are within a narrow range of maturity. The calculated vitrinite reflectances (VRc%) values range from 0.91 to 0.92%, indicating that the oils were generated at the peak of oil window (Radke, 1987, 1988). The MDR values in the oils range from 2.31 to 2.74 (Table 4.10). These values show a narrow maturity range, indicating similar maturity status. The triaromatic steroids maturity ratio C_{28}S-TAS/(C_{28}R+C_{28}S-TAS) is 0.52 for both oils, indicating that the oils are thermally mature (Lewan et al., 1986). The 2-/1-methylpyrene (2-/1-MPy) and 2-/1-methylchrysene (2-/1-MChy) range from 0.96 to 0.97 and 1.06 to 1.21, respectively, while the methylpyrene ratio (MPYR) values are constant at 0.49 for the two oil samples. These values show thatthe oils are thermally mature (Garrigues *et al*., 1988; Kruge, 2000; Li *et al*., 2012; Fang *et al*., 2015).

4.6 Stable Carbon Isotopic Composition of Niger Delta oils

4.6.1 Bulk stable carbon isotope

The bulk stable carbon isotope of the whole oils, saturate and aromatic fractions are presented in Tables 4.12 The bulk isotopic data were used in determining the origin and depositional environment of the oils.

4.6.1.1 ADL Field

The carbon isotopic values of the whole oil, saturate, and aromatic fractions of the oils range from -26.8‰ to -27.8‰, -27.7‰ to -28.3‰ and -24.9‰ to -26.9‰, respectively (Table 4.12). For each sample, the saturate fraction is more depleted in $\delta^{13}C$ than the aromatic fraction with values not more than -1.4‰. The isotopic differences between the whole oils, saturate and aromatic fractions of the oils are less than 1.0‰, indicating that the crude oils were derived from the same source (Table 4.12) (Peters and Moldowan, 1993). The oils plotted between terrigenous and marine zone on the cross plot of $\delta^{13}C_{aro}$ versus $\delta^{13}C_{sat}$ (Fig.4.42). However, the majority of the oils fall within the terrigenous region which further confirmed the terrestrial source input for the oil samples (Sofer, 1984).

4.6.1.2 OKN Field

The carbon isotopic values of the whole oil, saturate, and aromatic fractions of the oils range from -25.4‰ to -26.3‰, -25.9‰ to -27.0‰ and -23.6‰ to -25.3‰, respectively (Table 4.12). In all the samples, the saturate fraction is more depleted in $\delta^{13}C$ than the aromatic fraction with values not more than 1.0‰. The isotopic differences between the whole oils and saturate and aromatic fractions of the oils are less than 1.4‰, indicating that the crude oils were derived from the same source (Table 4.12) (Peters and Moldowan, 1993). The oils plotted between terrigenous and marine zone on the cross plot of $\delta^{13}C_{aro}$ versus $\delta^{13}C_{sat}$ (Fig. 4.42) indicating oils derived from source rocks of mixed sources.

4.6.1.3 MJI Field

The carbon isotopic values of the whole oil, saturate, and aromatic fractions of the oils range from -25.5‰ to -27.3‰, -26.2‰ to -28.4‰ and -25.2‰ to -26.0‰, respectively (Table 4.12). The isotopic differences between the whole oils, saturate and aromatic fractions of the oils are less than 1.9‰, indicating that the crude oils were derived from the same source (Table 4.12) (Peters and Moldowan, 1993). The oils plotted between the terrigenous and marine zones on the plots of $\delta^{13}C_{aro}$ versus $\delta^{13}C_{sat}$(Fig.4.42).

However, the majority of the oils fall within the terrigenous region indicating higher input of plant materials into the organic matter that formed the oils.

4.6.1.4 MJO Field

The carbon isotopic values of the whole oil, saturate, and aromatic fractions of the oils range from -25.6‰ to -26.2‰, -26.5‰ to -27.0‰ and -23.5‰ to -26.2‰, respectively (Table 4.12). The isotopic differences between the whole oils and saturate and aromatic fractions of the oils are less than 1.5‰, indicating that the crude oils were derived from the same source (Table 4.12) (Peters and Moldowan, 1993). The cross plot of $\delta^{13}C_{aro}$ versus $\delta^{13}C_{sat}$ (Fig. 4.42) for MJO samples show the oils plotted within the marine and terrigenous zone indicating oils derived from source rocks of mixed origin (terrestrial and marine).

Table 4.12: Bulk stable carbon isotopic data of Niger Delta oils

		$\delta^{13}C$, ‰			
Sample	Depth(m)	Oil	Sat	Aro	Polar
ADL-1	2602-2607	-27.7	-28.1	-26.9	-27.2
ADL-2	2602-2607	-27.8	-27.8	-25.8	-27.1
ADL-3	2702-2704	-26.8	-27.7	-24.9	-27.4
ADL-4	2718-2720	-27.3	-28.2	-25.3	-27.2
ADL-5	2759-2763	-27.7	-27.7	-25.1	-27.1
ADL-6	2766-2770	-27.7	-27.9	-25.8	-27.6
ADL-7	2905-2908	-27.3	-27.7	-26.9	-27.4
ADL-8	2964-2967	-27.3	-27.8	-25.0	-27.2
ADL-9	3064-3052	-27.5	-28.3	-26.5	-27.1
OKN-1	1749-1750	-25.4	-26.1	-24.2	-25.5
OKN-2	1892-1895	-25.8	-26.4	-23.6	-25.0
OKN-3	1905-1907	-25.4	-26.5	-24.3	-25.6
OKN-4	1952-1955	-25.6	-26.0	-24.3	-25.6
OKN-5	2050-2059	-25.8	-26.3	-24.9	-24.9
OKN-6	2369-2555	-25.9	-26.6	-24.9	-24.9
OKN-7	2377-2672	-25.5	-26.4	-24.3	-25.2
OKN-8	2469-2782	-25.7	-25.9	-23.9	-24.9
OKN-9	2485-2793	-25.8	-26.5	-24.1	-25.2
OKN-10	2489-2491	-25.5	-26.9	-25.3	-25.8
OKN-11	2521-2523	-26.1	-26.9	-23.9	-26.1
OKN-12	2530-2537	-26.3	-27.0	-24.8	-25.7
OKN-13	2566-2568	-25.6	-26.2	-24.5	-24.6
OKN-14	2677-2683	-25.5	-26.3	-24.8	-25.8
OKN-15	3148-3154	-26.1	-26.3	-25.0	-25.5
OKN-16	3593-3605	-25.2	-26.2	-23.7	-25.0

Table 4.12 contd: Bulk stable carbon isotopic data of Niger Delta oils

		$\delta^{13}C$, ‰			
Sample	Depth(m)	Oil	Sat	Aro	Polar
MJI-1	1607-1611	-25.5	-27.1	-25.6	-26.8
MJI-2	1777-1779	-26.2	-27.0	-25.0	-26.8
MJI-3	1795-1797	-26.1	-28.0	-25.6	-27.6
MJI-4	1920-1921	-26.9	-27.9	-25.6	-26.7
MJI-5	1936-2342	-26.1	-26.2	-25.2	-26.5
MJI-6	1944-1947	-26.3	-27.1	-25.4	-27.0
MJI-7	1948-1950	-26.8	-28.0	-26.0	-26.9
MJI-8	1979-2398	-26.2	-26.9	-25.5	-28.5
MJI-9	2442-2444	-26.2	-27.7	-25.3	-27.6
MJI-10	3030-3036	-27.3	-28.4	-25.4	-26.8
MJO-1	2207-2216	-26.2	-26.6	-23.5	-24.9
MJO-2	2070-2081	-25.6	-27.0	-24.4	-25.4
MJO-3	2091-2104	-25.9	-26.6	-24.2	-24.5
MJO-4	2096-2101	-25.7	-26.5	-26.2	-26.6
WZB-1		-25.9	-26.5	-25.7	-26.8
WZB-2		-25.2	-26.8	-25.4	-26.1

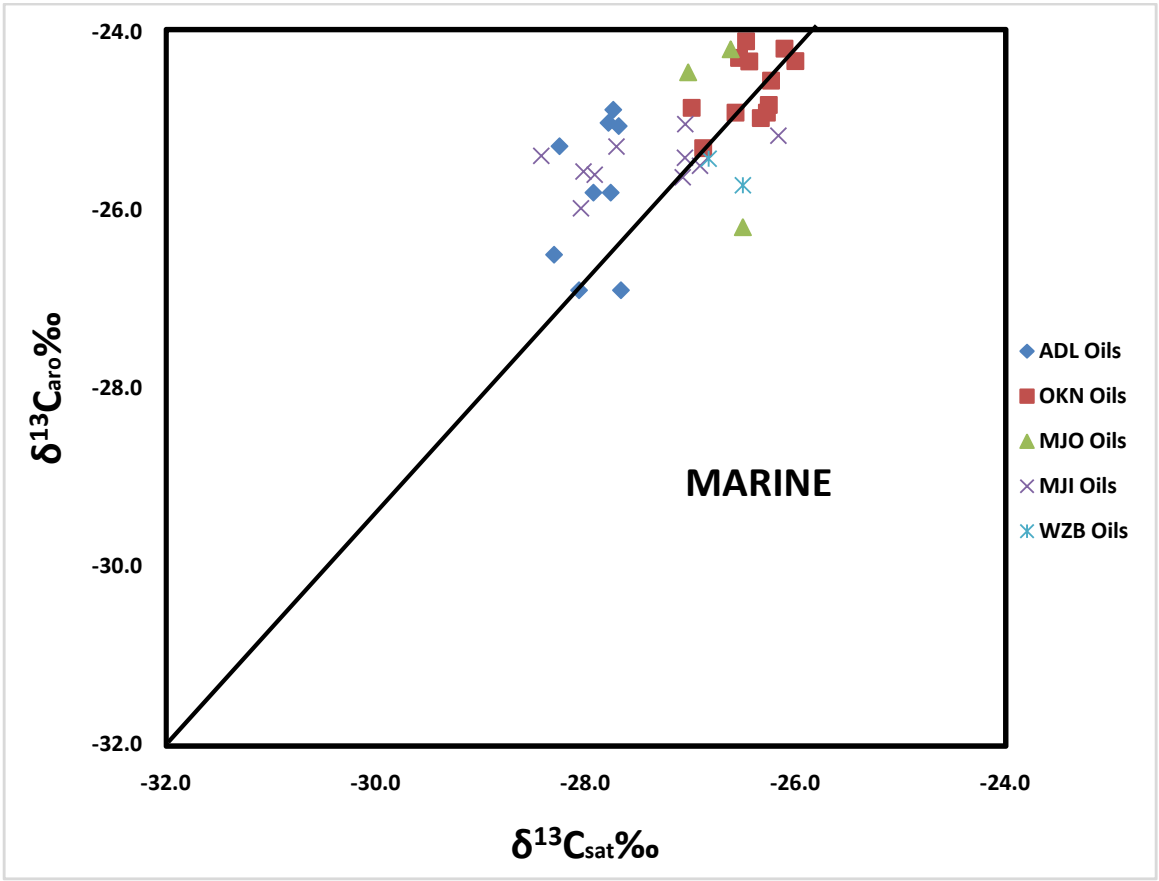

Fig. 4.42: Plot of the $\delta^{13}C$ values of aromatic fractions versus $\delta^{13}C$ values of saturate fractions for oil samples from the Niger Delta (after Sofer, 1984).

4.6.1.5 WZB Field

The carbon isotopic values of the whole oil, saturate, and aromatic fractions of the oils range from -25.2‰ to -25.9‰, -26.5‰ to -26.8‰ and -25.4‰ to -25.7‰, respectively (Table 4.12). In all the samples, the saturate fraction is more depleted in $\delta^{13}C$ than the aromatic fraction with values not more than 0.4‰. The isotopic differences between the whole oils and saturate and aromatic fractions of the oils are less than 1.6‰, indicating that the crude oils were derived from the same source (Table 4.12) (Peters and Moldowan, 1993). The cross plot of $\delta^{13}C_{aro}$ versus $\delta^{13}C_{sat}$ (Fig. 4.42) grouped the oils under marine zone.

4.6.2 Stable carbon isotopic composition of individual n-alkanes of Niger Delta oil

The $\delta^{13}C$ isotopic values for individual n-alkanes of the samples are presented in Table 4.13. The origin and depositional environment of the oils were determinedfrom the$\delta^{13}C$ isotopic values of the individual n-alkanes.

4.6.2.1 ADL Field

The average carbon isotopic compositions of individual alkanes (nC_{13}-nC_{33}) for the samples range between –30.4 to –27.6 δ^{13}‰. The most depleted values were noted for the long chain alkanes (nC_{21}-nC_{32}). These observations are characteristics of higher plant derived organic matter (Schouten *et al*., 2000; Hu *et al*., 2002; Samuel *et al*., 2009; Cai *et al.*, 2015). Low contribution from marine organic matter (i.e.C_3 algae or cyanobacteria) is observed in enriched $\delta^{13}C$ isotope values of short (nC_{13}-nC_{18}) n-alkanes. A negatively sloping n-alkane profile which shows lighter (more negative) carbon isotope ratio with increasing n-alkane chain length is obtained for the oil samples (Fig. 4.43). This negative slope fingerprint has been described as characteristic of oils derived from deltaic and terrigenous organic matter (Murray *et al*., 1994; Wilhelms *et al*., 1994; Samuel *et al*., 2009; Cai *et al*., 2015).

The carbon isotopic composition of n-alkanes for the samples ranges between –30.0 and –28.9 δ^{13}‰, supporting terrigenous organic matter for the oils (Murray *et al*., 1994; Cai *et al*., 2015). Hence, the oil samples are derived from source of mixed origin (terrestrial and marine) deposited in lacustrine-fluvial/deltaic depositional environment.

The $\delta^{13}C$ isotope ratios of Pr and Ph range from –32.0 to –26.2 δ^{13} ‰ (av. -29.3) and –30.1 to –27.6 δ13‰ (av. –29.2) respectively. The ^{13}C-values of Pr and Ph of the oils lack substantial variation which suggests that the oils were formed from source rocks of similar organic materials (Schwas and Spangenberg, 2007; Cai *et al*., 2015).

Table 4.13: Stable Carbon Isotopic Composition of n-Alkanes in Niger Delta Crude Oils (δ^{13}‰)

Sample	C13	C14	C15	C16	C17	C18	C19	C20	C21	C22	C23	C24	C25	C26	C27	C28	C29	C30	C31	C32	C33	Weighted Av.	Pr	Ph
ADL-1	-27.7	-27.7	-27.9	-28.1	-28.4	-28.6	-28.8	-28.9	-29.0	-29.1	-29.1	-29.0	-29.0	-28.9	-29.2	-29.3	-28.8	-29.8	-30.2	-30.2	-29.4	-28.9	-32.0	-30.1
ADL-2	-27.5	-28.6	-28.0	-28.1	-28.4	-28.9	-29.3	-29.5	-29.7	-29.6	-29.9	-29.9	-30.0	-30.1	-30.3	-30.4	-30.4	-30.1	-30.2	-30.4	-22.6	-29.1	-30.3	-30
ADL-4	-28.0	-27.9	-28.1	-28.3	-28.5	-28.9	-29.2	-29.4	-29.5	-29.5	-29.8	-30.1	-29.4	-29.7	-29							-29.0	-26.2	-27.6
ADL-5	-28.7	-28.6	-28.7	-29.2	-29.6	-29.7	-30.0	-30.1	-30.3	-30.3	-30.7	-30.7	-30.9	-31.0	-31.2	-31.0	-30.3	-30.8	-30.9			-30.2	-27.2	-28.7
ADL-6	-28.0	-28.2	-28.1	-28.3	-28.4	-28.6	-28.8	-28.8	-29.0	-29.2	-29.5	-29.5	-29.5	-29.6	-30.0	-30.2	-30.5	-30.2	-31.3			-29.3	-31.4	-30.4
ADL-7	-27.8	-27.9	-27.6	-28.1	-28.8	-29.3	-29.7	-30.1	-30.5	-30.7	-31.0	-31.0	-31.1	-31.0	-31.2	-31.1	-30.8	-30.4	-30.2	-30.3	-30.9	-30.0	-27.9	-28.4
ADL-8		-28.7	-28.5	-28.7	-28.6	-28.8	-28.9	-29.1	-29.1	-29.1	-29.3	-29.2	-29.2	-29.2	-29.1	-29.3	-29.4	-29.3	-29.8	-30.5		-29.1	-31.9	-30.5
ADL-9	-28.6	-28.7	-29.0	-29.3	-29.5	-29.4	-29.5	-29.5	-29.6	-29.5	-29.8	-29.8	-29.9	-30.0	-29.9	-29.9	-29.8	-29.5	-30.2			-29.5	-28	-28.2
Average of individual n-alkanes	-28.0	-28.3	-28.2	-28.5	-28.8	-29.0	-29.3	-29.4	-29.6	-29.6	-29.9	-29.9	-29.9	-29.9	-30.0	-30.2	-30.0	-30.0	-30.4	-30.4	-27.6		-29.3	-29.2
OKN-2		-27.0	-27.0	-27.0	-27.2	-27.6	-27.7	-27.9	-28.0	-28.0	-28.4	-28.3	-28.4	-28.3	-28.6	-28.3	-28.6	-28.5	-28.6	-27.4	-28.4	-28.0	-24.6	-27.8
OKN-3				-26.9	-26.9	-26.9	-27.0	-27.3	-27.4	-27.4	-27.7	-27.6	-27.8	-28.0	-28.0	-28.6	-28.8	-28.3	-29.7	-28.7	-28.3	-27.9	-29.7	-28.8
OKN-4		-26.5	-26.6	-26.3	-26.2	-26.2	-26.8	-26.8	-27.1	-27.2	-27.6	-27.3	-27.6	-27.5	-27.4	-28.3	-28.9	-29.0	-30.6	-30.4	-32.5	-27.8	-27.3	-28.3
OKN-5			-26.4	-26.5	-26.3	-26.5	-27.1	-27.9	-28.6	-29.1	-29.0	-28.9	-29.0	-29.0	-29.0	-29.3	-29.4	-29.1	-29.3	-28.8	-28.9	-28.3	-23.9	-27
OKN-7			-27.1	-26.6	-26.7	-26.5	-26.9	-27.0	-27.3	-27.5	-27.7	-27.7	-27.7	-27.7	-27.8	-28.3	-28.5	-28.3	-29.7	-28.5	-28.6	-27.7	-24.7	-27
OKN-8		-26.6	-27.1	-26.7	-27.0	-27.3	-27.4	-27.7	-27.9	-28.0	-28.2	-28.1	-28.4	-28.5	-29.0	-29.1	-29.8	-29.4	-29.4	-28.9	-29.0	-28.2	-29.8	-29.6
OKN-9	-25.9	-26.2	-26.0	-26.1	-26.3	-26.4	-26.5	-26.6	-27.2	-27.3	-27.9	-28.2	-28.9	-29.0	-29.3	-29.0	-29.3	-29.1	-29.7	-28.9	-28.6	-27.7	-24.6	-27.8
OKN-10	-25.8	-25.7	-25.7	-25.9	-26.1	-26.4	-26.6	-26.7	-26.9	-26.8	-26.9	-26.7	-26.8	-26.9	-27.1	-27.2	-27.5	-27.3	-27.9	-27.5	-28.1	-26.8	-24.9	-27.5
OKN-11		-27.0	-27.1	-27.0	-27.2	-27.4	-27.7	-27.7	-27.9	-27.8	-27.9	-27.6	-27.7	-27.5	-27.8	-27.7	-28.1	-27.8	-28.2	-27.9		-27.6	-28.2	-29.7
OKN-12	-26.6	-27.1	-27.5	-27.8	-27.8	-28.1	-28.2	-28.2	-28.5	-28.2	-28.2	-27.9	-27.6	-27.6	-27.3	-27.0	-27.0	-26.8	-26.3	-27.3	-24.8	-27.4	-25.4	-28.1
OKN-14	-26.4	-26.2	-25.9	-26.1	-26.3	-26.5	-26.7	-27.0	-27.3	-27.4	-27.6	-27.6	-27.6	-27.6	-27.7	-27.7	-27.8	-27.6	-27.9	-27.3	-27.3	-27.1	-29.9	-29
OKN-16	-25.2	-25.2	-25.8	-26.8	-27.2	-27.6	-27.9	-28.0	-27.8	-27.7	-27.3	-27.2	-26.9	-26.9	-26.7	-26.5	-26.6	-26.7	-27.0	-27.4		-26.9	-25.3	-27.2
Average of individual n-alkanes	-26.0	-26.4	-26.6	-26.6	-26.8	-26.9	-27.2	-27.4	-27.7	-27.7	-27.9	-27.8	-27.9	-27.9	-28.0	-28.1	-28.4	-28.2	-28.7	-28.3	-28.4		-26.5	-28.1

Table 4.13 contd

Sample	C13	C14	C15	C16	C17	C18	C19	C20	C21	C22	C23	C24	C25	C26	C27	C28	C29	C30	C31	C32	C33	Weighted Av.	Pr	Ph
MJI-1		-28.2	-28.4	-28.6	-28.9	-28.8	-29.1	-29.1	-29.4	-29.5	-29.7	-29.5	-30.0	-29.9	-29.9	-30.8	-30.8	-30.2	-30.8			-29.5	-26.0	-28.5
MJI-3		-28.2	-28.1	-28.2	-28.5	-28.5	-28.7	-28.7	-29.0	-28.9	-29.2	-29.2	-29.5	-29.4	-29.6	-30.7	-30.5	-30.5	-30.9	-30.0		-29.3	-26.4	-28.4
MJI-4	-28	-28.4	-28.8	-28.7	-28.9	-29.2	-29.5	-29.7	-29.9	-29.9	-30.1	-30.1	-30.1	-30.1	-30.4	-30.4	-30.6	-30.3	-30.8	-30.6	-30.3	-29.8	-32.1	-30.5
MJI-5		-28.0	-28.1	-28.2	-32.5	-28.7	-28.5	-28.7	-29.1	-29.2	-29.3	-29.5	-29.4	-29.5	-29.6	-30.3	-31.1	-30.2	-30.1	-27.1	-30.2	-29.4	-25.6	-27.6
MJI-7			-29.1	-28.9	-28.9	-29.0	-29.2	-29.4	-29.5	-29.4	-29.9	-29.6	-30.0	-30.1	-30.4	-30.7	-31.3	-31.2	-31.3	-32.1		-30.0	-29.1	-29.7
MJI-8				-28.8	-28.7	-28.6	-29.0	-29.3	-29.3	-29.4	-29.8	-29.7	-30.0	-30.5	-30.3	-30.8	-31.6	-32.6	-30.7			-29.9	-21.9	-29.0
MJI-9		-28.6	-28.7	-28.7	-29.0	-28.8	-28.7	-29.1	-29.5	-29.3	-29.7	-29.5	-30.2	-30.0	-30.5	-31.5	-31.2	-31.0	-31.5	-29.1		-29.7	-26.4	-28.9
MJI-10	-28.6	-28.6	-28.6	-28.9	-29.1	-29.4	-29.8	-30.1	-30.4	-30.5	-30.6	-30.7	-31.0	-31.1	-31.3	-31.5	-31.9	-31.6	-31.7	-31.3	-30.9	-30.4	-29.7	-30.4
Average of individual n-alkanes	-28	-28.3	-28.6	-28.6	-29.3	-28.9	-29.1	-29.3	-29.5	-29.5	-29.8	-29.7	-30.0	-30.1	-30.2	-30.8	-31.1	-31.0	-31.0	-30.0	-30.5		-27	-29.1
MJO-1			-25.2	-24.8	-24.9	-24.9	-24.9	-24.9	-25.2	-25.1	-25.3	-24.7	-24.4	-24.3	-24.2	-24.2	-24.8	-24.3	-24.5	-23.8	-24.9	-24.7	-23	-26.9

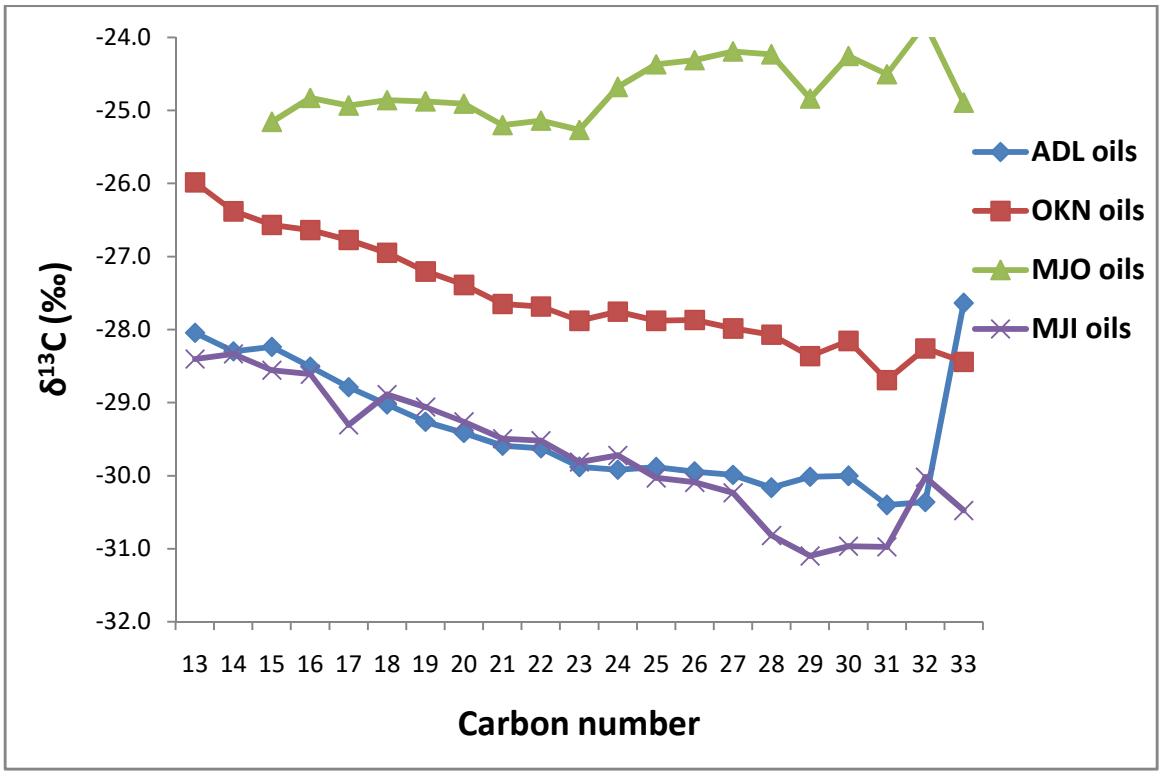

Fig.4.43 : Carbon isotopic distribution of individual n-alkanes in Niger Delta crude oils (after Murray *et al*., 1994).

4.6.2.2 OKN Field

The average carbon isotopic compositions of individual alkanes (nC_{13}-nC_{33}) for OKN samples range from –28.7 to –26.0 δ^{13}‰. The most depleted values were observed for the long chain alkanes (nC_{21}-nC_{33}). These observations are features of higher plant derived n-alkanes (Schouten *et al*., 2000; Hu *et al*., 2002; Samuel *et al*., 2009; Cai *et al*., 2015). A negatively sloping n-alkane profile which shows lighter (more negative) carbon isotope ratio with increasing n-alkane chain length is obtained for the oil samples (Fig. 4.43) (Murray *et al*., 1994; Wilhelms *et al*., 1994; Samuel *et al*., 2009; Cai *et al*., 2015). This negative slope n-alkane profile has been reported as characteristic of oils derived from deltaic and terrigenous organic matter (Murray *et al*., 1994; Wilhelms *et al*., 1994; Samuel *et al*., 2009; Cai *et al*., 2015). The carbon isotopic composition of n-alkanes for the samples range from –28.3 to –26.8 δ^{13}‰, typical of terrestrial organic input (Murray *et al*., 1994; Cai *et al*., 2015). A notable marine incursion is observed in the flat portions of n-alkane profile between C_{13} to C_{22} and C_{24} to C_{28} (Fig. 4.43). Hence, OKN samples were derived from source rocks of both terrestrial and marine organic matter deposited in lacustrine-fluvial/deltaic depositional environment.

The δ^{13}C isotope ratios of Pr and Ph range from –29.9 to –23.9 δ^{13} ‰ (av. -26.5) and –29.7 to –27.0 δ13‰ (av. –28.1‰) respectively. The δ^{13}C isotope ratios of Pr and Ph lack significant difference, which suggest that they were from similar organic material (Schwas and Spangenberg, 2007; Cai *et al*., 2015).

4.6.2.3 MJI Field

The average carbon isotopic compositions of individual alkanes (nC_{13}-nC_{33}) for Meji samples range between –31.1 to –28.3 δ^{13}‰. The long chain alkanes (nC_{21}-nC_{33}) were observed to have the most depleted values. These observations are features of oils derived from higher plant organic matter (Schouten *et al*., 2000; Hu *et al*., 2002; Samuel *et al*., 2009; Cai *et al*., 2015). Low input from marine organic matter (i.e.C_3 algae or cyanobacteria) is reflected in heavier δ^{13}C isotope values of short (nC_{13}-nC_{18}). A negatively sloping n-alkane profile is obtained for the oil samples (Fig. 4.43). This profile shows lighter (more negative) carbon isotope ratio with increasing n-alkane chain length (Murray *et al*., 1994; Wilhelms *et al*., 1994; Samuel *et al*., 2009; Cai *et al*., 2015). This

negative slope n-alkane profile have been described as features of oil derived from source rocks derived from deltaic and terrigenous organic matter (Murray *et al*., 1994; Wilhelms *et al*., 1994; Samuel *et al*., 2009; Cai *et al*., 2015).

The carbon isotopic compositions of n-alkanes for the samples range from –30.4 to –29.3 δ^{13}‰ indicating terrestrial organic input (Murray *et al*., 1994; Cai *et al*., 2015). A notable marine incursion is observed in the flat portions of n-alkane profile between C_{13} to C_{15} and C_{17} to C_{26} (Fig. 4.43). Therefore, MJI samples are derived from source rocks of mixed organic material (terrestrial and marine) deposited in lacustrine-fluvial/deltaic depositional environment.

The δ^{13}C isotope ratios of Pr and Ph range from –32.1 to –21.9 δ^{13} ‰ (av. -27.1) and –30.5 to –27.6 δ13‰ (av. –29.1) respectively. There is no substantial variation between these values which suggest that they were formed from the same source (Schwas and Spangenberg, 2007; Cai *et al*., 2015).

4.6.2.4 MJO Field

The average carbon isotopic compositions of individual alkanes (nC_{13}-nC_{33}) for the oil samples range between –25.3 to –23.8 δ^{13}‰. The most depleted values were noted for the light chain alkanes (nC_{15}-nC_{23}). This observation is a characteristic of higher plant derived n-alkanes (Schouten *et al*., 2000; Hu *et al*., 2002; Samuel *et al*., 2009; Cai *et al*., 2015). A positive to nearly flat n-alkane isotope profile is obtained for the oil samples with increasing chain length (Fig. 4.43). Nearly flat n-alkane δ^{13}C profiles have been previously noted to be diagnostic of oils from marine and lacustrine kerogen (Chung *et al*., 1994, Murray *et al*., 1994; Samuel *et al*., 2009; Cai *et al*., 2015). The carbon isotopic composition of n-alkanes for the samples is 24.7 δ^{13}‰, which is typical of marine organic input (Murray *et al*., 1994; Cai *et al*., 2015).

The δ^{13}C isotope ratios of Pr and Ph are –22.5 δ^{13} ‰ and –26.9 δ13‰, respectively. There is no significant variation between the ^{13}C-values of Pr and Ph, which suggest that they were formed from the similar organic matter (Schwas and Spangenberg, 2007; Cai *et al*., 2015).

4.7 Occurrence and Distribution of Dibenzofurans and Benzo[b]naphthofurans in Niger Delta Source Rocks

The representative m/z 168, 182, 196 and 218 mass chromatograms showing the distribution of dibenzofuran, methyldibenzofurans, dimethyldibenzofurans and benzo[b]naphthofurans in the rock samples are presented in Fig.4.44. The peak identities and relative abundances of identified compounds are listed in Tables 4.14 and 4.15, respectively.

4.7.1 Distribution of Dibenzofurans and Benzo[b]naphthofurans

The relative percentages of dibenzofuran, methyldibenzofurans (C_1-dibenzofurans) and dimethyldibenzofurans (C_2-dibenzofurans) in the rock samples range from 1.75 -29.82 %, 27.60 - 40.52 % and 29.66 - 68.89%, respectively (Table 4.15). The dibenzofurans are dominated by C_2-dibenzofurans (Table 4.14, Fig.4.44b). Among the C_1-dibenzofurans, 2- + 3-methyldibenzofuran is the most abundant in the rock samples while 1-methyldibenzofuran often appears to be the least (Table 4.15). This pattern of distribution has been reported in a paleozoic coals from Pennine Basin, Central and Northern England by Armstroff (2004). However, this observation is different from what was reported in source rocks from Sakoa basin Germany (Radke *et al*. 2000) and Beibuwan basin South China sea (Li and Ellis 2015) whereby 4-methyldibenzofuran was the dominant compound among the C_1-dibenzofurans. Among the C_2-dibenzofurans, ethyldibenzofuran-1 (EDBF-1), dimethyldibenzofuran-3 (DMDBF-3) and dimethyldibenzofuran-6 (DMDBF-6) were detected in high amounts (Table 4.14) while dimethyldibenzofuran-1 (DMDBF-1) is present in very low abundance.

Benzo[b]naphthofurans are detected in high abundance in the source rocks (Fig. 4.44c). Benzo[b]naphtho[1,2-d]furan is the least abundant isomer among the three isomers of benzo[b]naphthofurans detected.

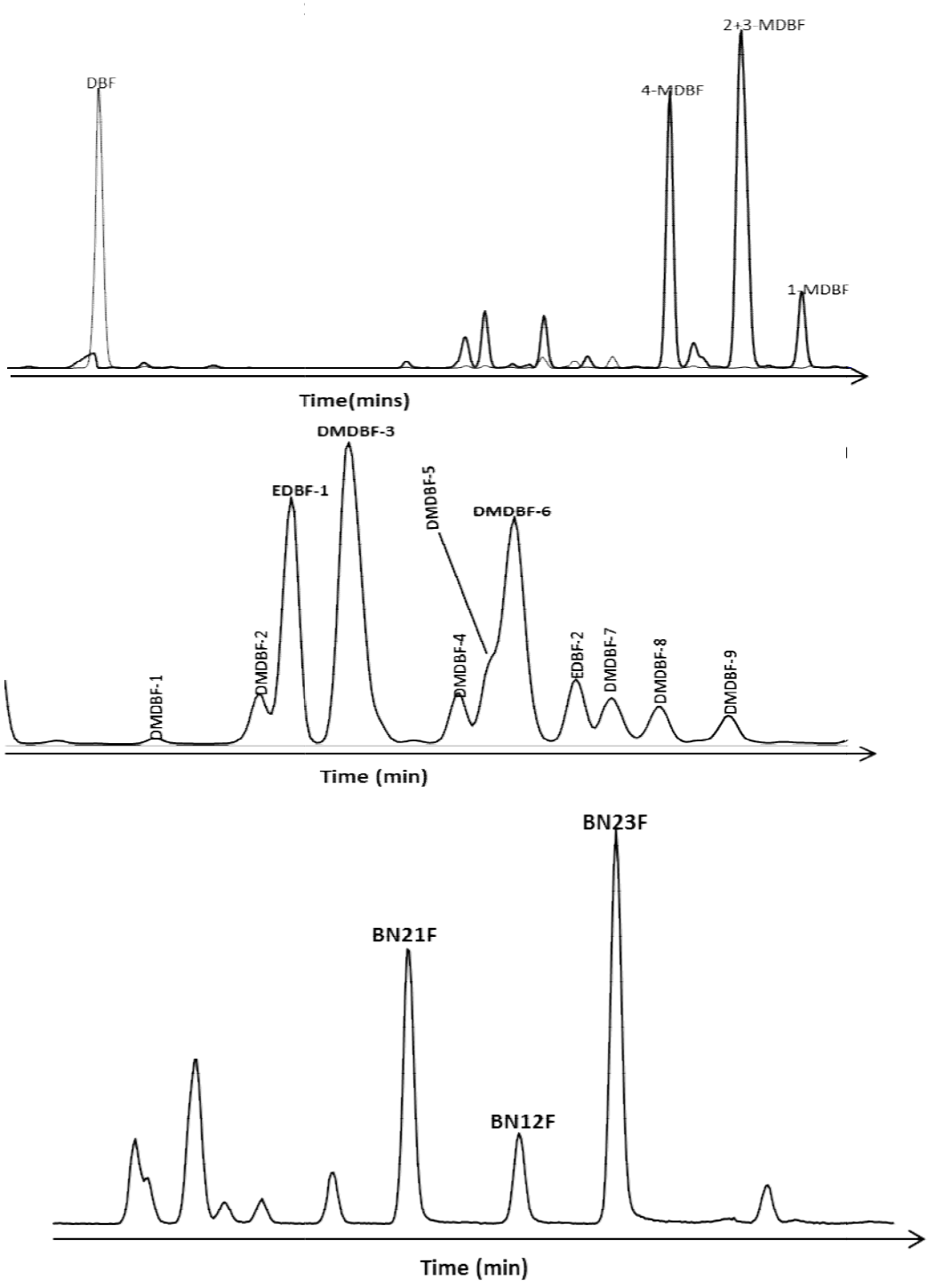

Fig. 4.44: m/z 168, 182, 196 and 218 showing the distributions of (a) dibenzofuran and methyldibenzofurans, (b) dimethyldibenzofurans and (c) benzo[b]naphthofurans in representative source rocks from Niger Delta

Table 4.14: Peak identification of dibenzofuran and Benzo[b]naphthofuran compounds in the Niger Delta source rocks and crude oils

Peak	Compound
DBF	Dibenzofuran
4-MDBF	4-methyldibenzofuran
2- + 3-MDBF	2- + 3-methyldibenzofuran
1-MDBF	1-methyldibenzofuran
DMDBF-1	Dimethyldibenzofuran-1
DMDBF-2	Dimethyldibenzofuran-2
EDBF-1	Ethyldibenzofuran-1
DMDBF-3	Dimethyldibenzofuran-3
DMDBF-4	Dimethyldibenzofuran-4
DMDBF-5	Dimethyldibenzofuran-5
DMDBF-6	Dimethyldibenzofuran-6
EDBF-2	Ethyldibenzofuran-2
DMDBF-7	Dimethyldibenzofuran-7
DMDBF-8	Dimethyldibenzofuran-8
DMDBF-9	Dimethyldibenzofuran-9
BN21F	Benzo[b]naphtho[2,1-d]furan
BN12F	Benzo[b]naphtho[1,2-d]furan
BN23F	Benzo[b]naphtho[2,3-d]furan

Table 4.15: Relative abundance of dibenzofuran compounds in rock extracts from Niger Delta, Nigeria

	Depth	Dibenzofurans (%)			C1-dibenzofurans (%)			C2- dimethyldibenzofurans (%)											BN21F/
Field	m	C0	C1	C2	4-	2- + 3-	1-	DM-1	DM-2	ET-1	DM-3	DM-4	DM-5	DM-6	ET-2	DM-7	DM-8	DM-9	(BN21F+BN12F)
OKN	1537	14.6	40.4	45.0	32.5	57.9	9.6	0.6	3.6	18.5	31.1	3.6	4.3	23.0	5.2	4.1	3.3	2.7	0.8
OKN	1729	29.8	40.5	29.7	37.6	52.7	9.7	0.8	5.1	17.4	30.0	4.1	6.0	19.8	5.2	4.7	3.8	3.0	0.8
OKN	2625	29.8	34.0	36.2	38.1	50.7	11.2	0.9	5.6	16.2	28.0	5.1	6.7	17.6	5.6	6.0	4.1	4.2	0.7
OKN	2780	20.2	30.4	49.4	33.1	55.7	11.2	0.7	6.1	15.5	28.5	4.3	5.6	20.8	5.5	5.7	3.9	3.4	0.8
OKN	2863	12.1	36.5	51.3	33.7	54.7	11.6	0.7	7.6	15.4	26.9	5.6	2.1	22.2	5.5	6.5	3.8	3.7	0.8
OKN	2909	12.7	31.4	55.9	31.5	56.4	12.0	0.6	6.8	15.5	27.9	4.4	3.8	22.1	5.6	5.8	4.0	3.4	0.8
MJI	2078	12.3	39.9	47.8	38.4	44.5	17.1	0.9	6.2	14.2	28.8	5.4	9.6	14.6	5.9	6.2	4.5	3.9	0.7
MJI	2299	1.7	30.1	68.2	30.1	49.6	20.3	0.7	6.4	13.9	26.3	5.6	4.9	19.0	7.1	6.6	5.4	4.0	0.7
MJI	2637	13.2	40.7	46.1	33.1	47.4	19.5	1.0	6.1	14.4	25.9	5.8	5.9	18.1	7.3	6.3	5.5	3.8	0.6
MJI	2857	10.2	34.9	54.9	32.1	46.8	21.1	0.9	7.8	13.9	25.1	5.8	6.0	17.2	6.9	6.8	5.7	3.9	0.5
MJI	2994	4.8	32.8	62.3	31.4	45.2	23.4	0.8	8.3	12.9	24.7	6.4	8.0	15.3	7.4	7.0	5.8	3.6	0.5
MJI	3085	14.8	39.8	45.3	32.6	46.9	20.4	0.9	6.1	14.0	25.0	5.2	5.7	19.6	7.7	6.4	5.4	4.0	0.5
MJI	3232	14.0	40.2	45.8	31.6	47.7	20.7	1.0	5.1	13.9	24.4	5.9	5.1	20.1	7.4	7.0	5.7	4.3	0.4
MJI	3323	18.1	38.0	43.9	33.3	47.4	19.2	1.1	6.0	13.7	25.2	5.3	4.7	19.8	6.9	7.5	5.3	4.3	0.4
MJI	3405	12.7	31.0	56.3	35.2	46.2	18.6	0.9	9.4	12.9	25.7	5.4	5.6	18.1	7.1	6.6	4.7	3.6	0.4
MJO	1616	7.3	35.0	57.7	35.2	52.5	12.3	0.8	5.4	15.2	28.9	4.8	6.1	18.9	5.3	6.4	4.3	4.0	0.8
MJO	1771	3.5	27.6	68.9	35.6	47.1	17.2	0.7	4.4	14.7	27.7	5.5	7.3	17.6	6.6	7.2	4.5	3.7	0.6
MJO	2091	4.1	34.0	61.9	35.9	50.0	14.1	0.7	4.2	15.7	28.6	5.8	6.8	17.7	5.8	7.6	3.9	3.3	0.8
MJO	2293	8.7	32.8	58.6	36.9	42.3	20.9	0.8	7.7	13.7	24.4	7.3	10.2	13.8	7.1	7.0	4.5	3.4	0.5
MJO	2570	6.9	31.5	61.6	35.5	45.4	19.1	0.7	8.2	13.6	24.5	6.3	8.5	15.7	6.8	7.8	4.5	3.5	0.6
MJO	2808	8.2	30.7	61.1	35.9	43.1	21.0	0.8	6.7	14.5	24.3	7.7	10.8	12.6	7.7	6.9	4.6	3.4	0.6

*BN21F/(BN21F+BN12F): benzo[b]naphtho[2,1-d]furan/(benzo[b]naphtho[2,1-d]furan + benzo[b]naphtho[1,2-d]furan); DM: dimethyl; ET: ethyl.

4.7.2 Influence of Facies/Depositional Environments on Dibenzofurans and Benzo[b]naphthofurans distributions

The effect of facies/depositional environments on the distributions of dibenzofurans in the source rocks was examined by comparing their relative abundance with Pr/Ph ratio. The rock samples from MJI and MJO fields have earlier been found to be deposited in oxic to suboxic conditions while those of OKN rocks were found to be deposited in the suboxic environment based on the ratios of Pr/Ph (Table 4.3). The C_{0-2}-dibenzofurans relative abundances show no visible variations that could suggest the influence of source facies on their distribution when plotted against Pr/Ph ratio (Fig. 4.45a). Similarly, the influence of source facies/depositional environments on benzo[b]naphthofurans distributions was examined by plotting Pr/Ph ratios against benzonaphthofurans ratios. The plots do not show much variation to indicate any possible source facies or depositional environment dependent (Fig. 4.45b).

The cross plots of Pr/Ph ratio against the relative abundance of methyldibenzofuran isomers and 4-/1-MDBF ratios show no trend to indicate the dependent of these isomers on source depositional environments (Fig.s 4.45c and d). Also, cross plots of the relative abundances of some selected dimethyldibenzofuran isomers and its ratios against Pr/Ph ratio lack significant variations to suggest any effects of facies or depositional environments on the dimethyldibenzofurans distributions in the source rocks (Fig.s 4.46a and b).

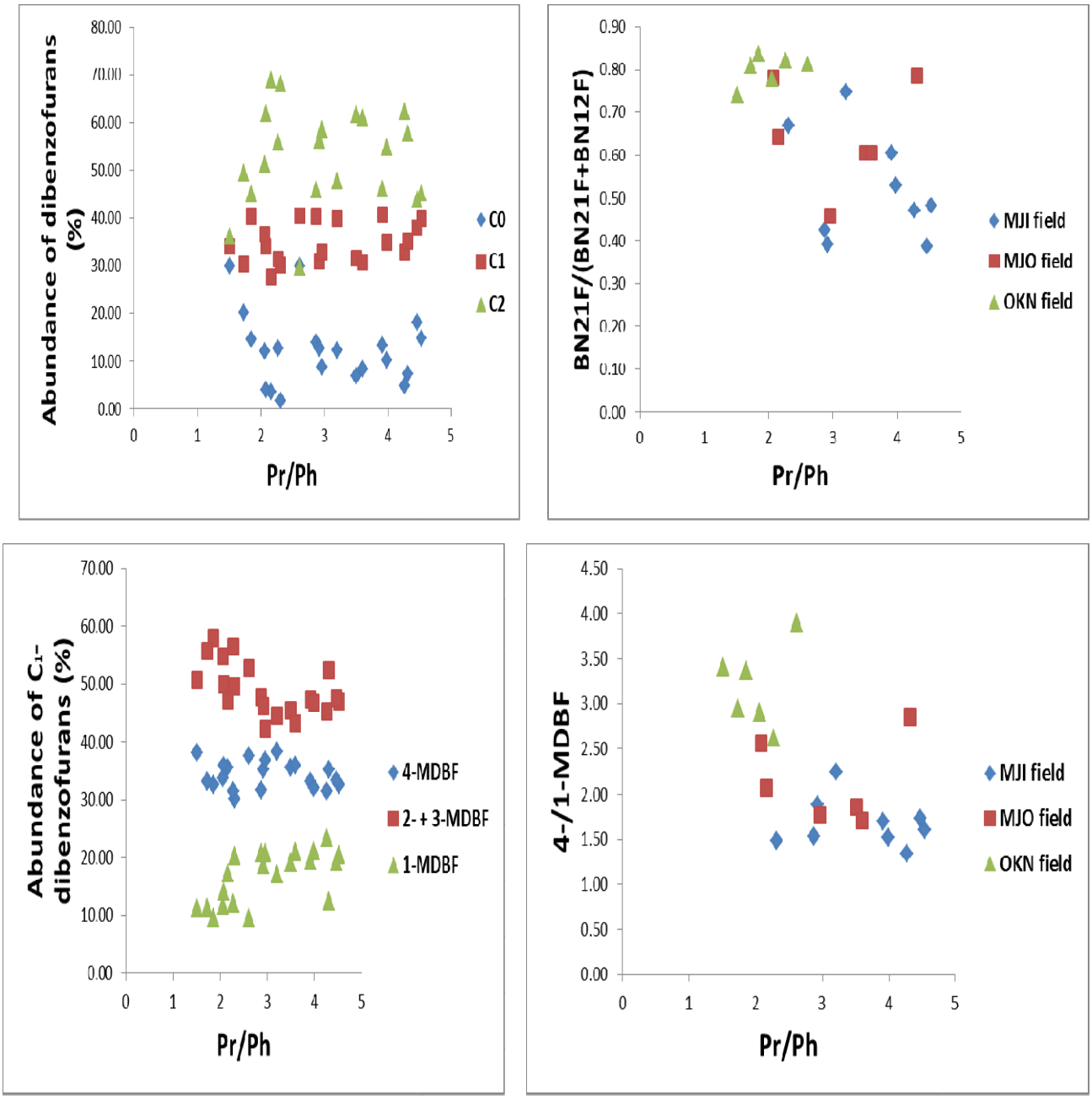

Fig. 4.45: Cross plots of Pr/Ph ratios versus (a) relative amounts of C_{0-2} dibenzofurans,(b) BN21F/(BN21F+BN12F), (c) relative amounts of C_1 dibenzofuransin and (d) 4-/1-MDBF in Niger Delta source rocks (after Li *et al.*, 2018).

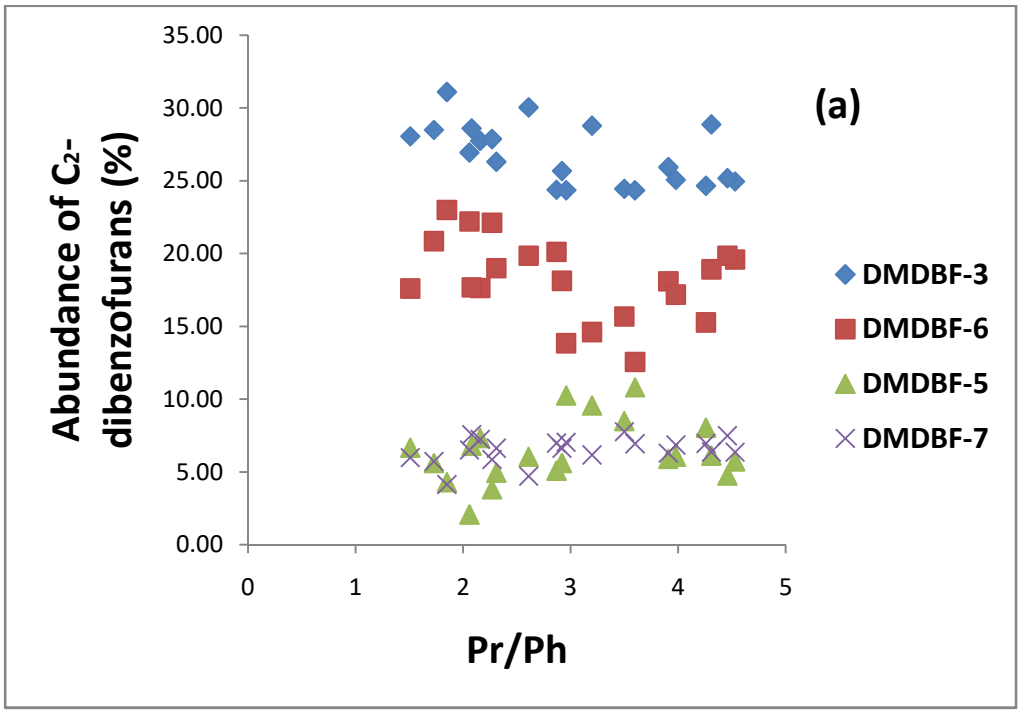

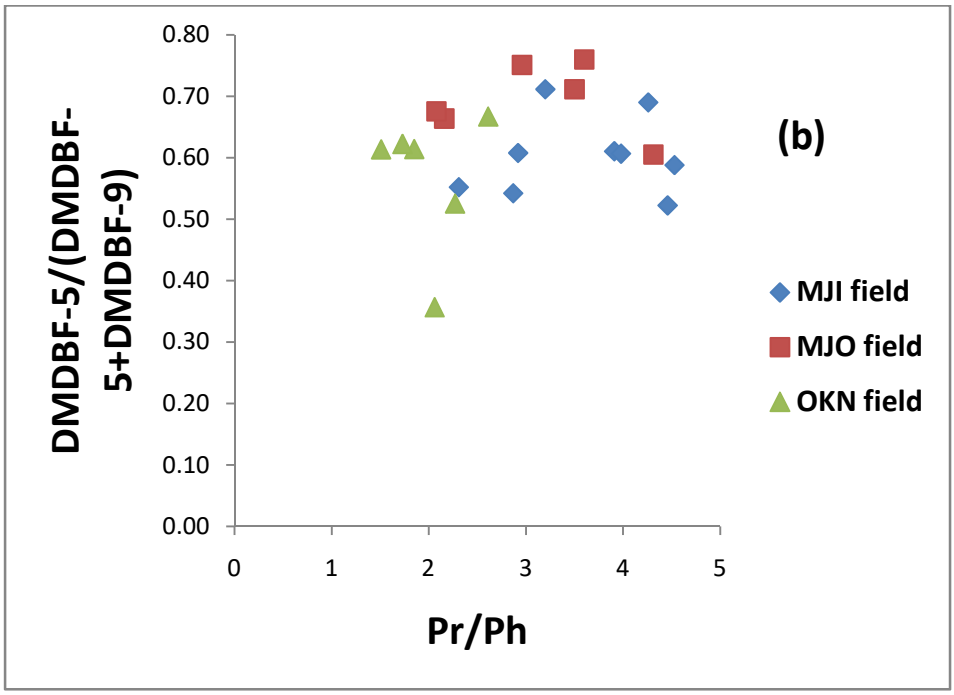

Fig. 4.46: Cross plots of Pr/Ph against (a) relative amounts of C_2-dibenzofurans (b) DMDBF-5/(DMDBF-5 + DMDBF-9) in Niger Delta source rocks (after Li *et al*., 2018).

4.7.3 Influence of Maturity on Dibenzofurans and Benzo[b]naphthofurans distribution

The relative abundance of dibenzofuran, methyldibenzofurans and dimethyldibenzofurans show no visible trend when plotted against depth suggesting that maturity has no influence on their distribution (Fig.4.47a). The benzo[b]naphtho[2,1-d]furan/(benzo[b]naphtho[2,1-d]furan + benzo[b]naphtho[1,2-d]furan) and 4-/1-methyldibenzofuran and dimethyldibenfuran-5/(dimethyldibenzofuran-5 + dimethyldibenzofuran-9) ratios show no trend with increasing burial depths (Fig. 4.47b and Fig. 4.48). This suggests that maturity has no influence on their distribution. The relative abundances of C_0, C_1 and C_2- dibenzofurans when plotted against S/S+R ratios of C_{29} sterane (Fig 4.49a) generally lack any significant variation that could suggest any effect of maturity on the dibenzofurans distribution. The plot of C_1- dibenzofurans and DMDBF-5/(DMDBF-5+DMDBF-9) versus S/S+R C_{29} sterane (Figs. 4.49b and 4.49c) also indicate no influence of maturity on the dibenzofurans distribution.

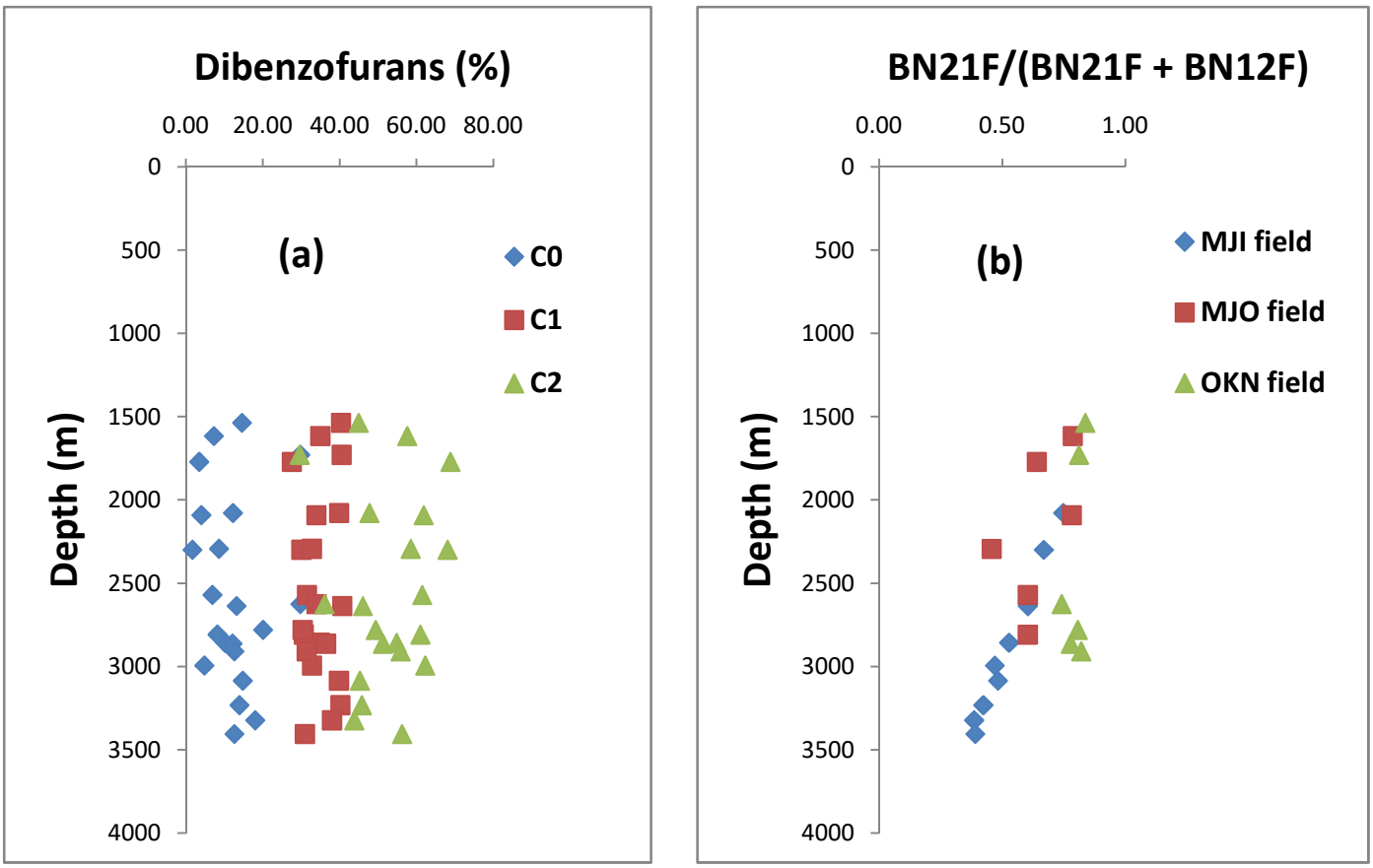

Fig. 4.47: Cross plots of depth versus (a) dibenzofuran concentrations and (b) BN21F/(BN21F + BN12F) in Niger Delta source rocks (after Li and Ellis, 2015)

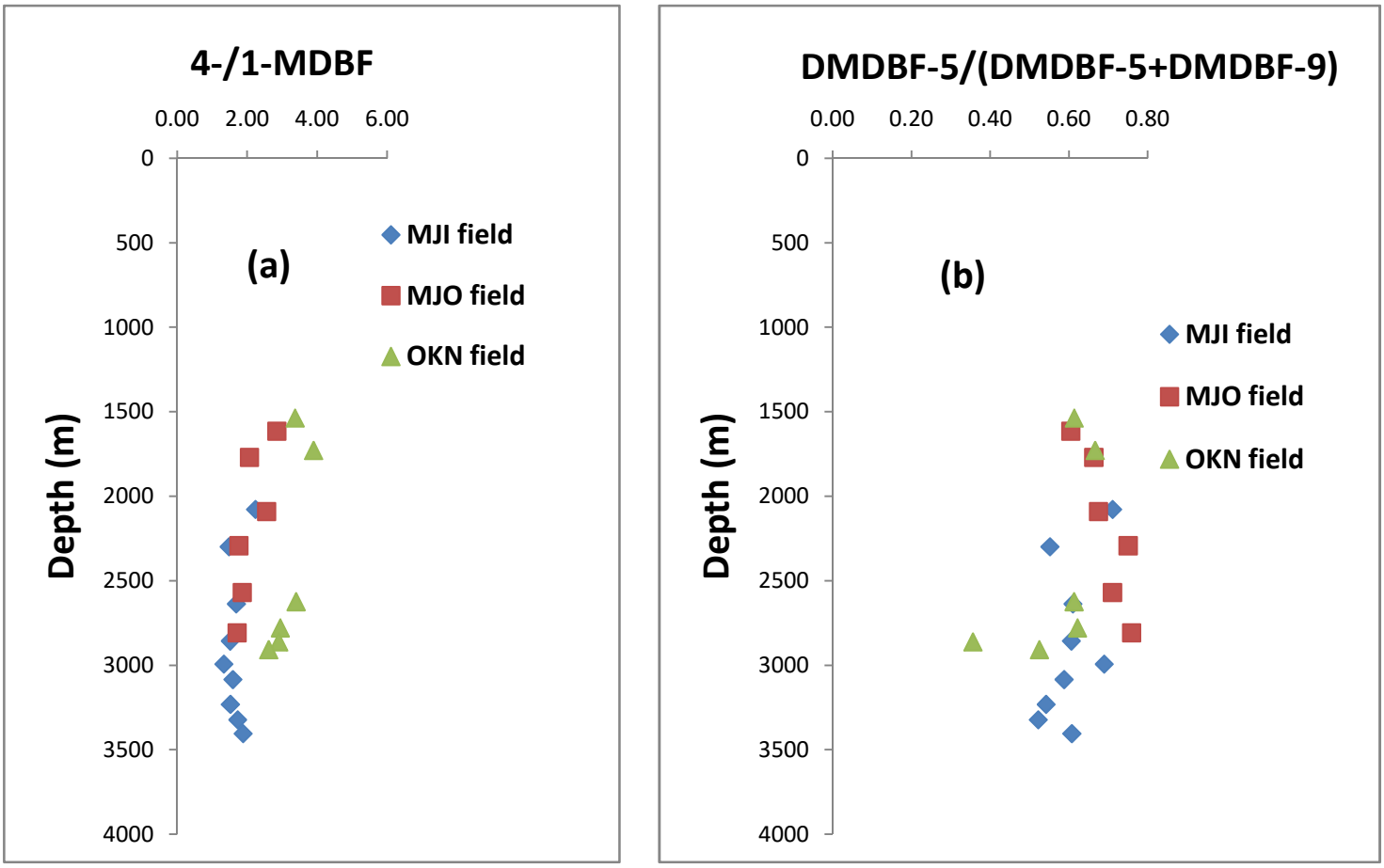

Fig. 4.48: Plots of depth against (a) 4-/1-MDBF and (b) DMDBF-5/(DMDBF-5 + DMDBF-9) in Niger Delta source rocks (after Li and Ellis, 2015).

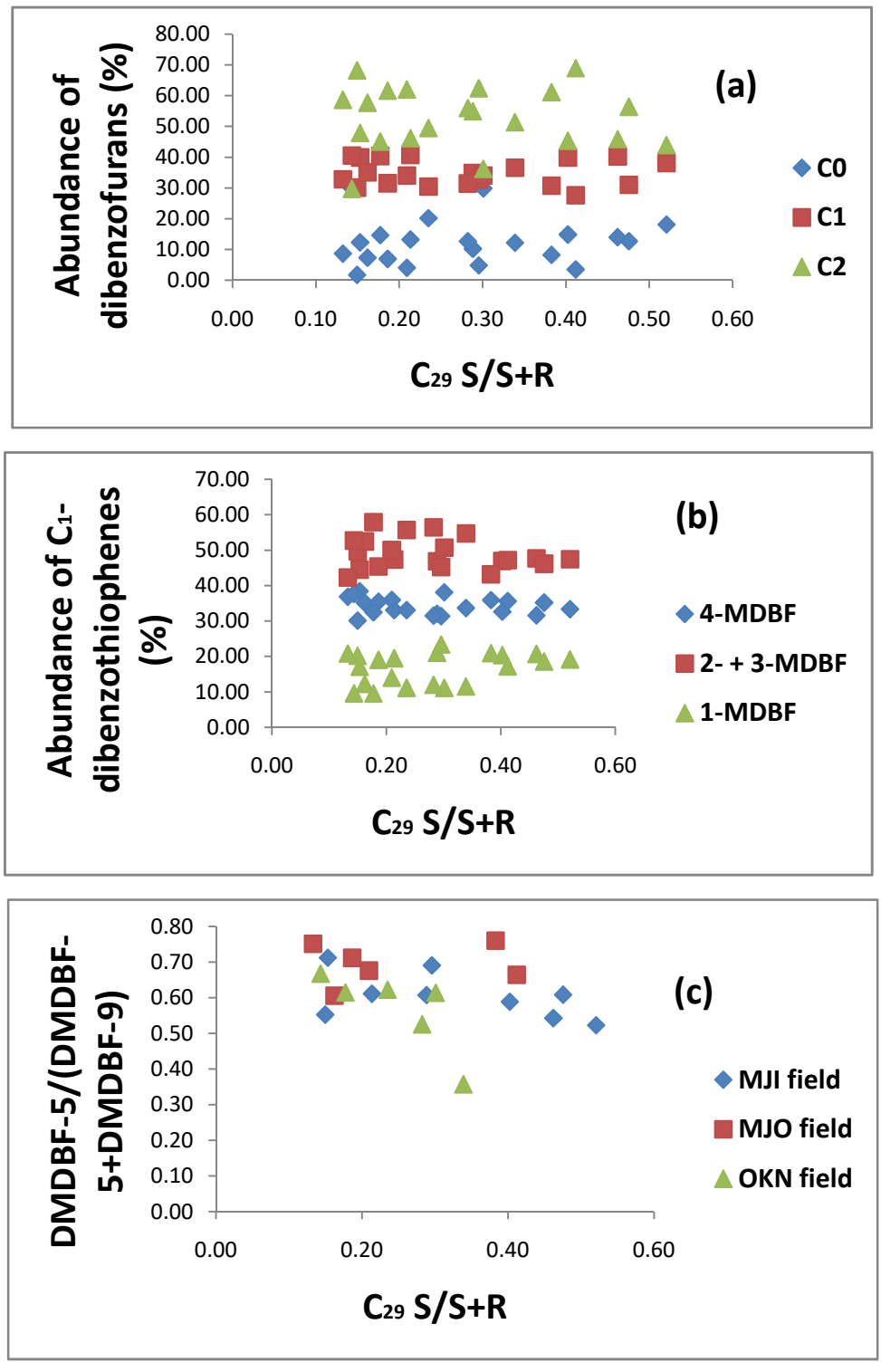

Fig. 4.49: Plots of C_{29} S/S+R vs. relative amounts of (a) $C_{0\text{-}2}$-dibenzofurans, (b) C_1-dibenzofurans and (c) DMDBF- 5/(DMDBF-5+DMDBF-9) in source rocks from Niger Delta (after Li and Ellis, 2015).

4.8 Occurrence and Distributions of Dibenzofurans and Benzo[b]naphthofurans in Crude Oils from Niger Delta

4.8.1 ADL Field

The representative mass chromatograms of the oilsamples showing the distribution of dibenzofurans and benzo[b]naphthofurans are presented in Fig. 4.51. The peak identities and relative abundance of the identified compounds are listed in Tables 4.14 and 4.16, respectively. The concentrations of dibenzofuran, C_1-dibenzofurans and C_2-dibenzofurans range from 4.65 to 76.45 µg/g, 22.88 to 147.52 µg/g and 76.98 to 469.91 µg/g, respectively (Tables 4.16 and 4.17). The dibenzofurans are dominated by C_2-dibenzofurans (Table 4.16). The C_1-dibenzofurans is dominated by 4-methyldibenzofuran (4-MDBF) while 1-methyldibenzofuran appears to be the least (Fig. 4.50). The dominance of 4-MDBF over other methyldibenzofurans has been reported in source rocks from Sakoa basin, Germany (Radke et al., 2000).

Among the C_2-dibenzofurans, dimethyldibenzofuran-2 (DMDBF-2), dimethyldibenzofuran-3 (DMDBF-3) and ethyldibenzofuran-1 (EDBF-1) are detected in higher amounts when compared with the other dimethyldibenzofurans (Table 4.16). Similar trend in the distribution of dimethyldibenzofurans have been reported in marine carbonate oils from Tarim basin, NW China (Li and Ellis, 2015). There is predominance of EDBF-1 over other C_2-dibenzofurans while DMDBF-1 is the least abundant (Fig. 4.50; Table 4.16).

The benzo[b]naphthofurans concentrations range from 2.75 to 58.28 µg/g (Table 4.17). Among the three isomers of benzonaphthofurans, benzo[b]naphtho[2,1-d]furan and benzo[b]naphtho[1,2-d]furan are the dominant compounds while benzo[b]naphtho[2,3-d] occurs as the least abundant (Fig. 4.50).

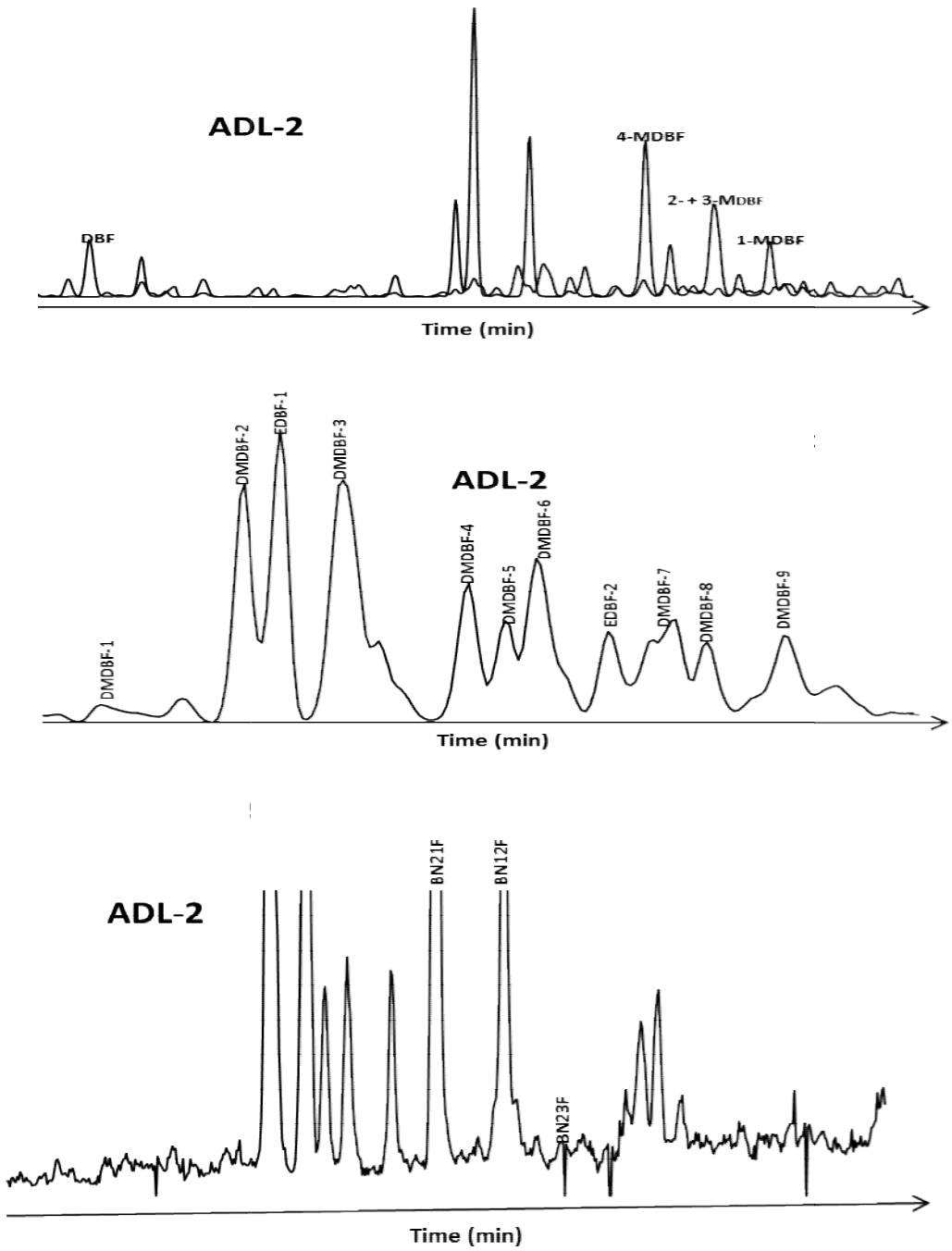

Fig. 4.50: Mass chromatograms showing the distribution of $C_{0\text{-}2}$- dibenzofurans (m/z 168+182, 196) and benzo[b]naphthofurans (m/z 218) in representative oil from ADL Field

Table 4.16: Absolute concentration (µg/g) of dibenzofurans in crude oils from ADL Field.

Sample	C0	4-MDBF	2- + 3-MDBF	1-MDBF	DMDBF-1	DMDBF-2	EDBF-1	DMDBF-3	DMDBF-4	DMDBF-5	DMDBF-6	EDBF-2	DMDBF-7	DMDBF-8	DMDBF-9
ADL1	20.28	34.82	26.99	11.72	4.86	26.94	31.66	41.91	17.81	11.47	27.44	12.40	22.74	10.60	17.99
ADL2	22.71	38.57	29.89	13.03	5.27	29.39	34.57	45.66	19.38	12.71	30.04	13.52	24.89	11.63	19.51
ADL3	4.65	10.92	7.92	4.04	1.25	11.93	10.19	17.81	5.64	4.21	8.39	3.78	5.91	3.26	4.62
ADL4	24.70	36.68	30.23	13.52	3.69	31.62	29.86	51.06	16.39	11.88	25.74	11.10	18.23	9.64	13.19
ADL5	17.61	30.01	22.63	10.15	4.14	22.93	27.05	45.42	15.22	9.69	23.12	10.73	19.39	9.06	15.59
ADL6	51.58	66.90	56.89	23.73	7.45	47.13	55.49	92.23	31.31	20.75	50.00	22.52	38.11	17.80	29.16
ADL7	25.93	50.84	43.09	26.69	6.61	26.42	31.56	40.57	19.73	15.09	29.44	15.89	24.12	13.02	16.50
ADL8	47.36	57.19	52.12	22.81	5.87	43.33	48.38	83.44	28.53	20.18	46.38	21.18	34.71	17.32	25.56
ADL9	76.45	82.18	82.29	36.86	9.42	51.09	63.02	101.62	36.14	27.54	60.62	27.65	40.09	23.99	28.73

Table 4.17: Absolute concentration (µg/g) of sum of dibenzofurans and benzonaphthofurans in crude oils from ADL Field.

Sample	Concentrations of DBFs and BNFs (µg/g oil)						BN21F/ (BN21F + BN12F)
	ΣMDBF	ΣDMDBF	BN21F	BN12F	BN23F	ΣBNF	
ADL1	73.52	225.83	7.03	3.64	0.90	11.58	0.67
ADL2	81.49	246.57	8.36	4.17	0.75	13.29	0.68
ADL3	22.88	76.98	1.47	0.59	0.70	2.75	0.72
ADL4	80.43	222.40	3.91	2.00	2.23	8.14	0.67
ADL5	62.78	202.33	6.15	3.05	0.05	9.25	0.68
ADL6	147.52	411.95	9.72	5.90	0.18	15.79	0.64
ADL7	120.63	238.96	24.92	18.16	15.19	58.28	0.62
ADL8	132.13	374.88	9.73	7.13	1.53	18.38	0.59
ADL9	201.33	469.91	22.27	18.83	8.12	49.22	0.56

*C_0: dibenzofuran;

ΣMDBF: total concentration of all methyldibenzofurans;

ΣDMDBF: total concentration of all dimethyldibenzofurans;

BN21F: Benzo[b]naphtho[2,1-d]furan

BN12F: Benzo[b]naphtho[1,2-d]furan

BN23F:Benzo[b]naphtho[2,3-d]furan

ΣBNF: total concentration of benzo[b]naphthofurans;

BN21F/(BN21F +BN12F):benzo[b]naphtho[2,1-d]furan/(benzo[b]naphtho[2,1-d]furan+ benzo[b]naphtho[1,2-d]furan);

4.8.2 OKN Field

The selective ion monitoring (SIM) representative chromatograms showing the distribution of dibenzofuran and its alkylated derivatives of the oil samples are presented in Fig. 4.51. The concentrations of dibenzofurans and benzonaphthofurans are listed in Tables 4.18 and 4.19. The concentrations of dibenzofuran, C_1-dibenzofurans and C_2-dibenzofurans range from 1.06 to 59.32 µg/g, 9.64 to 155.76 µg/g and 61.50 to 474.92 µg/g , respectively (Tables 4.18 and 4.19). C_2-dibenzofurans are the most abundant in the crude oils (Table 4.19). Among the C_1-dibenzofurans, 4-methyldibenzofurans (4-MDBF) is the dominant compound of the methyldibenzofurans while 1-methyldibenzofuran is the least abundant (Fig. 4.51).

Among the C_2-dibenzofurans, dimethyldibenzofuran-2 (DMDBF-2), ethyldibenzofuran-1 (EDBF-1), dimethyldibenzofuran-3 (DMDBF-3) and dimethyldibenzofuran-6 (DMDBF-6) occurred in higher amounts when compared with the other dimethyldibenzofurans (Fig.4.51b; Table 4.18). Similar trend of dimethyldibenzofurans distributions have been observed in the lacustrine oils from Beibuwan basin, South China Sea (Li and Ellis, 2015). Ethyldibenzofuran-1 is the dominant compound in the oils while dimethyldibenzofuran-1 is the least (Fig. 4.51; Table 4.18).

The benzo[b]naphthofurans concentrations range from 4.19 to 26.61 µg/g (Table 4.19). The three isomers of benzonaphthofurans show equal distributions in oils from OKN field (Fig. 4.51).

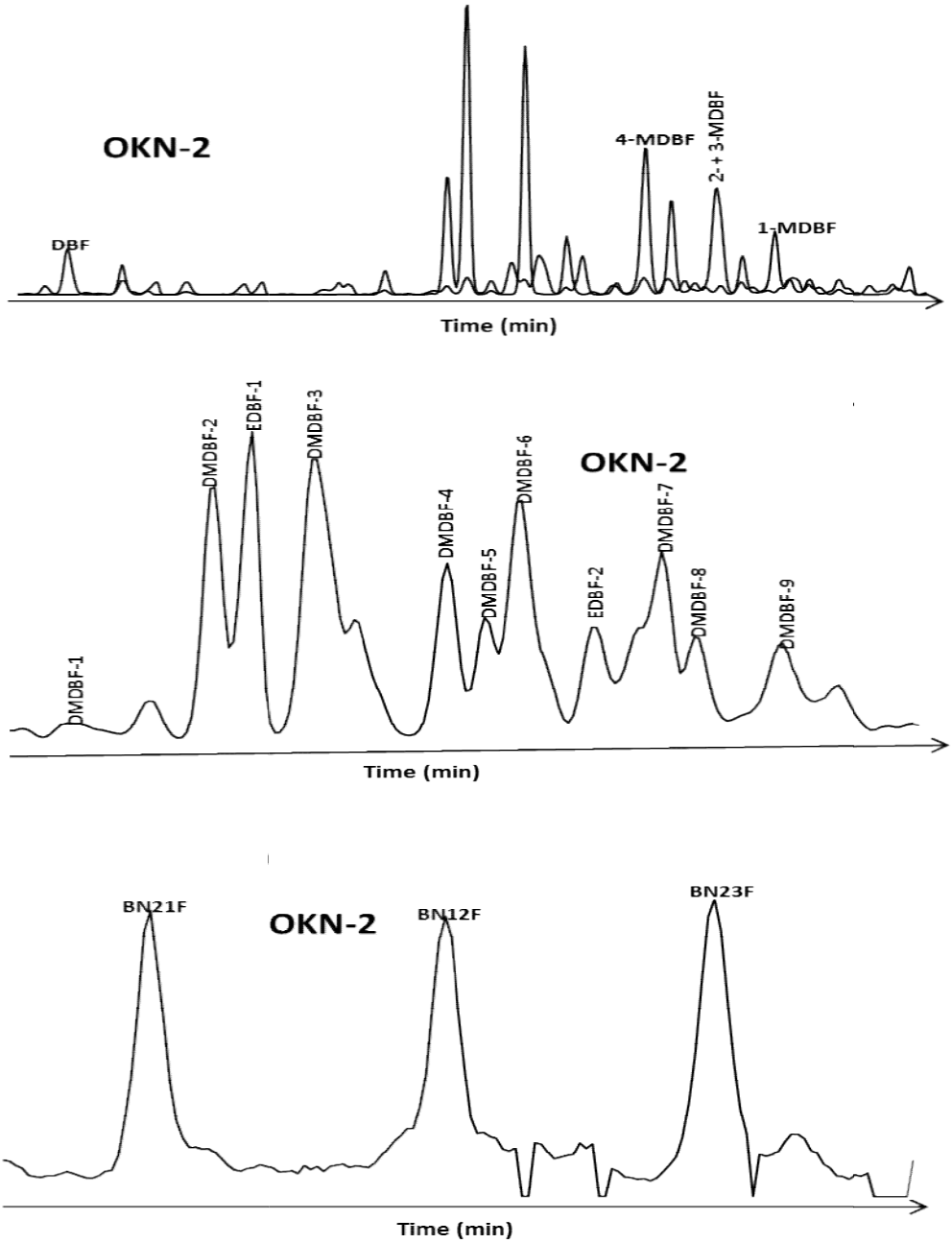

Fig. 4.51: Mass chromatograms showing the distribution of $C_{0\text{-}2}$-dibenzofurans (168+182,196) and benzo[b]naphthofurans (m/z 218) in representative oil from OKN Field

Table 4.18: Absolute concentration (μg/g) of dibenzofurans in crude oils from OKN Field.

Sample	C0	4-	2- + 3-	1-	DMDBF	DMDBF	EDBF	DMDBF	DMDBF	DMDBF	DMDBF	EDBF	DMDBF	DMDBF	DMDBF
		MDBF	MDBF	MDBF	-1	-2	-1	-3	-4	-5	-6	-2	-7	-8	-9
OKN1	22.99	36.69	27.67	13.72	3.03	73.48	38.88	52.42	27.92	16.26	41.23	16.46	56.52	13.67	23.99
OKN2	14.51	28.63	25.80	11.70	5.07	30.94	34.65	51.28	22.88	13.68	41.27	16.94	37.70	14.15	21.23
OKN3	15.36	28.67	23.92	10.50	5.26	29.33	32.51	48.23	21.74	12.47	38.63	15.64	35.47	13.27	20.17
OKN4	24.05	40.76	32.88	14.83	5.39	73.51	43.06	60.59	31.78	17.00	49.01	19.70	62.69	16.55	29.83
OKN5	15.86	26.46	22.88	10.06	2.60	27.07	30.27	44.64	19.63	11.69	35.63	14.15	31.79	11.56	17.22
OKN6	1.06	3.99	3.84	1.81	1.06	6.41	7.25	10.47	4.86	2.99	8.91	3.65	8.23	3.18	4.48
OKN7	25.83	36.59	31.25	14.03	5.90	34.36	38.68	57.51	25.68	15.30	45.85	18.56	41.80	15.47	23.71
OKN8	30.37	38.88	33.70	15.30	3.08	35.08	39.83	57.88	24.71	16.49	44.12	17.91	37.84	14.55	20.49
OKN9	13.98	28.21	25.61	11.33	3.80	31.51	34.73	51.86	22.64	13.85	41.10	16.59	37.56	14.00	21.02
OKN10	21.48	32.85	31.06	16.45	3.99	32.68	31.00	62.49	18.86	16.68	32.48	15.47	25.59	12.02	14.55
OKN11	29.13	38.88	33.87	16.78	4.69	34.43	34.82	68.85	20.32	16.69	35.77	16.90	28.13	12.61	16.89
OKN12	59.32	65.70	59.25	30.81	4.87	59.05	55.65	110.96	34.48	30.28	57.91	28.03	45.51	21.64	26.52
OKN13	22.39	34.32	27.62	12.13	4.62	68.07	36.13	48.73	27.28	14.33	41.21	15.70	57.74	14.56	25.35
OKN14	41.07	47.08	36.17	19.27	4.77	36.39	37.54	59.59	22.03	20.31	37.01	18.32	29.89	14.03	17.55
OKN15	26.12	41.88	36.82	19.21	5.00	38.17	38.15	60.55	22.39	20.67	39.18	18.94	31.61	14.46	17.60
OKN16	33.23	48.25	42.62	22.25	3.70	38.77	45.13	72.20	27.37	25.35	48.77	23.16	37.98	17.20	19.77

Table 4.19: Absolute concentration (µg/g) of sum of dibenzofurans and benzonaphthofurans in crude oils from OKN Field.

Sample	Concentrations of DBFs and BNFs (µg/g oil)						BN21F/ (BN21F + BN12F)
	ΣMDBF	ΣDMDBF	BN21F	BN12F	BN23F	ΣBNF	
OKN1	78.09	363.87	8.33	8.36	9.92	26.61	0.51
OKN2	66.13	289.79	5.09	5.90	6.53	17.53	0.48
OKN3	63.09	272.71	4.72	5.03	5.87	15.63	0.50
OKN4	88.47	409.09	8.16	8.90	10.56	27.62	0.49
OKN5	59.40	246.24	4.47	4.47	5.43	14.38	0.51
OKN6	9.64	61.50	1.26	1.43	1.49	4.19	0.48
OKN7	81.87	322.80	5.15	5.07	5.70	15.93	0.52
OKN8	87.89	312.00	5.18	5.88	6.28	17.34	0.48
OKN9	65.15	288.65	4.76	6.19	6.31	17.27	0.45
OKN10	80.35	265.79	3.79	3.55	4.64	11.98	0.53
OKN11	89.53	290.09	4.13	2.94	5.62	12.69	0.60
OKN12	155.76	474.92	6.77	5.44	8.56	20.77	0.57
OKN13	74.08	353.72	8.10	8.42	9.38	25.90	0.50
OKN14	102.52	297.44	5.42	4.31	5.87	15.61	0.57
OKN15	97.91	306.72	6.16	4.78	6.75	17.69	0.58
OKN16	113.11	359.40	6.19	7.68	6.81	20.68	0.46

*C_0: dibenzofuran;

ΣMDBF: total concentration of all methyldibenzofurans;

ΣDMDBF: total concentration of all dimethyldibenzofurans;

BN21F: Benzo[b]naphtho[2,1-d]furan

BN12F: Benzo[b]naphtho[1,2-d]furan

BN23F:Benzo[b]naphtho[2,3-d]furan

ΣBNF: total concentration of benzo[b]naphthofurans;

BN21F/(BN21F +BN12F):benzo[b]naphtho[2,1-d]furan/(benzo[b]naphtho[2,1-d]furan+ benzo[b]naphtho[1,2-d]furan);

4.8.3 MJI Field

The m/z 168+182, 196 and 218 mass chromatograms showing the distribution of dibenzofuran and its alkylated derivatives are shown in Fig. 4.52. The absolute concentrations of dibenzofuran compounds are presented in Tables 4.20 and 4.21. The concentrations of dibenzofuran, methyldibenzofurans and dimethyldibenzofurans in MJI oils range from 17.22 to 136.71 µg/g, 94.62 to 570.64 µg/g and 529.24 to 1346.81 µg/g, respectively (Tables 4.20 and 4.21). C_2- dibenzofurans are the most abundant in the crude oils (Table 4.21). Among C_1-dibenzofurans, 4-methyldibenzofuran is the most abundant in the oil samples (Fig. 4.52). Within the C_2-dibenzofurans, dimethyldibenzofuran-2 (DMDBF-2), dimethyldibenzofuran-3 (DMDBF-3) and ethyldibenzofuran-1 (EDBF-1) are detected in higher concentrations when compared with other C_2-dibenzofurans (Fig. 4.52; Table 4.20). This pattern of distribution has been reported in marine carbonate oils from the Tarim basin, NW China (Li and Ellis, 2015). The benzo[b]naphthofurans concentrations range from 16.81 to 352.602 µg/g (Table 4.21). Among the three isomers of benzo[b]naphthofurans, benzo[b]naphtho[2,3-d]furan is the dominant component while benzo[b]naphtho[1,2-d]furan is the least abundant (Fig. 4.52).

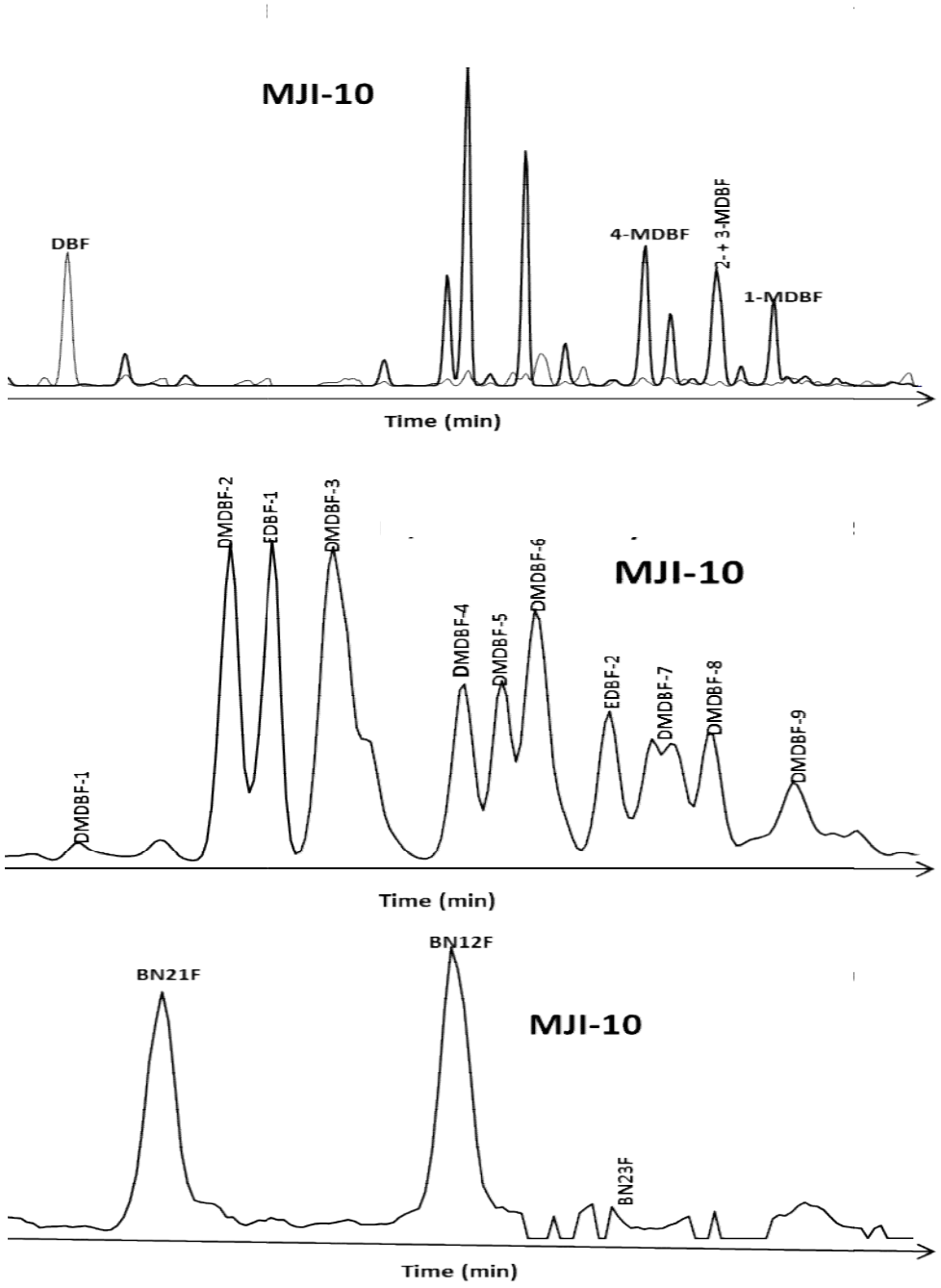

Fig. 4.52: Mass chromatograms showing the distribution of $C_{0\text{-}2}$-dibenzofurans (168+182, 196) and benzo[b]naphthofurans (m/z 218) in representative oil from MJI Field

Table 4.20: Absolute concentration (µg/g) of dibenzofurans in crude oils from MJI Field.

Sample	C0	4-MDBF	2- + 3-MDBF	1-MDBF	DMDBF-1	DMDBF-2	EDBF-1	DMDBF-3	DMDBF-4	DMDBF-5	DMDBF-6	EDBF-2	DMDBF-7	DMDBF-8	DMDBF-9
MJI1	15.79	47.38	38.42	10.77	6.42	78.56	64.43	106.18	48.31	16.67	79.58	23.93	68.33	25.30	50.27
MJI2	126.71	123.34	111.40	53.83	6.23	125.75	109.00	216.48	66.50	57.71	112.09	53.28	82.97	45.13	51.79
MJI3	104.44	101.74	92.66	41.80	7.07	96.64	89.56	178.47	56.73	45.01	97.65	40.42	67.64	40.22	38.80
MJI4	113.52	110.24	105.27	51.85	6.93	109.35	90.44	186.22	59.94	53.82	98.40	50.72	74.39	40.35	47.62
MJI5	17.22	46.39	36.57	11.66	5.18	74.97	59.93	102.99	46.06	17.80	73.31	23.84	63.90	22.12	39.15
MJI6	110.54	269.08	206.53	95.04	23.72	167.05	143.09	264.70	116.82	76.19	164.04	82.77	131.11	80.15	107.16
MJI7	112.60	110.02	102.41	49.17	5.93	101.74	93.46	183.03	56.62	50.32	100.34	47.25	69.60	40.65	40.19
MJI8	61.30	76.52	68.79	28.27	10.07	91.34	78.03	150.50	54.24	31.53	90.66	36.91	73.25	34.45	49.03
MJI9	135.72	133.30	119.73	56.90	7.57	132.44	114.95	234.25	73.48	60.47	126.92	56.87	89.83	48.95	59.52
MJI10	136.71	83.83	87.85	44.89	7.30	68.66	64.99	127.83	43.27	38.99	72.30	36.20	53.41	29.51	33.86

Table 4.21: Absolute concentration (µg/g) of sum of dibenzofurans and benzonaphthofurans in crude oils from MJI Field.

Sample	Concentrations of DBFs and BNFs (µg/g oil)						BN21F/ (BN21F + BN12F)
	ΣMDBF	ΣDMDBF	BN21F	BN12F	BN23F	ΣBNF	
MJI1	96.57	567.98	13.02	7.90	20.77	41.69	0.64
MJI2	288.57	926.93	18.56	16.02	21.04	55.62	0.55
MJI3	236.20	758.22	14.21	11.34	18.34	43.88	0.57
MJI4	267.36	818.18	12.36	11.71	13.78	37.85	0.53
MJI5	94.62	529.24	12.11	7.06	19.30	38.47	0.64
MJI6	570.64	1346.81	127.74	120.59	104.28	352.60	0.55
MJI7	261.60	789.12	12.09	11.91	16.75	40.75	0.52
MJI8	173.58	700.03	13.26	10.62	0.26	24.13	0.57
MJI9	309.93	1005.24	18.65	16.20	25.07	59.92	0.55
MJI10	216.56	576.32	7.75	8.91	0.15	16.81	0.48

*C_0: dibenzofuran;

ΣMDBF: total concentration of all methyldibenzofurans;

ΣDMDBF: total concentration of all dimethyldibenzofurans;

BN21F: Benzo[b]naphtho[2,1-d]furan

BN12F: Benzo[b]naphtho[1,2-d]furan

BN23F:Benzo[b]naphtho[2,3-d]furan

ΣBNF: total concentration of benzo[b]naphthofurans;

BN21F/(BN21F +BN12F):benzo[b]naphtho[2,1-d]furan/(benzo[b]naphtho[2,1-d]furan+ benzo[b]naphtho[1,2-d]furan);

4.8.4 MJO Field

The representative m/z 168+182, 196 and 218 mass chromatograms of the oil samples from MJO field showing the distribution of dibenzofuran and its derivatives are shown in Fig. 4.53. The absolute concentrations of dibenzofuran compounds are presented in Tables 4.22 and 4.23. The concentrations of dibenzofuran, methyldibenzofurans and dimethyldibenzofurans in the oils range from 55.15 to 73.96 µg/g, 161.27 to 215.91 µg/g and 437.66 to 657.48 µg/g, respectively (Tables 4.22 and 4.23). The dibenzofurans are dominated by C_2- dibenzofurans (Table 4.23). 4-methyldibenzofuran is the most abundant among the isomers of methyldibenzofurans in the oil samples (Fig. 4.53).

Within the C_2-dibenzofurans, dimethyldibenzofuran-3 (DMDBF-3),) are detected in higher concentrations when compared with other C_2-dibenzofurans (Fig. 4.53; Table 4.23). This pattern of distribution has been reported in marine carbonate oils from the Tarim basin, NW China (Li and Ellis, 2015). The benzo[b]naphthofurans concentrations range from 34.12 to 43.74 µg/g (Table 4.23). Among the three isomers of benzo[b]naphthofurans, benzo[b]naphtho[1,2-d]furan was detected in higher abundance while benzo[b]naphtho[2,1-d]furan and benzo[b]naphtho[2,3-d]furan are the least abundant (Fig. 4.53).

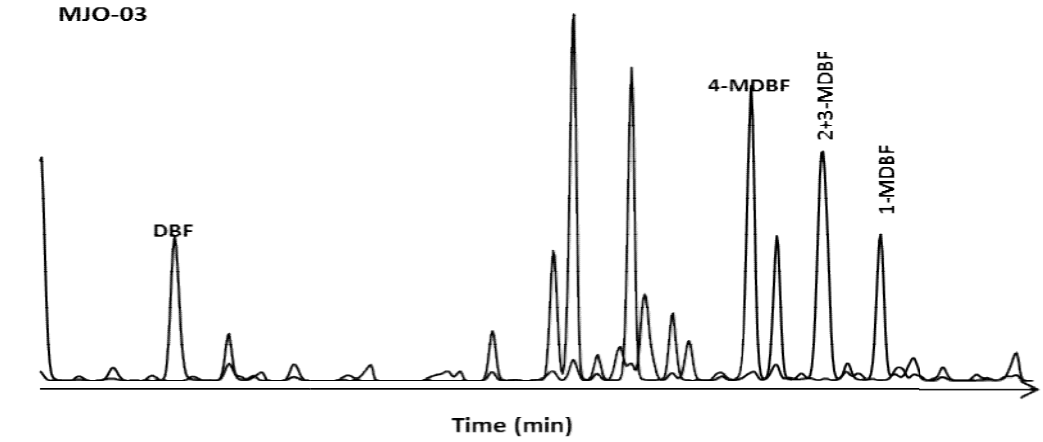
MJO-03
DBF
4-MDBF
2+3-MDBF
1-MDBF
Time (min)

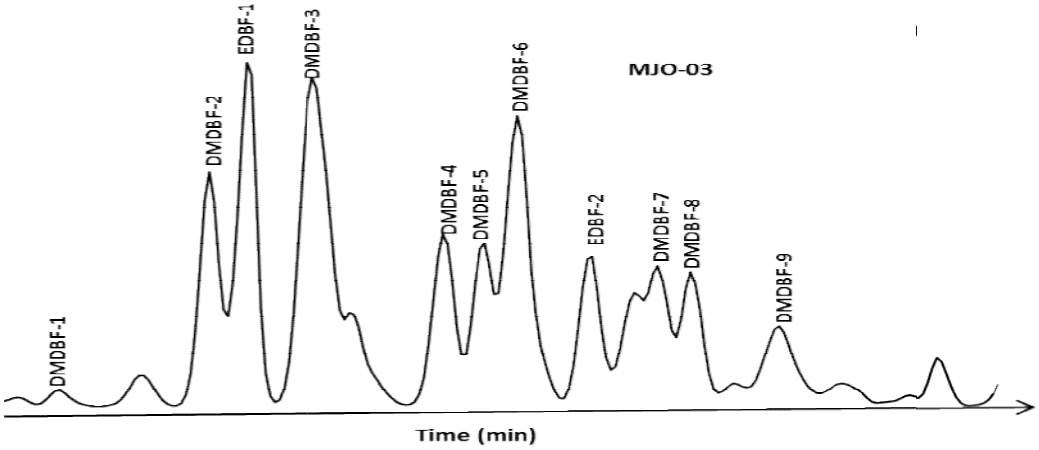
DMDBF-1
DMDBF-2
EDBF-1
DMDBF-3
DMDBF-4
DMDBF-5
DMDBF-6
MJO-03
EDBF-2
DMDBF-7
DMDBF-8
DMDBF-9
Time (min)

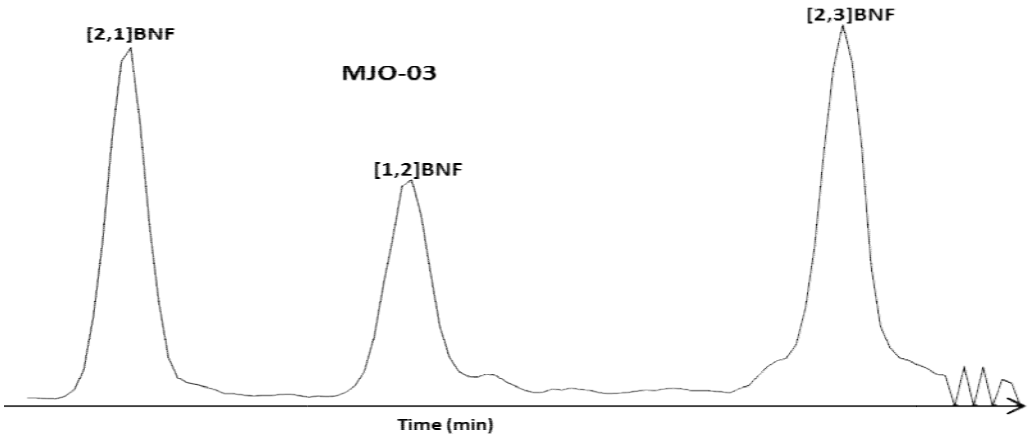
[2,1]BNF
MJO-03
[1,2]BNF
[2,3]BNF
Time (min)

Table 4.22: Absolute concentration (μg/g) of dibenzofurans in crude oils from MJO and WZB Fields.

Sample	C_0	4-MDBF	2- + 3-MDBF	1-MDBF	DMDBF-1	DMDBF-2	EDBF-1	DMDBF-3	DMDBF-4	DMDBF-5	DMDBF-6	EDBF-2	DMDBF-7	DMDBF-8	DMDBF-9
MJO1	55.15	62.85	66.43	32.00	3.60	44.56	62.51	91.80	33.95	31.42	67.85	29.71	23.96	25.90	22.40
MJO2	73.96	86.18	87.44	42.28	5.10	57.70	81.85	147.98	48.51	40.33	93.83	41.49	69.78	36.24	34.68
MJO3	60.39	69.51	72.10	34.21	3.93	46.88	68.13	120.62	38.62	32.90	76.40	33.52	50.75	29.29	26.86
MJO4	68.76	79.35	78.93	37.52	4.98	49.76	73.56	135.40	47.02	34.75	88.95	39.83	70.54	34.22	34.42
WZB1	54.99	54.09	61.50	29.96	4.00	52.29	69.10	128.61	4.69	33.56	116.79	28.36	40.49	24.90	29.50
WZB2	42.26	46.36	49.84	25.54	3.72	64.21	70.09	136.03	4.23	37.20	110.36	25.04	44.04	21.85	27.71

Table 4.23: Absolute concentration (µg/g) of sum of dibenzofurans and benzonaphthofuransin crude oils from MJO and WZB Fields.

Sample	Concentrations of DBFs and BNFs (µg/g oil)						BN21F/ (BN21F + BN12F)
	ΣMDBF	ΣDMDBF	BN21F	BN12F	BN23F	ΣBNF	
MJO1	161.27	437.66	9.24	16.83	8.05	34.12	0.37
MJO2	215.91	657.48	12.14	20.65	10.96	43.74	0.38
MJO3	175.83	527.90	9.81	17.53	8.86	36.20	0.37
MJO4	195.80	613.42	10.40	17.91	9.53	37.84	0.38
WZB1	145.55	532.29	9.97	16.33	7.79	34.10	0.39
WZB2	121.74	544.49	10.14	14.47	8.20	32.81	0.43

*C_0: dibenzofuran;

ΣMDBF: total concentration of all methyldibenzofurans;

ΣDMDBF: total concentration of all dimethyldibenzofurans;

BN21F: Benzo[b]naphtho[2,1-d]furan

BN12F: Benzo[b]naphtho[1,2-d]furan

BN23F:Benzo[b]naphtho[2,3-d]furan

ΣBNF: total concentration of benzo[b]naphthofurans;

BN21F/(BN21F +BN12F):benzo[b]naphtho[2,1-d]furan/(benzo[b]naphtho[2,1-d]furan+ benzo[b]naphtho[1,2-d]furan).

4.8.5 WZB Field

The representative m/z 168+182, 196 and 218 mass chromatograms of the oil samples showing the distribution of dibenzofuran and its derivatives are presented in Fig. 4.54. The absolute concentrations of dibenzofuran compounds are presented in Tables 4.22 and 4.23. The concentrations of dibenzofuran, methyldibenzofurans and dimethyldibenzofurans in the oils range from 42.26 to 54.99 µg/g, 121.74 to 145.55 µg/g and 532.29 to 544.49 µg/g, respectively (Tables 4.22 and 4.23). The dibenzofurans are dominated by C_2- dibenzofurans (Table 4.23). 4-methyldibenzofuran is the most abundant among the isomers of methyldibenzofurans in the oil samples (Fig.4.54).

Within the C_2-dibenzofurans, dimethyldibenzofuran-2 (DMDBF-2), dimethyldibenzofuran-6 (DMDBF-6), dimethyldibenzofuran-3 (DMDBF-3) and ethyldibenzofuran-1 (EDBF-1) are detected in higher concentrations when compared with other C_2-dibenzofurans (Fig.4.54; Table 4.22). This pattern of distribution has been reported in marine carbonate oils from the Tarim basin, NW China (Li and Ellis, 2015). The benzo[b]naphthofurans concentrations range from 32.81 to 34.10 µg/g (Table 4.23). Benzo[b]naphtho[2,3-d]furan is the least abundant among the three isomers of benzo[b]naphthofurans while benzo[b]naphtho[2,1-d]furan and benzo[b]naphtho[1,2-d]furan show almost equal distribution (Fig.4.54).

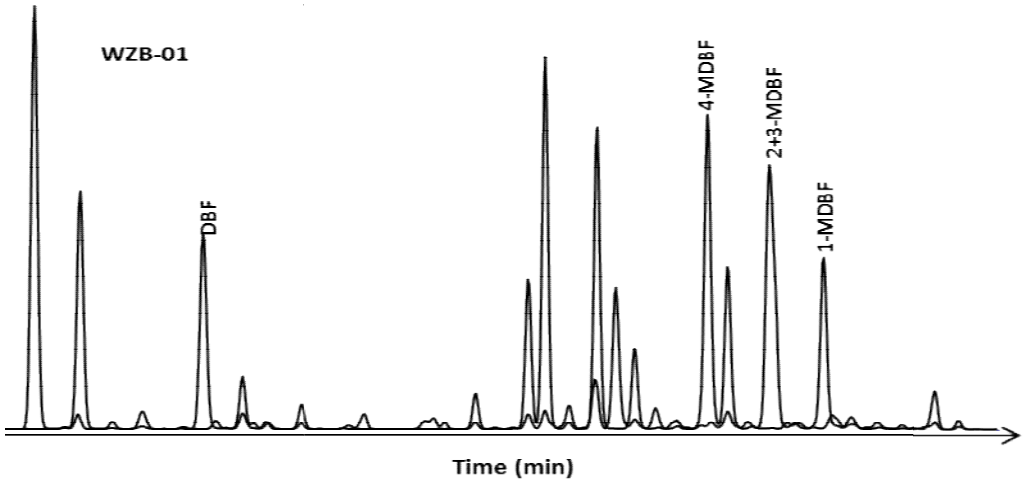
WZB-01
DBF
4-MDBF
2+3-MDBF
1-MDBF
Time (min)

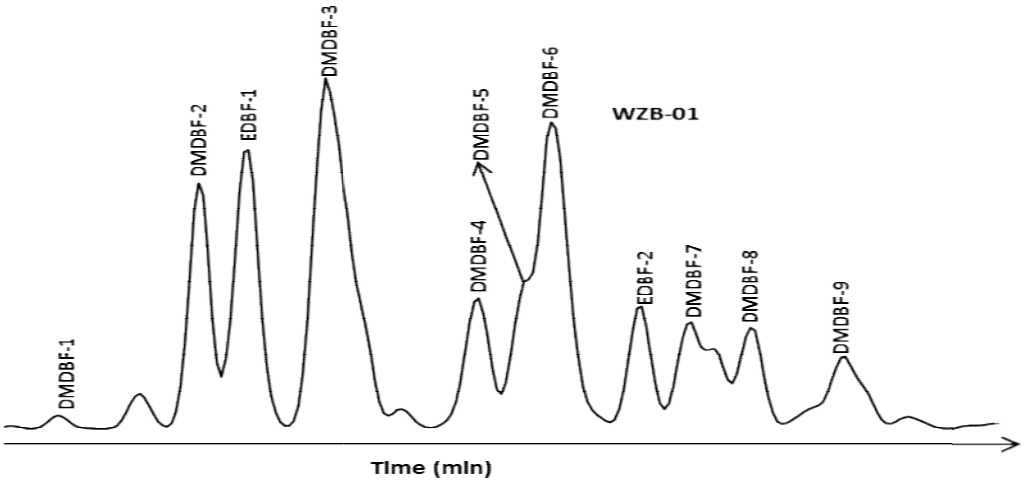
DMDBF-1
DMDBF-2
EDBF-1
DMDBF-3
DMDBF-4
DMDBF-5
DMDBF-6
WZB-01
EDBF-2
DMDBF-7
DMDBF-8
DMDBF-9
Time (min)

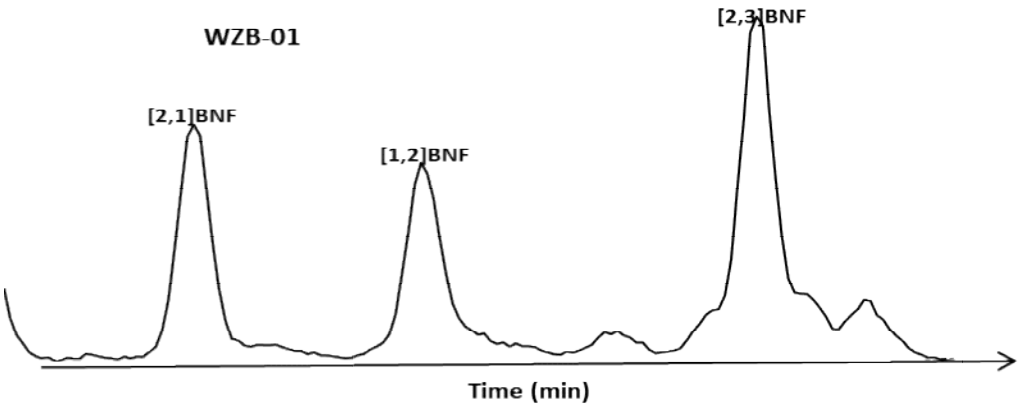
WZB-01
[2,1]BNF
[1,2]BNF
[2,3]BNF
Time (min)

4.9 Effects of source input, depositional environment, maturity and biodegradation on the distribution of dibenzofurans

The source, depositional environment, thermal maturity of organic matter and biodegradation are important factors controlling the distribution and concentrations of most molecular markers in source rocks and crude oils. In this study, the effect of source, depositional environment, maturity and biodegradation on the distribution of dibenzofurans in the oils were investigated by plotting the concentrations and ratios of dibenzofuran isomers against well-established source, maturity and biodegradation parameters obtained from the saturate and aromatic distributions in the oils (Fig.s. 4.55 to 4. 65).

4.9.1 ADL Field

Fig.s 4.55a and 4.55b show the plots of Pr/Ph against the total concentration of dibenzofurans and BN21F/(BN21F+BN12F) ratios. These plots clearly showed that the distribution of the dibenzofurans and benzo[b]naphthofurans have no significant correlation with the Pr/Ph ratio. The variations observed among the dibenzofurans may be due to other factors other than source facies.

It has been reported that maturity can have marked effects on the distribution of molecular isomers of alkylated dibenzofurans (Radke *et al*., 2000; Li *et al*., 2011, 2018). The total concentrations of dibenzofurans and benzo[b]naphthofurans were plotted against 20S/(20S+20R) C_{29} steranes in Fig. 4.56a. The plot clearly indicates the influence of maturity on the dibenzofurans and benzo[b]naphthofurans distributions. The plot of 4-/1-MDBF against MPI-1 also shows that maturity has influence on the distributions of dibenzofurans in the oils (Fig.4.56b).

The total concentrations of the dibenzofurans and benzo[b]naphthofurans show no significant correlation with biodegradation parameters, $C_{30}\alpha\beta$ hopane/(Pr+Ph) and (Pr+Ph)/(nC_{17}+nC_{18}) ratio (Fig.4.57). This indicates that there is no influence of biodegradation on the dibenzofuran and benzo[b]naphthofurans distributions in the oils.

4.9.2 OKN Field

The plot of total concentrations of dibenzofurans and benzo[b]naphthofurans (BN21F/(BN21F+BN12F) ratios against Pr/Ph ratios lack any significant correlation (Fig. 4.58). This indicates that source facie has no effect on the distribution of the dibenzofurans and benzo[b]naphthofurans in the oils.

Fig.4.59a shows the plots of total concentrations of dibenzofurans and benzo[b]naphthofurans against 20S/(20S+20R) C_{29} steranes. The plot shows that maturity has no effect on the distributions of dibenzofurans and benzo[b]naphthofurans in the oils. This is further supported by the plot of 4-/1-MDBF against MPI-1 (Fig.4.59a). The variations observed among the dibenzofurans and its derivatives must have been due to other factors other than maturity.

Fig.4.57 shows plots of the total concentrations of dibenzofurans and benzo[b]naphthofurans against $C_{30}\alpha\beta$ hopane/(Pr+Ph) and (Pr+Ph)/(nC_{17}+nC_{18}) ratios in the oils. This plot suggests no effect of biodegradation on the distributions of dibenzofuran and benzo[b]naphthofurans in the oils.

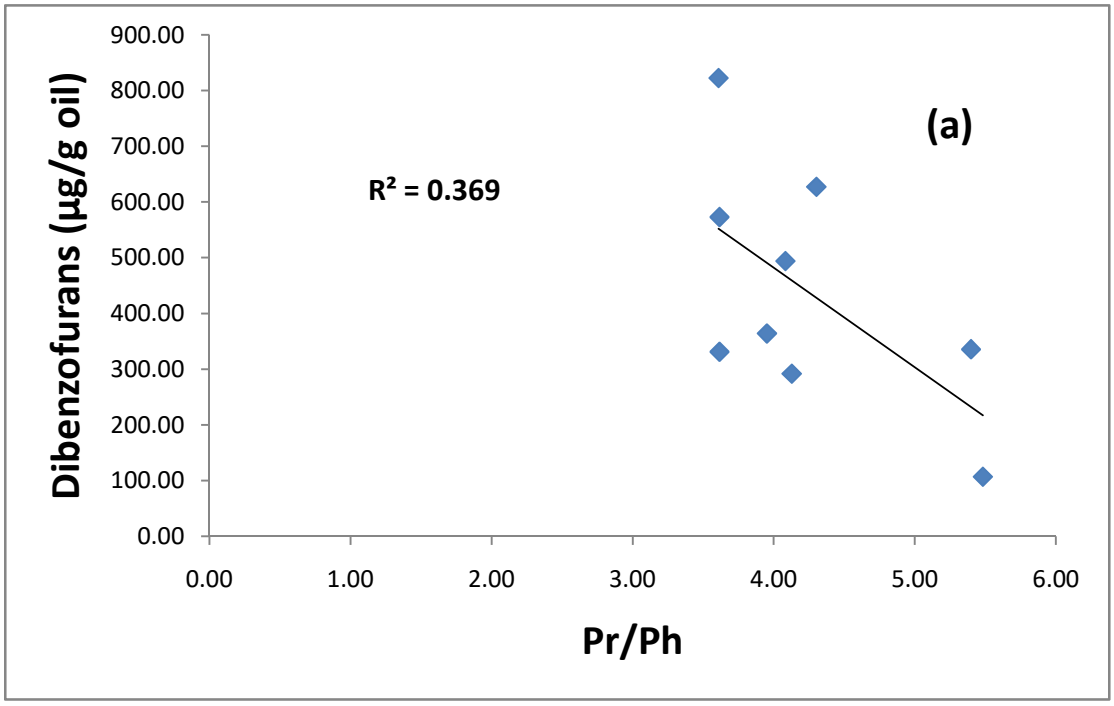

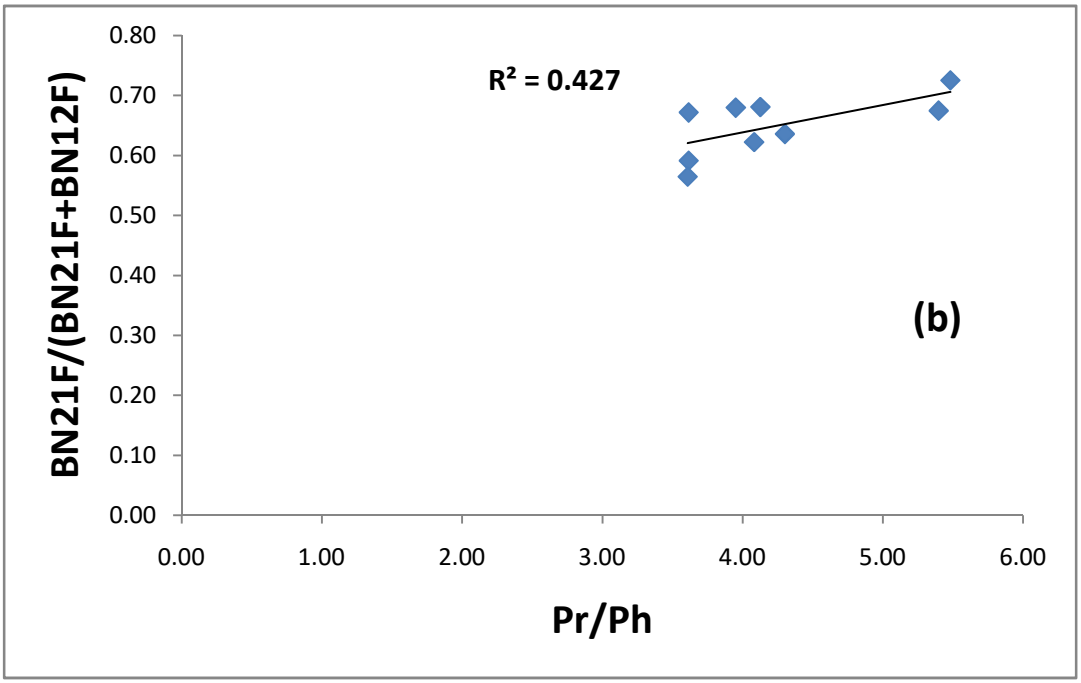

Fig. 4.55: Cross plots of Pr/Ph against (a) total concentration of dibenzofurans and (b) BN21F/(BN21F+BN12F) for ADL oils.

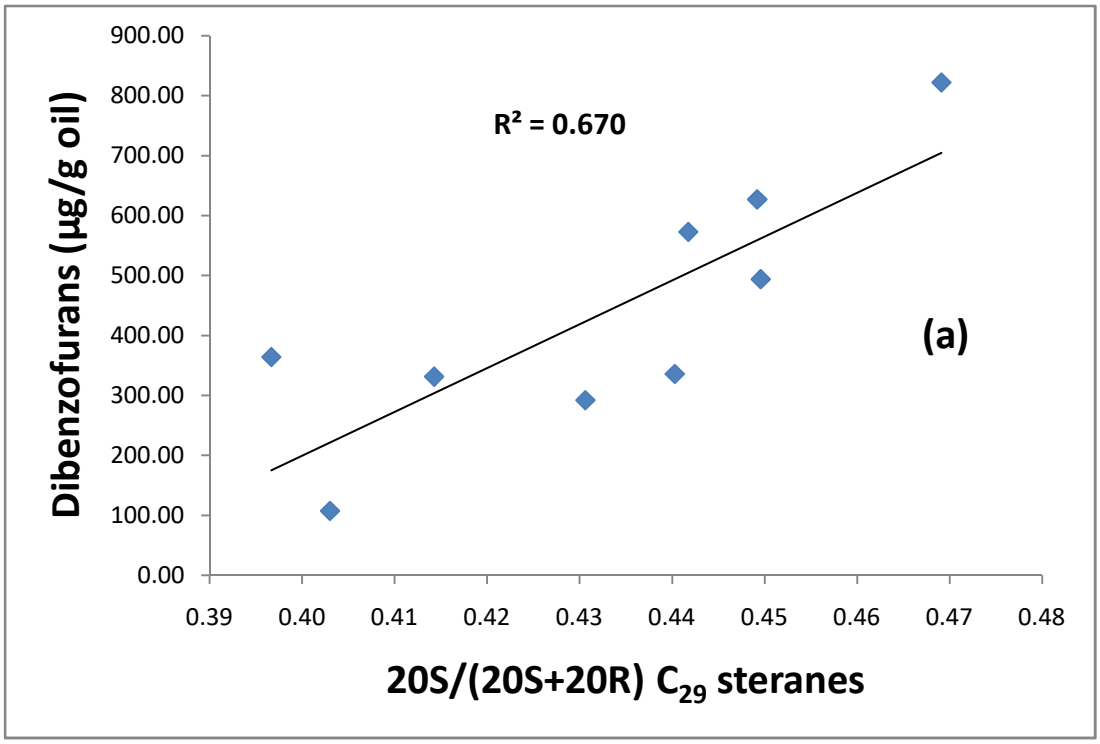

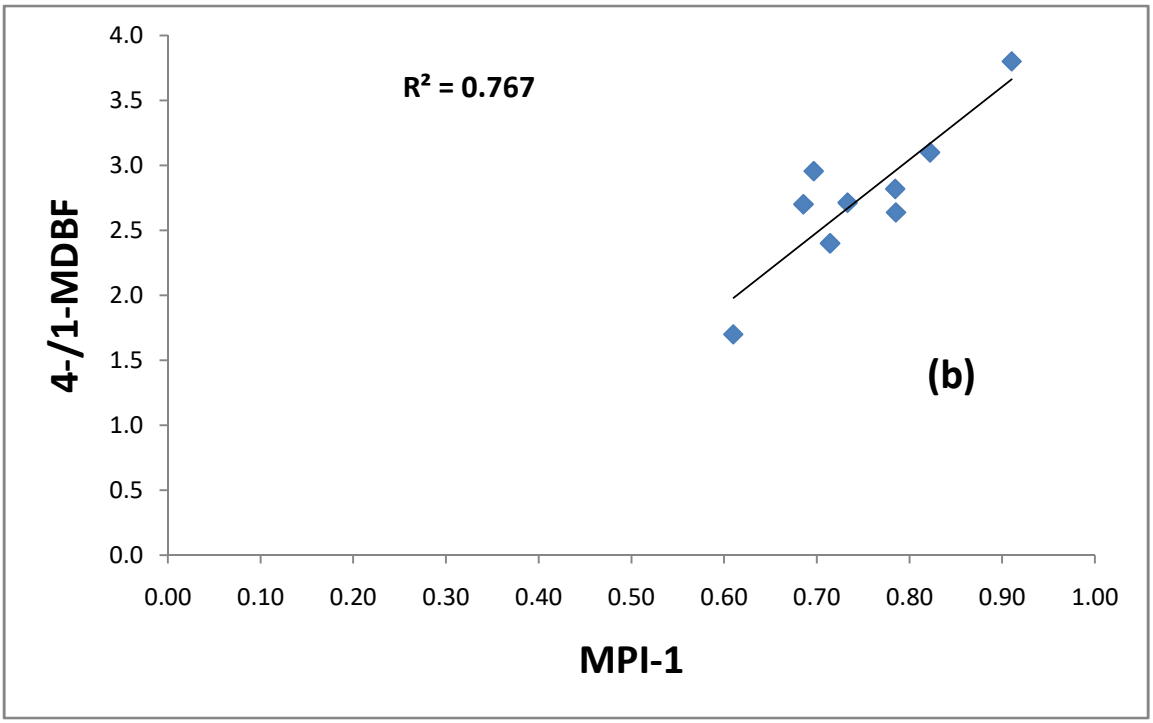

Fig.4.56: Cross plots of (a) total concentration of dibenzofurans versus 20S/(20S+20R) C_{29} steranes and (b) 4-/1-MDBF versus MPI-1 for ADL oils.

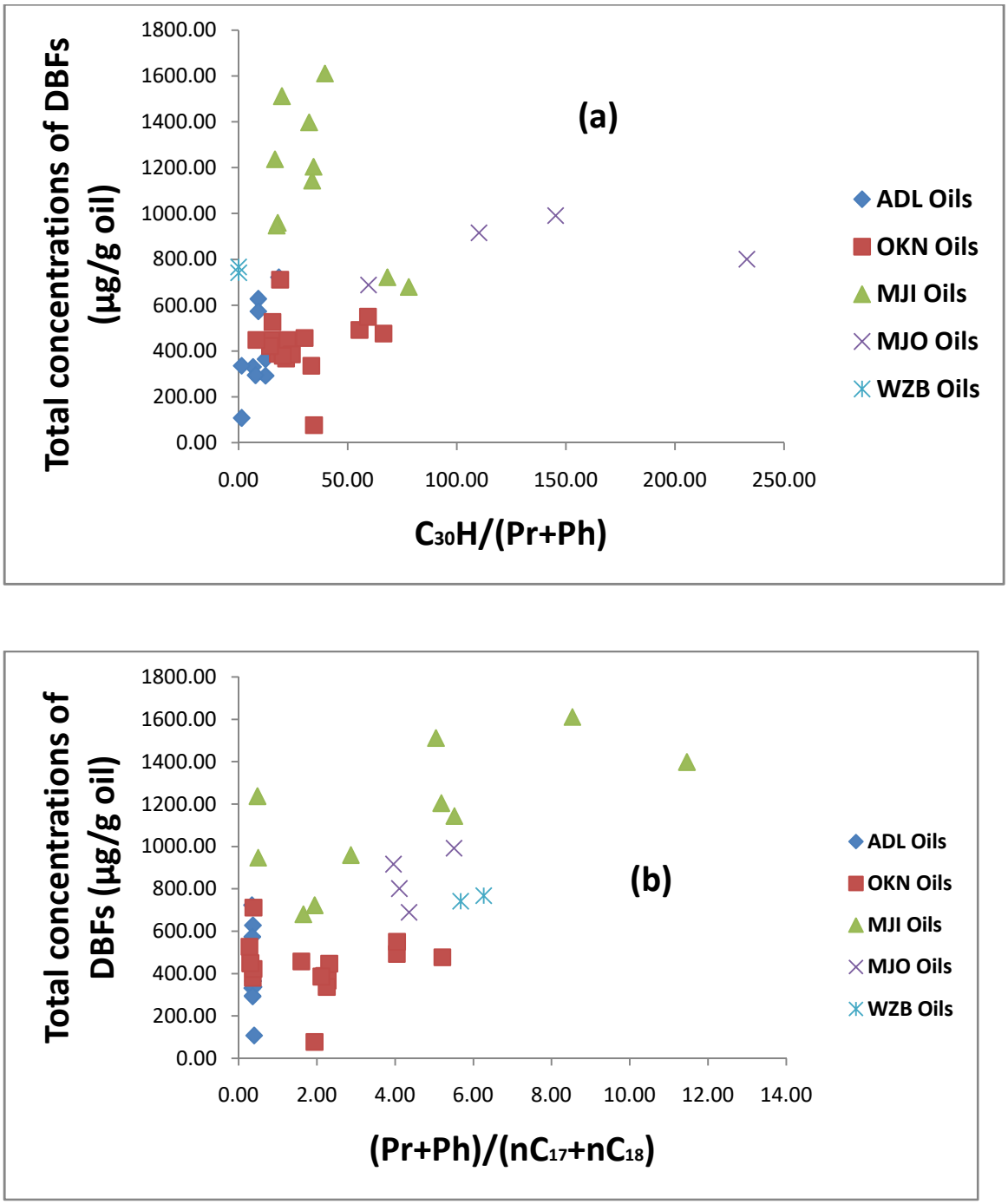

Fig.4.57: Cross plots of the total concentrations of dibenzofurans versus(a)$C_{30}\alpha\beta$ hopane/(Pr+Ph) and (b) (Pr+Ph)/(nC_{17} + nC_{18}) ratios in Niger Delta oils. (after Li and Ellis, 2015).

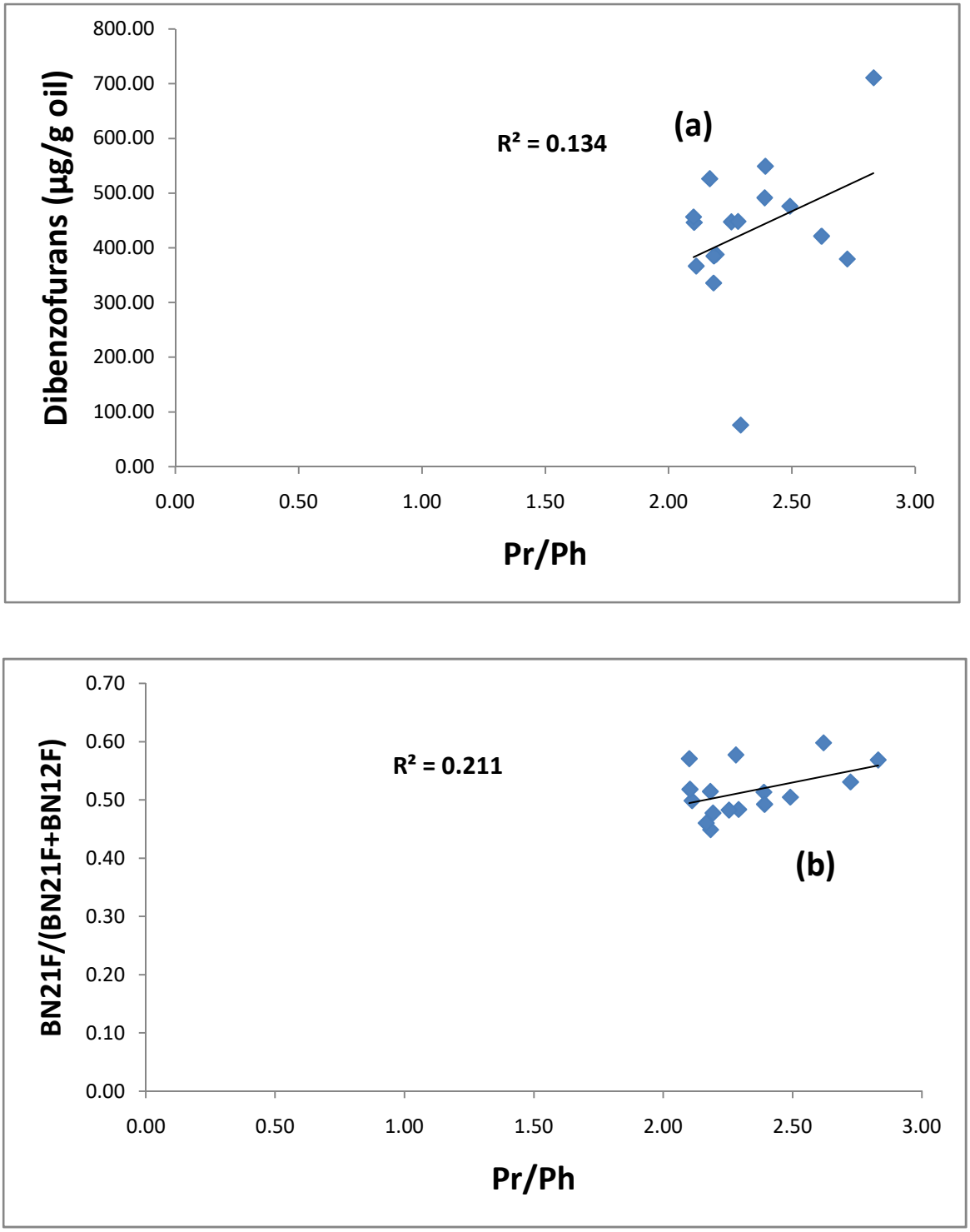

Fig. 4.58: Cross plots of Pr/Ph against (a) total concentration of dibenzofurans and (b) BN21F/(BN21F+BN12F) for OKN oils.

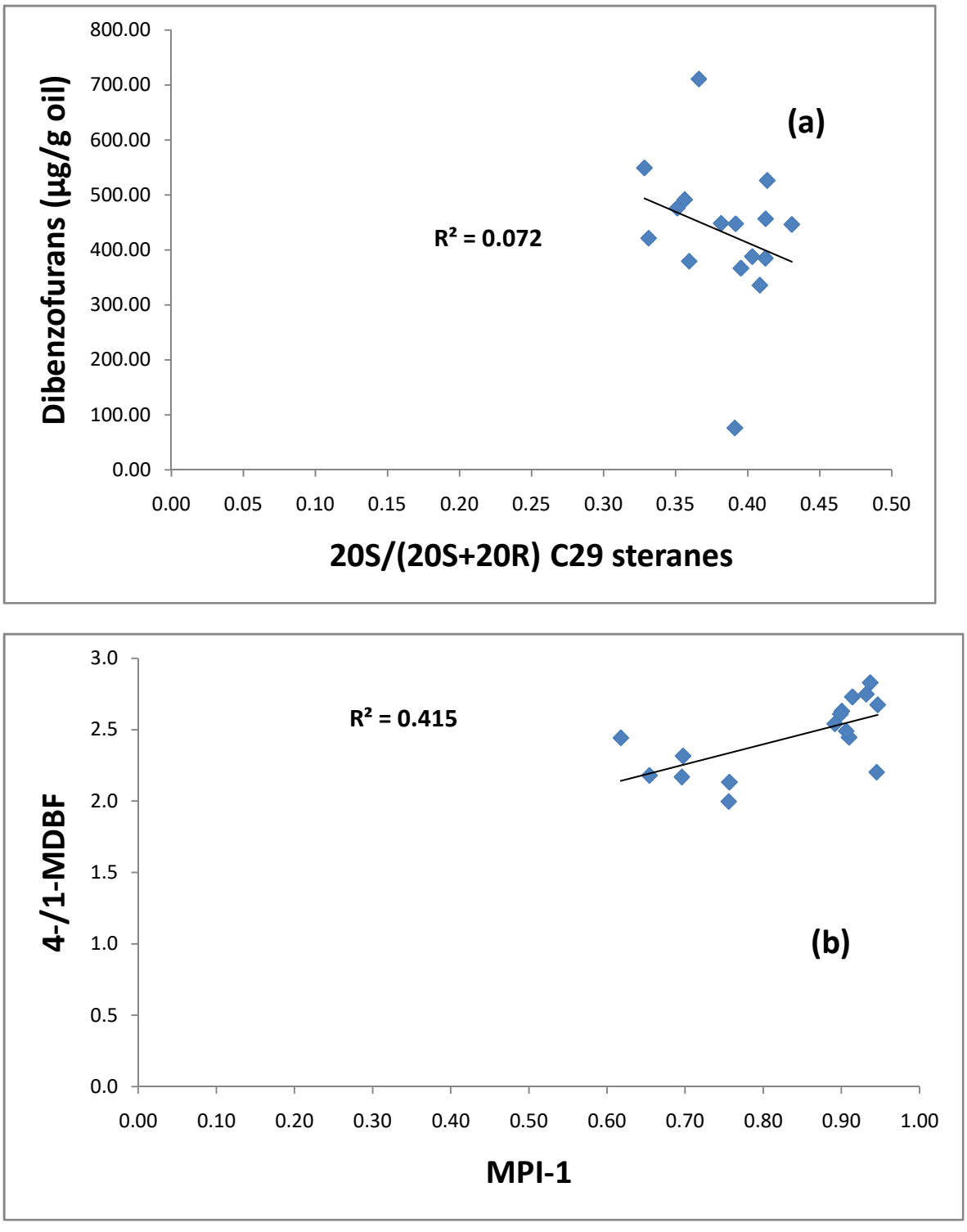

Fig. 4.59: Cross plots of (a) total concentration of dibenzofurans versus 20S/(20S+20R) C_{29} steranes and (b) 4-/1-MDBF versus MPI-1 for OKN oils

4.9.3 MJI Field

The plots of concentrations of dibenzofurans and benzo[b]naphthofurans (BN21F/(BN21F+BN12F) ratios against Pr/Ph ratios do not show any significant correlation(Fig. 4.60). This observation suggests that source facie has no influence on the distribution and abundance of the dibenzofurans and benzo[b]naphthofurans in the oils.

Fig. 4.61a shows the plot of the total concentrations of dibenzofurans and benzo[b]naphthofurans against 20S/(20S+20R) C_{29} steranes. This plot showed no effect of maturity on the abundance and distributions of the dibenzofurans in the oils. The plots of 4-/1-MDBF ratios against MPI-1 also indicate no influence of maturity on the abundance of dibenzofurans in the oils (Fig. 4.61b). Hence, the variations among the dibenzofurans and benzo[b]naphthofurans must have been due to other factor other than thermal maturity.

The plots of the total concentrations of dibenzofurans and benzo[b]naphthofurans against $C_{30}\alpha\beta$ hopane/(Pr+Ph) and (Pr+Ph)/(nC_{17}+nC_{18}) ratios (Fig. 4.57) indicate no effect of biodegradation on the distributions of the dibenzofuran and benzo[b]naphthofurans in the oils.

4.9.4 MJO Field

The concentrations of dibenzofurans and benzo[b]naphthofurans (BN21F/(BN21F+BN12F) ratios were plotted against Pr/Ph ratios in Fig.s 4.62a and 4.62b, respectively. These plots lack any correlation to suggest the influence of organic matter source on the dibenzofurans distribution in the oils. The total concentrations of dibenzofurans and benzo[b]naphthofurans showed a significant correlation when plotted against 20S/(20S+20R) C_{29} steranes in Fig. 4.63a. This observation shows that thermal maturity has significant influence on the abundance and distributions of the dibenzofurans in the oils. The plots of 4-/1-MDBF against MPI-1 further confirmed the influence of maturity on the abundance of the dibenzofurans in the oils (Fig. 4.63b).

The Fig.4.57 shows the plots of total concentrations of dibenzofurans and benzo[b]naphthofurans against $C_{30}\alpha\beta$ hopane/(Pr+Ph) and (Pr+Ph)/(nC_{17}+nC_{18}) ratios. These plots indicate no effect of biodegradation on the abundance of the dibenzofuran and benzo[b]naphthofurans in the oils.

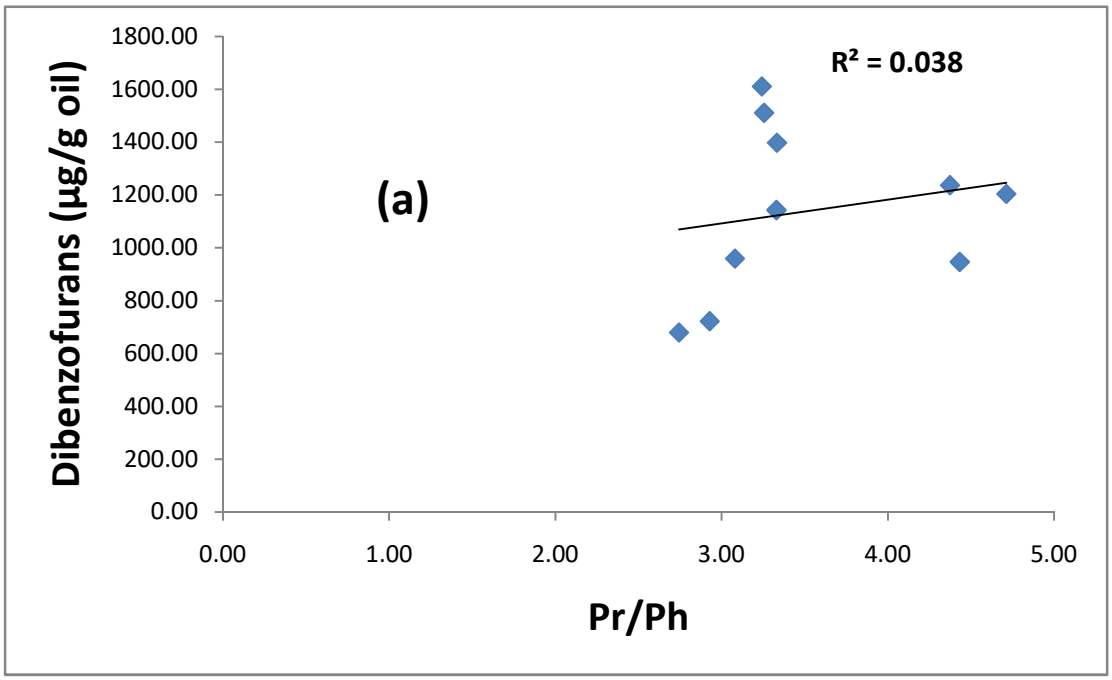

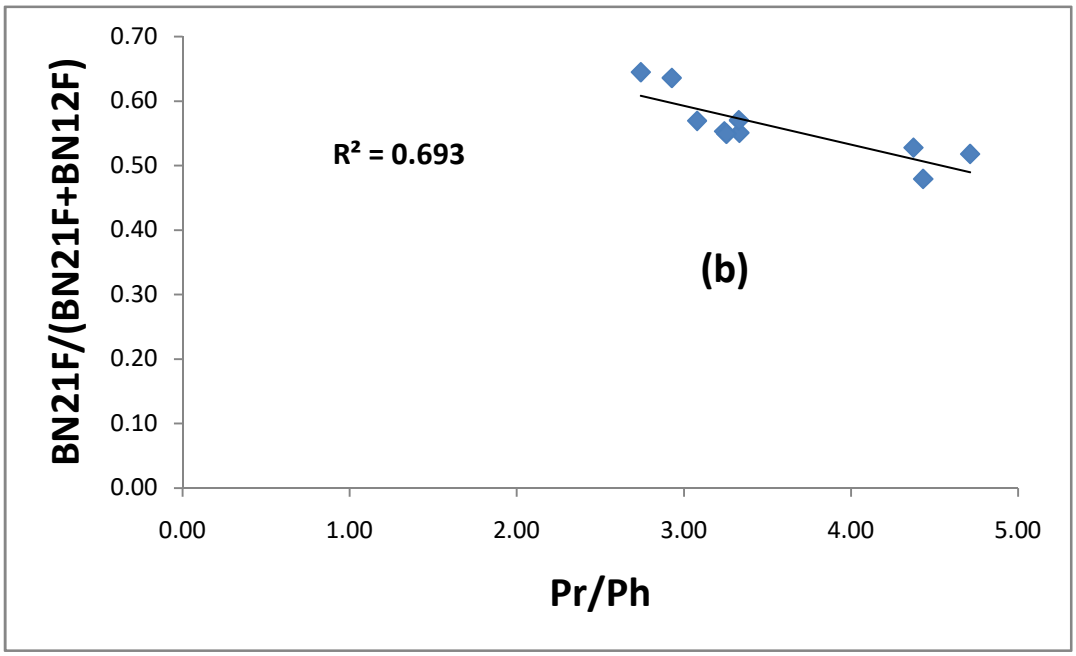

Fig. 4.60: Cross plots of Pr/Ph against (a) total concentration of dibenzofurans and (b) BN21F/(BN21F+BN12F) for MJI oils.

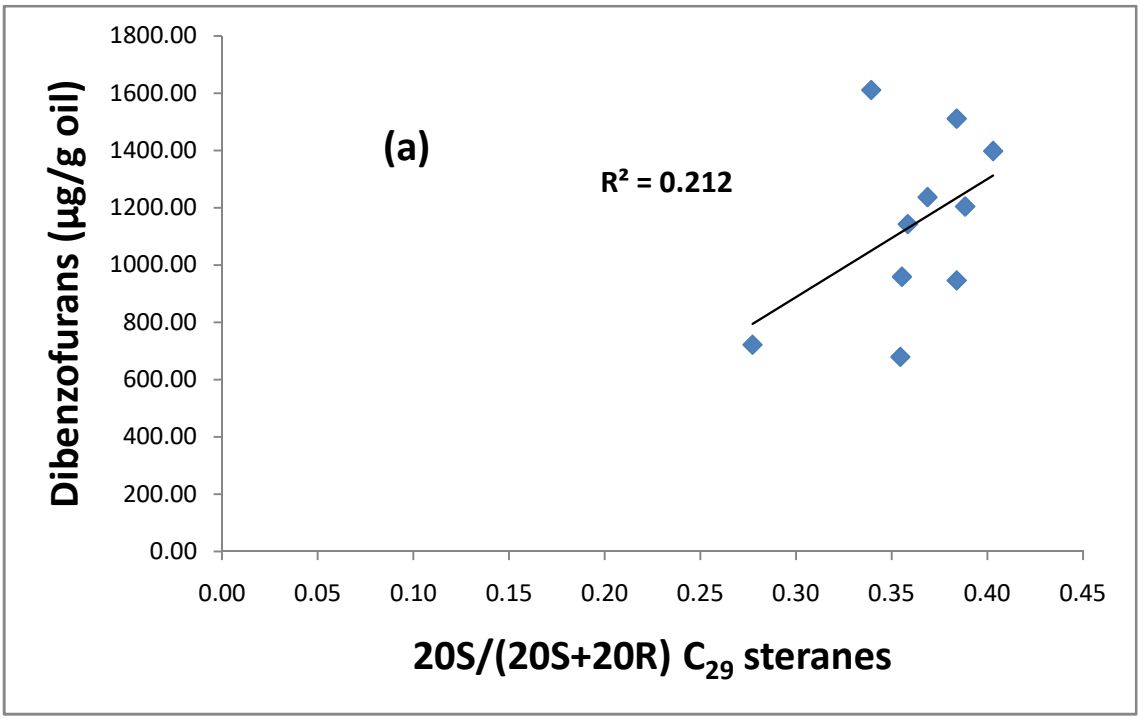

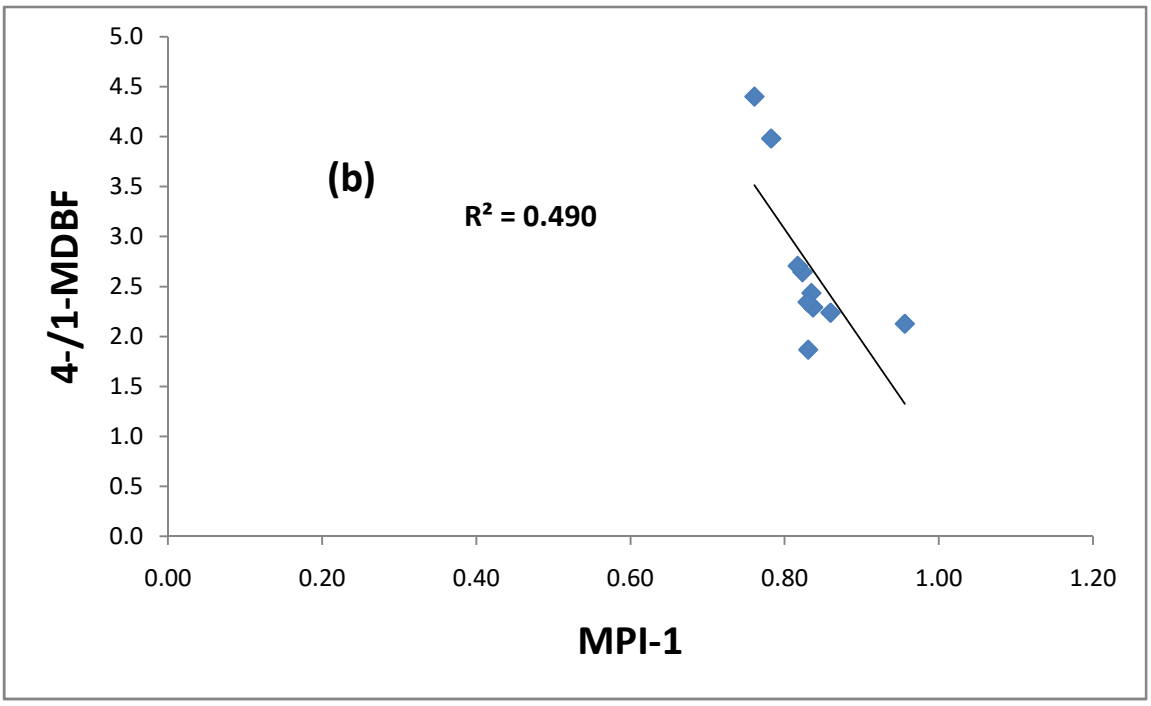

Fig.4.61: Cross plots of (a) total concentration of dibenzofurans versus 20S/(20S+20R) C_{29} steranes and (b) 4-/1-MDBF versus MPI-1 for MJI oils.

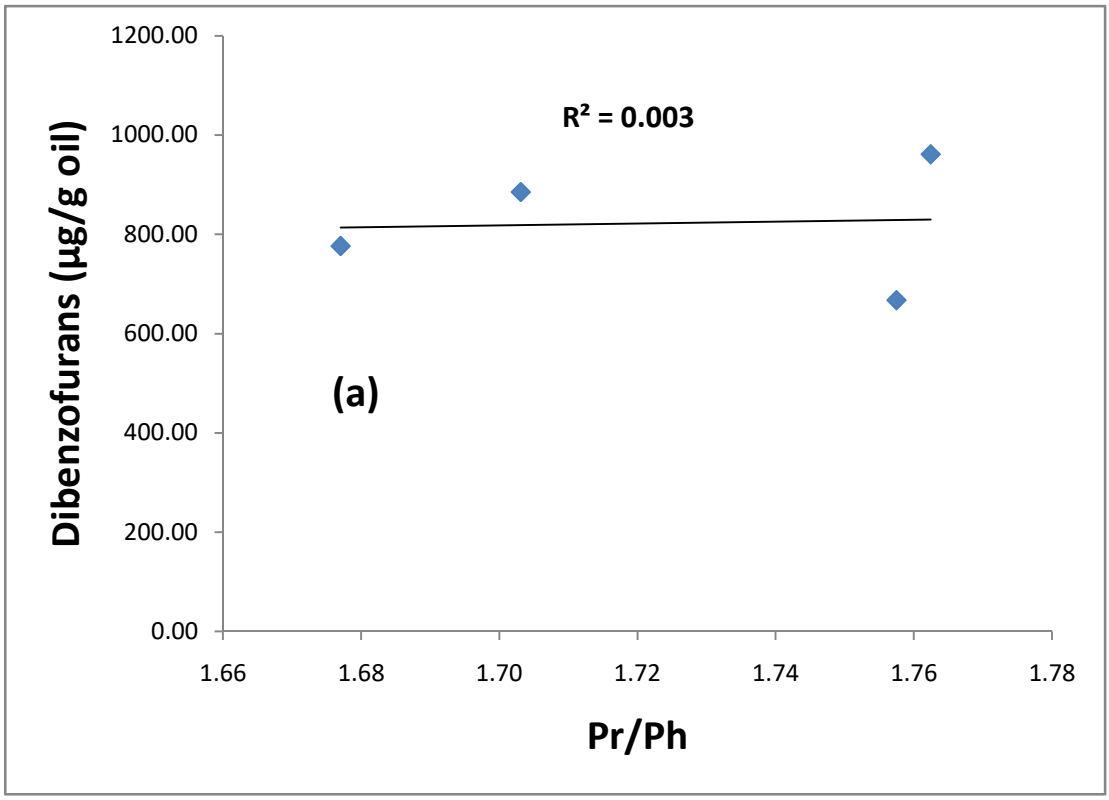

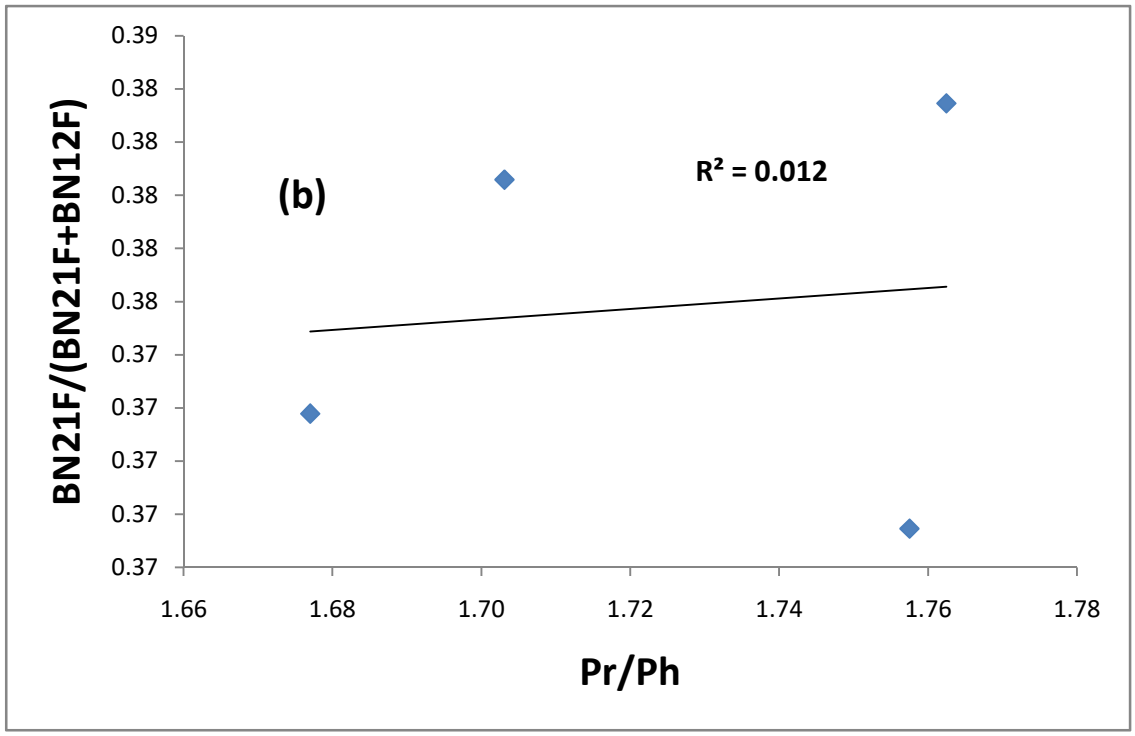

Fig. 4.62: Cross plots of Pr/Ph against (a) total concentration of dibenzofurans and (b) BN21F/(BN21F+BN12F) for MJO oils.

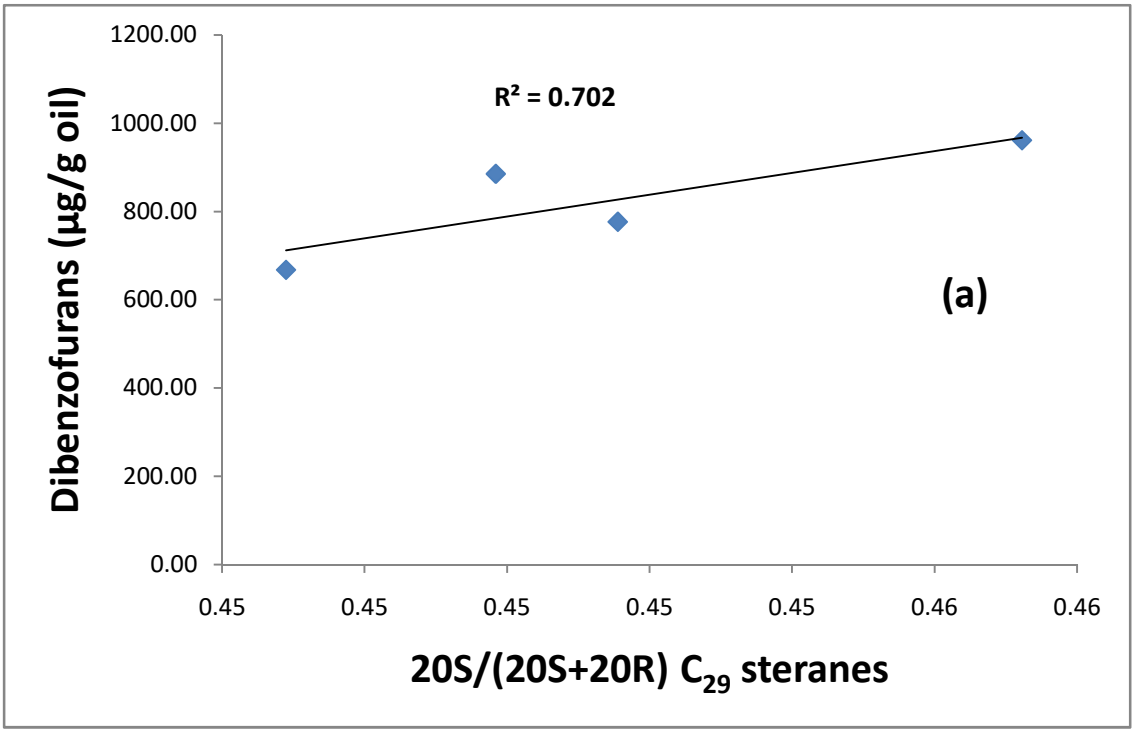

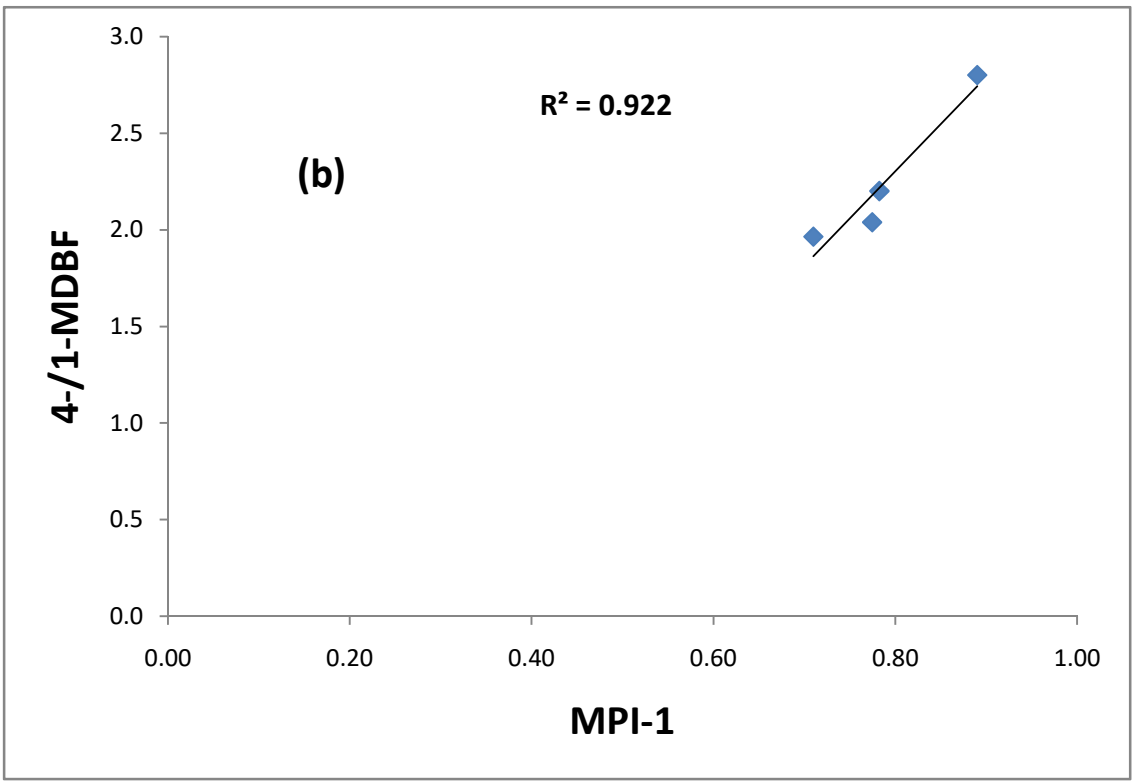

Fig. 4.63: Cross plots of (a) total concentration of dibenzofurans versus 20S/(20S+20R) C_{29} steranes and (b) 4-/1-MDBF versus MPI-1 for MJO oils.

4.10 Variation in Dibenzofurans concentrations during oil migration

The prerequisite for tracing oil migration direction and evaluating migration distances is that the distribution and abundance of the migration molecular markers to be used must not be influenced by source facies, depositional environment, thermal maturity and biodegradation. The present study has shown that the distributions and abundance of the dibenzofurans and benzo[b]naphthofurans in the oils from the same field were not influenced by the organic matter.ADL and MJO oils were found to show substantial maturity influence on the abundance and distribution of dibenzofurans (Fig.s 4.56 and 4.63), among the five fields. The distribution and abundance of dibenzofuran compounds in oils from OKN and MJI fields is found to be mainly controlled by migration induced fractionation and, thus, the dibenzofuran compounds can serve as potential migration tracers for the oils in these fields.

The concentrations of dibenzofuran and its derivatives have been proposed to decrease with increasing oil migration distance (Li et al., 2011, 2018; Li and Ellis, 2015). Therefore, the direction of decrease in total concentrations of DBFs can indicate the extent and direction of oil migration in MJI and OKN fields. The oil migration distance in OKN and MJI fields were estimated based on the gradual decrease in the total concentrations of the dibenzofuran compounds.

4.10.1 OKN Field

The total concentrations of dibenzofuran compounds (including the parent and all of the methyl-, dimethyl-, and ethyldibenzofuran and benzo[b]naphthofuran isomers) and the estimated relative migration distances for wells in OKN field are shown in Table 4.24. The total concentration of DBFs in the oils range from 76.39 to 710.77 µg/g oil, with an average of 431.64b µg/g oil (Table 4.25). The total concentrations of DBFs decrease from 710.77 (OKN-12) to 76.39 µg/g oil (OKN-6) (Table 4.24). This indicates that OKN-6 has migrated the longest distance from the source kitchen into its present position. The migration distances of other oils in OKN field are between OKN-6 and OKN-12 oils. Carbazoles have been successfully applied to oil migration study in Niger Delta (Faboya *et al*, 2015). The location map of the oil wells in the field is shown in Fig. 4.64. The variations in the total dibenzofuran concentration indicate south to east oil

migration in the field(Fig. 4.64). Therefore, it can be predicted that the oils originated from a source kitchen in the southern part of OKN field. This speculation is further supported by the plot of total concentrations of carbazoles on the location map of the oil wells in the field under study (Fig. 4.65). These findings suggest that the southern part of OKN field is the most prolific exploration region.

Different authors have successfully estimated the migration distances of some oil wells based on the nearest well to the speculated source kitchen along the migration orientation by arbitrarily assigning 1km to the nearest well (Larter *et al*., 1996; Li *et al*., 2014; Faboya *et al*., 2015). The present study takes OKN-12 as a reference well because of its highest DBFs concentration. Fig. 4.66a show the differences in the total concentrations of the dibenzofurans compounds as a function of relative migration distance for oils in the OKN field. It indicates that the concentrations of the total dibenzofurans compounds decrease with increasing secondary migration distance with general linear trend (R^2 = 0.8292) for the oils from OKN field. This is further supported by the plot of total concentration of carbazoles against relative migration distance (R^2 = 0.6772) (Fig. 4.66b). The maximum migration distance obtained from the present field is less than 100km and this has been associated with rift basin such as Niger Delta basin (Larter *et al*., 1996; Li *et al*., 2014).

Table 4.24: Total concentrations of dibenzofurans and carbazole compounds and the estimated relative migration distances.

Well	N (µg/g oil)	O (µg/g oil)	Relative migration distance (km)
OKN Field			
OKN1	10.53	491.56	7.8
OKN2	8.37	387.96	12.3
OKN3	7.85	366.79	19.8
OKN4	10.36	549.22	10.7
OKN6	1.17	76.39	38.4
OKN8	8.98	447.60	12.3
OKN9	7.06	385.04	11.4
OKN10	8.82	379.60	15.6
OKN11	7.63	421.45	6.4
OKN12	12.87	710.77	1
OKN13	7.03	476.09	7.4
OKN14	7.95	456.64	9.2
OKN15	9.64	448.44	11.8
OKN16	11.45	526.43	8.4
MJI Field			
MJI1	3.51	722.03	36.3
MJI2	16.83	1397.83	25
MJI3	16.89	1142.74	25.9
MJI4	7.12	1236.90	28.9
MJI5	1.12	679.56	64.3
MJI6	72.41	2380.59	1
MJI7	14.71	1204.06	24.4
MJI8	3.36	959.04	52
MJI9	14.83	1510.82	28.7
MJI10	42.45	946.40	28.6

O: total concentration of dibenzofuran, methyldibenzofurans, dimethyldibenzofurans and benzo[b]naphthofurans;

N: total concentration of carbazole, methylcarbazoles, dimethylcarbazoles and benzocarbazoles.

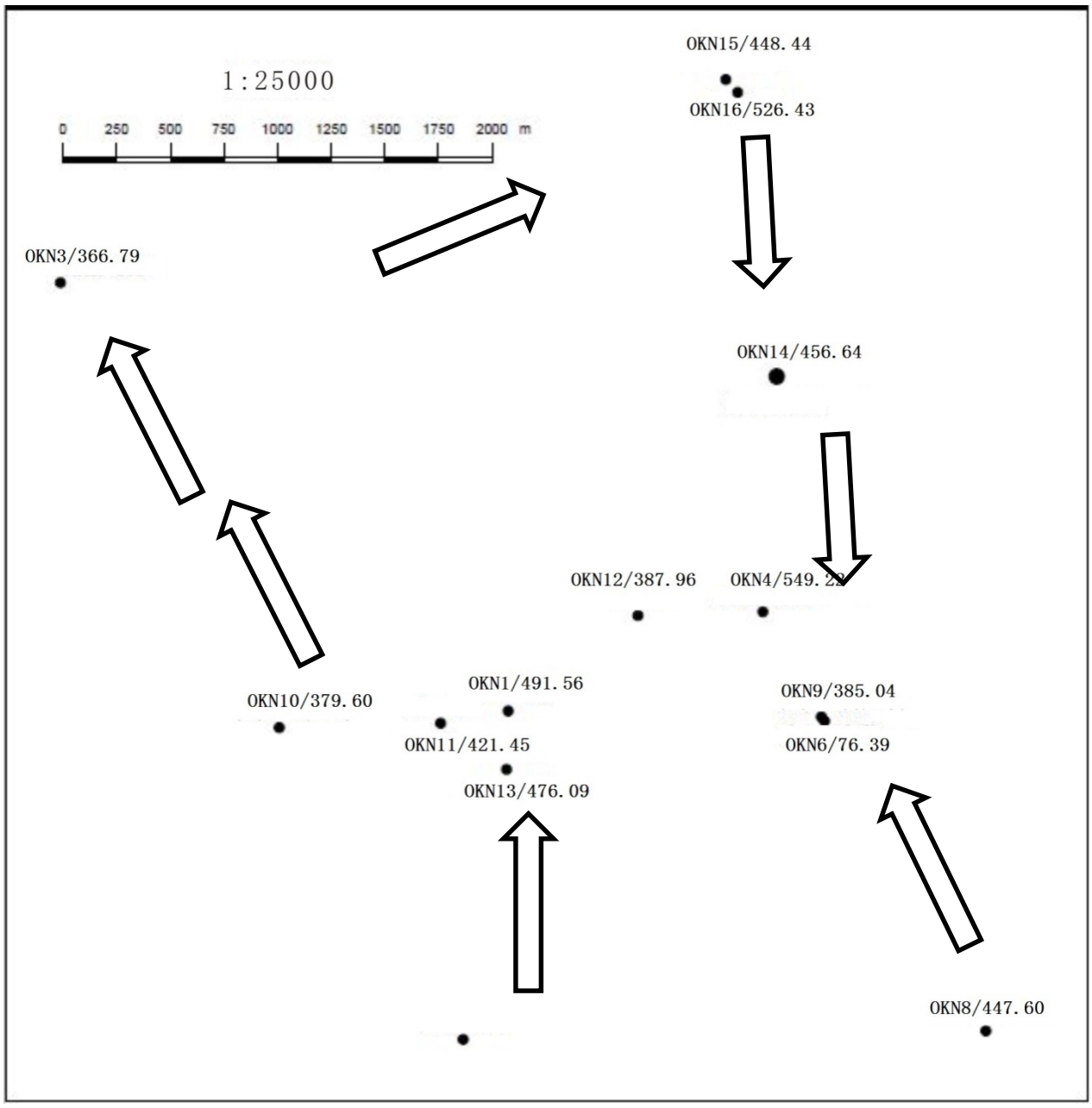

Fig. 4.64: Map showing the total concentration of dibenzofurans and the direction of oil migration in OKN Field.

.

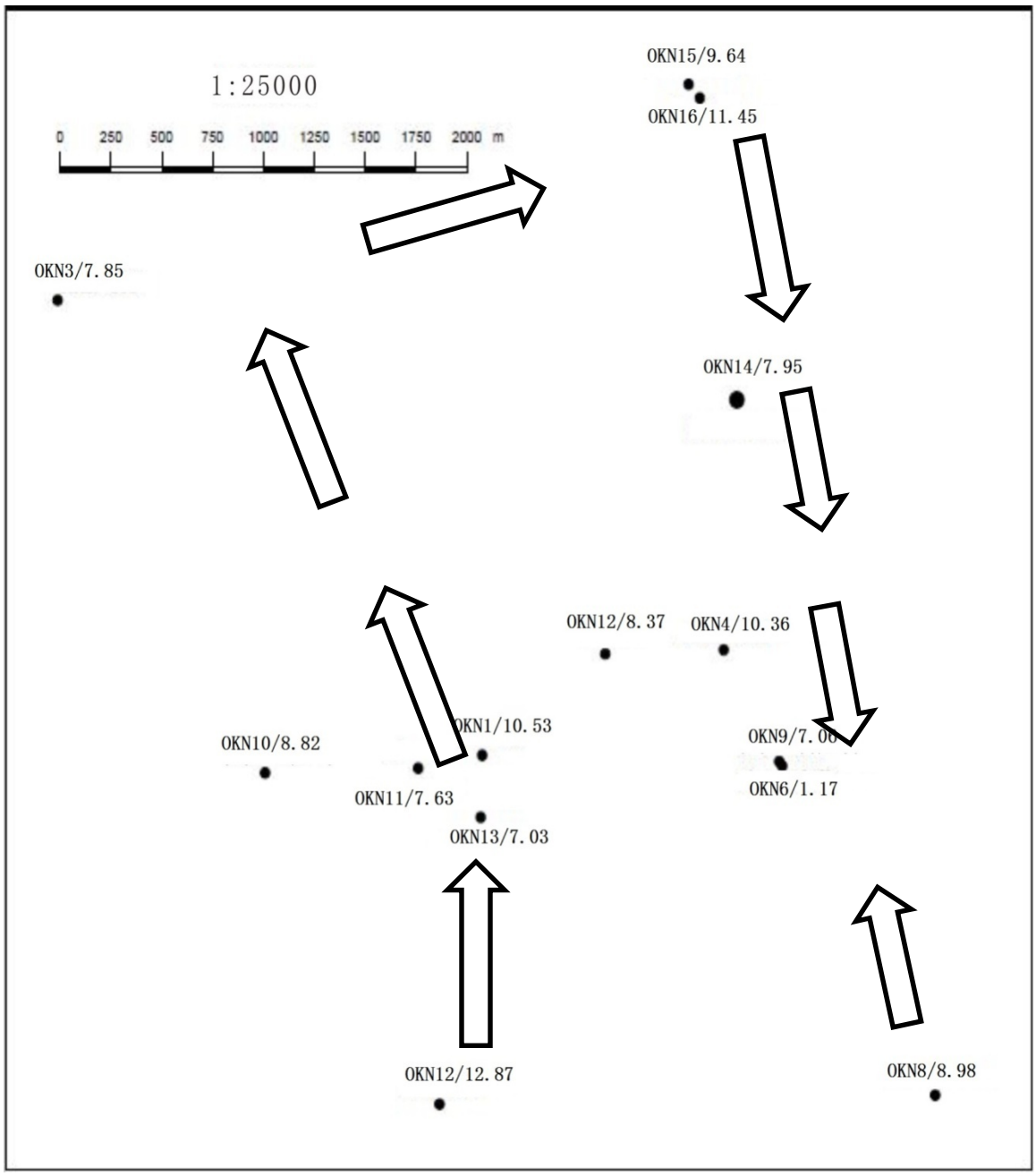

Fig. 4.65: Map showing the total concentration of carbazoles and the direction of oil migration in OKN Field.

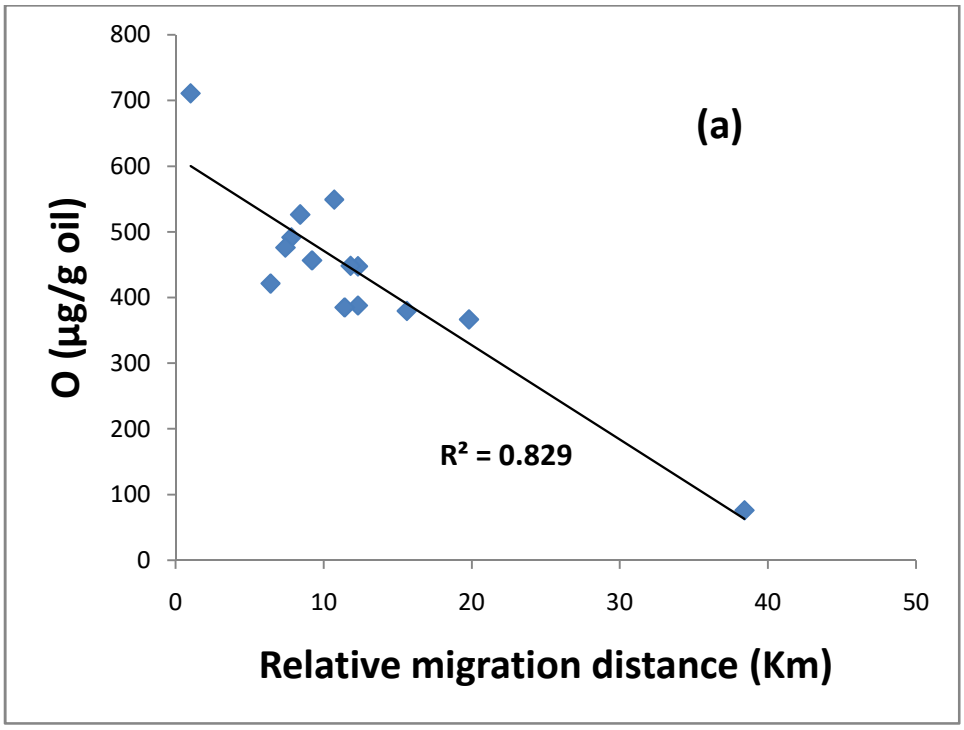

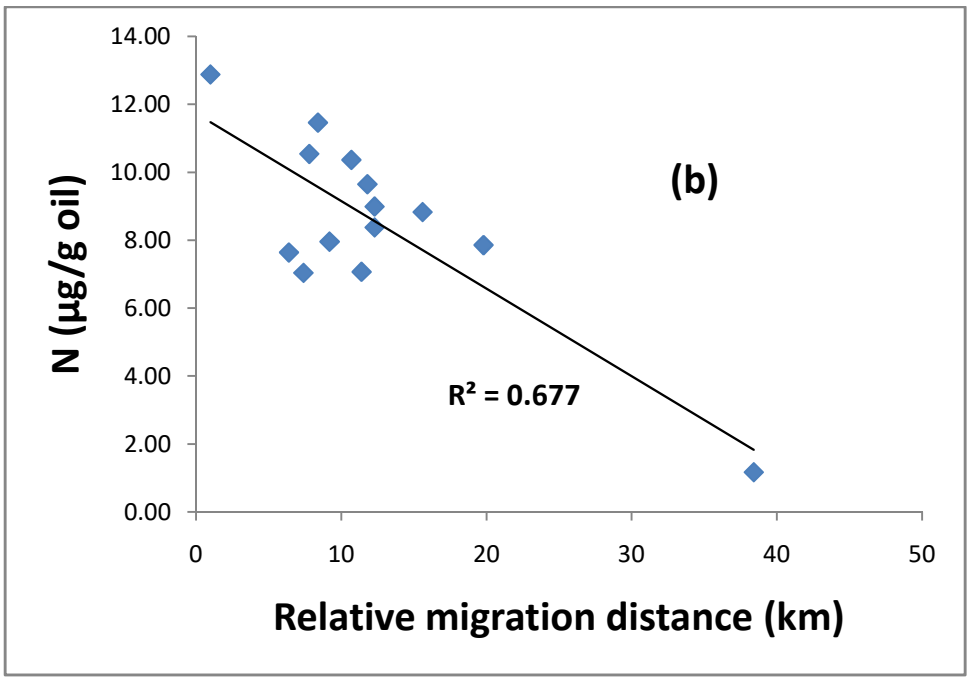

Fig.4.66: Plot of the relative migration distance against (a) absolute dibenzofurans concentration and (b) absolute concentration of carbazoles in OKN Field.

4.10.2 MJI Field

The total concentrations of DBFs (including the parent and all of the methyl-, dimethyl-, and ethyldibenzofuran and benzo[b]naphthofuran isomers) in the oils range from 679.56 to 2380.59µg/g oil, with an average of 1217.99µg/g oil. The total concentrations of DBFs decrease significantly from 2380.59 (MJI-6) to 679.56 µg/g oil (MJI-5) (Table 4.24). This shows that MJI-5 has migrated the longest distance from the source kitchen into its present habitat. The migration distances of other oils in MJI field are intermediate between MJI-5 and MJI-6 oils.

Fig. 4.67 shows the location map of the oil wells in the field. The variations in the total concentration of the DBFs reflect a south - east oil migration direction in the field(Fig. 4.67). Thus, it can be speculated that the oils originated from a source kitchen in the southern part of MJI field and as such, the most prolific region for petroleum exploration. This observation is consistent with the findings obtained from the plot of total concentration of carbazoles on the location map of the oil wells from the same field (Fig. 4.68).

Fig.4.69a show the changes in the total concentrations of the dibenzofurans as a function of relative migration distance for oils in the MJI field. The Fig. shows that the concentrations of the total dibenzofuran compounds decrease with increasing secondary migration distance with linear trend (R^2 = 0.6776). This is further confirmed by the plot of total concentration of carbazoles against relative migration distance (R^2 = 0.5835) (Fig. 4.69b). The maximum migration distance obtained from the present field is less than 100km and this has been associated with rift basin such as Niger Delta basin (Larter *et al*., 1996; Li *et al*., 2014).

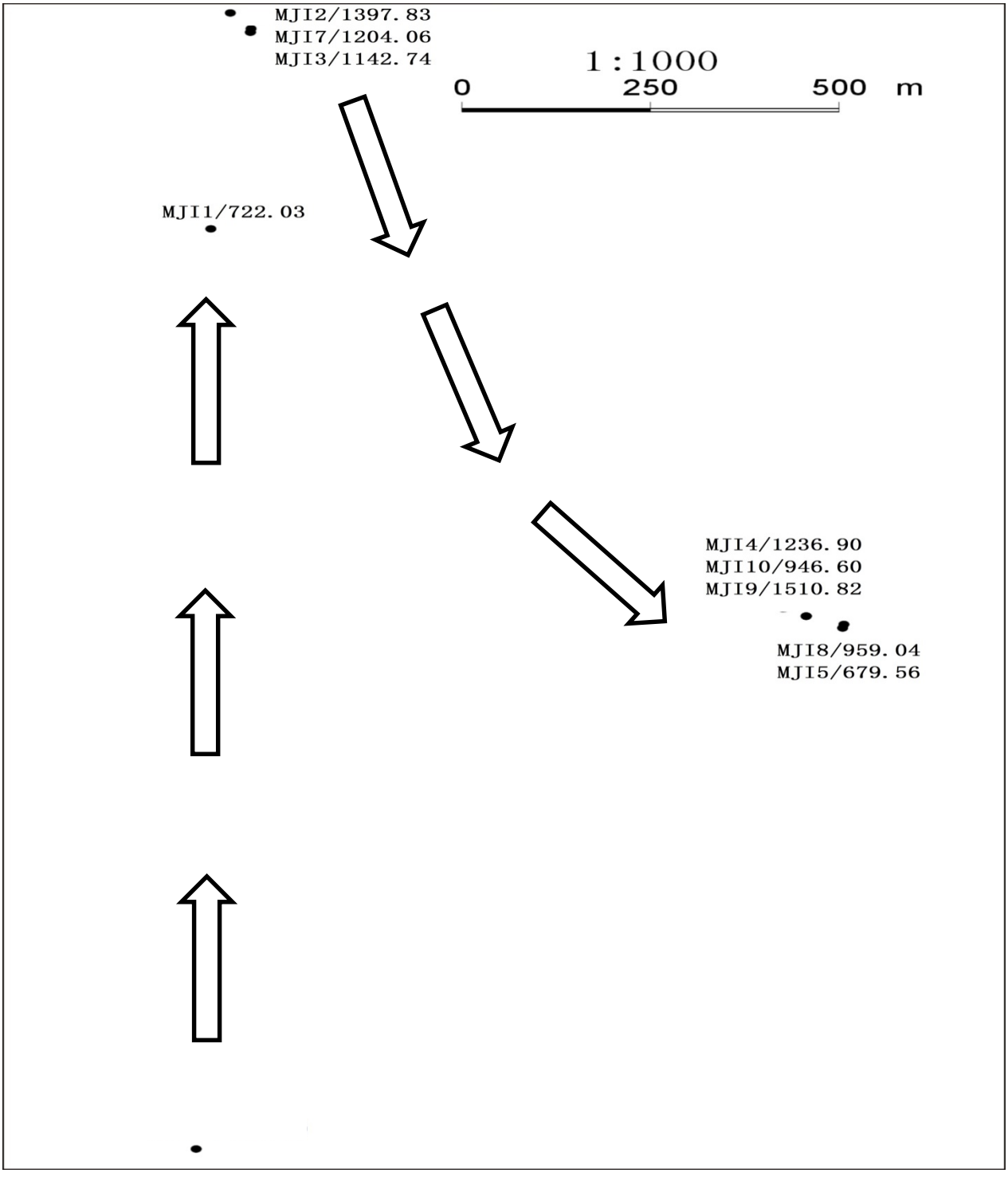

Fig. 4.67: Map showing the total concentration of dibenzofurans and the direction of oil migration MJI Field.

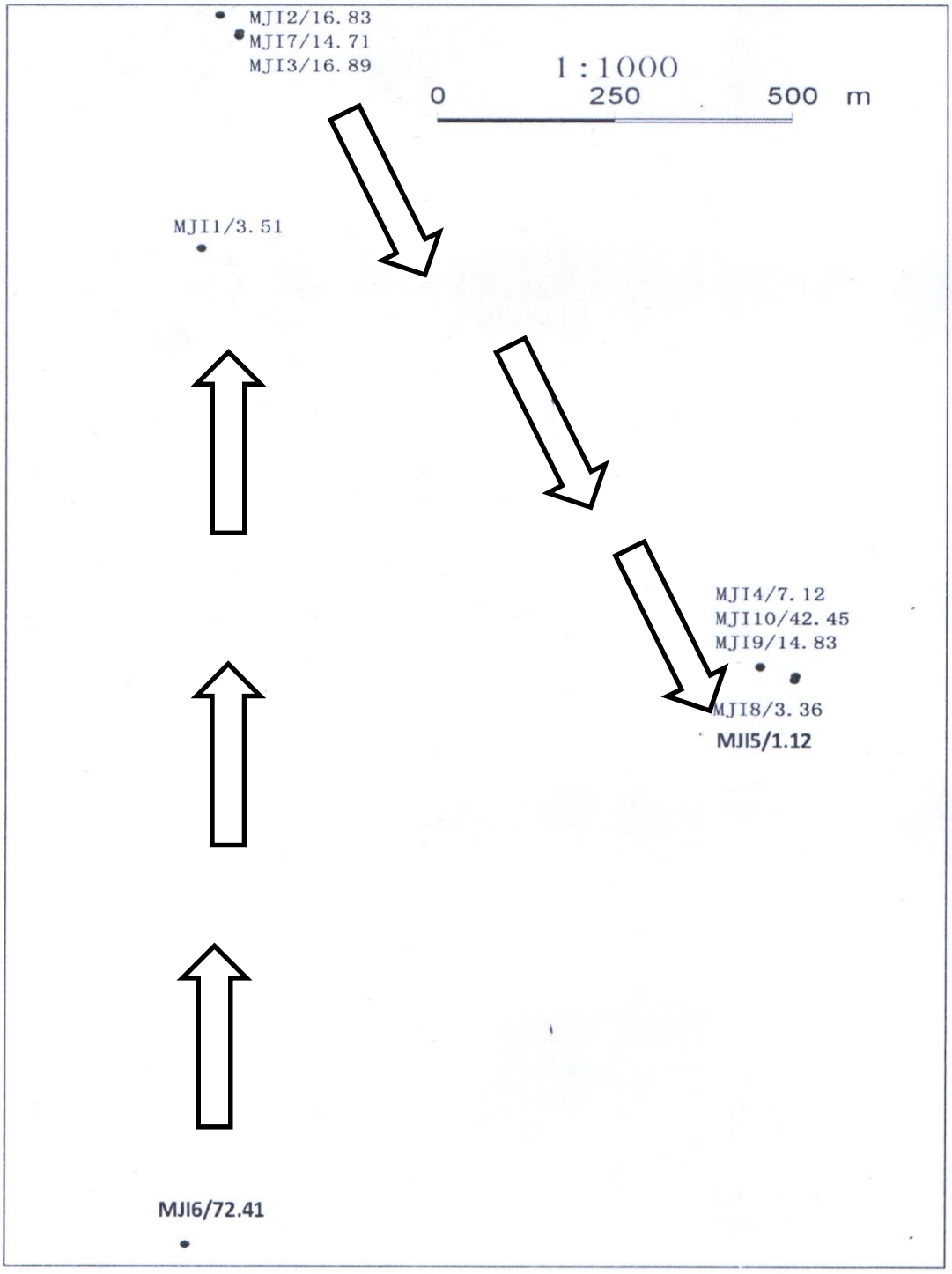

Fig. 4.68: Map showing the total concentration of carbazoles and the direction of oil migration in MJI Field.

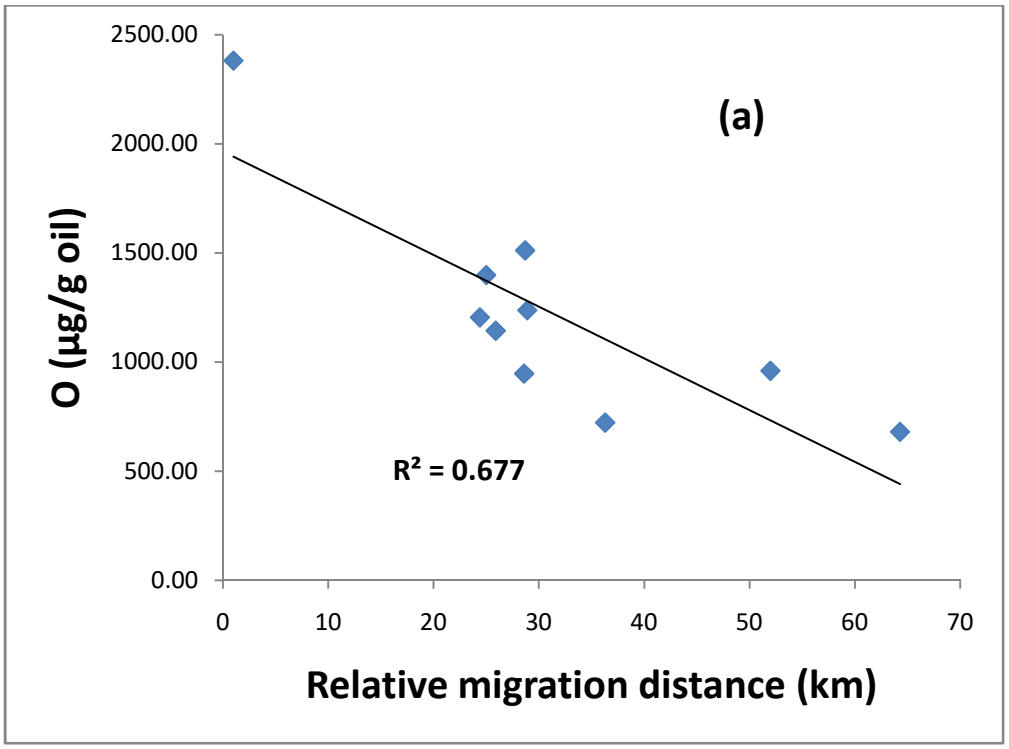

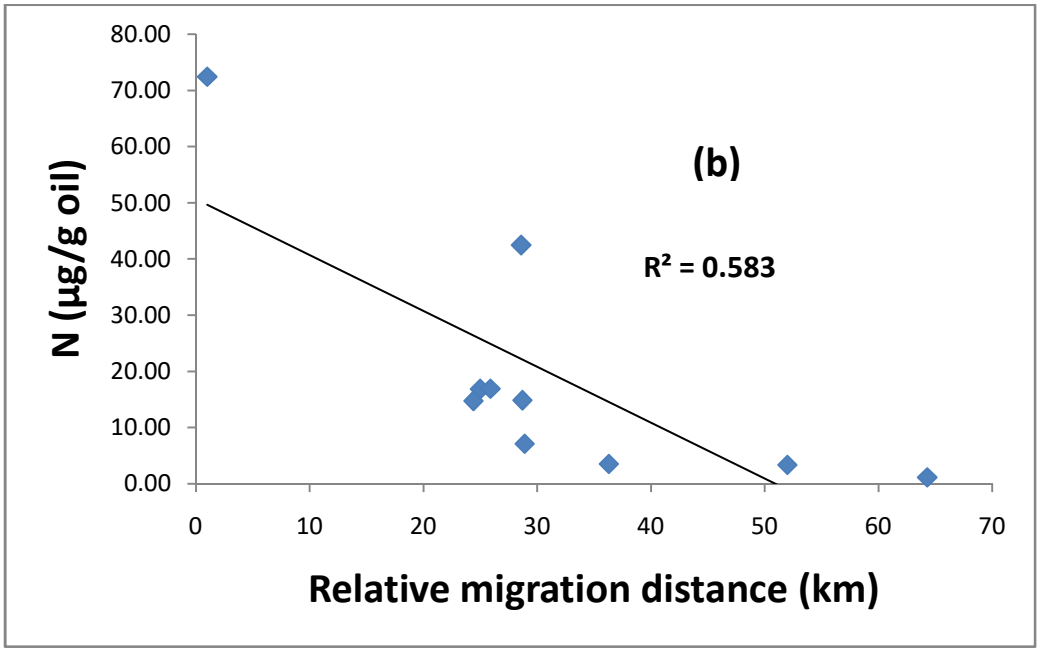

Fig.4.69: Plot of the relative migration distance against (a) absolute dibenzofurans concentrations and (b) absolute concentrations of carbazoles in MJI Field

CHAPTER FIVE

SUMMARY AND CONCLUSIONS

The present study investigated the occurrence and distribution of dibenzofurans and benzo[b]naphthofurans in Niger Delta source rocks and crude oils in relation to source facies, thermal maturity and oil migration for the first time. The hydrocarbon potential of the source rocks and the source and thermal maturity of the crude oils were also evaluated. The samples were analysed using Rock-Eval pyrolysis, gas chromatography-mass spectrometry (GC-MS), gas chromatography-isotope ratio- mass spectrometry (GC-IRMS),elemental analysis-isotope ratio mass spectrometry (EA-IRMS) and optical microscopy.

The TOC and GP values in the rock samples ranged exceed the minimal 0.5 wt% and 2.0 mg/g required for a potential source rock. The Hydrogen Index (HI) and Oxygen Index (OI) values and various plots from the Rock-Eval pyrolysis data showed that ADL, MJI, MJO and WZB source rocks were formed from organic matter of mixed origin (type II, III and IV) which has potential to generate both oil and gas. Most of the samples have major contribution from terrestrial materials (type III) with the exception of OKN samples. The Tmax, Production Index (PI) and Vitrinite Reflectance (Ro %) values in the rocks indicated that the source rocks are at immature to early mature stage.

The plots of OI against HI and maceral composition showed that MJI and MJO rock samples are derived mainly from terrigenous organic matter (type III) while OKN rock samples are mainly marine (type II kerogen). The Pr/Ph values of MJI and MJO rock samples indicated source rocks with significant terrigenous organic matter contribution deposited under oxic conditions while Pr/Ph values of OKN rock samples reflected suboxic conditions. The C_{27}, C_{28} and C_{29} sterane distributions in the source rocks showed source rocks with significant contributions from terrigenous organic matter. The presence of oleanane in the rock samples reflected terrestrial organic matter deposited in fluvial/deltaic environment. The Ts/(Ts+Tm), 22S/22S+22R C_{31} homohopane and 20S/20S+20R C_{29} sterane values for the rock samples showed that the source rocks are within immature to early mature stage.Thedistribution of aromatic hydrocarbons and carbon isotopic compositions in all the samples showed that the rock samples were

formed from organic matter derived from mixed origin (terrestrial and marine materials) deposited in lacustrine-fluvial/deltaic depositional environment.

The Pr/Ph and DBT/P values of the oils showed the oils were derived from lacustrine-fluvio-deltaic source rocks deposited in oxic to sub-oxic depositional environments. The relative abundance of C_{27}, C_{28} and C_{29} steranes in ADL and MJIindicated higher terrigenous organic matter input to the source rock that formed the oils while the relative abundances of C_{27}, C_{28} and C_{29} steranes in OKN, WZB and MJO oils reflected oils derived from source rocks of mixed origin but with significant contributions from marine source. The aromatic hydrocarbons and carbon isotopic compositions of the crude oils further confirmed that the oils were derived from source rocks of mixed organic origin deposited in an oxic to suboxic paleoenvironment. The aliphatic biomarkers maturity parameters showed that the oils were formed from early mature source rocks while the aromatic hydrocarbons maturity parameters indicated oil generated at the peak of oil generative window.

The relative percentages of dibenzofuran, methyldibenzofurans (C_1-dibenzofurans) and dimethyldibenzofurans (C_2-dibenzofurans) in the rock samples were characterized by the predominance of the C_2-dibenzofurans over other dibenzofurans. 2- and 3-methyldibenzofuran predominated over other methyldibenzofurans in the source rocks while ethyldibenzofuran-1 (EDBF-1), dimethyldibenzofuran-2 (DMDBF-2), dimethyldibenzofuran-3 (DMDBF-3) and dimethyldibenzofuran-6 (DMDBF-6) were detected in higher amounts among the C_2-dibenzofurans. Benzo[b]naphthofurans also occurred in the source rocks. The abundance and distributions of the dibenzofurans and benzo[b]naphthofurans in the rocks were found not to be influenced by source facie and thermal maturity.

The absolute concentrations of dibenzofuran, methyldibenzofurans (C_1-dibenzofurans) and dimethyldibenzofurans (C_2-dibenzofurans) in the oil samples were dominated by C_2-dibenzofurans. 4-methyldibenzofuran predominated over other methyldibenzofurans in all the oils. The ethyldibenzofuran-1 (EDBF-1), dimethyldibenzofuran-2 (DMDBF-2), dimethyldibenzofuran-3 (DMDBF-3) and dimethyldibenzofuran-6 (DMDBF-6) were detected in higher amounts when compared with the other dimethyldibenzofurans in the oil samples. Benzo[b]naphthofurans were

detected in appreciable amounts in the oil samples. The distribution of the dibenzofurans were influenced by thermal maturity in oils from ADL, MJO and WZB fields while the oil samples from OKN and MJI fields were not influenced by source facie, maturity and biodegradation. The oil migration direction and distances in OKN and MJI fields were determined based on the abundance of the dibenzofurans. The total concentrations of dibenzofurans decrease from 2380.59 to 76.39 μg/g in the longest migrated oil. This decrease in concentration resulted from migration induced fractionation effect. The migration distances estimated for the oils ranged between 1.0 and 64.0 km.

The results of this study showed that the variations in the abundance and distribution of dibenzofurans in oils from similar source facies and thermal maturities were effective in determining the oil migration direction and distances in the Niger Delta basin.

REFERENCES

Achari, R. G., Shaw, G. and Holleyhead, R. 1973. Identification of ionene and other carotenoid degradation products from the pyrolysis of sporopollenins derived from some pollen exines, a spore coal and the green river shale. *Chemical Geology*12: 229–234.

Adam, P., Schaeffer, P. and Albrecht, P. 2006. C_{40} monoaromatic lycopane derivatives as indicators of contribution of the algal Botryococcus braunii race L to the organic matter of Messel oil shale (Eocene, Germany). *Organic Geochemistry* 37:584-596

Akande, S.O., Ojo, O.J., Erdtmann, B.D. and Hetenyi, M. 2005 .Paleoenvironments, organic petrology and Rock-Eval studies on source rock facies of the Lower Maastrichtian Patti Formation, southern Bida Basin, Nigeria. *Journal of African Earth Sciences* 41:394-406.

Akinlua, A. and Torto, N. 2011. Geochemical evaluation of Niger Delta sedimentary organic rocks: a new insight. *Int. J. Earth Sci. (Geol. Rundsch)* 100:1401-1411.

Albrecht, P. and Ourisson, G. 1971. Biogenic substances in sediments and fossils.Angew.*Chemistry International Edition* 10:209-225.

Alexander, R., Strachan, M.G., Kagi, R.I. and van Bronswijk, W. 1986. Heating rates effects on aromatic maturity indicators. *Organic Geochemistry* 10:97-1003.

Alexander, R., Bastow, T. P., Kagi, R. I. and Singh, R. K. 1992. Identification of 1,2,2,5-Tetramethyltetralin and 1,2,2,3,4-Pentamethyltetralin as Racemates in Petroleum. *Journal of the Chemical Society, Chemical Communications* 1906:1712–1714.

Alpern, B. (Ed.), 1975. Petrographie de la matiere organique des sediments relations avec la paleotemperature et le potentiel petrolier. *Editions du CNRS, P*aris 278 pp.

Alpern, B., Durand, B., Espitalie, J., Tissot, B., 1972. Localization, characterization et classification petrographique, des substances organiques sedimentaires fossils. In: von Gaetner, H.R., Wehner, H.R. (Eds.), *Advances in Organic Geochemistry*, 1971, pergamon press, pp 1-28.

Armstroff, A. 2004.Geochemical Significance of Biomarkers in Paleozoic Coals.*Ph.D. Thesis*, Technischen Universistat Berlin, Berlin, Germany.

Andrusevich V. E., Engel M. H., Zumberge J. E. and Brothers L. A.1998. Secular episodic changes in stable carbon isotopic composition of crude oils. *Chemical Geology* 152:59-72.

Aquino Neto, F. R., Trendel, J. M., Restle, A., Connan, J. and Albrecht, P. A. 1983.Advances in Organic Geochemistry, chapter Occurrence and Formation of Tricyclic and Tetracyclic Terpanes in Sediments and Petroleums.*John Wiley & Sons Limited*, 659–667

Asif, M. 2010. Geochemical Applications of Polycyclic Aromatic Hydrocarbons in Crude Oils and Sediments from Pakistan.*Ph.D. Thesis*, *University of Engineering and Technology*, Lahore, Pakistan.

Asif, M. and Fazeelat, T. 2012. Petroleum geochemistry of the Potwar Basin, Pakistan: II – Oil classification based on heterocyclic and polycyclic aromatic hydrocarbons. *Applied Geochemistry* 27:1655–1665.

Audino, M., Grice, K., Alexander, R. and Kagi, R.I. 2002.Macrocyclic alkanes in crude oils from the algaenan of Botryococcus braunii.*Organic Geochemistry* 33:979-984.

Azevedo, D. A., Aquino Neto, F. R. and Simoneit, B. R. T. 1994. Extended saturate and monoaromatic tricyclic terpenoid carboxylic acids found in Tasmanian tasmanite. *Organic Geochemistry* 22:991-1004

Bakel, A. J. and Philp, R. P. 1990. Advances in Organic Geochemistry 1989, chapter The distribution and quantitation of organonitrogen compounds in crude oils and rock pyrolysates. *Pergamon Press*, London, 353–367.

Barakat, A.O. and Rullkötter, J. 1997. A comparative study of molecular paleosalinity indicators: chromans, tocopherols and C_{20} isoprenoid thiophenes in Miocene lake sediments (Nordlinger Ries, Southern Germany). *Aquatic Geochemistry* 3:169-190.

Bastow, T.P., Alexander, R., Fisher, S.J., Singh, R.K., van Aarssen, B.G.K. and Kagi, R.I. 2000.Geosynthesis of organic compounds. Part V-methylation of alkylnaphthalenes. *Organic Geochemistry* 31:523-534.

Bastow, T.P., Snigh, R.K., van Aarssen, B.G.K. and Alexander, R.I. 2001. 2-Methylretene in sedimentary material: a new higher plant biomarker. *Organic Geochemistry* 32:1211-1217.

Batten, D.J., 1973. Use of palynologic assemblage-types in wealden correlation.*Paleontology* 16:1-40.

Beka, F. T. and Oti, M.N. 1995. The distal offshore Niger delta: frontier prospects of a mature petroleum province, in Oti, M.N., and G. Postma, eds., Geology of deltas: Rotterdam, A. A. Balkema, p. 237-241

Benner, R., Fogel, M.L.Sprague, E.K. and Hodson, R.E. 1987. Depletion of 13C in lignin and its implications for stable carbon isotope studies.*Nature* 329:708-710.

Bordenave, M.L. and Espitalie, J. 1993. Elemental composition of kerogens. In: Bordenave, M.L. (Ed.), *Applied Petroleum Geochemistry*. Editions Technip, Paris. 334-339

Borrego, A.G., Hagemann, H.W., Prado, I. J. G., Guillen, M.D. and Blanco, C. G. 1996.Compar-ative petrographic and geochemical study of the Puertollano oil shale kerogens.*Organic Geochemistry* 24 (3):309–321.

Borrego, A.G., Blanco, C.G. and Püttmann, W. 1997. Geochemical significance of aromatic hydrocarbon distribution in the bitumens of the Puertollano oil shales, Spain. *Organic Geochemistry* 26.3/4:219-228.

Bostick, N. H. 1973. Time as a factor in thermal metamorphism of phytoclasts (coaly particles).*C. R. 7 Congres International de Stratigraphie et de Geologie du Carbonifere, Krefeld* 2:183–193.

Boulter, M.C., 1994. An approach to a standard terminology for palinodebris. In: Traverse, A. (Ed.), sedimentation of organic particles. Cambridge University Press, 119-216.

Boulter, M.C, Riddick, A., 1986. Classification and analysis of palinodebris from the palaeocene sediments of the Forties Field.*Sedimentology* 33:871-886.

Brassell, S.C., Eglinton, G., Marlowe, I.T., Pflaumann, U. and Sarnthein, M. 1986. Molecular stratigraphy: a new tool for climatic assessment. *Nature* 320:129-133.

Brondz, H. M., Simoneit, B.R.T. and Brassell, S. C. 2012.Molecular Indicators of Past Life. *The Anatomical Record*268:186-195

Budzinski, H., Garrigues, P.H., Connan, J., Devillers, J., Domine, D., Radke, M. and Oudin, J.L. 1995. Alkylated phenanthrene distributions as maturity and origin indicators in crude oils and rock extracts. *Geochimica et Cosmochimica Acta* 59.10:2043-2056.

Bugress, J.D., 1974. Microscopic examination of kerogen (dispersed organic matter) in petroleum exploration. In: Dutcher, R.R., Hacquebard, P.A., Schopf, J.M., Simon, J.A. (Eds.), Carbonaceous Materials as Indicators of Metamorphism: GSA Special Paper, 153, pp. 19-30.

Bujak, J.P., Barss, M.S., Williams, G.L., 1977. Organic type and color hydrocarbon potential. *Oil & Gas Journal* 75:96-100.

Bustin, R. M., Cameron, A. R., Grieve, D A. and Kalkreuth, W., 1983. Coal Petrology: Its Principles, Methods and Applications, Short Course Notes 3. *Geological Association Canada,* 230 pp.

Bustin, R. M. 1988. Sedimentology and characteristics of dispersed organic matter in Tertiary Niger Delta: Origin of source rocks in a deltaic environment. *American Association of Petroleum Geologists Bulletin* 72: 277-298.

Cai, C.F., Li, K.K., Ma, A.L., Zhang, C.M., Xu, Z.M., Worden, R.H., Wu, G.H., Zhang, B.S., Chen, L.X., 2009a. Distinguishing Cambrian from Upper Ordovician source rocks: evidence from sulfur isotopes and biomarkers in the Tarim Basin. *Organic Geochemistry* 40: 755–768.

Cai, C.F., Zhang, C.M., Cai, L.L., Wu, G.H., Jiang, L., Xu, Z.M., Li, K.K., Ma, A.L., Chen, L.X., 2009b. Origins of Palaeozoic oils in the Tarim Basin: evidence from sulfur isotopes and biomarkers. *Chemical Geology* 268:197–210.

Cai, C.F., Zhang, C.M., Worden, R.H., Wang, T.K., Li, H.G., Jiang, L., Huang, S., Zhang, B., 2015. Application of sulfur and carbon isotopes to oil–source rock correlation: A case study from the Tazhong area, Tarim Basin, China. *Organic Geochemistry* 83-84, 140-152.

Chakhmakhchev, A., Suzuki, M. and Takayama, K. 1997. Distribution of alkylated dibenzothiophenes in petroleum as tool for maturity assessments. *Organic Geochemistry*26:483-490.

Chen, Z., Yang, Y., Wang, T.G., Chen, B., Li, M., Luo, B., Chen, Y., Ni, Z., Yang, Z., Chen, T., Fang, R. and Wang, M. 2017. Dibenzothiophenes in solid bitumens: Use ofmolecular markers to trace paleo-oil filling orientations in the Lower Cambrian reservoir of the Moxi–Gaoshiti Bulge, Sichuan Basin, southern China. *Organic Geochemistry* doi: http://dx.doi.org/10.1016/j.orggeochem.2017.03.013.

Chung H. M., Rooney M. A., Toon M. B. and Claypool G. E. 1992. Carbon isotope composition of marine crude oils. *American Association of Petroleum Geologists Bulletin* 76:1000-1007.

Clayton C., 1991. Effect of maturity on carbon isotope ratios of oils and condensates. *Organic Geochemistry* 17:887–899.

Clarke, F. W. 1916. Data of geochemistry, third edition.*US Geological Survey Bulletin*, 616.

Clegg, H., Wilkes, H., Oldenburg, T., Santamaria-Orozco, D. and Horsfield, B. 1998b. Influence of maturity on carbazole and benzocarbazole distributions in crude oils and source rocks from the Sonda de Campeche, Gulf of Mexico. *Organic Geochemistry* 29:183–194

Combaz, A. 1980.Les kerogenes vus au microscope. In: Durand, B. (Ed.), *kerogen. Insoluble organic matter from sedimentary rocks.*Edtions Technip, Paris, pp. 55-113.

Cook, A.C., Sherwood, N.R., 1991. Classification of oil shales, coals and other organic rich rocks.*Organic Geochemistry* 17, 211-222

Correia, M. 1971. Diagenesis of sporopollenin and other comparable organic substances: application to hydrocarbon research. In: Brooks, J., Grant, P.R, Muir, M., van Gijzel, P., Shaw, G., (Eds.), *Sporopollenin. Academic Press*, New York, pp. 569-620.

Craig, H., 1953. The geochemistry of the stable carbon isotopes.*Geochimica et Cosmochimica Acta* 3:53–92.

Didyk, B.M., Simoneit, B.R.T., Brassel, S.C. and Eglinton, G. 1978.Organic geochemical indicators of paleoenvironmental conditions of sedimentation.*Nature* 272:216-222.

Dorbon, M., Schmitter, J. M., Garrigues, P., Ignatiadis, I., Evald, M., Arpino, P. and Guiochon, G., 1984. Distribution of carbazole derivatives in petroleum.*Organic Geochemistry* 7:111–120

Doust, H. and Omatsola, E. 1990.Niger Delta divergent/passive margin basins. *AAPG Bull. Mem.* 45:201–238

Durand, B. 1993.Composition and structure of organic matter in immature sediments. In: Bordenave, M.L. (Ed.), *Applied Petroleum Geochemistry*, Paris, pp. 77–100.

Durand, B., Nicaise, G., Roucaché, J., Vandenbroucke, M. and Hagemann, H.W. 1977.Etude géochimique d'une série de charbons. In: Campos, R., Goñi, J. (Eds.), *Advances in Organic Geochemistry* 1975. ENADIMSA, Madrid, pp. 601–631

Dzou, L. I. P., Noble, R. A. and Senflte, J. T. 1995. Maturation effects on absolute biomarker concentrations in a suite of coals and associated vitrinite concentrates. *Organic Geochemistry* 23:681–697.

Ejedawe, J.E., Coker, S.J.L., Lambert-Aikhionbare, D.O., Alofe, K.B. and Adoh, F.O. 1984.Evolution of oil-generative window and oil and gas occurrence in Tertiary Niger Delta Basin.*AAPG* 68:1744-1751.

Ekweozor, C.M., Okogun, J.I., Ekong, D.E.U. and Maxwell, J.R. 1979. Preliminary organic geochemical studies of samples from the Niger Delta, (Nigeria): II. Analysis of shale for triterpenoid derivatives.*Chemical Geology* 27:29–37.

Ekweozor, C.M. and Okoye, N.V. 1980. Petroleum source-bed evaluation of the Tertiary Niger Delta.*American Association of Petroleum Geologists Bulletin* 64:1251–1259

Ekweozor, C.M. and Daukoru, C.M. 1984. Petroleum Source bed evaluation of Tertiary Niger Delta—reply. *AAPG Bulletin* 68:390-394.

Ekweozor, C.M. and Udo, O.T., 1988. The oleananes: origin, maturation and limits of occurrence in southern Nigeria sedimentary basins. In: Mattavelli, L., Novelli, L. (Eds.), *Advances in Organic Geochemistry* 1987. Pergamon Press, Oxford, pp. 131–140.

Ekweozor, C.M. and Daukoru, C.M. 1994. Northern delta depobelt portion of the Akata-Agbada petroleum system, Niger Delta, Nigeria, in The petroleum system from source to trap. *AAPG Memoir* 60:599-613

England, W.A., Mann, A.L., Mann, D.M., 1991. Migration from source to trap. In: Merrill, R.K. (Ed.), Source and Migration Processes and Evaluation Techniques. *American Association of Petroleum Geologists Handbook of Petroleum Geology*:23–46.

Espitalié, J., Lar Porte, J.L.Madec, M., Marquis, F., Le Plat, P., Paulet, J. and Boutfen, A. 1977b. Method rapide de caracterisation des roches meres de leur potential petrolier et de leur degree d'evolution. *Revue l'Inst. Francais du Petrole* 32.1:23-42.

Evamy, B. D., Haremboure, J., Kamerling, P., Knaap, W. A., Molloy, F. A., and Rowlands, P. H. 1978. Hydrocarbon habitat of Tertiary Niger Delta.*American Association of Petroleum Geologists Bulletin* 62:277–298

Faboya, O. L., Sonibare, O. O., Liao, Z., Ekundayo, O., and Tian, Y. 2014. Occurrence and distribution of carbazoles and benzocarbazoles in Tertiary Niger Delta source rocks. *Petroleum Science and Technology* 32:2938–2952

Faboya, O. L., Sonibare, O. O., Liao, Z., Ekundayo, O., and Tian, Y. 2015. Oil-source Rock Correlation and Distributions of Pyrrolic Nitrogen Compounds in Oils from the Niger Delta, Nigeria.*Petroleum Science and Technology* 33:1253–1266.

Fan, P.; Philp, R. P., Li, Z.; Yu, X. and Ying G. 1991.Biomarker distributions in crude oils and source rocks from different sedimentary environments.*Chemical Geology* 93:61–78.

Fan, P., Philp, R.P., Zhenxi, L., Guangguo, Y., 1990. Geochemical characteristics of aromatic hydrocarbons of crude oils and source rocks from different sedimentary environments. *Organic Geochemistry* 16:427–435.

Fang, R., Li, M., Wang, T.G., Zhang, L., Shi, S., 2015. Identification and distribution of pyrene, methylpyrenes and their isomers in rock extracts and crude oils.*Organic Geochemistry* 83-84: 65-76.

Fang, R., Wang, T.G., Li, M., Xiao, Z., Zhang, B., Huang, S., Shi, S., Wang, D., Deng, W., 2016. Dibenzothiophenes and benzo[b]naphthothiophenes: Molecular markers for tracing oil filling pathways in the carbonate reservoir of the Tarim Basin, NW China.*Organic Geochemistry* 91:68-80.

Fenton, S.; Grice, K.; Twitchett, R.J.; Böttcher, M.; Looy, C.V. andNabbefield, B. 2007.Changes in Biomarker Abundances and their Stable Carbon Isotopes across

the Permian-Triassic (P-Tr) Schuchert Dal Section (East Greenland).*Earth and Planetary Science Letter* 262:230-239

Ficken, K.J., Li, B., Swain, D.L. and Eglinton, G. 2000. An n-alkane proxy for the sedimentary input of submerged/floating fresh water aquatic macrophytes. *Organic Geochemistry* 31.7-8:745-749.

Fischer, F. and Tropsch, H. 1926. Uber die direkte synthese von erdol-kohlenwasserstoffen bei gewohnlichem druck. *Berichte der Deutschen Chemischen Gesellschaft* 59:830–1.

Fischer, M.J., Barnard, P.C. and Cooper, B.S. 1981. Organic maturation and hydrocarbon generation in the Mesozoic sediments of the Sverdrup Basin, Arctic Canada.*Proceedings IV International Palynological Conference*, Lucknow (197-77), 2, pp. 581–588.

Forsman, J. P. and Hunt, J. M. 1958 Insoluble organic matter (kerogen) in sedimentary rocks of marine origin. In: Habitat of Oil: A Symposium (L. G. Weeks, ed.) *American Association of Petroleum Geologists*, Tulsa, OK, pp. 747–78.

Galimberti, R., Gheselli, C., and Chiaramonte, M. A., 2000. Acidic polar compounds in petroleum: a new analytical methodology and applications as molecular migration indices. *Organic Geochemistry* 31:1375-1386.

Garrigues, P., De Sury, R., Angelin, M.L., Bellocq, J., Oudin, J.L., Ewald, M., 1988. Relation of the methylated aromatic hydrocarbon distribution pattern to the maturity of organic matter in ancient sediments from the Mahakam delta. *Geochimica et Cosmochimica Acta* 52:375–384.

Garrigues, P.S., Marniesse, M.P., Ewald, M., 1987. Origin of polycyclic aromatic hydrocarbons (PAH) in Recent sediments from the continental shelf of the 'Golfe de Gascogne' (Atlantic Ocean) and in the Gironde Estuary. *International Journal of Environmental Analytical Chemistry* 28:121–131.

Grice, K., Audino, M., Alexander, R., Boreham, C.J.and Kagi, R.I. 2001.Distribution and stable carbon isotopic compositions of biomakers in torbanites from different palaeogeographical locations.*Organic Geochemistry* 32:1195-1210X.

Grice, K., Nabbefeld, B. and Maslen, E. 2007. Source and significance of selected polycyclic aromatic hydrocarbons in sediments (Hovea-3 well, Perth Basin,

Western Australia) spanning the Permian–Triassic boundary. *Organic Geochemistry* 38:1795–1803

Grice, K., Lu, H., Atahan, P., Asif, M., Hallmann, C., Greenwood, P., Maslen, E., Tulipani, S., Williford, K. and Dodson, J. 2009. New insights into the origin of perylene in geological samples. *Geochimica et Cosmochimica Acta* 73: 6531–6543

Gutjahr, C.C.M., 1983. Introduction to incident-light microscopy of oil and gas source rocks. In: van der Berg, M.W, Felix, R. (Eds.), Special Issue in the Honour of J.D., de Jong: *Geological Magazine* 62:417-425.

Habib, D. 1979. Sedimentary origin of North Atlantic Cretaceous palynofacies. Deep Drilling Results in the Atlantic Ocean: Continental Margin and Paleoenvironment: Am. Geophys. Union, pp. 420-437.

Habib, D. 1983. Sedimentation-rate-dependent distribution of organic matter in the North Atlantic Jurassic-Cretaceous. In: Sheridan, R.E, Gradstein, F.M. (Eds.), Initial Reports Deep Seas Drilling Project 76, U.S. Govt. Printing Office, Washington, D.C., pp. 781-794.

Hakimi, M.H., Abdullah, W.H. and Shalaby, M.R. 2011.Organic geochemical characteristics of crude oils from Masila Basin, Eastern Yemen.*Organic Geochemistry* 42:465-476.

Hart, G.F., 1986. Origin and Classification of organic matter in clastic systems.*Palynology* 10:1-23.

Hayes, T.M., Freeman, K.H., Popp, B. and Hoham, C.H. 1990. Compound specific isotope analyses: a novel tool for reconstruction of biogeochemical proceses. *Organic Geochemistry* 16:1115-1128.

Hayes, J.M. 1993. Factors controlling ^{13}C contents of sedimentary organic compounds: Principles and evidence. *Marine Geology* 113:111-125.

Helm, R. V., Latham, D. R., Ferrin, C. R. and Ball, J., 1960.Identification of Car-bazole in Wilmington Petroleum through Use of Gas-Liquid Chromatography and Spectroscopy.*Analytical Chemistry* 32:1765–1767.

Horsfield, B., 1984. Pyrolysis studies and petroleum exploration. In: Brooks, J., Welte, D., (Eds.), Advances in Petroleum Geochemistry, Vol. 1, *Academic Press*, London, pp. 247-298

Horsfield, B., Clegg, H., Wilkes, H. 1998. Effect of maturity on carbazole distribution in petroleum systems: new insights from the Sonda de Campeche, Mexico, and Hils Syncline, Germany. *Naturwissenschaften* 85:233–23

Huang, H., Zhang, S. and Su, J. 2015. Geochemistry of Tri- and Tetracyclic Terpanes in the Palaeozoic Oils from the Tarim Basin, Northwest China. *Energy & Fuels* 29:7014−7025

Huang, W.Y. and Meinschein, W. G., 1979.Sterols as ecological indicators.

Geochimica et CosmochimicaActa 43:739–745.

Hughes, W.B., Holba, A.G. and Dzhou, L.I.P. 1995. The ratios of dibenzothiophene to phenanthrene and pristane to phytane as indicatorsof depositional environment and lithology of petroleum source rocks. *Geochimica et Cosmochimica Acta* 59:3581-3598.

Hunt, J.M. 1996. Petroleum Geochemistry and Geology.Second Edition. New York: W.H. Freeman and Company.

Hwang, R. J., Heidrick, T., Mertanib, B., Qivayantib and Lic, M. 2002.Correlation and migration studies of Northern Central Sumatra oils.*Organic Geochemistry* 33:1361-1379

Ioppolo, M., Alexander, R. and Kagi, R. I. 1992.Identification and analysis of C0-C3 phenols in some Australian crude oils.*Organic Geochemistry* 18:603–609.

Jaffe, R. and Gallardo, M. T. 1993.Application of carboxylic acid biomarkers as indicators of biodegradation and migration of crude oils from the Maracaibo Basin, Western Venezuela.*Organic Geochemistry* 20:973-984.

Jaffe, R. and Gardinali, P. R. 1990. Generation and maturation of carboxylic acids in ancient sediments from the Maracaibo Basin, Venezuela. *Organic Geochemistry* 16:211-218.

Jinggui, L., Philp, P., Zifang, M., Wenhui, L., Jianjing, Z., Guojun, C., Mei, L. and Zhaoyun, W. 2005. Aromatic compounds in crude oils and source rocks and their

application to oil-source rock correlations in the Tarim Basin, NW China. *Journal of Asian Earth Science* 25:251–268.

Jinggui, L., Mei, L. and Zhaoyun, W. 2004. DibenzofuraN series in terrestrial source rocks and crude oils and applications to oil-source rock correlations in the Kuche Depression of Tarim Basin, NWChina. *Chinese Journal ofGeochemistry* 23:113-123

Johns, R.B. 1986. Biological markers in sedimentary record. Amsterdam: Elsevier Science Publisher.

Kalkreuth,W.D. and Macauley, G. 1989. Sedimentological and petrographical characteristics of Cretaceous strandplain coals: a model for coal accumulation from the North Ameri-can Western Interior Seaway. *International Journal of Coal Geology* 12:381–424.

Kalkreuth, W. and Macauley, G. 1987. Organic petrology and geochemical (Rock-Eval) studies in oil shales and coals from the Pictou and Antigonish areas, Nova Scotia, Canada. *Bulletin of Canadian Petroleum Geology* 35.3:263–295.

Kalkreuth, W. and Macauley, G. 1984. The organic petrology of selected oil shale samples from the Lower Carboniferous Albert Formation, New Brunswick, Canada. *Bulletin of Canadian Petroleum Geology* 32.1:38–51.

Kenney, J. F., Kutcherov, V. A., Bendeliani, N. A. and Alekseev, V. A. 2002. The evolution of multicomponent systems at high pressures. VI. The thermodynamic stability of the hydrogen–carbon system: the genesis of hydrocarbons and the origin of petroleum. *Proceedings of the National Academy of Science*, USA, 99:10976–81.

Killops, S.D. and Killops, V.J. 1993.An introduction to organic geochemistry. UK: Longman Group Ltd.

Killops, S.D. and Killops, V.J. 2005.Introduction to organic geochemistry.Second edition. U.K: Blackwell Publishing Limited.

Koopmans, M.P., Larter, S.R., Zhang, C., Mei, B., Wu, T. and Chen, Y. 2002.Biodegradation and mixing of crude oils in Eocene Es3 reservoirs of the Liaohe basin, northeastern China.*American Association of Petroleum Geologists Bulletin* 86:1833-1843.

Kruge, M.A., 2000. Determination of thermal maturity and organic matter type by principal components analysis of the distributions of polycyclic aromatic compounds. *International Journal of Coal Geology* 43, 27–51.

Lafargue, E., Espitalie, J., Marquis, F. and Pillot, D. 1998. Rock-Eval 6 applications in hydrocarbon exploration, production and in soil contamination studies. *In Revue de l'Institut Francais du Petrole* 53.4:421-437.

Lambert-Aikhionbare, D.O. and Ibe, A.C. 1984. Petroleum source-bed evaluation of the Tertiary Niger Delta: Discussion. *American Association of Petroleum Geologists Bulletin* 61:961–981.

Langford, F.F. and Blanc-Valleron, M.M. 1990. Interpreting Rock Eval pyrolysis data using graphs of pyrolyzable hydrocarbons versus total organic carbon. *American Association of Petroleum Geologists Bulletin* 74:799-804.

Larter, S.R., 1985. Integrated kerogen typing in the recognition and quantitative assessment of petroleum source rocks. In: Thomas, B.M., Dore, A.G., Eggen, S.S., Home, P.C., Larsen, R.M., (Eds.), Petroleum Geochemistry in Exploration of the Norwegian Shell. Graham & Trotman, pp. 269-286

Larter, S.R., Bowler, B.F.J., Li, M., Chen, M., Brincat, D., Bennett, B., Noke, K., Donohoe, P., Simmons, D., Kohnen, M., Allan, J., Telnaes, N., Horstad, I., 1996.Molecular indicators of secondary oil migration distances.*Nature* 383:593–597.

Larter, S.R. and Douglas, A.G. 1982. Pyrolysis methods in organic geochemistry: An overview. *Journal of Analytical and Applied Pyrolysis* 4:1-19.

Lesquereux, L. 1866. Report on the fossil plants of Illinois. *Illinois Geological Survey* 2:425–70.

Lewan, M.D., Bjoroy, M. and Dolcater, D.L., 1986.Effects of thermal maturation on steroid hydrocarbons as determined by hydrous pyrolysis of Phosphoria Retort shale.*Geochimica et Cosmochimica Acta* 50:1977-1988.

Li, M., Yao, H., Stasiuk, L. D., Fowler, M. G., Larter, S. R. 1997. Effect of maturity and petroleum expulsion on pyrrolic nitrogen compound yields and distributions in Duvernay Formation petroleum source rocks in central Alberta, Canada.*Organic Geochemistry* 26:731–744

Li, M., Larter, S.R., Stoddart, D., Bjoroy, M., 1995. Fractionation of pyrrolic nitrogen compounds in petroleum during migration: derivation of migration-related geochemical parameters. In: The Geochemistry of Reservoirs (Ed. By J. M. Cubitt, W. A. England), p. 103-123. *Geological Society*, London.

Li, M., Larter, S. R., Frolov, Y. B., Bjoroy, M. 1994.Adsorptive Interaction be-tween Nitrogen Compounds and Organic and/or Mineral Phases in Subsurface Rocks.*Journal of High Resolution Chromatography* 19:230–236.

Li, M., Liu, X., Wang, T.G., Jiang, W., Fang, R., Yang, L. and Tang, Y., 2018. Fractionation of dibenzofurans during subsurface petroleum migration: Based on molecular dynamics simulation and reservoir geochemistry. *Organic Geochemistry* 115: 220–232.

Li, M. and Ellis, G.S., 2015. Qualitative and Quantitative Analysis of Dibenzofuran, Alkyldibenzofurans, and Benzo[b]naphthofurans in Crude Oils and Source Rock Extracts. *Energy and Fuels* 29:1421−1430.

Li, M., Wang, T.G., Shi, S., Liu, K., Ellis, G.S., 2014. Benzo[b]naphthothiophenes and alkyl dibenzothiophenes: molecular tracers for oil migration distances. *Marine and Petroleum Geology* 57:403–417.

Li, M**.;** Wang, T.; Zhong, N.; Zhang, W.; Sadik, A. And Li, H. 2013. Ternary diagram of fluorenes, dibenzothiophenes and dibenzofurans: Indicating depositional environment of crude oil source rocks. *Energy, Exploration & Exploitation* 31:569-588

Li, M., Shi, S. and Wang, T.G. 2012. Identification and distribution of chrysene, methylchrysenes and their isomers in crude oils and rock extracts. *Organic Geochemistry* 52:55–66.

Li, M.; Wang, T.; Yang, F.; Shi, Y.J., 2011. Molecular tracer markers for filling pathway in condensate reservoirs: Alkyldibenzofurans. *Oil and Gas Technology* 33:6−11 (in Chinese with English abstract).

Li, M., Wang, T., Liu, J., Zhang, M., Lu, H., Ma, Q., Gao, L., 2008. Total alkyl dibenzothiophenes content tracing the filling pathway of condensate reservoir in the Fushan Depression, South China Sea. Science in China Series D: *Earth Sciences* 51:138–145

Ling, M. and Zhihuan, Z. 2009. Aromatic geochemical characteristics of crude oil of beach area in Nanpu Sag. *Journal of Oiland Gas Technology*31:11-15(in Chinese with English abstract).

Ioppolo, M., Alexander, R. and Kagi, R. I., 1992.Identification and analysis of C_0-C_3phenols in some Australian crude oils.*Organic Geochemistry* 18:603–609.

Lu, H., Peng, P. and Sun, Y. 2003. Molecular and stable carbon isotopic composition of monomethylalkanes from one oil sand sample: source implications. *Organic Geochemistry* 34:745-754.

Mackenzie, A.S. 1984. Application of biomarkers in petroleum geochemistry. In: Brooks, J., Welte, D.H. (Eds.), Advancesin Petroleum Geochemistry, vol. 1. London: Academic Press.115–214.

Marynowski, L., Czechowski, F. and Simoneit, D. R. T., 2000. Phenylnaphthalenes and polyphenyls in Paleozoic source rocks of the Holy Cross Mountains, Poland. *Organic Geochemistry* 32:69–85.

Masran, T.C., Pocock, S.A.J., 1981. The classification of plant-derived particulate organic matter in sedimentary rocks. In: Brook, J. (Ed.), Organic Maturation Studies and Fossil Fuel Exploration. *Academic Press*, London, pp. 145-175.

Mathews, D.E. and Hayes, J.M. 1978. Isotope-ratio-monitoring gas chromatography mass spectrometry.*Analytical Chemistry* 50:1465-1473.

McCollom, T. M. and Seewald, J. S. 2001. A reassessment of the potential for reduction of dissolved CO_2 to hydrocarbons during serpentinization of olivine. *Geochimica et Cosmochimica Acta* 65: 3769–78.

McCollom, T. M. and Seewald, J. S. 2003. Experimental constrainsts on the hydrothermal reactivity of organic acids and acid anions: I. Formic acid and formate. *Geochimica et Cosmochimica Acta* 67:3625-3644

Mello, M.R. and Maxwell, J.R. 1990. Organic geochemical and biological marker characterization of source rocks and oils from lacustrine environments in the Brazillian continental margin. In: Katz, B.J. (Ed.), Lacustrine Basin Exploration. *American Association of Petroleum Geologists Bulletin* 50:77-97

Mello, M.R., Gallianone, P.C., Brassel, S.C. and Maxwell, J.R. 1988.Geochemical and biological marker asesment of depositional environments using Brazillian offshore oils.*Marine and Petroleum Geology* 3:205-223.

Mendeleev, D. 1877. L'origine du petrole. *Revue Scientifique*, 2e Ser., VIII:409–16.

Moldowan, J.M., Seifert, W.K. and Gallegos, E.J. 1985. Relationship between petroleum composition and depositional environmentof petroleum source rocks. American *Association of Petroleum Geologists Bulletin* 69:1255-1268.

Moldowan, J.M., Dahl, J., Huizinga, B.J., Fago, F.J., Hickey, L.J., Peakman, T.M. and Taylor, D.W. 1994.The molecular fossil record of oleanane and its relation to angiosperms. *Science* 265:768-771.

Mukhopadhyay, P.K., Wade, J.A. and Kruge, M.A. 1995. Organic facies and maturation of Jurassic/Cretaceous rocks, and possible oil-source correlation based on pyrolysis of asphaltenes, Scotian Basin, Canada. *Organic Geochemistry* 22:85-104.

Murray, A.P., Summons, R.E., Boreham, C.J. and Dowling, L.M. 1994. Biomarker and normal alkane isotope profiles of Tertiary oils: Relationship to source rock depositional setting. *Organic Geochemistry* 22:521-542.

Newberry, J. S. 1873. The General Geological Relations and Structure of Ohio.*Ohio Geological Survey Report 1*, Part1. Division of Geological Survey, Columbus, OH.

Nwachukwu, J.I. and Chukwura, P.I. 1986. Organic matter of Agbada Formation, Niger Delta, Nigeria.*American Association of Petroleum Geologists Bulletin* 70:48–55.

Oakwood, T. S., Shriver, D. S., Fall, H. H., McAleer, W. J. and Wunz, P. R. 1952. Optical activity of petroleum.*Industrial and Engineering Chemistry* 44: 2568–70.

Okoh, A.F. and Nwachukwu, J.I. 1997. Organic geochemistry of Para-35 and Mina-3 wells Niger Delta, Nigeria. *Journal of Mining and Geology.* 33:103-114.

Orr, W.L. 1986. Kerogen/asphaltene/sulphur relationships in sulphur-rich Monterey oils. In: Advances in Organic Geochemistry, 1-3 (Ed. By D. Leythaeuser, J. Rullkotter), *Pergamon Press*, Oxford.499-516.

Ourrison, G., Albrecht, P. and Rohmer, M. 1979. Thehopanoids: palaeo-chemistry and biochemistry of a group of natural products. *Pure and Applied Chemistry* 51:709-729.

Ourisson, G., Albrecht, P. and Rohmer, M. 1982.Predictive microbial biochemistry-from molecular fossil to prokaryotic membranes.*Trends in Biochemistry Sciences* 7:236-239.

Ourisson, G., Rohmer, M. and Poralla, K. 1987. Prokaryotic hopanoids and other polyterpenoid sterol surrogates. *Annual Review of Microbiology* 41:301–333.

Ottenjann, K., Teichmuller, M., Wolf, M., 1975. Spectral fluorescence measurements of sporinites in reflected light and their applicability for coalification studies. In: Alpern, B. (Ed.), Petrographie de la matiere organique des sediments relations avec la paleotemperature et le potentiel petrolier. Editions du CNRS, Paris, pp. 67-91.

Parry, C.C., Whitley, P.K.J., Simpson, R.D.H., 1981. Integration of palynological and sedimentation methods in facies analysis of the Brent Formation. Petroleum Geology of the Continental Shelf of Northwest Europe, Heyden, London, pp. 205-215.

Pastorova**,** R.E.**;** Botto**,** A.P.W. and Boon**,** J.J.1994. Cellulose char structure: a combined analytical Py–GC–MS, FTIR, and NMR study. *Carbohydr.Res***.** 262**:**7–47

Peters, K. E. 1986. Guidelines for evaluating petroleum source rocks using programmed pyrolysis. *American Association of Petroleum Geologists Bulletin* 70:329

Peters, K.E. and Moldowan, J.M. 1993. The Biomarker Guide. Interpreting Molecular Fossils in Petroleum and Ancient Sediments. New Jersey: Prentice-Hall, Englewood Cliffs.

Peters, K.E., and Cassa, M.R. 1994. Applied source rock geochemistry. In: Magoon, L.B., Dow, W.G. (Eds.), The Petroleum Systems- From Source to Trap. *American Association of Petroleum Geologists Memoir* 60:93-120.

Peters, K.E., Walters, C.C. and Moldowan, J.M. 2005. The Biomarker Guide. Biomarkers and Isotopes in the Environment and Human History (I).*Cambridge University Press.*

Peters, K.E. and Fowler, M.J. 2005. Applications of Petroleum geochemistry to Exploration and Reservoir management. *Organic Geochemistry* 33:5-36

Philp, R.P. 1985. Methods in Geochemistry and Geophysics, 23.Fossil Fuel Biomarkers.Applications and spectra. NY: *Elsevier Science Publishing Company Inc.*

Philp, R.P. and Gilbert, T.D. 1986. Biomarker distributions in Australian oils predominantly derived from terrigenous source material. *Organic Geochemistry* 10: 73-84.

Picha, F.J. and Peters, K.E. 1998. Biomarker oil-to-source rock correlation in the western Carpathians and foreland Czech Republic.*Petroleum Geosci*ence 4:289–302

Pompeckj, J. F. 1901. Die Juraablagerungen zwischen Regensburg und Regenstauf. *Geologisches Jahrbuch* 14:139–220.

Potter, J., Rankin, A. H. and Treloar, P. J. 2001. The nature and origin of abiogenic hydrocarbons in the alkaline igneous intrusions, Khibina and Lovozero in the Kola Peninsula, N. W. *Presented at the Geological Society London Meeting on Hydrocarbons in Crystalline Rocks*, February 13–14, 2001, London.

Püttmann, W. and Villar, H. 1987. Occurrence and geochemical significance of 1,2,5,6-tetramethylnaphthalene. *Geochimica et Cosmochimica Acta* 51:3023-3029.

Radke, M., Welte, D.H. and Wilsch, H. 1982. Geochemical study on a well in the Western Canada Basin: relation of the aromatic distribution pattern to maturity of organic matter. *Geochimica et Cosmochimica Acta* 46:1-10.

Radke, M. and Welte, D.H. 1983. The methylphenanthrene index (MPI): a maturity parameter based on aromatic hydrocarbons. In: Bjoroy M, editor. *Advances in Organic Geochemistry* 10:51-63.

Radke, M., Welte, D. and Willsch, H. 1986. Maturity parameters based on aromatic hydrocarbons: influence of the organic matter type. *Organic Geochemistry* 10:51-63.

Radke, M. 1987. Organic geochemistry of aromatic hydrocarbons. In: Brooks, J., Welte, D.H. (Eds.). *Advances in Petroleum Geochemistry*, Vol. 2. London: Academic Press.141-207.

Radke, M., Vriend, S. P. and Ramanampisoa, L. R. 2000. Alkyldibenzofurans in terrestrial rocks: Influence of organic facies and maturation. *Geochimica et Cosmochimica Acta* 64:275–286.

Requejo, A. G. 1994. Maturation of petroleum sourcerocks-II. Quantitative changes in extractable hydrocarbon content and composition associated with hydrocarbon generation. *Organic Geochemistry* 21:91–105

Rooney, M.A., Vuletich, A.K. and Griffith, C.E. 1998. Compound-specific isotope analysis as a tool for characterizing mixed oils: an example from West of Shetlands area. *Organic Geochemistry* 29:241-254.

Samuel, O.J., Cornford, C., Jones, M., Adekeye, O.A. and Akande, S.O. 2009.Improved understanding of the petroleum systems of Niger Delta Basin, Nigeria.*Organic Geochemistry* 40:461–483

Samuel, O. J., Kildahl-Andersen, G., Nytoft, H. P., Johansen, J. E. and Jones, M. 2010. Novel tricyclic and tetracyclic terpanes in Tertiary deltaic oils: Structural identification, origin and application to petroleum correlation. *Organic Geochemistry* 41:1326–1337

Schimmelmann, A., Sessions, A.L., Boreham, C.J., Edwards, D.S., Logan, G.A. and Summons, R.E. 2004. D/H ratios in terrestrially sourced petroleum systems.*Organic Geochemistry* 35:1169-1195.

Schouten, S., Eglinton, T. E., Sinninghe Damste, J. S. and de Leeuw, J. W. 1995. Influence of sulphur-crosslinking on the molecular size distribution of sulphur-rich macromolecules in bitumen. In: Vairavamurthy M. A., Schoonen, M. A. A. (Eds.), Geochemical Transformations of Sedimentary Sulphur. *American Chemical Society Symposium Series* 612:80-92

Schuchert, C. 1915. The conditions of black shale deposition as illustrated by Kuperschiefer and Lias of Germany.*Proceedings of the American Philosophical Society* 54:259–69.

Schwab, V.F. and Spangenberg, J.E. 2007.Molecular and isotopic characterization of biomarkers in the Frick Swiss Jura sediments: A palaeoenvironmental reconstruction on the northern Tethys margin. *Organic Geochemistry* 38:419-439.

Seifert, W. K., 1975. Carboxylic acids in petroleum and sediments.*Fortschritte der Chemie organischer Naturstoffe* 32:1–49.

Seifert, W.K. and Moldowan, J.M. 1981. Palaeoreconstruction by Biological markers.*Geochimica et Cosmochimica Acta* 45:783-794.

Seifert, W. K. and Moldowan, J.M. 1986. Use of biological markers in petroleum exploration. In: Methods in Geochemistry and Geophysics vol.24 (R.B. Johns, ed.). Amsterdam: Elsevier. 261-290.

Selley, R. C. 1998. Elements of petroleum geology, San Diego (CA), Academic Press.

Sephton, M. A., Looy, C. V., Veefkind, R. J., Visscher, H., Brinkhuis, H. and de Leeuw, J. W. 1999. Cyclic diaryl ethers in a Late Permian sediment. *Organic Geochemistry* 30:267–273

Senftle, J.T., Landis, Ch.R. and MacLaughlin, R.L. 1993. Organic petrographic approach to kero-gen characterization. In: Engel, M.H., Macko, S.A. (Eds.), Organic Geochemistry. : Principles and Applications. *Plenum Publishing Corporation*, New York, pp. 355–374. Chapter 15.

Shanmugam, G. 1985. Significance of coniferous rain forest and related organic matter in generating commercial quantities of oil, Gippsland Basin, Australia.*AmericanAssociation of Petroleum Geologists Bulletin* 69:1241-1254

Sherwood Lollar, B.S., Frape, S. K., Weise, S. M., et al. 1993. Abiogenic methanogenesis in crystalline rocks.*Geochimica et Cosmochimica Acta* 57:5087–97.

Sherwood Lollar, B., Westgate, T. D., Ward, J. A., et al. 2002. Abiogenic formation of alkanes in the Earth's crust as a minor source for global hydrocarbon reservoirs.*Nature* 416:522–4.

Short, K. C., and Stauble, A. J. 1967. Outline of geology of Niger Delta .*AAPG* 51:761-779.

Simoneit, B.R.T. 1998. Biomarker PAHs in the environment. In: Neilson, A., Hutzinger, O., editors. *The handbook of environmental chemistry*. Berlin: Springer Verlag. 175-221.

Simoneit, B.R.T. 2002. Molecular Indicators of Past Life. *The Anatomical Record* 268:186-195.

Sinninghe Damsté, J.S., Knock-van Dalen, A. S., de Leeuw, J.W., Schenck, P.A., Guoying, S. and Brassell, S. C. 1987. The identification of mono-, di- and trimethyl 2-methyl-2-(4,8,12-trimethyldecyl)chromans and their occurrence in the geosphere. *Geochimica et Cosmochimica Acta* 57:2393-2400

Sinninghe Damste, J. S. and de Leeuw, J. W. 1990.Analysis, structure and geochemical significance of organically-bound sulphur in the geosphere: State of the art and future research. *Organic Geochemistry* 16, 1077–1101

Sinninghe Damsté, J.S., Keely, B. J., Betts, S. E., Baas, M., Maxwell, J. R. and de Leeuw, J.W. 1993. Variations in abundances and distributions of isoprenoid chromans and long-chain alkylbenzenes in sediments of the Mulhouse Basin: A molecular sedimentary record of palaeosalinity. *Organic Geochemistry* 20:1201-1215

Sinninghe Damsté, J.S., Kenig, F., Koopmans, M.P., Koster, I., Schouten, S., Hayes, J.M. and De Leeuw, J.W. 1995. Evidence for gammacerane as an indicator of water coloumn stratification. *Geochim et Cosmochim Acta* 59:1895-1900.

Sivan, P., Datta, G. C. and Singh, R. R. 2008.Aromatic biomarkers as indicators of source, depositional environment, maturity and secondary migration in the oils of Combay Basin, India.*Organic Geochemistry* 39:1620-1630

Sonibare, O., Alimi, H., Jarvie, D. and Ehinola, O. A. 2008.Origin and Occurrence of crude oils in the Niger Delta, Nigeria.*Journal of Petroleum Science and Engineering* 61:99-107

Stach, E., Mackowsky, M-Th., Teichmuller, M., Taylor, G.H., Chandra, D. and Teichmuller, R. (Eds.) 1982.Coal Petrology.*Gebruder Borntraeger*, Berlin - Stuttgart, 535 pp

Stacher, 1995.Present Understanding of the Niger Delta Hydrocarbon Habitat. In: Oti, M.N., Postma, G. (Eds.), Geology of Deltas. Frotterdam, A.A., Bakkerma, pp. 57–267.

Staplin, F.L., 1969. Sedimentary organic matter, organic metamorphism, and oil and gas occurrences.*Bulletin of Canadian Petroleum Geology* 17:47–66.

Suárez-Ruiz, I., Flores, D., Mendonça Filho, J.G. and Hackley, P.C. 2012. Review and update of the applications of organic petrology: Part 1. Geological applications.*International Journal of Coal Geology* 59:54-112.

Taylor, P., Bennettt, B., Jones, M. and Larter, S. 2001.The effect of biodegradation and water washing on the occurrence of alkylphenols in crude oils.*Organic Geochemistry* 32:341–358.

Taylor, P., Larter, S., Jones, M., Dale, J., Horstad, I., 1997.The effect of oil-water-rock partitioning on the occurrence of alkylphenols in petroleum systems.*Geochimica et Cosmochimica Acta* 61:1899–1910.

Taylor, G.H., Teichmuller, M., Davis, A., Diessel, C. F. K., Littke, R. and Robert, P. 1998. Organic Petrology.*Gebrüder Borntraeger*, Berlin. 704 pp

ten Haven, H.L. 1996. Applications and limitations of Mango''s light hydrocarbon parameters in petroleum correlation studies. *Organic Geochemistry* 24:957–976

Thode, H.G. 1981.Sulfur isotope ratios in petroleum research and exploration: 202 Williston basin.*American Association of Petroleum Geologists Bulletin*:1527-1535.

Tissot, B.P., Pelet, R. and Ungerer, P. H. 1987.Thermal history of sedimentary basins, matu-ration indices and kinetics of oil and gas generation.*American Association Petroleum Geology Bulletin* 71:1445–1466

Tissot, B.T. and Welte, D.H. 1984. Petroleum Formation and Occurrences.Second Edition. Berlin: Springer-Verlag.

Tissot, B.T. and Welte, D.H. 1978. Petroleum Formation and Occurrences: A New Approach to Oil and Gas Exploration. Berlin, Heidelberg, New York: Springer-Verlag.

Treibs, A. 1934. The occurrence of Chlorophyll derivatives in an oil shale of the upper Triassic. *Annalen* 517:103-114.

Treibs, A. 1936.Chlorophyll and hemin derivatives in organic mineral substances.*Angewandte Chemie* 49:682–6.

Tuttle, M.L.W., Charpentier, R.R. and Brownfield, M.E., 1999. The Niger Delta petroleum system: Niger Delta Province, Nigeria, Cameroon, and Equitorial Guinea, Africa. *US Geological Survey Open-File Report* 99-50-H.

Van Aarssen, B. G. K., Bastow, T. P., Alexander, R. and Kagi, R.I. 1999. Distribution of methylated naphthalenes in crude oils: indicators of maturity, biodegradation and mixing. *Organic Geochemistry* 30:1213-1227

van Krevelen, D.W. 1961. Coal: Typology–Chemistry–Physics–Constitution, 1st ed. *Elsevier*, Amsterdam. 514 pp

van Krevelen, D.W. 1993. Coal: Typology–Chemistry–Physics–Constitution, 3rd ed. *Elsevier*, The Netherlands. 979 pp

Volkman, J.K., Alexander, R., Kagi, R.I., Rowland, S.J. and Sheppard, P.N. 1984.Biodegradation of aromatic hydrocarbons in crude oils from the Barrow Sub-basin of Western Australia.*Organic Geochemistry* 6:619-632.

Volkman, J.K. 1988. The biological marker compoundsas indicators of the depositional environments of petroleum source rocks. In: Fleet, A.J., Kelts, K., Talbot, M.R. (Eds.), Lacustrine Petroleum Source Rocks. *Geological Society Special Publication* 40:103-122

Wang, T., He, F., Li, M., Hou, Y. and Guo, S. 2004. Alkyldibenzothiophenes: molecular tracers for filling pathway in oil reservoirs. *Chinese Science Bulletin* 49:2399-2404

Waples, D. 1985. Geochemistry in petroleum exploration.*International Human Resources Development Corporation*, Boston. 232 pp

Waples, D.W. and Machiara, T. 2001. The Geology of Niger Delta.*Bulletin of Canadian Petroleum Geology* 38:357-380.

Wendebourg, J. and Harbaugh, J.W. 1997. Simulating Oil Entrapment in Clastic Sequences. Pergamon, New York.

Whitehead, E.V. 1974. The structure of petroleum pentacycles. In: Tissot, B., Bienner, F. (Eds.), Advances in Organic Geochemistry. *Editions techniq.* 1973:225-243.

Whiteman, A.1982. Nigeria: Its Petroleum Geology, Resources and Potentials. vol. 1 and 2. *Graham and Trontman Ltd*., 394 pp

Xiao, Z., Li, M., Huang, S., Wang, T.G., Zhang, B., Fang, R., Zhang, K., Ni, Z., Zhao, Q. and Wang, D. 2016. Source, oil charging history and filling pathways of the Ordovician carbonate reservoir in the Halahatang Oilfield, Tarim Basin, NW China. *Marine and Petroleum Geology* 73:59–71.

Xiangchun, C., Zuozhen, H., Xiaofei, S. and Chengpeng, Y. 2011. Geochemical characteristics of aromatic hydrocarbons in crude oils from the Linnan Subsag, Shandong Province, China.*Chinese Journal of Geochemistry* 30:132–137.

Yang, F., Wang, T.G. and Li, M. 2016.Oilfilling history of the Mesozoic oil reservoir in the Tabei Uplift of Tarim Basin, NW China.*Petroleum Science and Engineering* 142:129-140.

Yangming, Z., Huanxin, W., Aiguo, S., Digang, L. and Dehua, P. 2005. Geochemical characteristics of Tertiary saline lacustrine oils in the Western Qaidam Basin, northwest China. *Applied Geochemistry* 33:1225-1240.

Yule, B., Roberts, S., Marshall, J.E.A. and Milton, J. A. 1998. Quantitative spore colour mea-surement using colour image analysis. *Organic Geochemistry* 28 (3–4):139–149.

Yunker, M.B., Macdonald, R.W., Vingarzan, R., Mitchell, R.H., Goyette, D. and Sylvestre, S. 2002. PAHs in the Fraser River basin: a critical appraisal of PAH ratios as indicators of PAH source and composition. *Organic Geochemistry* 33:489–515.

Yunker, M.B., Macdonald, R.W., Snowdon, L.R. and Fowler, B.R. 2011.Alkane and PAH biomarkers as tracers of terrigenous organic carbon in Arctic Ocean sediments.*Organic Geochemistry* 42:1109–1146.

Yunker, M.B., McLaughlin, F.A., Fowler, M.G. and Fowler, B.R. 2014. Source apportionment of the hydrocarbon background in sediment cores from Hecate Strait, a pristine sea on the west coast of British Columbia, Canada. *Organic Geochemistry* 76:235–258.

Zhang, C., Zhang, Y., Zhang, M., Zhao, H., and Cai, C. 2008. Carbazole distributions in rocks fromnon-marine depositional environments.*Organic Geochemistry* 39:868–878.

Zumberge, J. E. 1987. Prediction of source rock characteristics based on terpane biomarkers in crude oils: A multivariate statistical approach. *Geochimica et Cosmochimica Acta* 51.6:1625-1637